Signal Processing and Soft Computing Approaches to Power Signal Frequency and Harmonics Estimation

Pravat Kumar Ray

Department of Electrical Engineering
National Institute of Technology, Rourkela
Rourkela-769 008, Orissa, India

Signal Processing and Soft Computing Approaches to Power Signal Frequency and Harmonics Estimation

Thesis submitted in partial fulfillment

of the requirement for the degree of

Doctor of Philosophy

in

Electrical Engineering

by

Pravat Kumar Ray
(Roll No-507EE004)

Under the Guidance of

Dr. Bidyadhar Subudhi
Dr. Abani Mohan Panda

Department of Electrical Engineering
National Institute of Technology, Rourkela
Rourkela-769 008, Orissa, India
January 2011

Department of Electrical Engineering
National Institute of Technology, Rourkela
Rourkela-769 008, Orissa, India

Certificate

This is to certify that the work in the thesis entitled ***Signal Processing and Soft Computing Approaches to Power Signal Frequency and Harmonics Estimation*** submitted by Pravat Kumar Ray is a record of an original research work carried out by him under our supervision and guidance in partial fulfillment of the requirements for the award of the degree of Doctor of Philosophy in Electrical Engineering during the session 2007-2010 in the Department of Electrical Engineering, National Institute of Technology, Rourkela. Neither this thesis nor any part of it has been submitted for the degree or academic award elsewhere.

Professor A. M. Panda
 Department of Electrical Engineering
Indira Gandhi Institute of Technology, Sarang

Professor Bidyadhar Subudhi
Department of Electrical Engineering,
National Institute of Technology, Rourkela

Acknowledgement

I would like to gratefully acknowledge the enthusiastic supervision and guidance of Prof. B. Subudhi and Prof. A. M. Panda during this work. They are my source of inspiration. As my supervisors, their insight, observations and suggestions helped me to establish the overall direction of the research and contributed immensely to the success of the work. I would like to thank Prof. G. S. Rath, Prof. K. B. Mohanty, Prof. A. K. Panda, Prof. S.Ghosh and Prof. S. R. Samantaray for their detailed comments and suggestions during the final phases of the preparation of this thesis.

I acknowledge all staffs, research scholars and friends of Center for Industrial Electronics and Robotics, Department of Electrical Engineering, NIT, Rourkela for helping me during my research work.

I must acknowledge the academic resource that I have got from NIT, Rourkela and IGIT, Sarang giving me a comfortable and active environment for pursuing my research.

Finally, I would like to thank my parents and my wife for their endless encouragement for pursuing my research.

Pravat Kumar Ray

Abstract

Frequency and Harmonics are two important parameters for power system control and protection, power system relaying, power quality monitoring, operation and control of electrical equipments. Some existing approaches of frequency and harmonics estimation are Fast Fourier Transform (FFT), Least Square (LS), Least Mean Square (LMS), Recursive Least Square (RLS), Kalman Filtering (KF), Soft Computing Techniques such as Neural Networks and Genetic Algorithms etc. FFT based technique suffers from leakage effect i.e. an effect in the frequency analysis of finite length signals and the performance is highly degraded while estimating inter-harmonics and sub-harmonics including frequency deviations. Recursive estimation is not possible in case of LS. LMS provides poor estimation performance owing to its poor convergence rate as the adaptation step-size is fixed. In case of RLS and KF, suitable initial choice of covariance matrix and gain leading to faster convergence on Mean Square Error is difficult. Initial choice of Weight vector and learning parameter affect the convergence characteristic of neural estimator. Genetic based algorithms takes more time for convergence.

To achieve faster convergence and more accuracy in estimation, in this thesis a Variable Leaky Least Mean Square (VL-LMS) is proposed for frequency estimation. The proposed approach uses a variable leak adjustment technique to avoid drifting of the parameters involved in the estimation mechanism. A variable adaptation step-size is also incorporated in the algorithm to yield faster convergence. The performance of the proposed algorithm is studied through simulations and on experimental data for several critical cases such as in presence of noise, jump in frequency, harmonics and sub-harmonics and inter-harmonics that often arise in a power system. These studies show that the VLLMS algorithm is superior to the existing ones in estimating power system frequency.

Subsequently, a nonlinear state estimation technique for estimation of harmonics, inter-harmonics and sub-harmonics based on Ensemble Kalman Filtering (EnKF) is proposed. This algorithm is suitable for problems having more numbers of variables. In harmonics estimation problem, there are twelve unknown variables for distorted signal containing

noise and d.c. offsets. EnKFs represent the distribution of power system states using a collection of state vectors known as ensemble, which replaces the covariance matrix by sample covariance computed from ensemble. The proposed EnKF estimation technique accurately estimates the harmonics, sub-harmonics and inter-harmonics including possible variations in amplitude in the time domain signal. Further, performance of the proposed EnKF method is compared with existing techniques such as Least Mean Square (LMS), Recursive Least Square (RLS), Recursive Least Mean Square (RLMS) and Kalman Filter (KF) algorithms, and it provides highly improved results with respect to tracking time and accuracy.

The thesis also proposed four hybrid estimation algorithms such as KF-Adaline, RLS-Adaline and RLS-BFO (Bacterial Foraging Optimization), Adaline-BFO, for estimation of power system frequency and harmonics. In case of KF-Adaline and RLS-Adaline, weights of the Adaline are updated using KF and RLS algorithm(s). Efficacies of the above hybrid estimation algorithms have been studied through simulation on numerical and experimental data that in terms of estimation accuracy, processing and tracking time, KF-Adaline outperforms RLS-Adaline. In this thesis, the proposed hybrid approaches to power system frequency and harmonics estimation first optimize the unknown parameters of the regressor of the input power system signal exploiting evolutionary optimization approach (BFO) and then RLS or Adaline are applied for achieving faster convergence in estimating the frequency and harmonics of distorted signal.

The estimation achieved by application of the proposed estimation approaches are exploited to design a Hybrid Active Power Filter (HAPF) for achieving pure sinusoidal signal. A HAPF has been proposed that uses modified PWM control technique for elimination of harmonics in distorted power system signals. This filter uses the estimation obtained from KF-Adaline approach. The modified PWM control technique used in HAPF is based on comparing simultaneously a triangular high frequency carrier signal with a controlling signal and its 180^0 out of phase signal. A laboratory prototype for HAPF with modified PWM control is developed for harmonics elimination in a distorted power system signal arising due to rectifier load. Simulation and experimentation are performed to verify the efficacy of the modified PWM control based HAPF. The above designed HAPF exhibits better filtering ability as compared to passive and active filters.

Contents

List of Figures

List of Tables

Acronyms

- ADALINE: Adaptive Linear Neural Network

- ANN: Adaptive Neural Network

- APF: Active Power Filter

- AR: Autoregressive

- ASD: Adjustable Speed Drive

- ASIC: Application Specific Integrated Circuit

- BFO: Bacterial Foraging Optimization

- CHARMDF: Characteristic Harmonics Digital Filter

- DFT: Discrete Fourier Transform

- DG: Distributed Generation

- DKF: Discrete Kalman Filter

- ECKF: Extended Complex Kalman Filter

- ELS: Extended Least Square

- EnKF: Ensemble Kalman Filter

- ES: Escalater

- ESPIRIT: Estimation of Signal Parameters Via Rotational Invariance Techniques

- FPGA: Field Programmable Gate Array

- GA: Genetic Algorithm

- GAP: Genetic Adaline Perceptrons

- HAPF: Hybrid Active Power Filter

- IAR: Integrated Autoregressive

- IC: Integrated Circuits

- KF: Kalman Filter

- KH: Kawatake Hirasaka

- LAV: Least Absolute Value

- LMS: Least Mean Square

- LOH: Low Order Harmonics

- LS: Least Square

- MSE: Mean Squared Error

- NKZ: Normalized Karni Zeng

- PCC: Point of Common Coupling

- PLL: Phase Locked Loop

- PSO: Particle Swarm Optimization

- PWM: Pulse Width Modulation

- RLMS: Recursive Least Mean Square

- RLS: Recursive Least Square

- RLS-C: Recursive Least Square Covariance Form

- RLS-I: Recursive Least Square Information Form

- SNR: Signal to Noise Ratio

- SVC: Static VAR Compensator

- SVD: Singular Value Decomposition

- THD: Total Harmonics Distortion

- TLS: Total Least Square

- TRU: Transformer Rectifier Unit

- UPS: Uninterruptible Power Supplies

- VAR: Volt Ampere Reactive

- VHDL: VHSIC Hardware Description Language

- VHSIC: Very High Speed Integrated Circuits

- VLLMS: Variable Leaky LMS

- VLSWBLS: Variable Length Sliding Window Block Wise Least Square

- VSSLMS: Variable Step Size Least Mean Square

- WLS: Weighted Least Square

- WT: Wavelet Transform

Chapter-1

Introduction

1.1 Background

Frequency is an important operating parameter of a power system because it reflects the energy balance between load and generating power. Hence, frequency is regarded as an index of operating practices and utilities can able to know the system energy balance situations by observing frequency variations. Frequency variation occurs over a small allowable range depending upon the load condition. Deviation of the system frequency from nominal frequency results in a change in reactance of system, which influences different relay functionalities such as frequency relay used in load shedding, reactive power reduction or severe damage, may occur in the system devices. Therefore, for power system control and protection, power system relaying, power quality monitoring, operation and control of devices, accurate monitoring of power system frequency is important. Further, many power electronic equipments and arc furnaces etc. generate lots of harmonics and noise in modern power systems. It is therefore essential for utilities to develop a reliable method for measurement of frequency in presence of harmonics and noises. Since frequency variation is a dynamic phenomenon, the conventional phasor estimation techniques such as Discrete Fourier Transform (DFT), Least Square (LS) and Kalman Filtering may not be suitable for achieving accurate frequency estimation under dynamic conditions.

Extensive usage of power electronic devices such as diodes, thyristor rectifiers, lighting equipments, uninterruptible power supplies (UPS) etc. introduces more amounts of harmonics to power system. But devices such as computers, UPS's which inject harmonics in power system are worst affected as the harmonics content in power system increases. These power electronic devices are very much sensitive to harmonics and they malfunction in presence of harmonics. If suitable harmonics estimation and filtering are not undertaken then these devices may inject inter-harmonics and sub-harmonics to power system. Harmonic currents and voltages also yield increased I^2R losses, over

1

voltage, saturation of transformer core and the reduction of the lifespan of sensitive equipments. The aforesaid adverse affects of harmonic necessitate guidelines to maintain acceptable harmonic labels in the power system. The interests in harmonic studies include modeling, measurements, mitigation and estimation of fundamental as well as harmonic components. Accurate analysis of power system measurements is essential to determine harmonic levels and effectively design harmonics filters. To provide the quality power, it is imperative to know the harmonic parameters such as magnitude and phase. This is essential for designing filters for eliminating and reducing the effects of harmonics in a power system. Thus, harmonic estimation is one of the critical and challenging issues to while dealing with power system signals.

1.2 A Review on Power System Frequency Estimation Algorithms

This section reviews different power system frequency estimation techniques based on signal processing and soft computing techniques.

1.2.1 Recursive Methods

A Least Mean Square (LMS) algorithm in complex form has been presented by Pradhan et al. [1] to estimate power system frequency. A complex signal for LMS algorithm is derived from three-phase signal using $\alpha - \beta$ transformation. This algorithm suffers poor convergence rate as the step size of the LMS is fixed. Variable step size is incorporated to enhance the convergence characteristics of standard LMS. This estimation of frequency is verified in the presence of noise, with frequency jump and with data collected from real time system. The presence of 3rd harmonic in the signal does not affect the performance of algorithm as 3rd harmonic component is eliminated during $\alpha - \beta$ transformation. But the presence of 5th harmonic component affects the performance of the algorithm, so a Butterworth filter used for pre-filtering and the estimation is correct with very less error. For step change in frequency, estimation is found to be correct within $1/3^{rd}$ of a cycle. They have collected power system voltage data in the laboratory by using a 16-channel data recorder at a sampling rate of 5 kHz.

Estimation achieved by using complex LMS was found to be correct with only peak-to-peak variation in the estimation of 0.001Hz without using prefilter.

A Variable Step Size LMS (VSSLMS) has been used in [4, 5] with a view to achieve more accuracy and better convergence in estimation over conventional LMS algorithm. It was observed that using VSSLMS un-correlated noise disturbances exist in the signal do not affect the estimation performance. Its step size is adjusted according to square of time averaging estimate of the autocorrelation of error and previous error. The auto-correlation error is a good measure of the proximity to the optimum and it rejects the effect of uncorrelated noise sequence in the step size update. The step size of the VSSLMS increases or decreases with the increase or decrease of mean square error of signal [4]. The convergence and steady state behavior of the algorithm are also analyzed. However this VSSLMS provides faster convergence at early stages of adaptation while there is little deviation in the later stage. In ref. [6], a new class of Gradient adaptive step-size LMS algorithm has been presented that is one type of Variable Step Size-LMS (VSS-LMS) algorithm. As a fixed μ may not respond to time varying signal parameters, authors in ref. [6] have demonstrated that by using a multiple step size parameter in LMS, one can overcome the above problem. Gradient adaptive step size LMS has been reported in [6] to outperform compared to Mathews [72] and Benveniste's algorithm [73].

A variable Leaky LMS algorithm has been proposed in [7] to avoid the slow convergence of standard LMS algorithm. Where, a leak parameter γ was used in the LMS algorithm. The name comes from the fact that when the input turns off, the weight vector of standard LMS stalls. However, at this time the weight vector of Leaky LMS leaks (spreads out). The Leaky LMS algorithm defined as adding zero mean white noise with autocorrelation matrix γI to the input x. If $\lambda_1, \lambda_2 .... \lambda_n$ are the input eigen value spread of standard LMS algorithm. Then eigen spread in the Leaky LMS algorithm is $(\lambda_1 + \gamma, \lambda_2 + \gamma, ... \lambda_n + \gamma)$. This means that if $\gamma >= 0$, the new eigen value spread is less than initial eigen value spread i.e. $\dfrac{\lambda_{max} + \gamma}{\lambda_{min} + \gamma} \leq \dfrac{\lambda_{max}}{\lambda_{min}}$. Therefore, Leaky LMS's worst-case transient performance is better than the standard LMS algorithm. This paper has also

discussed about when to adjust the leak and how much to adjust the leak. It is found that if error in VL-LMS is less than error in standard LMS, then leak is to be increased, otherwise it should be decreased. Regarding how much to increase or decrease the leak, they have explained a leak adjustment algorithm. They have also verified that VL-LMS outperforms the standard LMS algorithm.

A modified Leaky LMS algorithm has been proposed in [8] which is unbiased and cost-effective because authors have solved the weight drift and bias problems of LMS and Leaky-LMS at an additional cost of only one comparison, one addition and one multiplication per iteration. The mean square error (MSE) performance of the adaptive algorithm (Leaky LMS) for Gaussian input data has been presented in ref. [9]. Inadequacy of excitation in the input sequence results in unbounded parameter estimates. This behavior causes degraded performances as a consequence of unbounded prediction error. The above problem has been stabilized by introducing leakage in the LMS algorithm. Therefore, the Leaky LMS algorithm was successful in abolishing "stalling" where gradient estimate is very less. It describes MSE analysis both for white input signal and for correlated input signal using Leaky LMS algorithm. A new adaptive filtering algorithm called subspace Leaky LMS has been designed in [10] to mitigate the problem of parameter drift of non-persistently exciting input signals. Algorithm proposed by the authors' in [10] leaks only in the unexcited modes and introduces insignificant bias on retaining the low computational complexity of LMS.

Tobias and Seara [11] described the adaptation path of an active noise and vibration control system having a nonlinear block cascaded with the adaptive filter. This type of nonlinearity is inherent in some of the components of an active control system (e.g. power amplifiers, sensors and actuators etc.). Weight updates equation has been derived by considering the gradient of the instantaneous cost function. A leak factor updatation algorithm has been proposed for variable leakage factor in VLLMS [11]. This leak adaptation in the proposed VLLMS has the advantage of using measurable signals in the system to perform the adjustment of the leak factor.

Douglas [12] compared the performance of two types of Leaky LMS adaptive filters. In one case, it is directly implemented and in another case, a random white noise is added to the input signal of LMS adaptive filter. The MSE analysis of second type of adaptive filter was reported to be worse than that of the Leaky LMS adaptive filter and this performance difference is quite large for large SNR and moderate values (10^{-5}) of leakage factor.

Frequency is considered as a state and estimated using extended complex Kalman Filter (ECKF) [13]. In this ECKF estimation method, the initial covariance matrix is chosen as $P_0 = \rho I$, where ρ >1. Estimation was performed under various system changing conditions such as presence of harmonics in the signal, sudden change in amplitude, phase and frequency of signal, presence of noise and unbalances in the magnitudes of phase voltages in three phases. At low values of SNR (20dB), convergences to the true frequency of the signal is achieved in almost 2 cycles (40ms) and if SNR value reduced to 20dB, time required for convergence reduces to less than 20ms. It is found from the result that with increase in SNR value, the corresponding estimation error decreases. It was also verified in [13] that ECKF is very stable and yields accurate frequency estimation. However, this method suffers from the choice of initial co-variance matrix, which is the key factor for determining the speed of convergence of the algorithm.

Huang et al. [14] proposed a robust algorithm based on an Extended Complex Kalman Filter (ECKF) for the estimation of power signal frequency. This algorithm is called robust because it suppressed the abnormalities from abnormal data (data that causes noises and disturbances in power systems as well as affect the accuracy of frequency estimation) of measurement and efficiency of frequency estimation is enhanced. They have verified the proposed approach using test signals, signals recorded from an arc furnace, signals obtained from the stainless steel factory and signals generated in the laboratory. It also shows that this new robust ECKF performs better than ECKF. Design of an Extended Complex Kalman Filter (ECKF) [15], [16] is discussed for measurement of power signal frequency. During the change in signal parameters, the covariance matrix and Kalman Gain should be reset to track them quickly. Authors have

used hysteresis type decision block to solve this type of problem. The authors determined hysteresis band by the nature of noise and nature of convergence. The test signal is derived using an experimental setup from the signal generator through an unshielded ribbon cable. A digital storage oscilloscope first measures signal frequency. Step change in frequency is realized by allowing sudden jump in the signal generator with introduction of delay subroutines. Kalman Filter resolves the distortion in the transmission line, which is introduced due to CT (or PT) and instrumentation cable.

Kalman Filter in Linear form has been implemented [17] for estimation of phasors of single phase and three-phase system. Authors used a single state frequency estimation technique that avoids the stability problem like the previously proposed Kalman Filter. This algorithm is tested through both simulation and power system data collected in the laboratory using data acquisition card. They have verified that this algorithm performs well in both cases but they have not taken into account the frequency change in the system. Grimble et al. [18] considered a plant, where state estimates are needed for feedback control purposes and parameter estimates are needed for unknown and varying output disturbances. Authors have reduced the order of the Extended Kalman Filter by omitting the model constant states or parameter vectors. Disturbance model is obtained using a modification of Panuska's model [74].

A linear prediction method has been proposed in [19] for the estimation of real harmonic sinusoidal frequency of a signal. According to this method, fundamental frequency is first estimated by using the standard least square approach and final estimate has been obtained by optimizing a Weighted Least Square concept. Chan and So [19] presented an iterative weighted least square approach for estimation of real harmonic sinusoidal frequency but have not take into account the computation of sinusoidal amplitudes and phases. They also verified the fullifilment of Cramer-Rao Lower Bound for high SNR. A variable length sliding window block wise least square (VLSWBLS) method for parameter estimation is proposed in [20]. Both Least Square (LS) and Recursive Least Square (RLS) methods have been employed for parameter estimation. In order to avoid the weak tracking ability of Block wise Least Square (BLS), a sliding window block wise least square approach with an adjustable window length is proposed

to extend the LS approach for parameter estimation of the system with abrupt parameter changes. The proposed approach outperforms the Least Square algorithms significantly and has excellent tracking ability for abrupt parameter changes and steady state performance. Djuric et al. [21] proposed an algorithm, which is derived from Fourier, and Zero crossing technique is applied to cosine or sine components of original signal, which is corrupted by higher harmonics. Fourier and Zero crossing algorithms show high measurement accuracy over a wide frequency change. The proposed algorithm is verified using computer simulation, fields and laboratory tests. For the estimation of power system frequency, a method [22] based on adaptive notch filter has been proposed. A voltage or current signal with d.c component and noise is taken. Its performance is studied with various conditions such as in presence of harmonics, step variations of frequency, ramp variations of frequency, oscillatory variations of frequency, oscillatory variations of amplitude etc. Its performance is also compared with a phase-locked loop (PLL). It has been found that the dynamic performance of the proposed method is faster than that of using PLL. Owing to its simpler structure, it can be used for both hardware and software environments. This technique [23] is based on implementation of two orthogonal digital filters. It provides accurate estimates to a resolution of 0.01-0.02 Hz for near nominal, nominal and off-nominal frequencies in about 20ms. This technique is also tested with voltage signals from a dynamic frequency source and from a power system. This technique requires less computation and is suitable for microprocessor-based relays. Karimi-Ghartemani and Iravani [24] implemented a method based on phase locked loop for estimation of power system frequency. The main features of this method are simple structure, robustness with respect to harmonics and variation of internal parameters, immune to noise and having negligible steady state error.

1.2.2 Soft Computing approaches to Power System Frequency Estimation

A technique based on fuzzy linear regression is proposed in [25] for frequency and harmonics evaluation in a power network, which used digitized voltage signals as fuzzy

numbers for estimation of frequency and harmonics components of voltage signal. They have investigated the effects of sampling frequency, data window size and degree of fuzziness on the estimated parameters. They have verified the proposed technique using simulated data but not verified using experimental data.

An adaptive neural network is presented in [26] for estimation of power system frequency. Authors have used a linear adaptive neuron "Adaline" for identifying parameters of a discrete signal model of a power system voltage. They have adjusted parameter learning to get a stable difference error equation. Proposed algorithm is able to track the frequency over a wide range of frequency changes. This algorithm tracks the frequency at different conditions of power system and also immune to presence of harmonics and noise in signal.

Neural network and genetic algorithm have been used in [27] for estimation of power system frequency. In that proposed algorithm, the learning of weights of neural network was carried out by genetic algorithm. They have compared the performance of this proposed technique with the conventional error back propagation and LMS algorithm. But they found that the proposed algorithm outperforms over other two. They have judged the performance using simulation only.

A technique based on neural network has been proposed in [23] for real time application of frequency in a power network. They have represented frequency as a weight of neural network and adjusted it through a suitable learning process. They have judged the dynamic behavior and steady state accuracy of the proposed technique. It also able to track the change in power system frequency within very less time

1.3 A Review on Power System Harmonic Estimation

This section provides a review on Harmonics Estimation based on Signal Processing, and Soft Computing techniques such as Fuzzy Logic, Neural Network and Evolutionary Computation.

1.3.1 Recursive Methods

Kennedy et al [37] proposed Kalman Filtering approach to harmonic analysis in power system. They used three test signals (Normal operating conditions, sudden drop in fundamental frequency and fault signal) for analyzing power system containing 5th, 7th, 11th and 13th harmonic components with a Gaussian noise of standard deviations 0.01 and a SNR of 40dB. First test signal considered was under normal operating condition, second was due to sudden drop in fundamental frequency and third was a fault signal. Both for linear and non-linear models estimation of harmonics has been carried out for the three test signals. In an unbalanced three-phase system, for the measurement of harmonics, the optimal locations of the installations of harmonic meters and optimal dynamic estimates of the harmonics injections are found out in ref. [38]. In this case, each harmonic injection has been treated as a random state model. Error covariance analysis of harmonic injection by the Kalman filter is used to determine the optimal metering locations. Estimation of harmonics [39] is necessary to minimize harmonic line currents and optimize the load power factor. It also discussed about estimation of harmonics with limited use of harmonic meters. The performance of proposed algorithm has been compared with EKF under different conditions such as normal load conditions, sudden load change, and presence of measurement bad data in IEEE 14 bus system [31]. They have verified that the proposed algorithm outperforms EKF.

Beides and Heydt [40] estimated bus voltage magnitudes and phase angles of the fundamental and higher harmonics from noisy measurement using Kalman Filter method. This algorithm is also tested with IEEE 14 bus system. These results are helpful in studying the total harmonic distortion over a full cycle. It is also helpful in designing power filter to minimize harmonics.

An approach combining both Fourier Linear Combiner and Extended Complex Kalman Filter (ECKF) has been proposed in [41] for power system harmonic estimation. Kalman Filter estimates amplitude and phase when frequency is fixed. However, when frequencies vary, it is unable to retune itself to the frequency changes. Similarly, Fourier Linear Combiner, using single layer neural network able to estimate harmonics at static frequency but during frequency change tracking time becomes much larger and there is

more error in estimation. Therefore, Dash et al. proposed a hybrid combination of Kalman Filter and Fourier Linear Combiner for time varying harmonics in presence of frequency changes. They have verified that proposed algorithm performed well even with frequency jump. A Discrete Kalman Filter (DKF) is designed in [42], which provides power system harmonics and unbalances to identify properly with minimum execution times. They compared for single phase and three phases line current signals of a 3 phase nonlinear load experimentally. The analyzed method has been implemented using Dspace (ds-1104) and able to track odd harmonics up to 19th order. This proposed $3\phi - 3\omega$ signal model could be used where low cost micro controllers and accurate measurements are required.

Several variants of Recursive Least Square (LS) algorithms such as Weighted Least Square (WLS), Recursive Least Square information form (RLS-I), Recursive Least Square Covariance form (RLS-C), Extended Least Square form 1 (ELS-1) and Extended Least Square form 2 (ELS-2) have been used in [43] for estimation of power system harmonics. They have used a noisy harmonic signal from an AC bus of a six-pulse rectifier as a test signal and applied various RLS algorithms to signals having different SNR values. Their analysis showed that good estimates of amplitudes and phases are produced even for 0 dB SNR. Therefore, this algorithm can be used for on-line implementation in a polluted power system.

Three methods such as Discrete Fourier Transform (DFT), Least Square (LS) and Least Absolute Value (LAV) techniques are applied in [44] to the voltage harmonic estimation of a three-phase six-pulse converter. In case of ideal noise free data, all the algorithms have provided exact estimate of the harmonics for sufficiently high sampling rate. For noisy case, LS method provides good estimates for large number of samples at the same time DFT fails. However, LAV provides a better result for high range of samples.

An online technique for estimation of parameters of harmonic signal based on LS and Total Least Square (TLS) optimization criteria has been presented in [45]. The network model under TLS criteria optimized the estimates assuming the fluctuation of frequency and sampling interval. On higher sampling frequencies, TLS estimates are better than LS

estimates. No real time data has been taken to validate the algorithm. A method based on Least Square has been presented in [46] to compute power system harmonic detection and Total Harmonic Distortion. The method has been compared with FFT and Kalman Filter. Simulation and experimental results showed that harmonic component detection scheme using Least Square method has great advantages over other methods because of its less computational cost when used for reconstructing the fundamental component and calculating the compensation current template online for active power filters. THD index can be calculated with little computational cost using this method as compared to other methods.

Lobos et al. [47] discussed Linear Least Square method for harmonic detection in a power system using singular value decomposition (SVD). This method has been investigated under using simulated waveforms as well as current waveforms at the output of a three phase frequency converter supplying an induction motor load and found that it is very versatile and efficient method for detection and locations of all higher harmonics existing in the power system. It is also applicable for estimation of inter-harmonics in a power system.

Dominguez et al. [48] presented the introduction of digital filter for estimation of harmonics components of signal. The digital filter charmDF (characteristic harmonics Digital Filter) incorporated on treatment of samples before applying Discrete Fourier Transform (DFT). The convergence of the algorithm during signal change is also improved. The main advantage is that same algorithm has been used during pre-fault and post-fault periods. So there is no need to know the time of occurrence of fault. But authors in [48] had not taken into account the effect of inter and sub-harmonics components.

Tao et al. [49] proposed an approach based on M-Estimators (i.e a broad class of estimators, which are obtained as the minima of sums of functions of the data e.g. LS estimator and many Maximum-Likelihood estimators) for harmonic estimation to overcome the error in estimation in presence of noise in signal. The initial values for harmonic frequencies are acquired using Estimation of Signal Parameters via Rotational

Invariance Techniques (ESPIRIT) algorithm to avoid local minima and to improve the convergence rate of optimization.

Yilmaz et al. [50] suggested parametric spectral estimation methods for the estimation of harmonics, inter-harmonics and sub-harmonics. Yule Walker, Burg, Co-variance and Modified Co-variance methods were applied for estimation of harmonics. They have successfully determined both integer and non-integer multiple harmonics through computer simulations. A harmonic model based on Wavelet Transform (WT) has been proposed in [51] for online tracking of power system harmonics using Kalman Filtering. Authors have estimated the harmonics amplitudes and phase angles by solving the coefficient of wavelet and scaling functions. Also they have combined Kalman Filtering Technique with it for developing an online harmonic tracking method. A Morlet Wavelet Transform based approach for the study of time-varying power system harmonics has been proposed in [52], where time frequency localization characteristics are embedded in Wavelets. They have applied Wavelet Transform for visualizing the inrush current harmonics of transformer and for investigation of arc furnace generated signal.

Mandel [53] suggested Ensemble Kalman Filter (EnKF) a recursive filter for harmonics estimation problem having large number of variables. It is a new version of the Kalman Filter and is an important data assimilation component of ensemble forecasting. This ref. described the derivation and practical implementation of the basic version of EnKF. Ref. [54] suggested that EnKF can be implemented without access to the observation matrix but only an observation function is required. When the data covariance matrix is easy to decompose, their EnKF is easy to implement. EnKFs represent the distribution of system state using a random sample, called an ensemble and Co-variance matrix is replaced by sample covariance of the ensemble. Gillijns et al. [47] suggested that classical Kalman filter provides a solution of state estimation for linear systems under Gaussian noise but estimation of nonlinear system using different algorithms have limited applicability and computationally expensive. Ensemble Kalman Filter (EnKF) is used as a nonlinear state estimation. It is widely used in weather forecasting, where models are nonlinear with high order. Initial states are also uncertain

and a large number of states are also available. The number of ensembles required in EnKF is heuristic. It was suggested in [55] that an ensemble of size 50 to 100 is often adequate for systems having thousands of states. They applied EnKF to three different examples, one linear and two non-linear for getting tradeoff between ensemble size and estimation accuracy.

1.3.2 Soft Computing approaches to Power System Harmonics Estimation

A technique based on Fuzzy LMS has been applied in [56] for estimation of harmonics voltage and current signals in power network. They have used fuzzy gain scheduling method for the adjustment of step size to provide faster convergence and noise rejection for tracking fundamental as well as harmonics components from signal.

Joorabian et.al. [57] decomposed total harmonics estimation problem into a linear and non-linear problem. Linear Estimator (Least Square (LS)) has been used for amplitude estimation and an adaptive linear combiner "Adaline" which is very fast and simple is used for harmonics phase estimation. There is improvement in convergence and processing time using this algorithm. This algorithm estimates correctly for static, dynamic and fault signal, but estimation using inter and sub harmonic components is not discussed. Lai et al. [58] applied the Least Square technique with artificial neural networks to harmonic extraction in time varying situations. If there is any frequency drift in the signal, then conventional FFT based on fixed measurement window is unable for effective power system monitoring. However, this proposed method is capable of dealing simultaneously the measurement of varying frequency, amplitude and any harmonic components present in the power system. In this case, there is no restriction about evaluation of the number of harmonic component excepting increasing complexity of neural network as the number of harmonics components is increased. Using parallel processing one can solve this problem of high complexity. A new method called power system digital harmonics analyzer [59] for frequency and amplitudes of fundamental and higher harmonic estimation from a voltage or current signal has been presented. It

consists of three stages, first one for an adaptive filter of input signal, second for frequency estimation, third for harmonic amplitude estimation. Simulated data and data from experimental setup have been used. It provided accurate frequency estimates with errors in the range of 0.002 Hz and amplitude estimates with error in the range of 0.03% for SNR=60dB in about 25 ms. Dash et al. [60] applied a neural network approach that is adaptive by Widow-hoff delta rule for the estimation of harmonic components in a power system. The authors adjusted the learning parameter α so that error between the actual and desired output is minimized. Signals corrupted with random noise and decaying DC component, data collected from an AC system using resistance, inductance and data acquisition card have been applied to this proposed method. This method was able to track harmonics and DC components accurately in comparison to KF-based algorithm. The adaptive nature of the algorithm is suitable in tracking harmonics with time varying amplitudes and phase angles. Mori et al. [61] presented a method based on back propagation learning for feed-forward neural network for harmonics prediction. For the effectiveness of the proposed method, it has been applied to the voltage harmonics observed through a computer based measurement system and its performance has been compared with different conventional methods such as Autoregressive (AR) model, Integrated Autoregressive (IAR) model, Escalater (ES) algorithm, Kalman Filter, Recursive Least Square (RLS), Kawatake Hirasaka (KH) method, Normalized Karni Zeng (NKZ) method and Adaptive Auto regressive model.

A neural network based algorithm has been developed in [62] to estimate both magnitude and phase up to eleventh harmonics (550 Hz) of a power system. They used a method for value determination of model parameters involving the noise environment. Performance of the proposed method is also tested with the conventional DFT method. It has fast response and high accuracy compared to DFT. Conventional FFT requires more than two cycles to detect component of harmonics but proposed approach takes ½ of the distorted wave as the input signal. So there is an improvement in the harmonic detection four times compared to FFT. Experimental results confirmed that proposed ANN model well performed in practice.

A number of hybrid algorithms such as Genetic Algorithm (GA), Genetic Algorithm-Least Square(GA-LS), Particle Swarm Optimization-Least Square(PSO-LS) and Adaptive neural Network(ANN) techniques has been proposed in [63] for estimation of harmonics in a power system. Estimation of the magnitude and phase angle of the harmonics has been accomplished by analyzing the waveforms. Out of the above hybrid schemes of harmonics estimation, comparison in terms of processing time and percentage error suggests that ANN is the effective for the estimation of harmonics in a power system.

Seifossadat et al. [64] presented an adaptive neural network based on Genetic Method called GAP (Genetic Adaline Perceptrons) for tracking the harmonics components of current and voltage waveforms in faulted power system. At each iteration of Adaline, Genetic Adaline Perceptrons (GAP) uses GA for selection of optimized value for learning parameter. The results were compared with DFT, KF, GA and Adaline methods. Results showed that GA has minimum deviation though it is not as fast as other methods like Adaline and GAP. The Adaline is the fastest and GA is most accurate. So authors had taken GAP as the trade off between speed and accuracy for harmonics evaluation in power system.

Bettayeb and Qidwai [65] presented a new algorithm for estimation of harmonics using GA's. The proposed algorithm estimates phase of power system signal using GA. After the estimation of phase, amplitude has been estimated using Least Square (LS) algorithm. Signals taken across load from a two-bus three-phase system with a full-wave six-pulse bridge rectifier were applied to this algorithm. Voltage data taken from an offshore industrial facility was also applied to this proposed algorithm and the algorithm performed well. They showed that there is an improvement of more than 60 % in convergence time of this proposed algorithm over the ordinary GA. With the use of fast machine such as Pentium 300MHz, convergence time reduces to few seconds. Thus online implementation is possible.

Mishra [69] presented the foraging behavior of E. Coli bacteria to estimate the harmonic components present in power system voltage/current waveforms. The foraging strategy becomes adaptive by using Takagi-Sugeno scheme. Linear Least Square has

been combined with Bacterial Foraging and Takagi-Sugeno scheme for estimation of amplitude. The cost function that is to be optimized using bacteria foraging, has been taken as the sum of squares of the error of the estimated and actual signal. Validation of proposed hybrid method has been accomplished with data collected across the load of a three-phase system with a full-wave six-pulse bridge rectifier at the load bus. It was found that this hybrid method outperformed over DFT and its performance was satisfactory for change in parameters as well as for decaying DC-contaminated signal.

Although RLS and ELS have been applied for power system harmonic estimation but the attention of many researchers have skipped in applying RLS and ELS to power system amplitude and frequency estimation problems with different signal to noise ratios and system changing condition. An immediate motivation was to apply RLS and ELS to frequency estimation problem on comparing their performance with Kalman Filter and LMS. LMS method applied to power system frequency estimation exhibits less speed of convergence and more estimation error. We have proposed a method called Variable Leaky LMS to avoid the aforesaid drawbacks of LMS in the power system frequency estimation problem. Several methods such as KF, CKF have been applied for power system harmonics estimation. But covariance matrix in case of Kalman Filtering can be replaced by sample covariance found from ensemble in EnKF and for high order system, maintenance of sample covariance is not difficult. Motivated by this benefit of EnKF we also attempt to apply this method for estimation of power system harmonics. Again for achieving better harmonic estimation accuracy, attempts have been made to combine some classical techniques such as RLS and Kalman Filter with soft computing techniques such as (Adaline and BFO)

It is found in literature that most work consider validation of estimation methods using synthetic signal from power system. But it would be interesting to verify the estimation algorithms by using real time power system data or laboratory data. Hence, we have applied dataset obtained from a power plant and from experimental setup to frequency and harmonic estimation for validation.

1.4 Motivation of the work

- Although RLS and ELS have been applied for power system harmonic estimation however attention has not been paid in applying RLS and ELS to power system frequency estimation problems. An immediate motivation was to apply RLS and ELS to frequency estimation problem on comparing their performance with available results.

- To devise efficient power system frequency estimation methods.

- To investigate the effectiveness of new signal processing techniques to power system harmonics estimation.

- To exploit benefits of individual algorithms (RLS, ELS, KF, LMS) in developing hybrid identification techniques employing both classical and soft computing techniques for both frequency and harmonics estimation.

- Most works in literature consider validation of estimation methods using synthetic signal from power system. Tests have been carried out on dataset from a power plant and experimental setup for frequency and harmonics estimation.

- For improvement in power quality, application of estimation algorithms may be exploited.

1.5 Problem Statement

The problem addressed in the thesis comprises of the following two sub problems as described below.

1.5.1 Frequency Estimation Problem
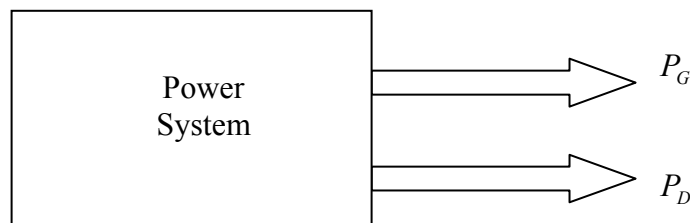
Fig. 1.1 Schematic of frequency estimation problem

P_G : Active Power Generation

P_D : Active Power Demand

If $P_D > P_G$, then frequency (f) of the system decreases

If $P_D < P_G$, then frequency (f) of the system increases

The load in a power system is not constant and system frequency remains at its nominal value only when there is a match between active power demand and active power generation. During the period of load change, the nominal frequency deviates. Thus the power system voltage/current signal gets distorted. Deviation of system frequency from nominal frequency, is called frequency error Δf , is an index of mismatch and can be used to send the appropriate command for changing the generation by adjusting Load Frequency Control (LFC). It is thus necessary to estimate power system frequency accurately before sending command to LFC to yield increase or decrease in generation. Thus, the frequency estimation problem is concerned with developing efficient algorithms with a view to obtain accurate estimation of frequency of the resulting distorted power system voltage signal.

1.5.2 Harmonics Estimation Problem
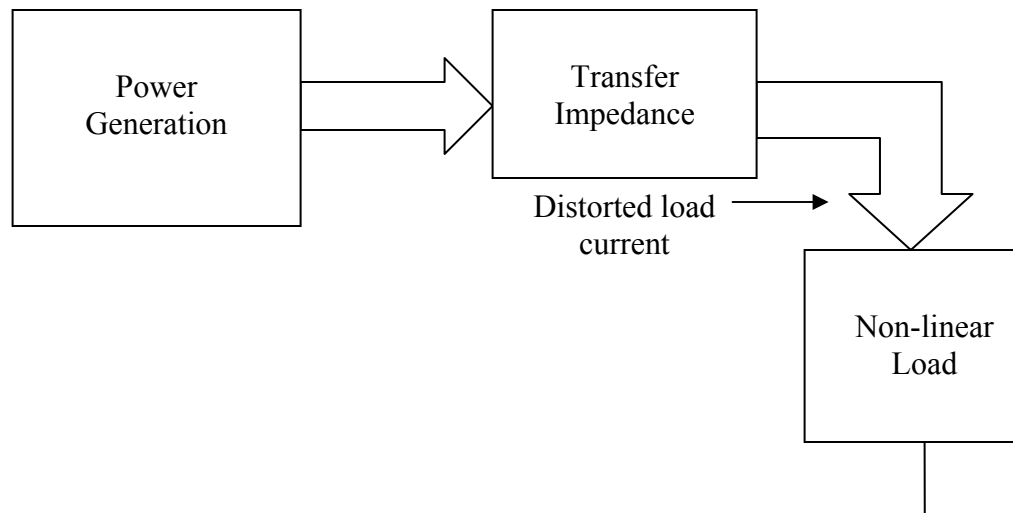
Fig. 1.2 Schematic of harmonics estimation problem

More usage of nonlinear loads such as power electronics devices introduces more amounts of harmonics into power system. As a matter of fact, power system voltage or current signal deviates from pure sinusoidal waveform and in particular the distortion of the current waveform becomes more complex. If suitable filtering is not undertaken then these devices will introduce inter-harmonics and sub-harmonic components to power system. Both harmonics and interharmonics have adverse effects on the power system operation. It is pertinent that accurate estimation of harmonics in distorted power system current/voltage signal to effectively design filters for eliminating harmonics. Hence, the harmonics estimation problem is intended to develop accurate estimation algorithms for obtaining amplitude and phase of the harmonics of the distorted voltage/current signal.

1. 6 Objectives of the Thesis

The following are the objectives of the Thesis.

- To apply recursive algorithms such as RLS and ELS to power system frequency estimation problem and to compare these results with the available Kalman Filter and LMS based results.

- Variable Leaky LMS is proposed to avoid less speed of convergence and more estimation error of LMS in the power system frequency estimation problem.

- Covariance matrix in case of Kalman Filtering can be replaced by sample covariance found from ensemble in EnKF and for high order system; maintenance of sample covariance is not difficult.

- To achieve accurate frequency and harmonic estimation, attempts have been made to combine some classical techniques such as RLS and Kalman Filter with soft computing techniques such as Adaline and BFO.

- To validate the proposed estimation algorithms on data obtained from laboratory and industrial setup.

- To exploit the efficacies of the developed estimation algorithms such as KF, Adaline and KF-Adaline for designing active power filters.

1.7 Thesis Organization

The thesis is organized as follows

Chapter-1 provides a brief background on the research area of estimation of frequency and harmonics in power system. It includes a critical review on research reported in frequency and harmonics estimation followed by motivation/objectives followed by statement of problem. It also provides the thesis organization.

Chapter-2 presents the estimation of frequency of single phase and three-phase signals, by using different variants of recursive techniques such as RLS, ELS, Kalman Filter and LMS. Simulation studies are made by considering signals with different SNR values and with step change in frequency. The effectiveness of the recursive estimation algorithms in estimating power system frequency has been verified. This chapter also presents the estimation of frequency, which is an important power system parameter by Variable Leaky Least Mean Square (VLLMS) algorithm.

In the first section of this chapter, LMS outperforms over KF but in second section, to enhance the convergence characteristics of the complex form of the LMS algorithm, a variable adaptation step-size is also incorporated. The proposed algorithm uses a quantized leak adjustment function to vary the leak. The performance of the new algorithm is studied through simulations at different situations of the power system. Proposed algorithm is verified using both simulation and experimental results.

Chapter-3 depicts combined RLS-Adaline (Recursive Least Square and adaptive linear neural network) and KF-Adaline (Kalman Filter-Adaline) approaches for the estimation power system frequency. In the previous chapter, only signal processing techniques are described but in this chapter, we have switched over to combination of signal processing and soft computing technique for better accuracy and less tracking time of estimation. The neural estimator is based on the use of an adaptive perceptron comprising a linear adaptive neuron called Adaline. The weight of the Adaline is updated by Kalman Filter and Recursive Least Square algorithm (RLS). The estimators' track the signal corrupted with noise and decaying DC components very accurately. The proposed approaches are tested in case of signal containing noise, harmonics, inter and sub-harmonics and signal obtained from laboratory setup.

First section of this chapter gives idea about frequency estimation using combined signal processing and Neural Network technique. But in second section, Evolutionary Computational technique is hybridized with signal processing technique for frequency estimation. BFO is used for the optimization of the unknown parameters by minimization of the cost function, which is the sum of the squared error of the signal. Out put of BFO is taken as the initial weights of the Adaline in case of Adaline-BFO and of the RLS incase of RLS-BFO. Then weights are updated using each of the algorithms. Frequency of signal is estimated from the updated weights of the Adaline and RLS. Their effectiveness is tested on taking signal containing noise, harmonics, inter and sub harmonics and also from the experimental data obtained from laboratory setup.

Chapter-4 suggests a nonlinear state estimation approach known as Ensemble Kalman Filtering (EnKF), for the detection of harmonics, inter-harmonics and sub-harmonics in a power system. After the discussion of estimation of frequency in previous two chapters, estimation of power system harmonics is carried out in this chapter. EnKFs represent the distribution of systems state using a collection of state vectors known as ensemble and replaces the covariance matrix by sample covariance computed from ensemble. While EnKF estimation has not been studied except some specialized applications, it is widely used in weather forecasting, where model is having high order, initial states are highly uncertain and non-linearity is more. In EnKF, the number of ensembles required is heuristic. Not only integer multiple harmonics but also non-integer multiple harmonics are successfully determined using computer simulations. Further performances of the proposed method are compared with other existing techniques such as RLS, LMS, RLMS and KF algorithms.

Chapter-5 describes a number of hybrid estimation algorithms such as combined RLS-Adaline and KF-Adaline for estimation of harmonic components of a power system. In chapter 4, only application of signal processing techniques have been described for harmonics estimation but in this chapter, we have switched over to combination of signal processing and soft computing technique for better accuracy and less tracking time of estimation. The way of implementation of these hybrid algorithms are the same as discussed in chapter 3 for frequency estimation. The proposed approaches are tested for

static and dynamic signal, signal containing inter and sub-harmonics and signal obtained from laboratory setup.

First section of this chapter gives idea about harmonics estimation using combined signal processing and Neural Network technique. But in second section, Evolutionary Computational technique is combined with signal processing technique for harmonics estimation. Here also the way of implementation of these hybrid algorithms are the same as discussed in chapter 3 for frequency estimation. Their effectiveness is also tested on taking signal containing harmonics, inter and sub harmonics and also from the experimental data obtained from laboratory setup.

Chapter 6 describes the application of a hybrid algorithm (KF-Adaline) to design of a Hybrid Active Power Filter (HAPF) for power conditioning. After estimation of harmonics with the proposed KF-Adaline algorithm, HAPF with a modified PWM control (indirect current control technique for generation of switching signal) is applied for harmonics compensation in distorted power signals. The modified PWM control technique is based on comparing simultaneously a triangular high frequency carrier signal with a slow varying regulation signal and its opposite. The simulated results of this hybrid power filter using modified PWM technique are compared with the active and passive filter. The performance of HAPF is also verified from the experimental results by making a laboratory prototype setup. In all three cases of filters such as passive, active and hybrid, harmonics components are estimated using KF-Adaline estimation algorithm. The total harmonic distortion (THD) is reduced from 19.2% before compensation to 1.82% after compensation using HAPF.

Chapter 7 provides comprehensive summary and conclusions of all different estimation approaches for power system frequency and harmonics. It focuses on contributions of the thesis and scope for future work.

Chapter-2

Power system Frequency Estimation Using Recursive Algorithms

2.1 Introduction

To ensure pure sinusoidal voltage or current signal in a power system i.e. for better power quality, it is intended that the power system should function without significant loss of performance. It deteriorates due to voltage surges, under voltage, over voltage, variation in frequency and variation in wave shape called harmonics. Hence, for improvement in power quality (issues of power quality related to frequency, is harmonics in power system), there is a need of fast and accurate estimation of supply frequency and voltage for an integrated power system, which may be corrupted by noise and higher harmonics. Owing to the power mismatch between the generation and load demand, there is a variation in system frequency from its normal value, which calls for a corrective action for its restoration to its original value. The problem of frequency estimation has been addressed using a large number of numerical methods such as Newton-Raphson, Weighted Least Square and adaptive FIR filtering from the digitized samples of the system voltage. The use of the zero crossing detection and calculation of the number of cycles within a predetermined time interval is one of the simple methods for determining the system frequency of a purely sinusoidal power system voltage waveform. However, signal processing techniques such as Discrete Fourier Transforms, Least Square Error technique [1], Kalman Filter [13, 41], Adaptive notch filters [75-78] have been used for frequency estimation of distorted power system signals. A large number of numerical techniques based on extending the measurement range of Least Square Error, Cramer-Rao bounds and Maximum Likelihood estimation and their practical implementations are reported in the literature [22-24] but these approaches suffer from yielding inaccurate results due to the presence of noise and harmonics and other system changing conditions such as change in fault inception angle and change in fault resistance. Although RLS and ELS methods are very

popular estimation techniques but unfortunately these have been overlooked for application to power system frequency estimation. Keeping this in mind, iterative techniques such as Recursive Least Square (RLS), Extended Least Square (ELS), Kalman Filter (KF) and Least Mean Square (LMS) are applied for estimation of power system frequency both for single phase and three-phase power system signals. In this chapter, these recursive techniques have been employed to obtain power system frequency estimation. Taking into account the real time power system signal, all the algorithms are implemented for frequency estimation at different SNR values and sudden change in frequency of signal.

2.2 Recursive Estimation of Frequency of single-phase distorted signal

2.2.1 Recursive Least Square (RLS) Algorithm applied to Frequency Estimation

Let a distorted power system signal buried with noise is represented by the following structure

$$y(t) = A_1 \sin(\omega_0 t + \phi_1) + \varepsilon(t) \tag{2.1}$$

To estimate the signal $y(t)$, the amplitude (A_1), phase (ϕ_1) and frequency (f_0), equation (2.1) can be written in discretized form as

$$y(k) = A_1 \sin \omega_0 kT \cos \phi_1 + A_1 \cos \omega_0 kT \sin \phi + \varepsilon(k)$$

$$y(k) = [\sin \omega_0 kT \quad \cos \omega_0 kT][\alpha \quad \beta]^T + \varepsilon(k) \tag{2.2}$$

where

$$\alpha = \theta_{11} = A_1 \cos \phi_1$$

$$\beta = \theta_{21} = A_1 \sin \phi_1$$

Further notational simplification of (2.2) can be made by expressing this in regressor form given by

$$y(k) = H(k)\theta + \varepsilon(k) \tag{2.3}$$

where $\varepsilon(k)$ is the noise of signal

Using the RLS estimation technique, the parameters can be estimated using the following computing steps

$$\hat{\theta}(k) = \hat{\theta}(k-1) + K(k)\varepsilon(k) \tag{2.4}$$

where $\hat{\theta}(k) =$ current value of estimate

$\hat{\theta}(k-1) = $ Past value of estimate

$K(k) = $ Kalman Gain

The error in the measurement is given by

$$\varepsilon(k) = y(k) - H(k)^T \hat{\theta}(k-1) \tag{2.5}$$

The gain K is updated using the following expression

$$K(k) = P(k-1)H(k)[\eta I + H(k)^T P(k-1)H(k)]^{-1} \tag{2.6}$$

where $P(k) = $ Error Covariance matrix and $\eta(0 < \eta < 1) = $ Forgetting factor

The covariance matrix can be updated using the following updatation law as given by

$$P(k) = [I - K(k)H(k)^T]P(k-1)/\eta \tag{2.7}$$

Equations (2.4) to (2.7) are initialized at $k = 0$. Initial covariance matrix $P(0)$ is usually chosen to be very large. i.e. $P = \delta I$, where δ is a large number and I is a square identity matrix.

After getting the final estimate of $\theta = \begin{bmatrix} \alpha & \beta \end{bmatrix}^T$, the fundamental amplitude (A_1) and phase (ϕ_1) can be estimated as given below

$$A_1 = \sqrt{(A_1 \cos\phi_1)^2 + (A_1 \sin\phi_1)^2}$$
$$A_1 = \sqrt{\alpha^2 + \beta^2} \tag{2.8}$$
$$\tan\phi_1 = \frac{\beta}{\alpha}$$

$$\phi_1 = \tan^{-1}\frac{\beta}{\alpha} \tag{2.9}$$

Once the estimates of amplitude and phase are obtained, then fundamental frequency (f_0) can be estimated as follows. f_0 is given by $f_0 = \frac{\omega_0}{2\pi}$ can be evaluated from the noisy measurement $y(k)$ using equation (2.1) as given below

$$\sin(\omega_0 kT + \phi_1) = \frac{y(k)}{A_1}$$

$$\omega_0 kT + \phi_1 = \sin^{-1}\left(\frac{y(k)}{A_1}\right)$$

$$f_0 = \frac{1}{2\pi kT}[\sin^{-1}\left(\frac{y(t)}{A_1}\right) - \phi_1]$$ (2.10)

2.2.2 Extended Least Square (ELS) Algorithm for Frequency Estimation

Same signal and model as described in section 2.2 (a) is also considered for estimation of frequency using ELS algorithm. Here, the estimation of the unknown parameter $\theta = \begin{bmatrix} \alpha & \beta \end{bmatrix}^T$ is done by rearranging the observation matrix H and the steps for the algorithms are given below.

$$P(k+1) = P(k) + [H^T(k)H(k)]^{-1}$$ (2.11)

$$\hat{\theta}(k+1) = \hat{\theta}(k) + P(k+1)H^T(k)[y(k+1) - H(k)\theta(\hat{k})]$$ (2.12)

After updatation of the unknown parameters, frequency is estimated using equation (2.10)

2.2.3 Kalman Filtering (KF) for frequency Estimation

The discretized voltages signal as described in section 2.2 (a) is also considered for applying KF to frequency estimation. The regressor form of signal as described in (2.3) is also taken. Then applying Kalman Filtering algorithm to (2.3), unknown parameters $\theta = \begin{bmatrix} \alpha & \beta \end{bmatrix}^T$ are estimated as follows

$$K(k) = \hat{P}(k/k-1)H^T(H\hat{P}(k/k-1)H^T + Q)^{-1}$$ (2.13)

where K is the Kalman gain, H is the observation matrix, $P = \delta I$ is the covariance matrix, where δ is a large number and I is a square identity matrix. Q is the noise covariance of the signal. So the covariance matrix is related with Kalman gain with the following equation.

$$\hat{P}(k/k) = \hat{P}(k/k-1) - K(k)H\hat{P}(k/k-1)$$ (2.14)

Hence the updated estimated state is related with previous state with the following equation.

$$\hat{\theta}(k/k) = \hat{\theta}(k/k-1) + K(k)(y(k) - H\hat{\theta}(k/k-1))$$ (2.15)

After updatation of the unknown parameter matrix, θ by Kalman Filtering, using equations (2.8-2.10), frequency is estimated.

2.2.4 Least Mean Square (LMS) Algorithm applied to frequency Estimation

The same signal as described in (2.1) is considered again to apply LMS for frequency estimation.

$$y(t) = A_1 \sin(\omega_0 t + \phi_1) + \varepsilon(t)$$

Above equation can be rewritten in discretized form as

$$y_k = imag \ (A_1 e^{j(w_k T + \phi_1)}) \tag{2.16}$$

If $\hat{y}_k$ is the estimated value of voltage at the kth instant, so equation (2.16) becomes

$$\hat{y}_k = imag(W_k \ \hat{y}_{k-1}) \tag{2.17}$$

$$W_k = e^{j\hat{\omega}_k T} \tag{2.18}$$

where W_k denotes the weight of the voltage signal, $\hat{\omega}$ is the estimated angular frequency. The error signal in this case is

$$e_k = y_k - \hat{y}_k \tag{2.19}$$

This algorithm minimizes the square of the error recursively by altering the complex weight vector W_k at each sampling instant using equation (2.18) as given below

$$W_k = W_{k-1} + \mu_k e_k \ \hat{y}^*_k \tag{2.20}$$

where * represents the complex conjugate of a variable. The step size μ_k is varied for achieving faster convergence of the LMS algorithm in the presence of noise. For complex states, the equations are modified as

$$\mu_{k+1} = \lambda \mu_k + \gamma R_k R_k^* \tag{2.21}$$

where R_k represents the autocorrelation of e_k and e_{k-1} and R_k^* represents the complex conjugate of R_k. It is computed as

$$R_k = \rho R_{k-1} + (1-\rho)e_k e_{k-1} \tag{2.22}$$

where ρ is an exponential weighting parameter and $0 < \rho < 1$, and $\lambda(0 < \lambda < 1)$ and $\gamma > 0$ control the convergence time. μ_{n-1} is set to μ_{max} or μ_{min} when it falls below or above the lower and upper boundaries respectively. These values are chosen based on signal statistics. At each sampling interval, the frequency is calculated from (2.18) as

$$W_k = e^{j\hat{\omega}_k T} = \cos \hat{\omega}_k T + j \sin \hat{\omega}_k T$$

$$\sin \hat{\omega}_k T = \text{Im}(W_k)$$

$$\hat{\omega}_k T = \sin^{-1}\left[\text{Im}(W_k)\right]$$

$$\hat{f}_k = \frac{1}{2\pi T} \sin^{-1}\left[\text{Im}(W_k)\right] \tag{2.23}$$

where $\omega_k = 2\pi f_k$

Fig. 2.1a shows the implementation of RLS, ELS and KF based algorithms for power system frequency estimation and Fig. 2.1b describes the implementation of LMS algorithm for power system frequency estimation. Fig. 2.1 shows the implementation procedure of the three estimation algorithms (RLS, ELS, and KF) for estimation of frequency of power system signal given by (2.1). Fig. 2.2 shows the flow chart of the LMS algorithm for convenience in implementation.

1. Initialize Amplitude, phase, frequency and unknown parameter matrix

2. Generate a power system signal

3. Estimate the discretized signal using initial value of unknown parameter

4. Evaluate: Estimation error = Actual signal - Estimated signal

5. Update gain and covariance matrix

6. Update unknown parameter

7. If final iteration is not reached, go to step 4

8. Estimate Amplitude, phase and followed by frequency using (2.8), (2.9) and (2.10)

Fig. 2.1a Description of (RLS, ELS and KF) algorithms for Frequency Estimation

1. Initialize $A, \phi, f, \lambda, \rho, \gamma, \mu, R, W$

2. Generate a power system signal

3. Estimate the discretized signal using initial value of weight vector

4. Evaluate: Estimation error = Actual signal - Estimated signal

5. Update Auto correlation matrix and step size using (2.22) and (2.21)

6. Update the weight vector using (2.20)

7. If final iteration is not reached, go to step 4

8. Estimate frequency from final updated weight vector using (2.23)

Fig. 2.1b Description of LMS algorithm for Frequency Estimation
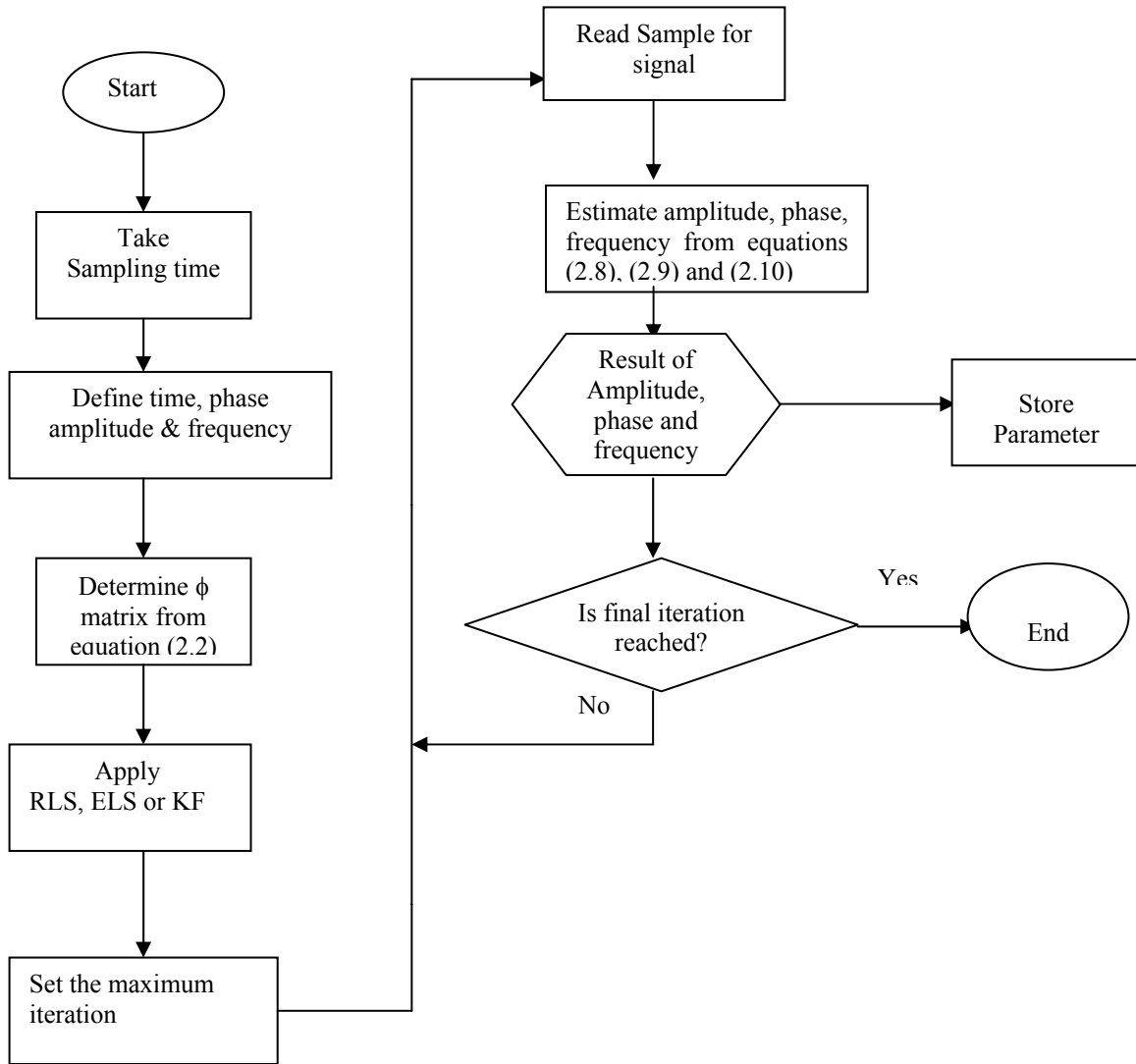
Fig.2.1c Estimation procedure for Recursive Estimation algorithms (RLS, ELS and KF)

```
                          ┌─────────────┐
                          │    Start    │
                          └─────────────┘
                                 │
                                 ▼
              ┌──────────────────────────────────────┐
              │  Initialize λ, β, ρ, P₀, γ,          │
              │  W, μ_max  and  μ_min                │
              └──────────────────────────────────────┘
                                 │
                                 ▼
              ┌──────────────────────────────────────┐
              │  Estimate signal with a Weight        │
              │  vector using (2.17)                  │
              └──────────────────────────────────────┘
                                 │
                                 ▼
              ┌──────────────────────────────────────┐
              │  Evaluate Error=Actual – Estimated    │
              │  signal using (2.19)                  │
              └──────────────────────────────────────┘
                                 │
                                 ▼
              ┌──────────────────────────────────────┐
              │  Update Step Size and Weight Vector   │
              │  on minimizing error from (2.21) and  │
              │  (2.20)                               │
              └──────────────────────────────────────┘
                                 │
                                 ▼
                          ◇ Is final ◇      No
                          ◇ iteration ◇ ──────────►
                                 │
                               Yes
                                 ▼
              ┌──────────────────────────────────────┐
              │  Get final updated Weight Vector      │
              └──────────────────────────────────────┘
                                 │
                                 ▼
              ┌──────────────────────────────────────┐
              │  Estimate frequency from updated      │
              │  Weight Vector using (2.23)           │
              └──────────────────────────────────────┘
                                 │
                                 ▼
                          ┌─────────────┐
                          │    Stop     │
                          └─────────────┘
```
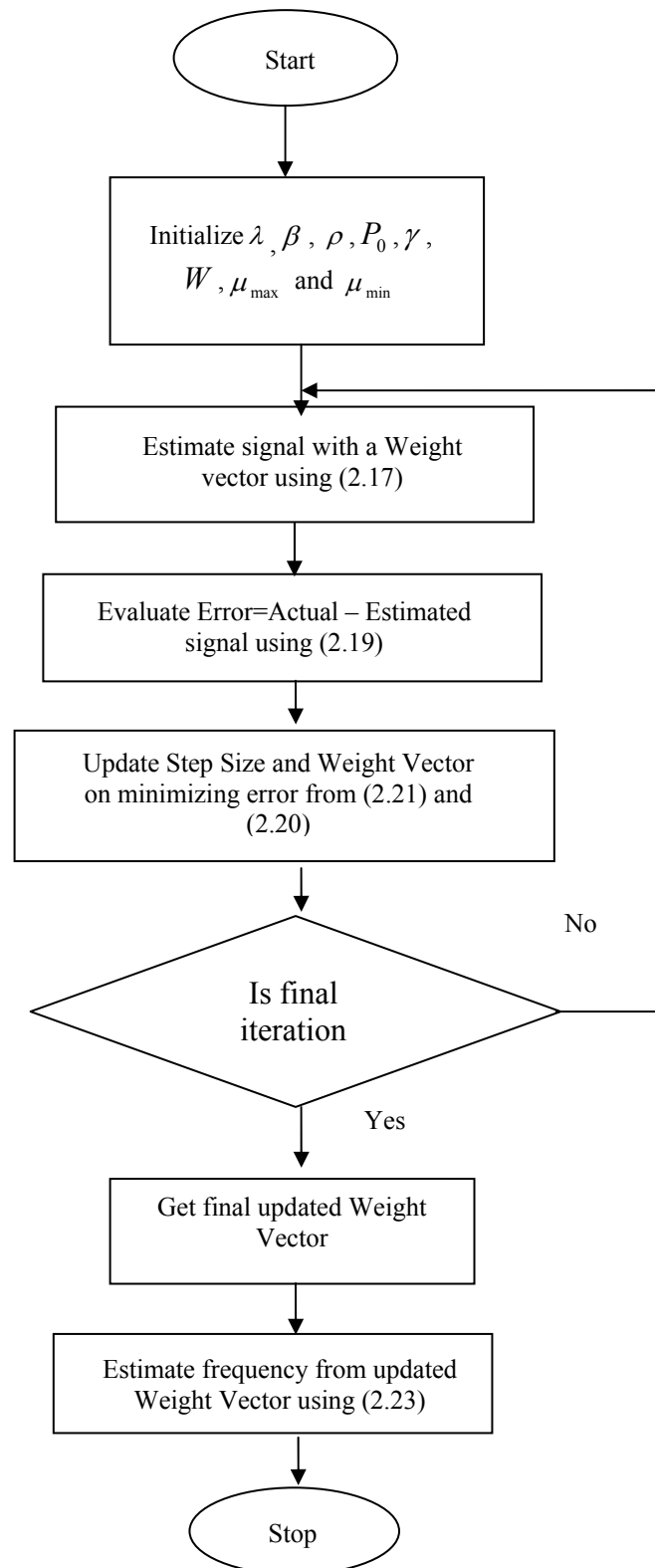
Fig.2.2 Flow chart of the Estimation Scheme of LMS algorithm

2.3 Results and Discussion (Single phase distorted signal)

A synthetic signal of 1 p.u. amplitude, 50 Hz frequency and 0.5236 p.u. phase angle generated using MATLAB. Then the recursive algorithms (RLS, ELS, KF and LMS) are implemented for estimation of power system frequency with the sampling interval of 1ms at different SNR of 20, 30 and 40 dB. Estimation of frequency is done after the estimation of amplitude and phase of the single phase signal using equations (2.8) to (2.10)

2.3.1 Comparison of Estimation performances (RLS, ELS, KF and LMS) at different SNRs. (Single phase signal)

Table-2.1
Parameters used for simulation studies (RLS, ELS, KF and LMS)

Algorithms	δ	η	ρ	λ	γ	Initial μ	Initial W
RLS	100	0.96	-	-	-	-	-
ELS	100	-	-	-	-	-	-
KF	100	-	-	-	-	-	-
LMS	-	-	0.99	0.97	0.001	0.001	0.018
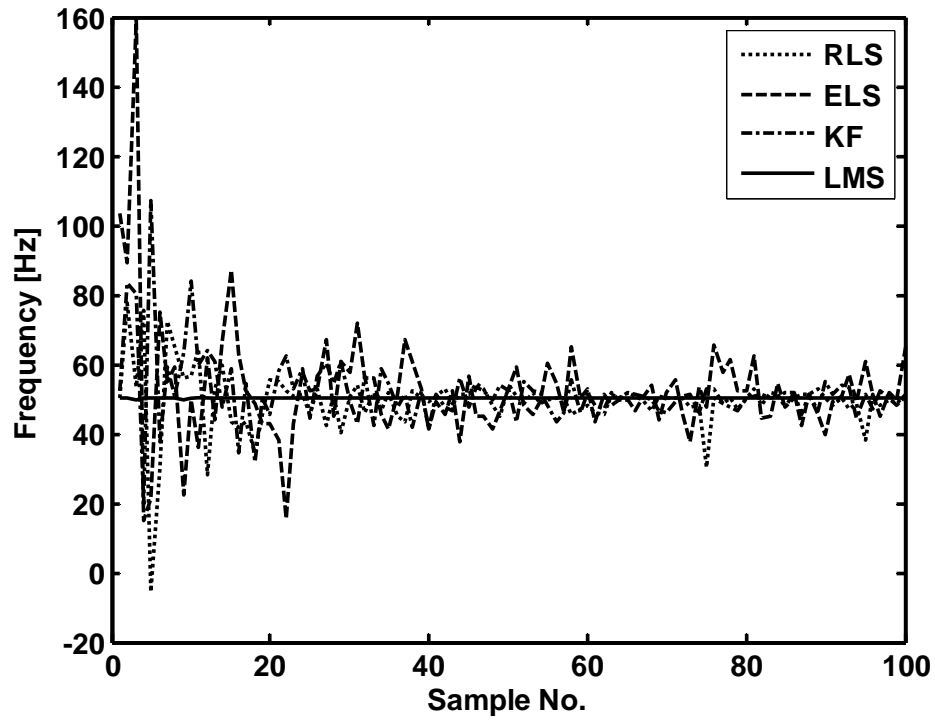
Fig.2.3 LMS estimation performance of Frequency of single phase signal (SNR 20dB)
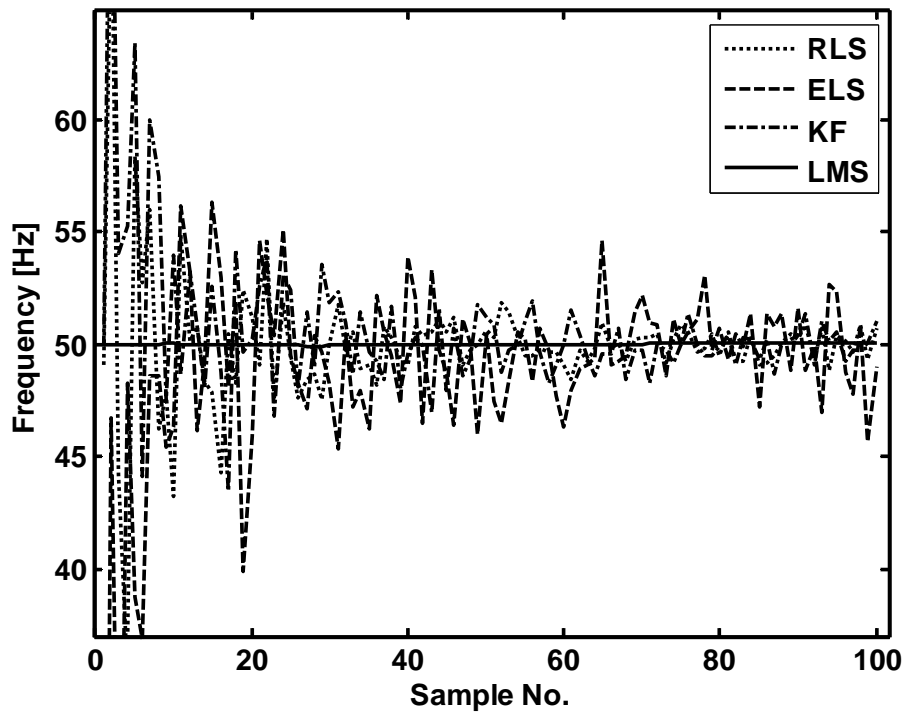
Fig.2.4 LMS estimation performance of Frequency of single phase signal (SNR 30dB)
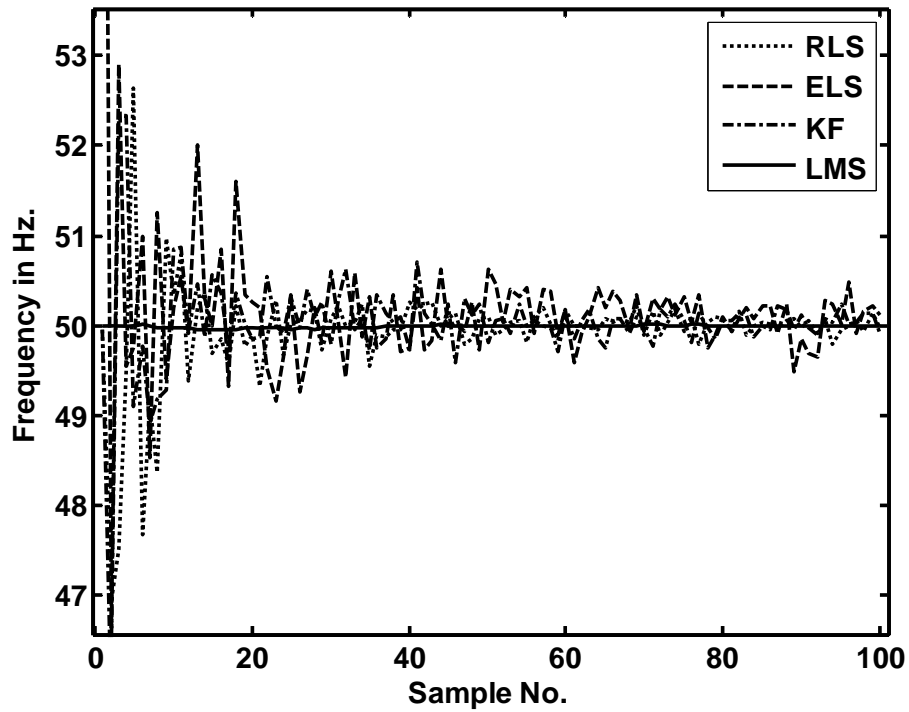
Fig.2.5 LMS estimation performance of Frequency of single phase signal
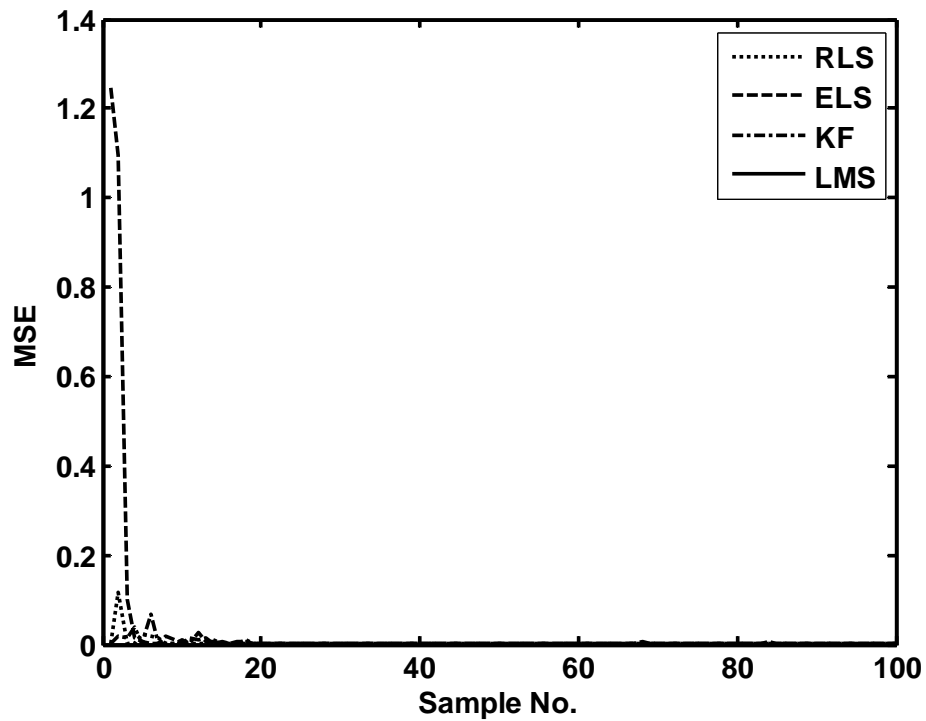
Fig.2.6 Performance comparison of LMS for MSE in estimation of Frequency of signal
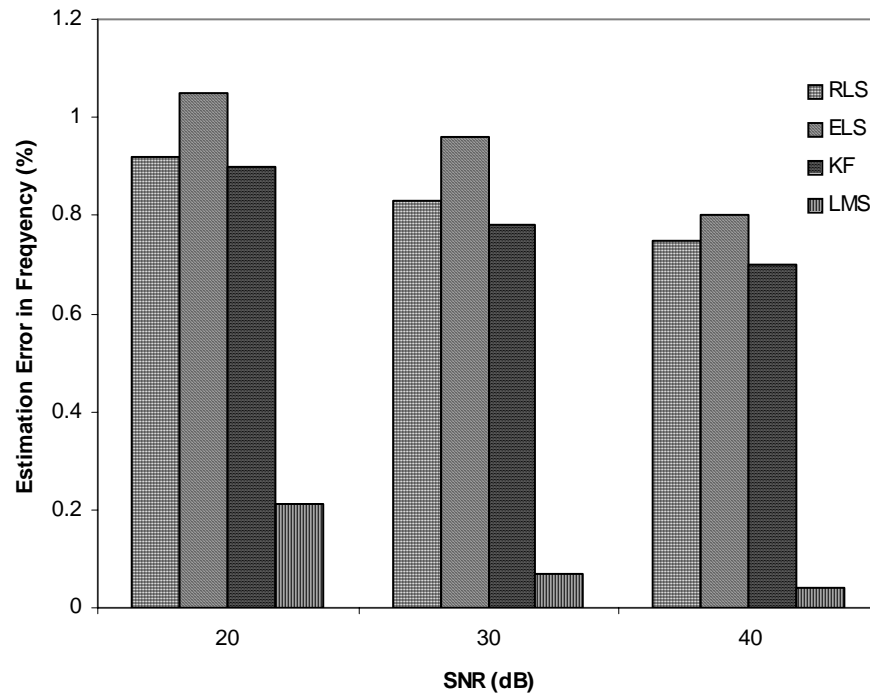
Fig. 2.7 SNR (dB) vs. Estimation error in frequency of single phase signal (%)

Table 2.1 shows the different values of parameters of different algorithms taken during simulation. Figures 2.3, 2.4 and 2.5 show estimated frequency using RLS, ELS, KF and LMS methods at SNR of 20, 30 and 40 dB respectively. From these figures it is clear that as SNR value increases estimation becomes more and more accurate in all the four cases but LMS outperforms over other three. Figure 2.6 shows Mean Squared Error in the estimation of frequency of signal at SNR 40 dB. It is found from the figure that maximum MSE in case of ELS with noise is of the order of 1 where as for RLS, it is of the order of 0.1. In case of LMS algorithm, MSE converges to zero over the samples. So in this case (frequency jump) also LMS outperforms over other three algorithms (RLS, ELS and KF). The comparison of estimation error using different algorithms is more clearly shown in Fig. 2.7 using bar charts.

2.3.2 Estimation performance comparison during sudden frequency change at SNRs (20dB, 30 dB and 40 dB) (Single phase signal)

Figures 2.8, 2.9 and 2.10 show the estimation of power system frequency with a jump in frequency of 50 to 49 Hz at 20th sample of the signal by using all the four algorithms at SNR of 20, 30 and 40 dB respectively. In case of estimation using RLS and ELS, there is more oscillation in all figures. LMS algorithm estimates frequency accurately in case of jump i.e sudden change in frequency of signal, but within few initial samples (having very less tracking time) its estimation of frequency value rises to 50 Hz. The physical idea of taking jump is the sudden change in frequency of signal. It is found from the above figures that as SNR value increases, accuracy in estimation improves (SNR refers to signal to noise ratio and for increase in SNR, there in a reduction in noise level).
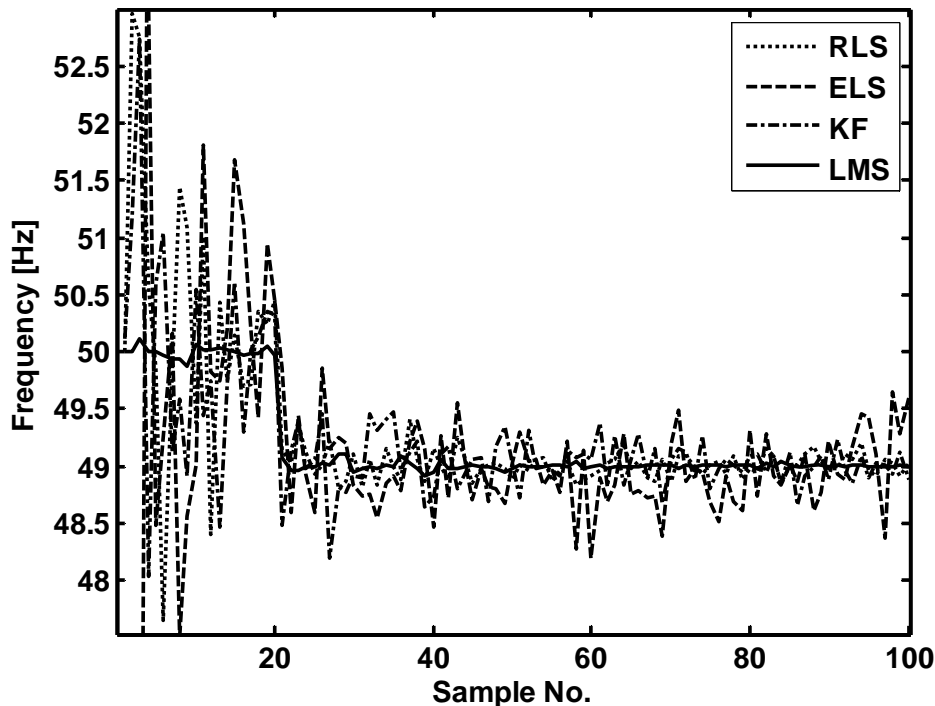
Fig.2.8 LMS estimation performance during sudden frequency change of 49 Hz from 50Hz (SNR 20dB)
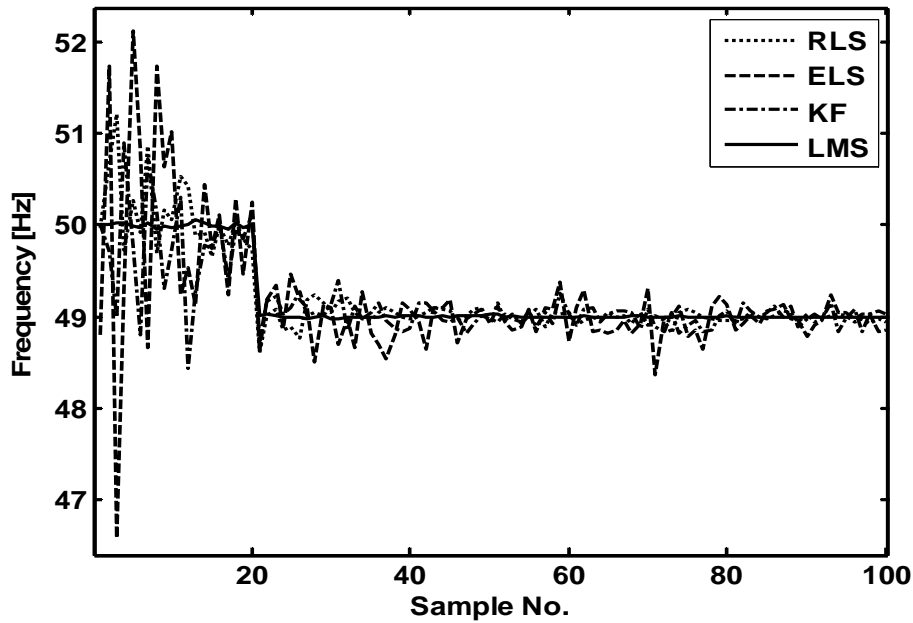
Fig.2.9 LMS estimation performance during sudden frequency change of 49 Hz from 50Hz (SNR 30dB)
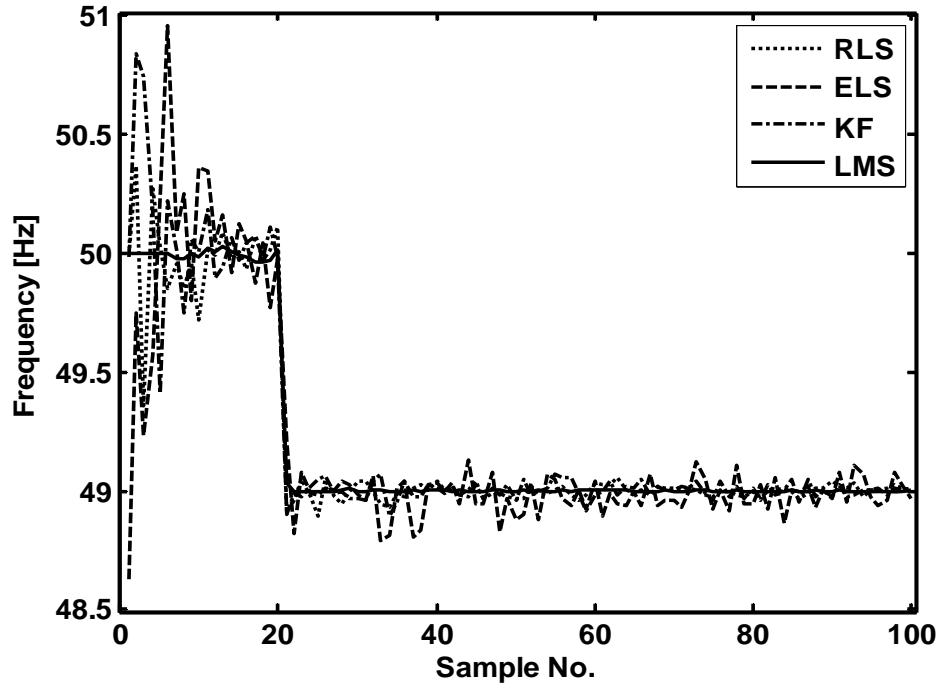
Fig.2.10 LMS estimation performance during sudden frequency change of 49 Hz from 50Hz (SNR 40dB)

2.4 Recursive Estimation of Frequency based on three-phase distorted signal

2.4.1 RLS approach for frequency estimation:

From the discrete values of the three-phase voltage signal of a power system, a complex voltage vector is formed using the well-known $\alpha - \beta$ transformation [1, 13]. A non-linear state space formulation is then obtained for this complex signal and RLS approach is used to compute the true state of the model. As frequency is modeled as a state, the estimation of the state vector yields the unknown power system frequency.

Continuous time representation of three phase voltages of power system is

$$v_a(t) = V_m \cos(\omega t + \phi) + \varepsilon_a(t)$$

$$v_b(t) = V_m \cos(\omega t + \phi - \frac{2\pi}{3}) + \varepsilon_b(t)$$

$$v_c(t) = V_m \cos(\omega t + \phi + \frac{2\pi}{3}) + \varepsilon_c(t)$$

The discrete representation of three phase voltages of a power system can be expressed as

$$v_a(k) = V_m \cos(\omega kT + \phi) + \varepsilon_a(k)$$

$$v_b(k) = V_m \cos(\omega kT + \phi - \frac{2\pi}{3}) + \varepsilon_b(k) \tag{2.24}$$

$$v_c(k) = V_m \cos(\omega kT + \phi + \frac{2\pi}{3}) + \varepsilon_c(k)$$

where v_a, v_b and v_c are three phase voltage signals. V_m is the amplitude of the signal, ω is the angular frequency, $\varepsilon_a(k), \varepsilon_b(k), \varepsilon_c(k)$ are the noise terms, T is the sampling interval, k is the sampling instant, ϕ is the phase of fundamental component. The complex form of signal derived from the three-phase voltages is obtained by transform as mentioned below

$$v_\alpha(k) = \sqrt{\frac{2}{3}}(v_a(k) - 0.5v_b(k) - 0.5v_c(k))$$

$$v_\beta(k) = \sqrt{\frac{2}{3}}(0.866v_b(k) - 0.866v_c(k)) \tag{2.25}$$

A complex voltage can be obtained from above equation (2.25) as follows

$$v(k) = v_\alpha(k) + jv_\beta(k) = \sqrt{\frac{3}{2}} V_m e^{j(\omega kT + \phi)}$$

$$= Ae^{j(\omega kT + \phi)} + \varepsilon(k)$$

(2.26)

where A is the amplitude of the signal and ε_k is the noise component.

Taking the states x_1 and x_2 as

$$x_1(k) = e^{j\omega kT} = \cos k\omega T + j \sin k\omega T$$

(2.27)

$$x_2(k) = Ae^{j(\omega kT + \phi)}$$

(2.28)

The observation signal v_k can be modeled in a state space form as

$$\begin{bmatrix} x_1(k+1) \\ x_2(k+1) \end{bmatrix} = \begin{bmatrix} 1 & 0 \\ 0 & x_1(k) \end{bmatrix} \begin{bmatrix} x_1(k) \\ x_2(k) \end{bmatrix}$$

(2.29)

$$y(k) = v(k) = \begin{bmatrix} 0 & 1 \end{bmatrix} \begin{bmatrix} x_1(k) \\ x_2(k) \end{bmatrix} + \varepsilon(k)$$

(2.30)

From equation (2.19) one can obtain

$$H = \begin{bmatrix} 0 & 1 \end{bmatrix}$$

(2.31)

Then RLS algorithm is applied to the above system equations (2.4) to (2.7).After the convergence of state vector is attained, the frequency is calculated from equation (2.27) as

$$\sin(\hat{\omega} kT) = \text{Im}(\hat{x}_1)$$

$$\hat{\omega} kT = \sin^{-1}(\text{Im}(\hat{x}_1))$$

$$\hat{f}(k) = \frac{1}{2\pi T}(\sin^{-1}(\text{Im}(\hat{x}_1)))$$

(2.32)

where $\omega = 2\pi f$

$\hat{f}$ is the estimated frequency of the signal

where Im () stands for the imaginary part of a quantity.

2.4.2 Extended Least Square (ELS) approach for frequency estimation:

After study on RLS applied to frequency estimation subsequently ELS has been applied for frequency estimation with a view to achieve better frequency estimation and easier computation due to lack of calculation of gain vector. Same model as described in RLS is used for the estimation of frequency using ELS. Unknown parameters in this case are estimated using equations (2.13) and (2.14). After estimation of unknown parameter, frequency is estimated using equation (2.32)

2.4.3 Kalman Filtering (KF) application to frequency estimation:

Kalman Filter [13, 14, 39-42] is a stochastic state estimator for parameter estimation. The discretized voltage signal as described in 2.4.1 is considered. Equations (2.24) to (2.31) describe observation plant model. Then applying Kalman Filtering algorithm to the above model i.e. using equations (2.13) to (2.15), unknown parameters are estimated. From the unknown parameter vector, frequency has been estimated using equation (2.32)

2.4.4 LMS Algorithm application to frequency estimation:

To enhance the convergence characteristics of frequency estimation of a power system signal, Least Mean Square algorithm is used where the formulated structure looks very simple and this algorithm is found to be accurate one under various systems changing condition to estimate correct measure of frequency. The complex voltage signal as expressed in Section 2.4.1 is taken.

The voltage (2.26) can be modeled as

$$\hat{V}_k = V_{k-1}e^{j\omega kT} \tag{2.33}$$

This model is utilized in the proposed frequency estimation algorithm and the scheme that describes the estimation process. The error signal in this case is

$$e_k = V_k - \hat{V}_k \tag{2.34}$$

where V_k is the estimated value of voltage at the kth instant. So Equation (2.33) can be rewritten

as

$$\hat{V}_k = W_k \hat{V}_{k-1} \tag{2.35}$$

$$W_k = e^{j\hat{\omega}_k T} \tag{2.36}$$

where W_k denotes the weight of the voltage signal, $\hat{\omega}$ is the estimated angular frequency. Then W_k is updated using equations (2.20) to (2.22). Frequency is estimated using (2.23).

2.5 Results and Discussions (Three phase distorted signal)

A synthetic signal of 1 p.u amplitude, 50 Hz frequency and 0.5 p.u phase angle is generated in MATLAB platform. Then the algorithms such as RLS, ELS, KF and LMS have been implemented with a sampling time of 1 ms so that sampling frequency becomes 1 kHz which is required for power system signal. A three-phase signal with 1p.u amplitude in each phase is also generated using MATLAB with SNR of 20, 30 and 40 dB respectively. From the complex signal a two-phase signal is generated by $\alpha - \beta$ transformation. The initial covariance matrix $P(0)$ is taken as δI where I is the identity matrix and $\delta > 1$. The observation vector H is taken as $\begin{bmatrix} 0 & 1 \end{bmatrix}$. The frequency estimation has been accomplished using the steps illustrated in the RLS, ELS and KF algorithms in section 2.3(a) to 2.3(c). Similarly for LMS algorithm the complex signal is also generated as that of the method adopted in other three algorithms. The complex weight matrix is updated with the right choice of step size $(\mu = 0.18)$ and initial value of correlation matrix $(R = 0)$. From the complex weight matrix the estimation of frequency is made using equation (2.23). All other parameters used for simulation studies of single phase signal as in Table 2.1 are also taken here. Results of estimating frequency using four different algorithms, namely RLS, ELS, KF and LMS are presented in this section.

2.5.1 Comparison of Estimation performances (RLS, ELS, KF and LMS) at different SNRs. (Three phase signal)

Frequency estimation performances of RLS, ELS, KF and LMS at different SNRs of 20 dB, 30 dB and 40 dB have been compared in figures 2.11 to 2.13. From these figures it is clear that as SNR value increases more accurate estimation in all the cases is achieved know that as SNR value goes on increasing estimation becomes more and more accurate in all the cases but LMS outperforms over other three so far as estimation error in frequency is concerned.
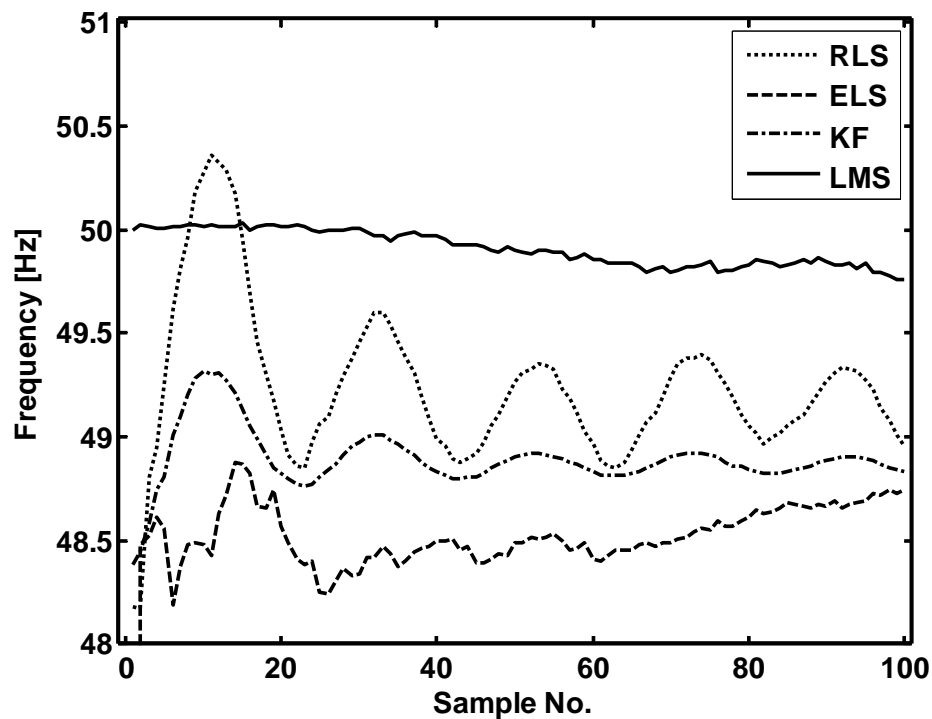
Fig.2.11 LMS estimation performance of Frequency of three phase signal (SNR 20dB)
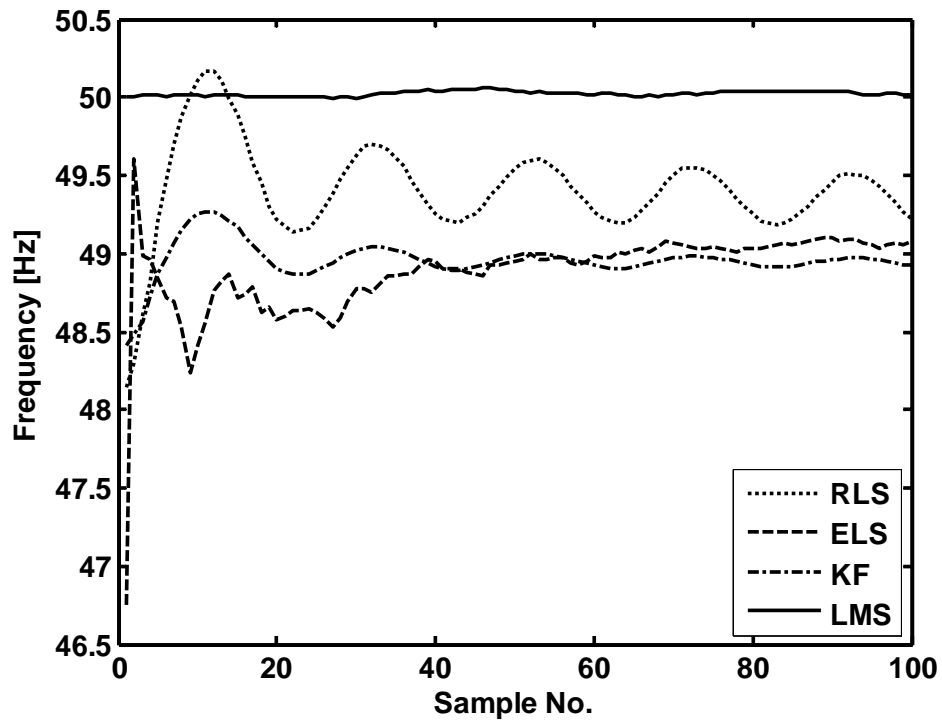
Fig.2.12 LMS estimation performance of Frequency of three phase signal (SNR 30dB)
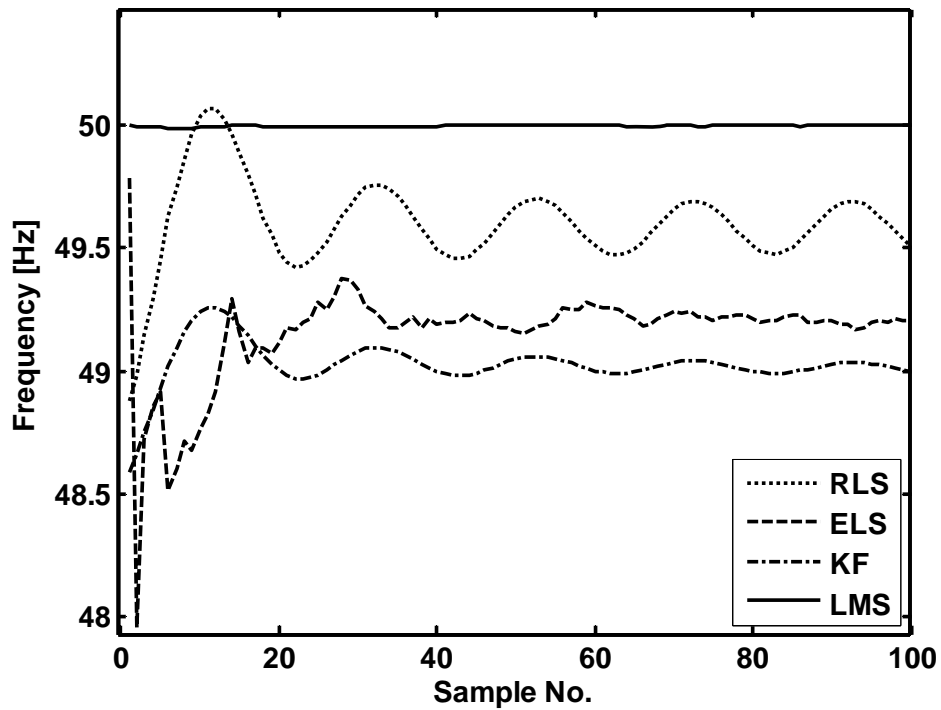
Fig.2.13 LMS estimation performance of Frequency of three phase signal (SNR 40dB)
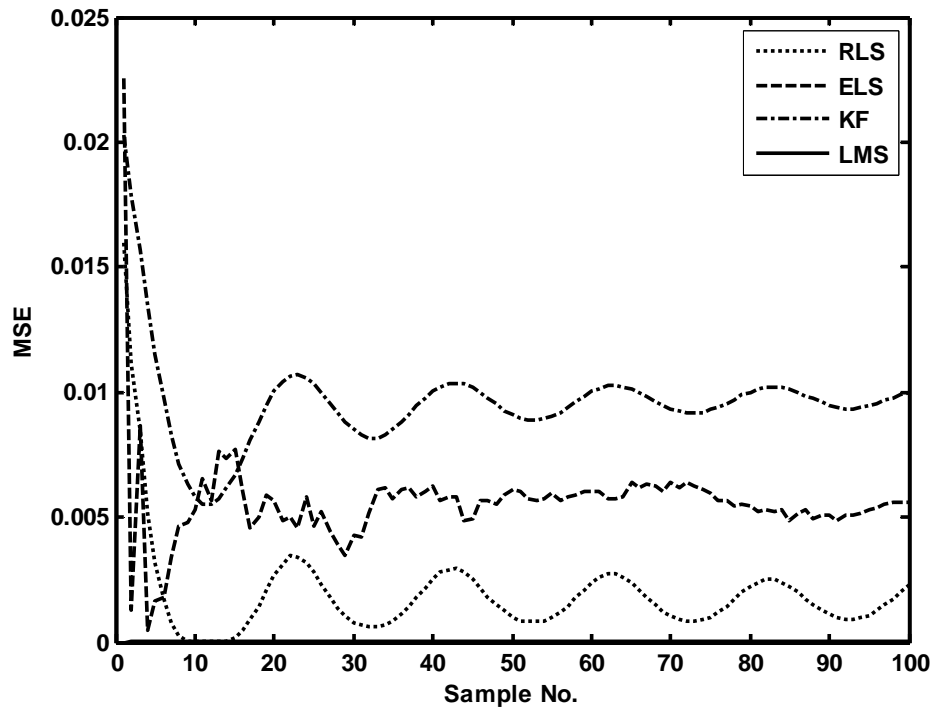
Fig.2.14 LMS estimation performance in MSE of frequency of three phase signal
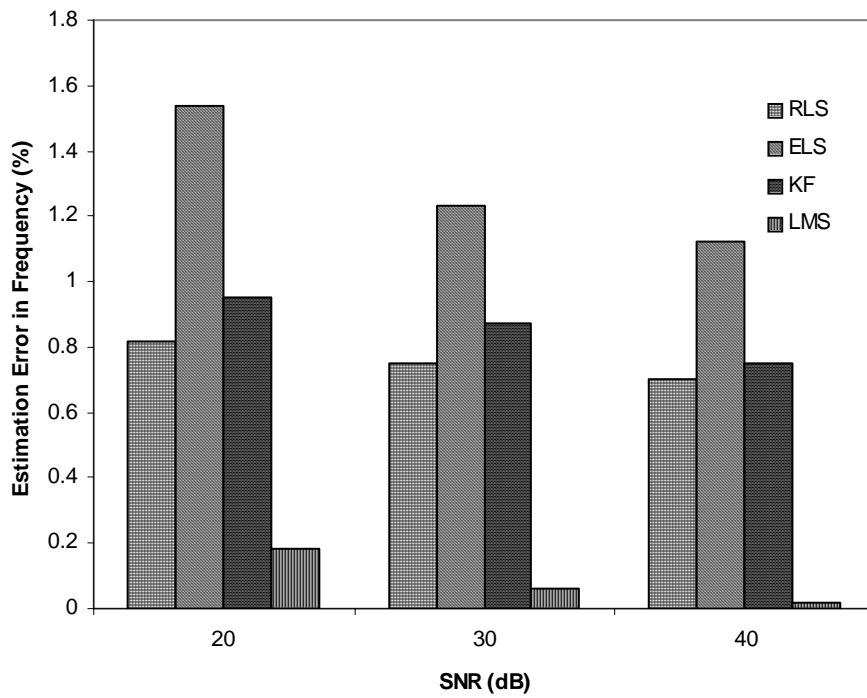
Fig. 2.15 SNR (dB) vs. Estimation error in frequency of three phase signal (%)

Figure 2.14 shows MSE in the estimation of frequency of signal at SNR 40 dB. It is found from the figure that maximum MSE in case of RLS, ELS and KF with noise is of the order of 10^{-2}. But MSE, in case of LMS algorithm, converges to zero over the samples. Hence in this case also LMS outperforms over other three algorithms (RLS, ELS and KF). Fig. 2.15 gives the comparison of estimation errors obtained using different algorithms.

2.5.2 Estimation performance comparison during sudden frequency change at SNRs (20dB, 30 dB and 40 dB) (Three phase signal)

Figures 2.16, 2.17 and 2.18 show the estimation of power system frequency with a jump in frequency of 50 to 49 Hz at 20th sample of the signal by using all the four algorithms with SNR of 20, 30 and 40 dB respectively. In case of estimation using RLS, ELS and KF, there are oscillations. LMS algorithm estimates frequency accurately with very less estimation error (0.02%) in case of jump, but within few initial samples (having very less tracking time) its estimation of frequency value rises to 50 Hz. It is found from the figures that as SNR value increases, accuracy in estimation improves.
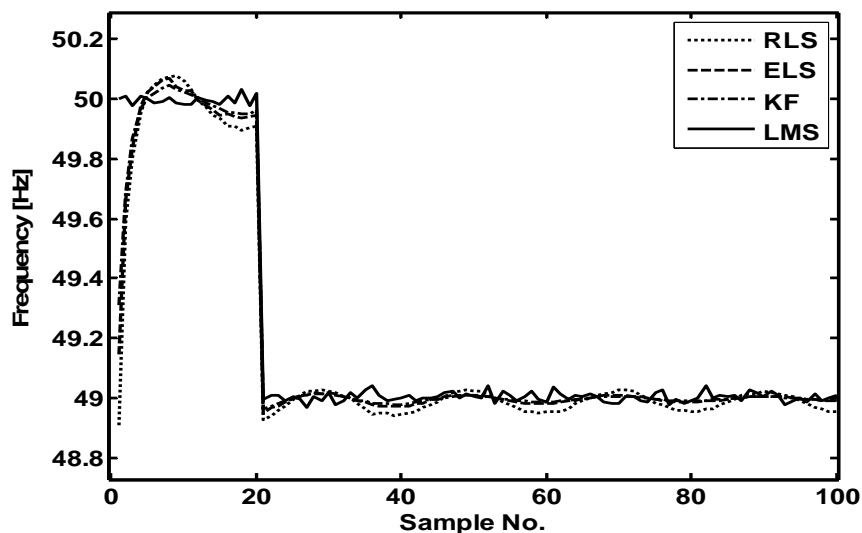
Fig.2.16 LMS estimation performance during sudden frequency change of 49 Hz from 50Hz of three phase signal (SNR 20dB)
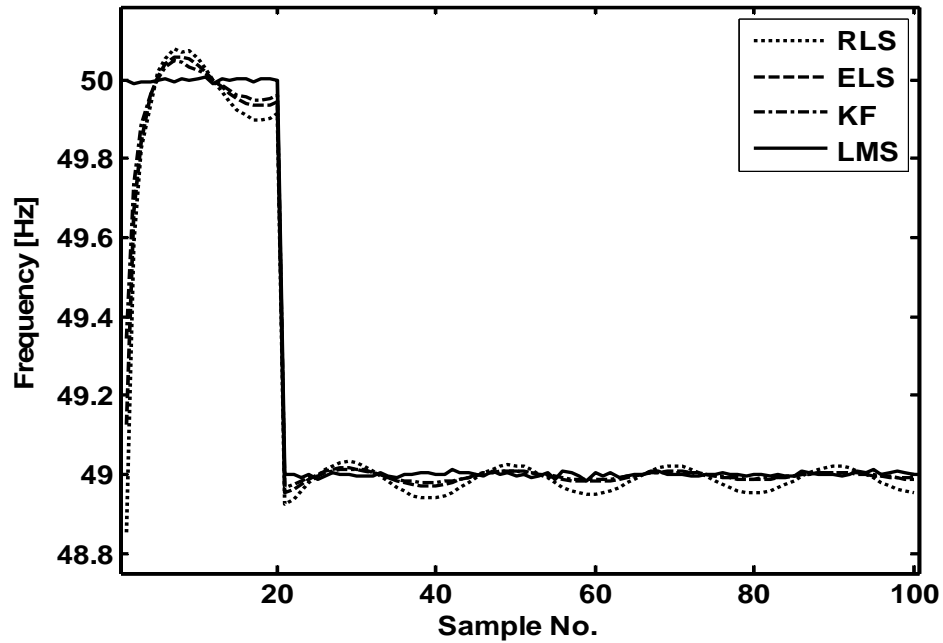
Fig.2.17 LMS estimation performance during sudden frequency change of 49 Hz from 50Hz of three phase signal (SNR 30dB)
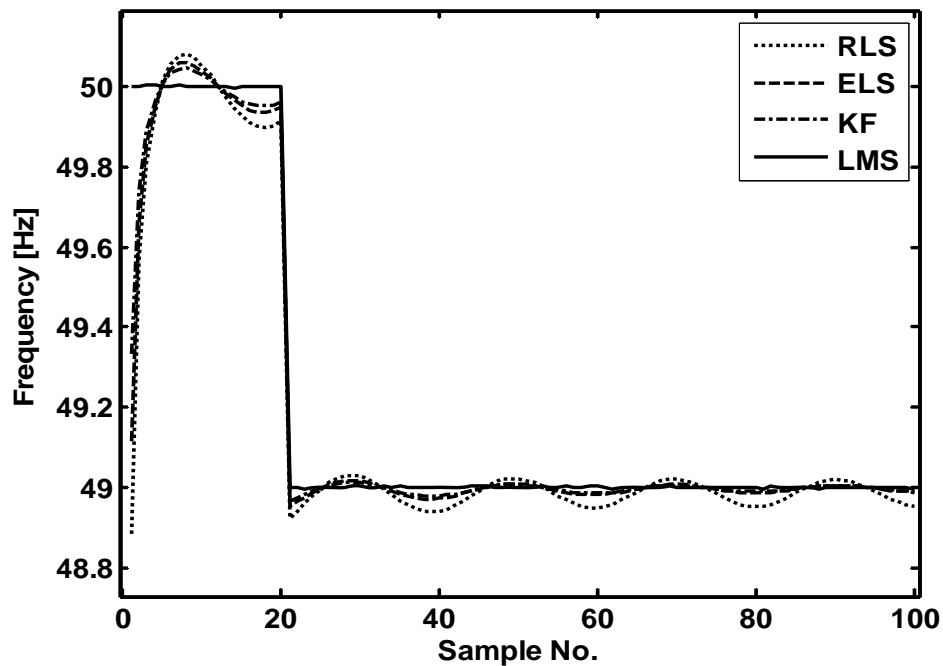
Fig.2.18 LMS estimation performance during sudden frequency change of 49 Hz from 50Hz of three phase signal (SNR 40dB)

2.6 Proposed VLLMS Algorithm

Least Mean Square algorithm [1], which is discussed in previous section of chapter 2, is adopted where the formulated structure looks very simple and this algorithm is found accurate under various systems changing condition to estimate correct measure of frequency. The LMS technique as cited possesses the advantages of simplicity in its underlying structure, computational efficiency, and robustness. However, such an algorithm suffers the problem of poor convergence rate as the adaptation step-size is fixed [1]. In case of LMS algorithm, since step size depends inversely on input power, when step size is small, it takes more time to learn about it's input with minimum mean square error and vice versa. So it suffers the problem of poor convergence rate as the adaptation step-size is fixed and estimation error is more. To overcome this, time varying step-size is usually employed in the standard LMS algorithm [4]. In the proposed method both leakage factor and step size are updated for more accuracy and less computational burden in the estimation. A Variable Leaky LMS algorithm [7] has faster convergence and less computational burden. It can be seen that the algorithm converges much slower along the worst-case eigen direction (the direction of the eigenvector corresponding to the smallest eigen value of auto correlation matrix) as opposed to the best-case eigen direction (the direction of the eigenvector corresponding to the largest eigen value). This disparity increases as the eigen value spread $\lambda max/\lambda min$ increases. Thus, the key step in improving the transient performance of LMS lies in decreasing the input eigen value spread.

In this chapter, a Variable Leaky LMS (VLLMS) [7], [9], [11] based frequency estimation technique is proposed which uses three-phase voltages. A complex signal is derived from the three-phase voltages using $\alpha - \beta$ transformation [1]. As the signal in the model is complex, the Variable Leaky LMS algorithm applied is in complex form. Then proposed algorithm is implemented to find out the frequency of that signal. At different SNR, frequency of signal is estimated using the proposed algorithm. The proposed algorithm is implemented to estimate the frequency during sudden change in frequency of signal, in case of the presence of harmonics, sub and inter-harmonics in the signal. Frequency estimation of real data generated from the laboratory experiment is carried out. Finally, frequency estimation of the industrial data collected from generator terminals of an Aluminium industry is also implemented. In all cases

of estimation, the performance of the proposed algorithm is compared with that of LMS and VSS-LMS algorithms. Apart from the contributions of the chapter as cited above, one vital contribution of the chapter is the parameter drifting that does not allow the estimated values beyond limit gives advantage in implementing other correcting circuitry based on the estimator.

2.6.1 Description on VLLMS algorithm

The basic block-diagram representation of an adaptive linear filtering scheme is shown in Fig. 2.19. The linear filter is given by

$$y_n = w_n^T x_n ,$$
(2.37)

where the subscript n represents the discrete time-instant, $x_n \in \mathfrak{R}^m$ is the input to the filter and $w_n \in \mathfrak{R}^m$ is the filter gain that maps the input to the output $y_n \in \mathfrak{R}$, which is required to be matched with a desired value d_n. The objective is to tune w_n in such a way that the error

$$e_n = d_n - y_n ,$$
(2.38)

or a suitable function of it converges to certain optimal value.

Several adaptive algorithms are available in literature for tuning w_n. A conventional one is the LMS one in which the updation is executed such that an instantaneous cost function defined as

$$J_n = e_n^2$$
(2.39)

converges to zero. However, use of such a cost function does not take care of the drifting of w_n in presence of external disturbances resulting in high filter gains. This problem can be overcome by considering the Leaky LMS algorithm in which the cost function (2.39) is modified as

$$J_n = e_n^2 + \gamma w_n^T w_n ,$$
(2.40)

where $0 \leq \gamma < 1$ is to be chosen so as to avoid the parameter drifting. The additional term in (2.40), $w_n^T w_n$, is known as the regularization component of it. Note that, selecting a constant γ may lead to over/under-parameterization of this regularization component. One way to avoid this is by using a variable γ, updation of which may be governed by a suitable cost function.
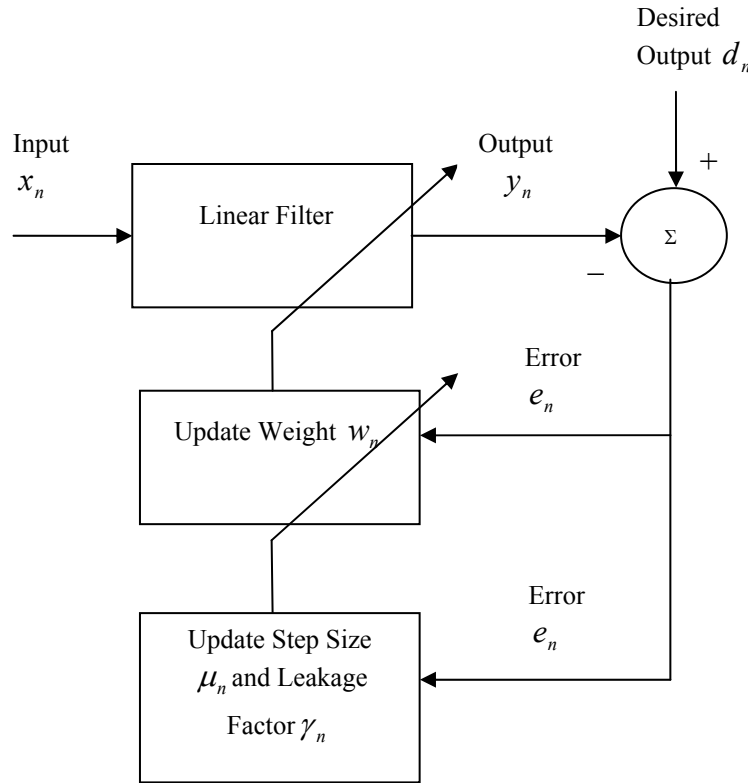
Fig. 2.19 The Adaptive Linear Estimation Scheme

This way, the cost function may further be modified from (2.40) as

$$J_n = e_n^2 + \gamma_n w_n^T w_n .$$

(2.41)

The above cost function is used for updating w_n in the VLLMS algorithm.

Now, one may try to define the adaptive laws for updating w_n and γ_n. First, for updating w_n, following the classical steepest descent rule, one may write

$$w_{n+1} = w_n - \mu \frac{\partial J_n}{\partial w_n} ,$$

(2.42)

where $\mu > 0$ is a step-size parameter to be chosen by the designer. Obviously, choosing a constant μ puts same weight on the correction term throughout the estimation process that may endure the convergence of the algorithm. Alternatively, for achieving faster convergence, one may use larger μ initially when the error is large and smaller one when the estimator has converged around its optimal values. This feature may be incorporated using a variable step-

size updatation scheme for μ that yields a faster convergence [4]. Incorporating this, (2.42) may be modified as:

$$w_{n+1} = w_n - \mu_n \frac{\partial J_n}{\partial w_n},$$
(2.43)

where μ_n is a variable step-size parameter and may be updated following [4] as:

$$\mu_{n+1} = \lambda\mu_n + \gamma_n e_n^2$$
(2.44)

Further, since we will be using this estimator for power system frequency estimation and it is well known that the desired signal d_n in our problem formulation (described in next section) may contain noises arising out from measurement or process disturbances, it will be better to incorporate a robust variable step-size algorithm of [5] rather than (2.44) that takes care of the effect of the external disturbances in the step-size update. To have such a facility, updatation of μ_n is required to utilize the autocorrelation of the error rather than the exact square of error value. Then (2.44) may be modified as:

$$\mu_{n+1} = \lambda\mu_n + \gamma_n p_n^2,$$
(2.45)

where p_n represents autocorrelation of e_n and that can be computed for an ergodic process by using a time average of it that can be computed following [1] as:

$$p_n = \beta p_{n-1} + (1-\beta)e_n e_{n-1}$$
(2.46)

Now, we are ready to obtain the final updatation equations for w_n and γ_n. For this, in view of (2.38), one may write

$$e_n^2 = d_n^2 + \left(w_n^T x_n\right)^2 - 2d_n w_n^T x_n.$$
(2.47)

From the above, one obtains

$$\frac{\partial e_n^2}{\partial w_n} = 2\left(w_n^T x_n - d_n\right)x_n = -2e_n x_n.$$
(2.48)

Using (2.41) in (2.43) and then using (2.48) in that, one obtains the corresponding update law as

$$w_{n+1} = (1 - 2\mu_n\gamma_n)w_n + 2\mu_n e_n x_n$$
(2.49)

Next, to update γ_n, one may use the same steepest descent rule but with the cost function (2.39) since the parameter drift of w_n is no more required to be controlled. Hence, one may use the update law as

$$\gamma_{n+1} = \gamma_n - \frac{\rho}{2} \frac{\partial e_n^2}{\partial \gamma_{n-1}} , \tag{2.50}$$

where $\rho > 0$ is also to be chosen by the designer. The derivative term in (2.50) may further be

rewritten as

$$\frac{\partial e_n^2}{\partial \gamma_{n-1}} = \left[\frac{\partial e_n^2}{\partial w_n} \right]^T \frac{\partial w_n}{\partial \gamma_{n-1}} . \tag{2.51}$$

Using (2.49), one may write

$$\frac{\partial w_n}{\partial \gamma_{n-1}} = -2 \mu_n w_{n-1} . \tag{2.52}$$

Substituting (2.48) and (2.52) into (2.51), and that in (2.50), one finally obtains

$$\gamma_{n+1} = \gamma_n - 2\mu_n \rho e_n x_n^T w_{n-1} . \tag{2.53}$$

This completes the VLLMS algorithm. The next section presents a formulation of the frequency

estimation problem in the above framework.

2.6.2 VLLMS based Frequency Estimation

The discretized voltage signal described in previous chapter can be represented as

$$V_{an}(k) = V_m \cos(\omega nT + \phi) + \varepsilon_{an}(k)$$

$$V_{bn}(k) = V_m \cos(\omega nT + \phi - \frac{2\pi}{3}) + \varepsilon_{bn}(k) \tag{2.54}$$

$$V_{cn}(k) = V_{mn} \cos(\omega nT + \phi + \frac{2\pi}{3}) + \varepsilon_{cn}(k)$$

where V_{an}, V_{bn}, V_{cn} are the voltages of the three phases at the nth instant, V_m is the maximum

amplitude of the signal, ω is the angular frequency, T is the sampling interval, ϕ is the phase of

fundamental component and $\varepsilon_{an}, \varepsilon_{bn}, \varepsilon_{cn}$ are uncorrelated noises in the respective phases.

The three-phase voltage (2.54) may be transformed to a complex quantity as

$$V_n = V_{\alpha n} + j V_{\beta n} , \tag{2.55}$$

by using the well-known α-β transformation [1], where

$$V_{\alpha n} = \sqrt{\frac{2}{3}}\left(V_{an} - 0.5V_{bn} - 0.5V_{cn}\right) \Bigg\}$$
$$V_{\beta n} = \sqrt{\frac{2}{3}}\left(0.866V_{bn} - 0.866V_{cn}\right) \Bigg\} \qquad (2.56)$$

Replacing nominal voltages from (2.54) into (2.56), one obtains

$$V_{\alpha n} = \sqrt{\frac{3}{2}}V_m \cos(\omega nT + \phi)$$
$$V_{\beta n} = \sqrt{\frac{3}{2}}V_m \sin(\omega nT + \phi) \qquad (2.57)$$

Therefore, following (2.55), V_n may alternatively be represented using the Euler's formula as

$$V_n = \sqrt{\frac{3}{2}}V_m e^{j(\omega nT + \phi)}. \qquad (2.58)$$

Using a cumulative noise term ε_n, a discretized model of (2.58) may easily be written as

$$V_n = e^{j\omega T}V_{n-1} + \varepsilon_n. \qquad (2.59)$$

Now, let $\hat{V}_n$ be the estimate of V_n. Then, following (2.59) and considering $\hat{\omega}_n$ be the estimate of ω at the nth instant one may write a linear filter corresponding to (2.37) as:

$$\hat{V}_n = W_n \hat{V}_{n-1}, \qquad (2.60)$$

where $W_n = e^{j\hat{\omega}_n T}$. The error signal corresponding to (2.38) may then be defined as

$$e_n = V_n - \hat{V}_n \qquad (2.61)$$

In the above model, the input of the filter, i.e. $\hat{V}_{n-1}$ and the weight vector W_n both are complex. The VLLMS algorithm presented in Section 3.2 may now be applied in complex form to estimate the frequency.

The algorithm minimizes the squared of the error by recursively altering the complex weight vector W_n at each sampling instant. In (3.13) section 2.3 replacing w by W and x_n by V_n^*, W_n can be updated as

$$W_{n+1} = (1 - 2\mu_n \gamma_n)W_n + 2\mu_n e_n V_n^* \qquad (2.62)$$

where μ is constant step size , μ_n is variable step size and $*$ represents the complex conjugate of that value and the variable step size μ_n is varied [4] for better convergence of the VL-LMS algorithm in the presence of noise. For complex states, the equation (2.45) becomes

$$\mu_{n+1} = \lambda\mu_n + \gamma_n P_n P_n^* \qquad (2.63)$$

where P_n represents the autocorrelation of e_n and e_{n-1}, where e_n and e_{n-1} are the errors at n th

and $(n-1)$ th instant and P_n is computed as [1]

$$P_n = \beta P_{n-1} + (1-\beta)e_n e_{n-1} \qquad (2.64)$$

β : exponential weighting parameter($0 < \beta < 1$)

λ : constant $(0 < \lambda < 1)$

γ : control the convergence time $(\gamma > 0)$

In (2.53) section 2.3, replacing $x_n{}^T$ by $\hat{V}_n$ and w_{n-1} by W_{n-1}. The variable leakage factor γ_n can be adjusted as

$$\gamma_{n+1} = \gamma_n - 2\mu_n \rho e_n \hat{V}_n W_{n-1} \qquad (2.65)$$

μ_{n+1} is set to μ_{max} or μ_{min} when it falls below or above the lower and upper boundaries, respectively. These values are chosen based on signal statistics. At each sampling interval, we

can estimate the frequency from the updated value of W_n i.e $W_n = e^{j\hat{\omega}_n T}$ as

$$\sin(\hat{\omega}_n T) = \mathrm{Im}(W_n)$$

$$f_n = \frac{1}{2\pi T}\sin^{-1}\left[\mathrm{Im}(W_n)\right] \qquad (2.66)$$

A flow chart of the above algorithm is presented in Fig. 2.20 for convenience in implementation.
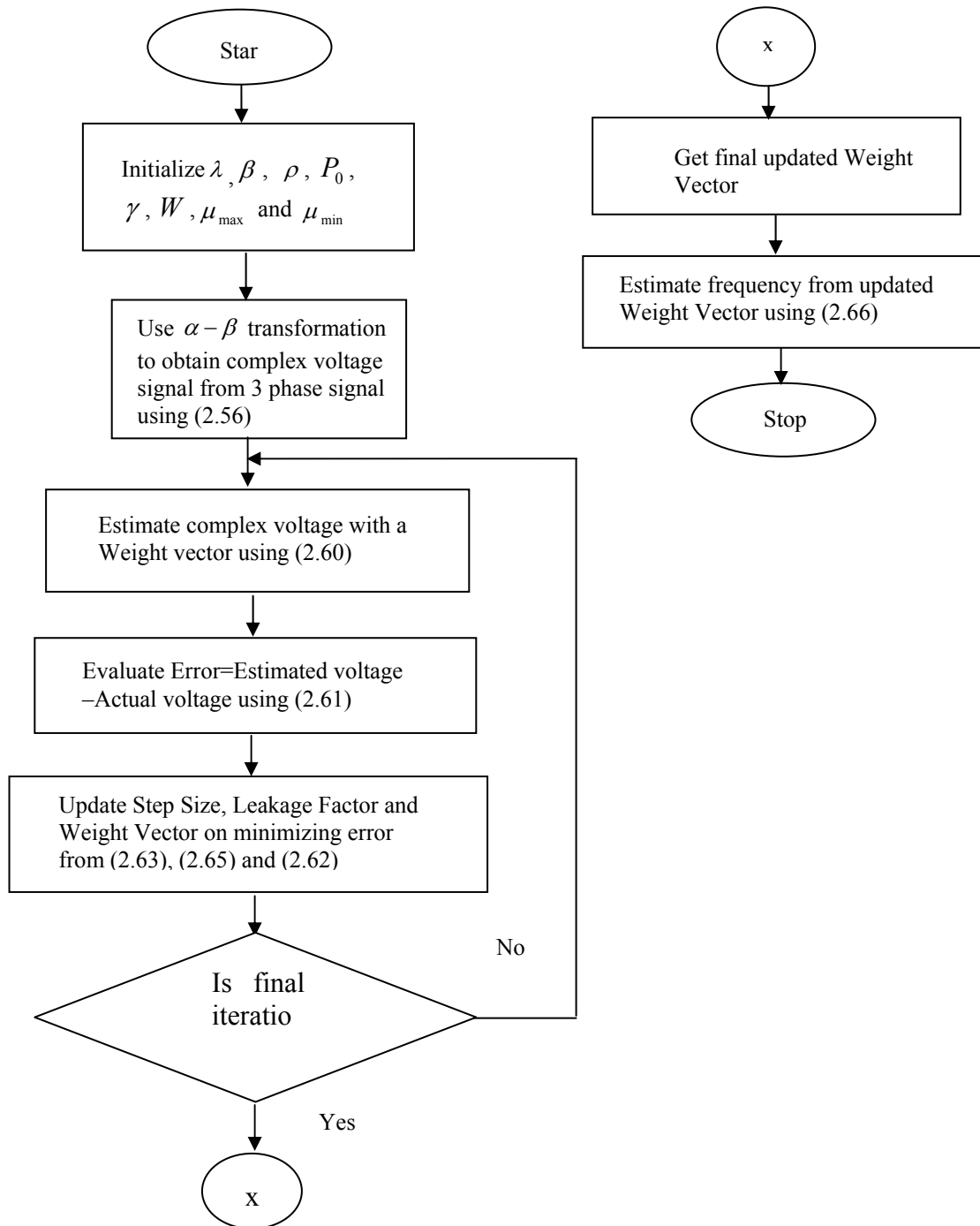
Fig. 2.20 Flow chart of the Estimation Scheme of VLLMS algorithm

2.7 Simulation Results (Frequency Estimation using VLLMS Algorithm)

2.7.1 Sinusoidal Signal in presence of noise

To have a simulation, note that, one first requires setting values of the parameters λ, β and, and the initial values of P_0, γ and W for running the algorithm. Table 2.2 shows the values of parameters taken during simulation. In fact μ_{max} is usually used to ensure that the mean square error (MSE) of the algorithm remains bounded and μ_{min} is used to provide a minimum level of tracking ability [4]. Next, we present the performance of the algorithm in estimating frequency in different simulated cases along with the results obtained using LMS [1] and VSSLMS [4] algorithms. MATLAB-SIMULINK is used for this purpose. For simulation studies we consider different cases of simulated signal that may represent several well-known properties of real-time power system voltage signal. First we start a sinusoidal signal with random noises that may arise due to measurement errors or external disturbances in the system.

Table 2.2
Parameters used for simulation studies (VLLMS)

Parameters	λ	β	ρ	Initial γ	Initial P_0	Initial W	μ_{max}	μ_{min}
Values	0.97	0.99	1.1	0.01	0	0.018	0.008	0.0001
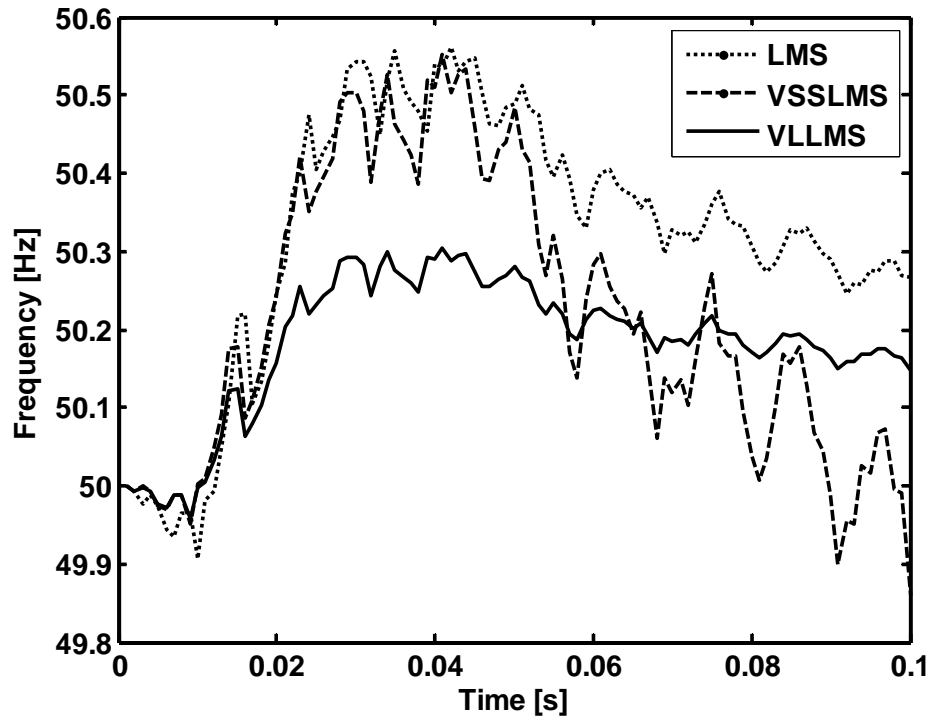
Fig.2.21 VLLMS estimation performance of frequency with noise (SNR 10dB)
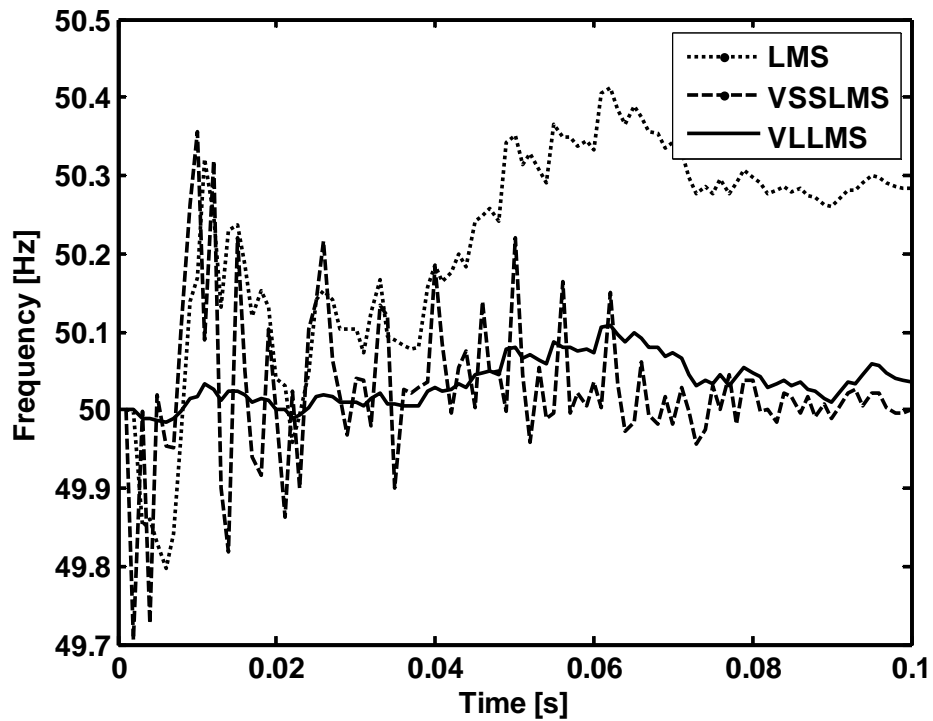
Fig.2.22 VLLMS estimation performance of frequency with noise (SNR 20 dB)
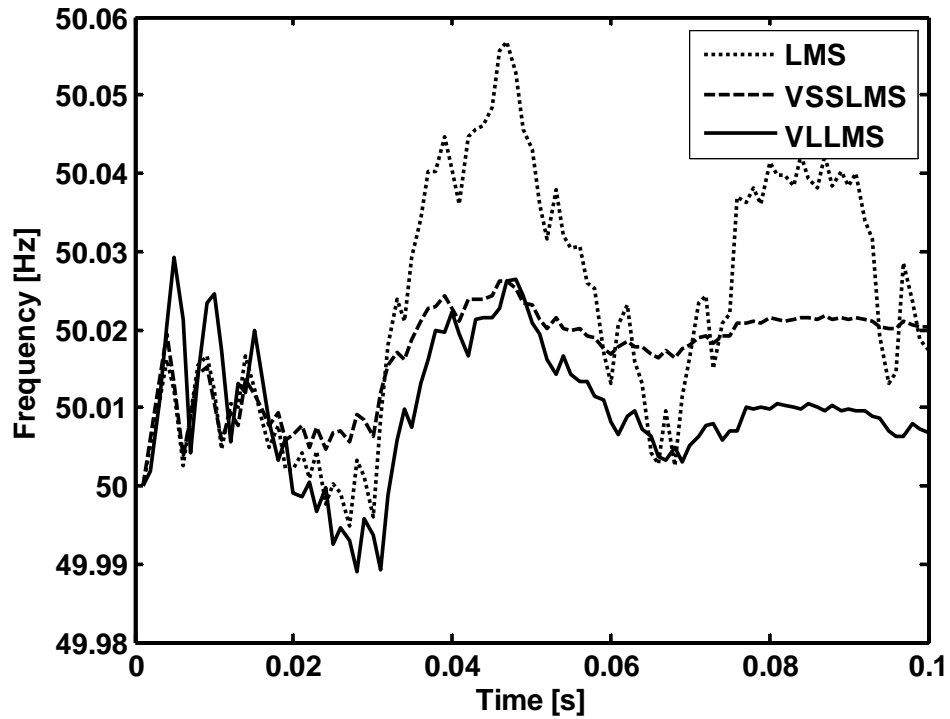
Fig.2.23 VLLMS estimation performance of frequency with noise (SNR 30dB)
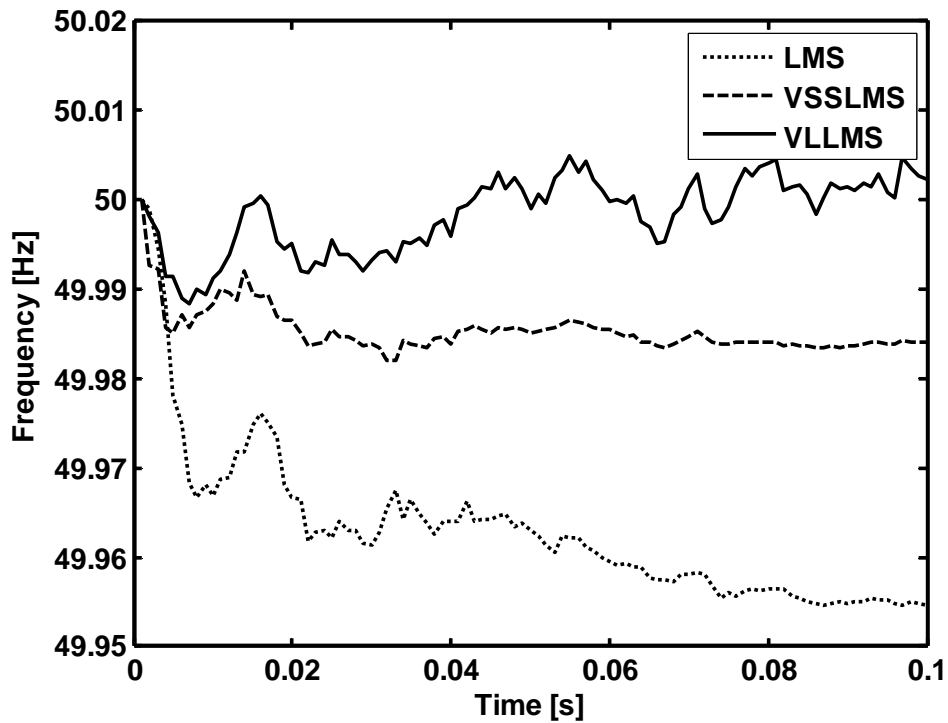
Fig.2.24 VLLMS estimation performance of frequency with noise (SNR 40dB)
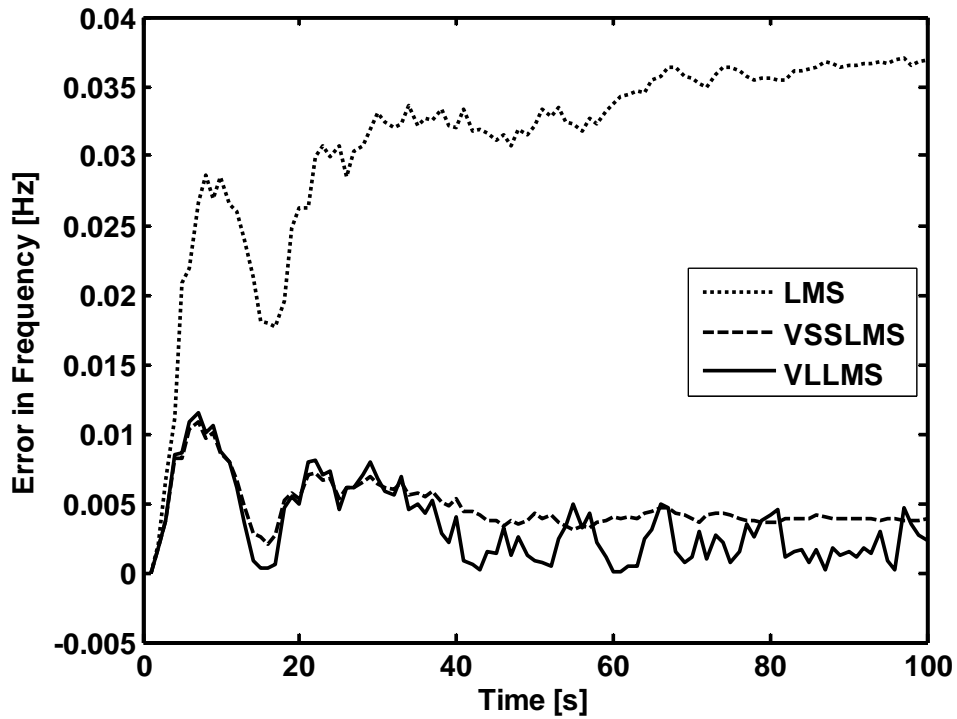
Fig.2.25 Estimation error in Frequency (LMS, VSSLMS and VLLMS)
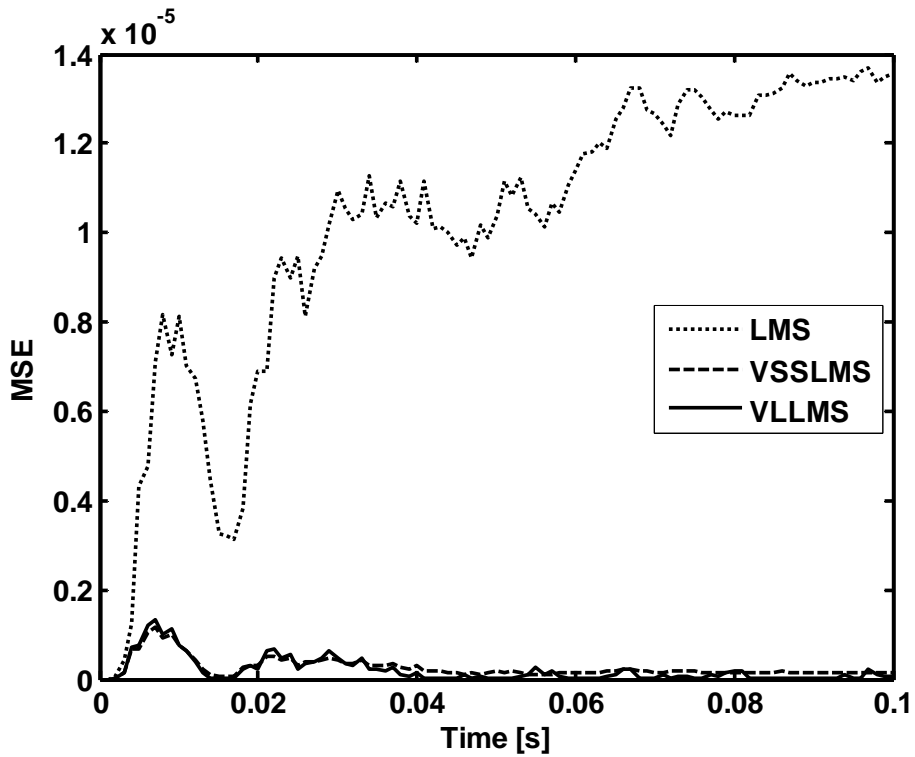
Fig.2.26 Mean Squared Error in estimation of Frequency (LMS, VSSLMS and VLLMS)
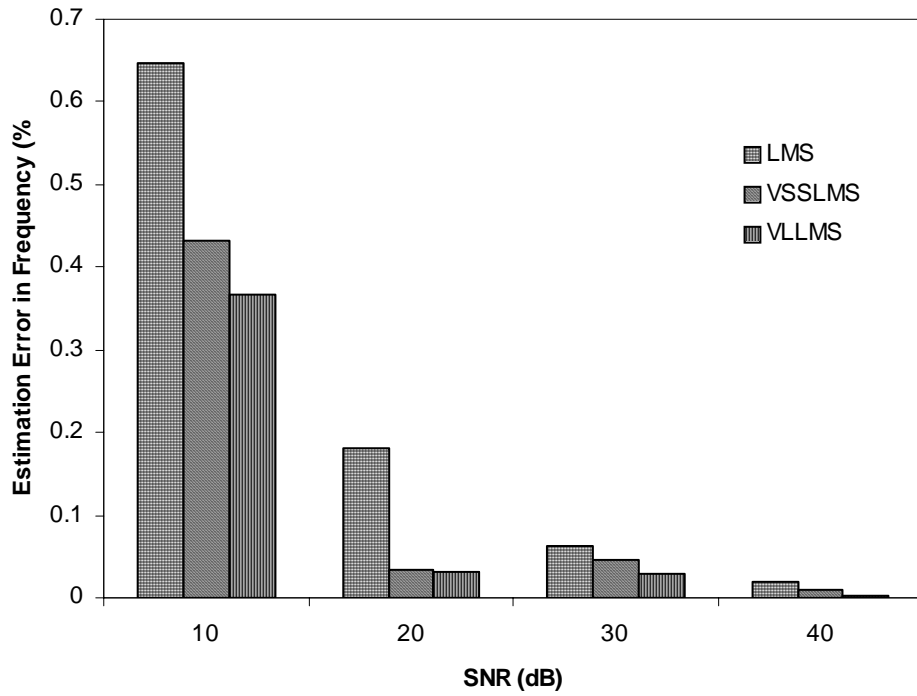
Fig. 2.27 SNR (dB) vs. Estimation error in frequency (%) (LMS, VSSLMS and VLLMS)
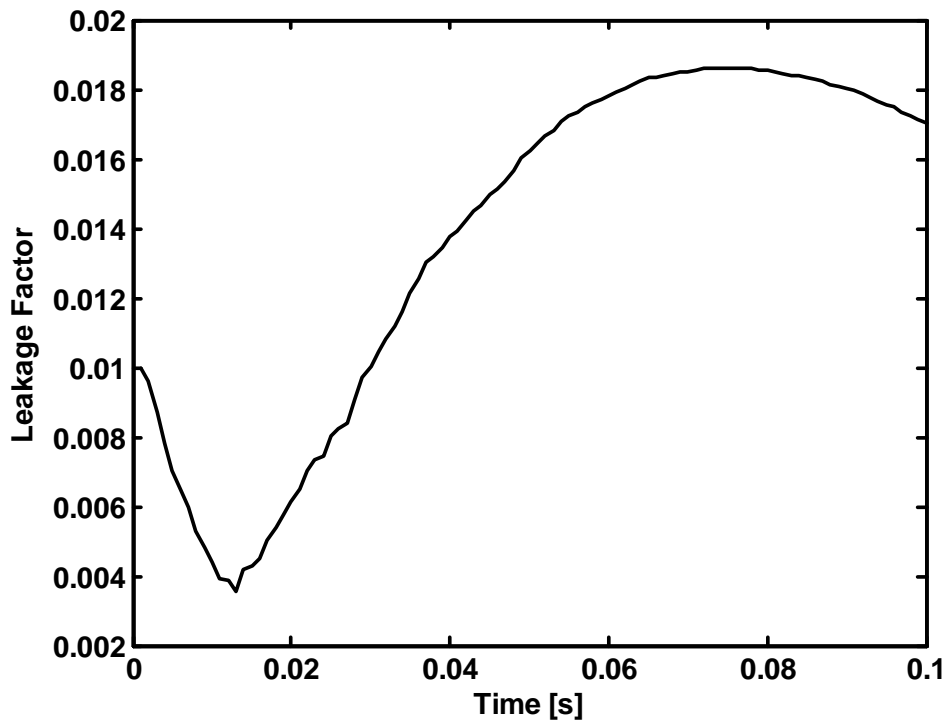
Fig.2.28 Variation of Leakage Factor of VLLMS algorithm

A 50 Hz signal with constant frequency but with random noises is generated with a 1-millisecond sampling interval. The performances of different algorithms for SNRs of 10 dB, 20 dB and 40 dB are shown respectively in Figs. 2.21, 2.22 and 2.23. It is clear that with the increase in signal to noise ratio, there is expectedly more accuracy in the estimation irrespective of the algorithm used. For further analysis, we consider only the 40 dB SNR case since in the other cases the errors using the existing algorithms are quite large. Fig. 2.24 and 2.25 show respectively the error in frequency estimation and its MSE values using different methods. These figures show that the error is minimized in case of the present VLLMS algorithm. Also, we present the estimated voltage signal using different methods, an MSE of which is shown in Fig.2.26. The comparison of estimation error using different algorithms is more clearly shown in Fig. 2.27 using bar charts. It is noted that in case of present algorithm, the estimation accuracy is more as compared to LMS and VSSLMS algorithms. An interesting reader may see the variation of the Leakage factor in Fig. 2.28.

Table 2.3
Comparative Assessment of LMS, VSSLMS and VLLMS Methods

Parameter	LMS	VSSL MS	VLLMS
Frequency	49.7473	49.7682	49.7767
Deviation (%)	1.0044	0.9628	0.9458
Computational time (seconds)	0.3120	0.2970	0.2500

A comparative assessment among these four methods taking into account a 50 Hz signal at SNR of 40 dB is presented in Table-2.3. From this table we conclude that deviation (%) in frequency and computational time are minimum in case of VL-LMS Algorithm also the accuracy in estimation of frequency (49.7767Hz) is more as compared to other three algorithms. The computation time is also less in the VLLMS algorithm compared to others that favor the feasibility of its real time implementation.

2.7.2 Jump in frequency in the signal

The next case is considered to be the performance of the algorithm in presence of jump in frequency (sudden change in frequency of signal). For this, we consider that the frequency changes from 50 Hz to 49 Hz. Two sub cases, one as it changes after the convergence of the algorithm and the other as the change occurs within one cycle. The corresponding results are shown in Figs. 2.29 and 2.30. Note that, in these cases also, the present algorithm outperforms the existing ones.
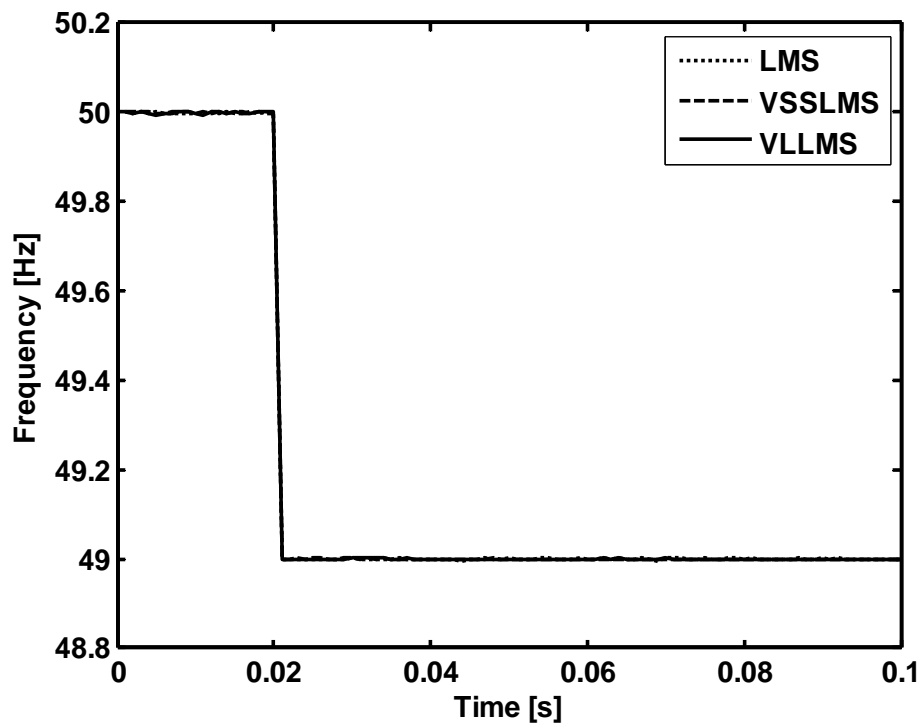
Fig. 2.29 VLLMS estimation performance during sudden frequency change of 49 Hz from 50 Hz (SNR 40 dB)
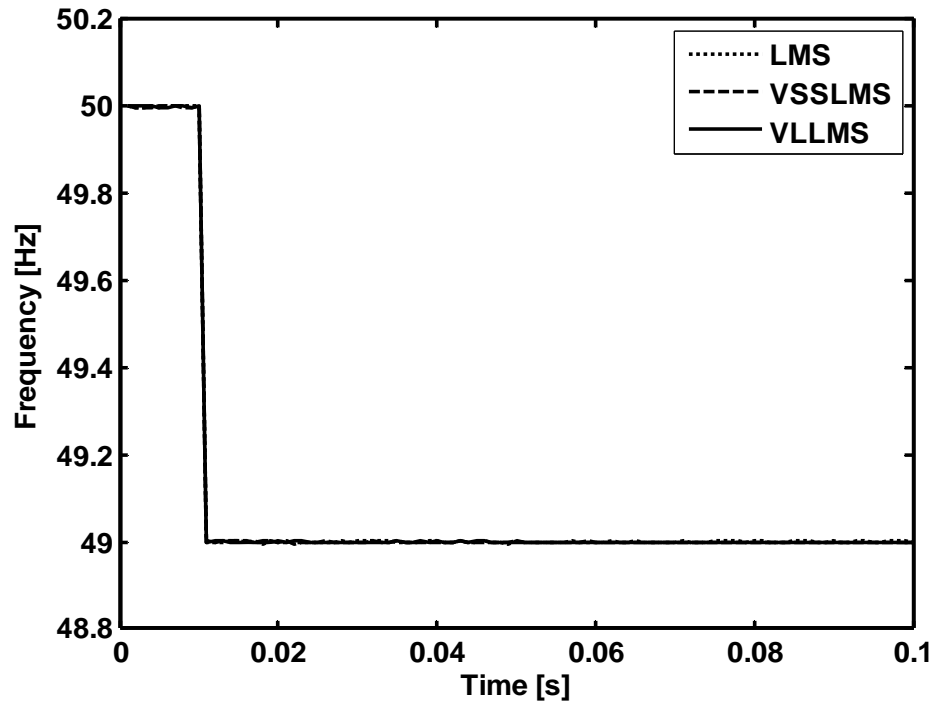
Fig. 2.30 VLLMS estimation performance during sudden frequency change of 49 Hz from 50 Hz within one cycle (SNR 40 dB)

2.7.3 In the presence of Harmonics

Next, we consider the problem of estimating fundamental frequency from signals having harmonics content in them. The common case of 3rd harmonic is considered. Fig. 2.31 shows the three-phase voltage signal containing this harmonic. Fig. 2.32 shows the estimation of frequency using different algorithms from the signal with harmonics. It can easily be concluded that a comparatively better performance is obtained in case of VLLMS algorithm
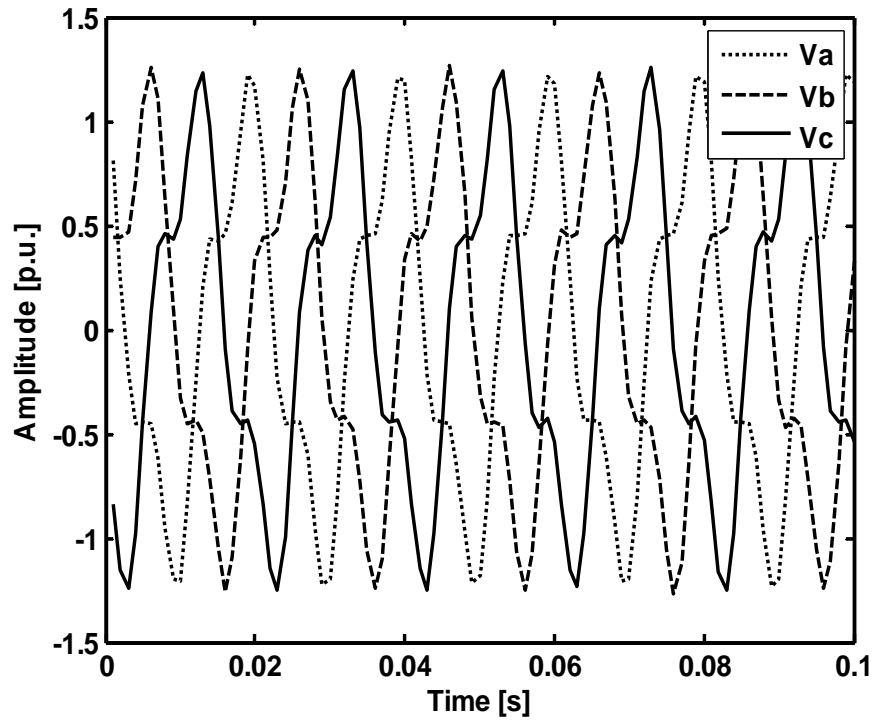
Fig. 2.31 Three phase signal-containing harmonics
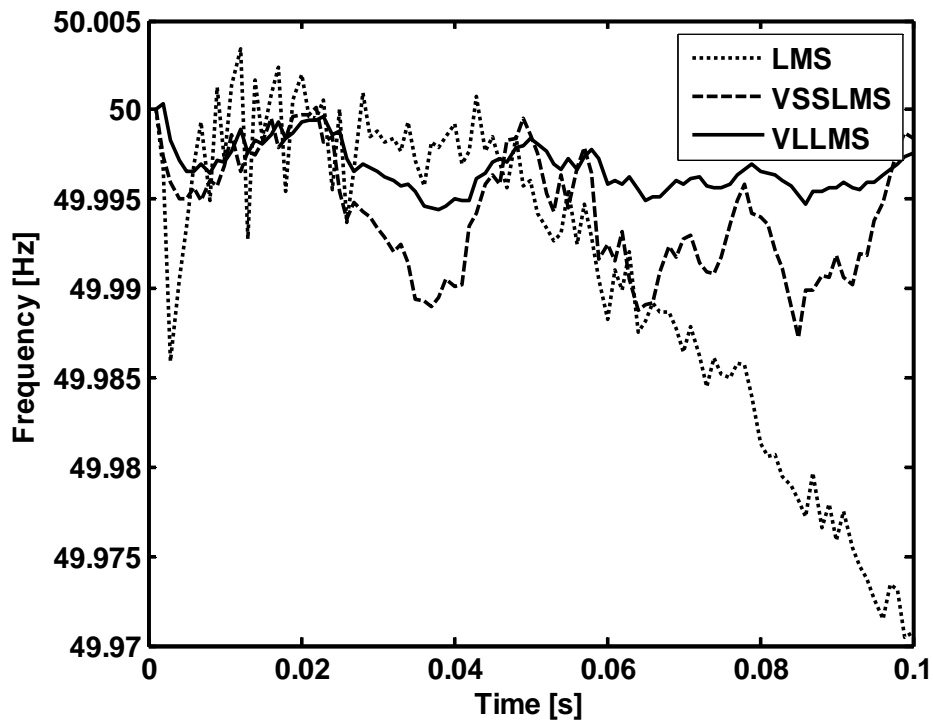
Fig. 2.32 VLLMS estimation performance of frequency in presence of harmonics

2.7.4 In the presence of Sub harmonics and Inter Harmonics

To evaluate the performance of the proposed algorithm in the estimation of a signal in the presence of Sub-harmonics and inter-harmonics, these components are added into the original signal. The frequency of sub-harmonic is 20 Hz, the amplitude is set as 0.5 p.u. and the phase is equal to 75 degrees. The frequency, amplitude and phase of the inter-harmonics is 140 Hz, 0.25 p.u. and 65 degrees respectively. Fig. 2.33 shows the three-phase signal containing sub and inter-harmonics.
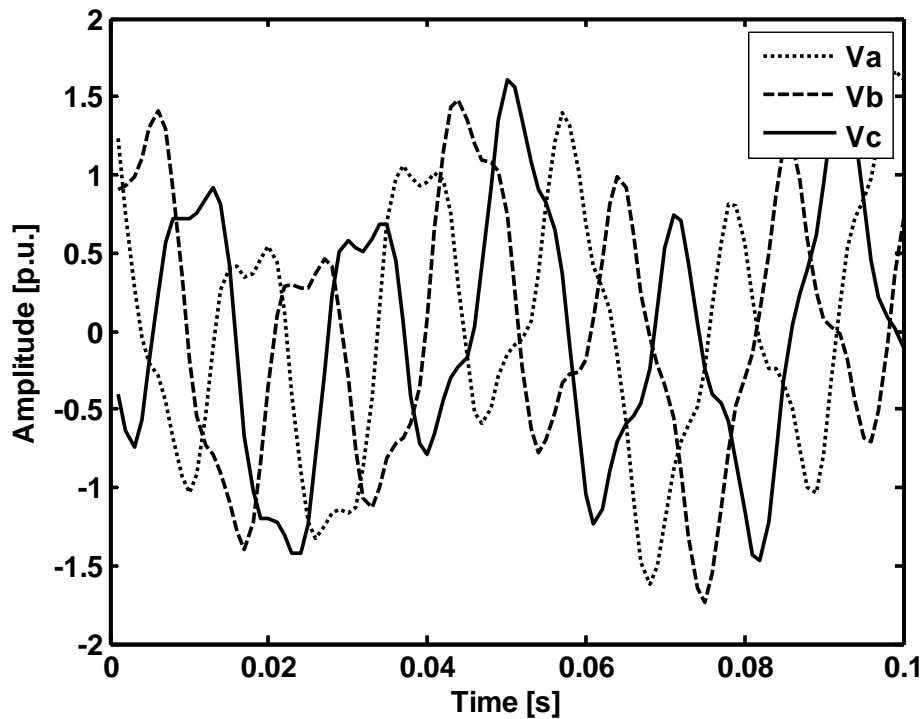
Fig. 2.33 Three-phase signal containing sub and inter harmonics
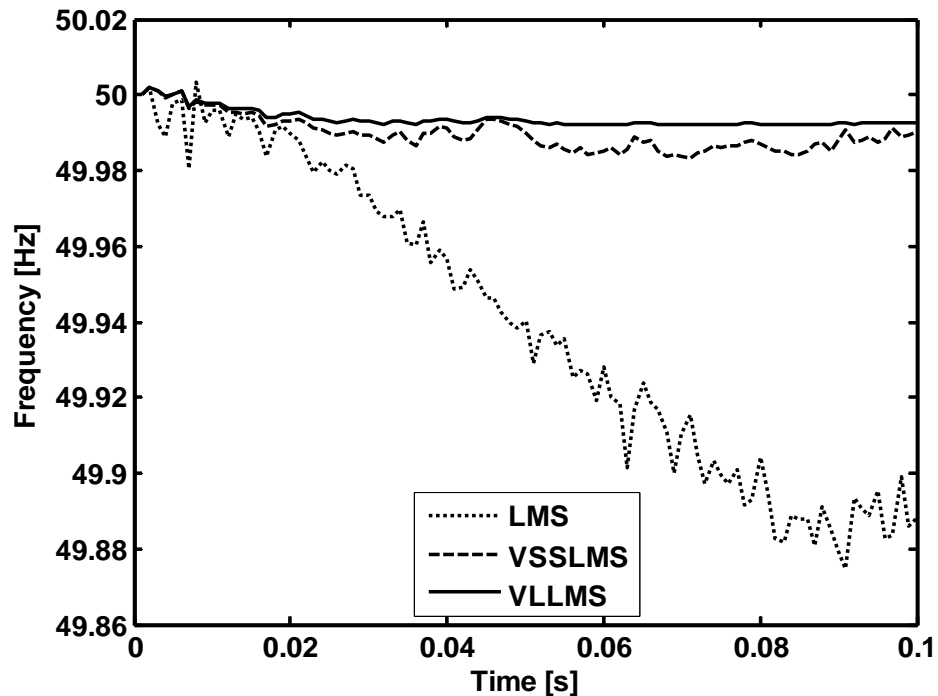
Fig. 2.34 VLLMS estimation performance of frequency in presence of sub and inter harmonics

Fig. 2.34 shows the estimation of fundamental frequency in presence of sub and inter-harmonics and is found that estimation is very much accurate in case of VSS-LMS and VL-LMS algorithm but there is small error in case of LMS algorithm.

2.8 Experimental Studies

So far performances of different algorithms have been studied on simulated signals. It would be interesting to have the same on some experimental data that captures many more features arises due to measurement and instrumentation for obtaining these. This section presents such studies.

2.8.1 Validation on real-time (Laboratory Setup) data

First we consider data collected from a laboratory setup. The data is obtained in laboratory from the supply on normal working day as per the experimental setup shown in Fig. 2.35 and laboratory prototype in Fig. 2.36.

Specifications of the Instruments used are:

1. Rheostats: $100\,\Omega$, 5 A (3 in no.)

2. Non-linear load: 3 Phase diode bridge rectifier with a 5 Ω resistor in series with a 100 mH inductor at the d.c side.

3. Digital Storage Oscilloscope (Make-Falcon): Band Width-25 MHz, Sample rate-100 MS/s, Channels-2, Record length-5000 data points, PC Connectivity- USB Port and PC Communication software.

4. PC: 1.46 GHz CPU and 1GB RAM, Notebook PC

. The voltage waveform is stored in a Digital Storage Oscilloscope and then through PC Communication software, data is acquired to the personal computer. The used PC had a 1.46 GHz CPU and 1GB RAM. The sampling time in this case is fixed at 0.04ms. Comparison of estimated frequency with respect to a 50 Hz constant frequency is shown in Figs. 2.37 and is found that LMS is better compared to the others.
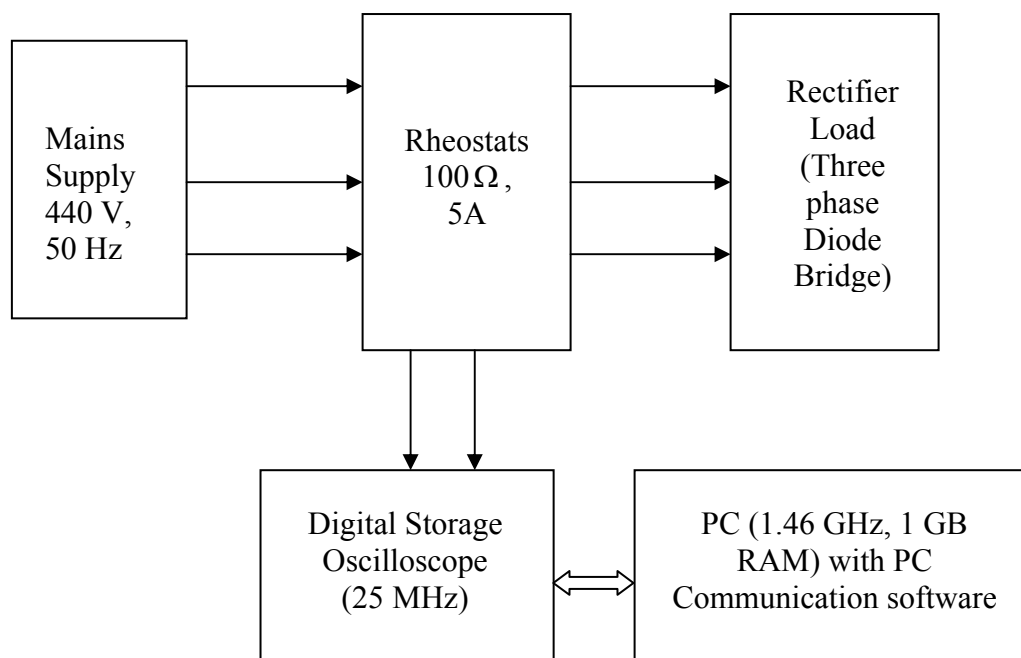
Fig.2.35Experimental setup for online data generation
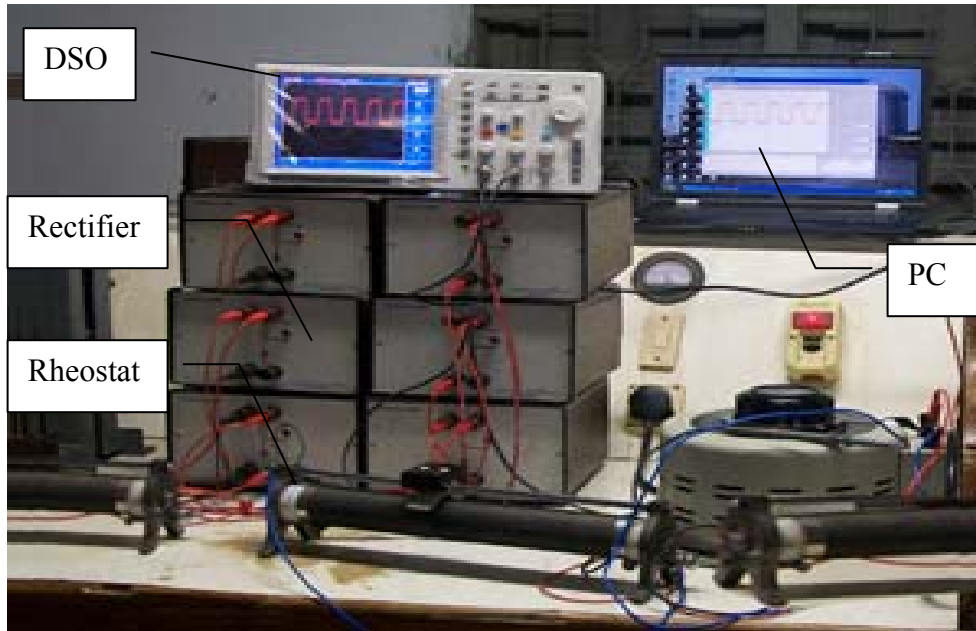
Fig. 2.36 Photograph of laboratory setup for online data generation
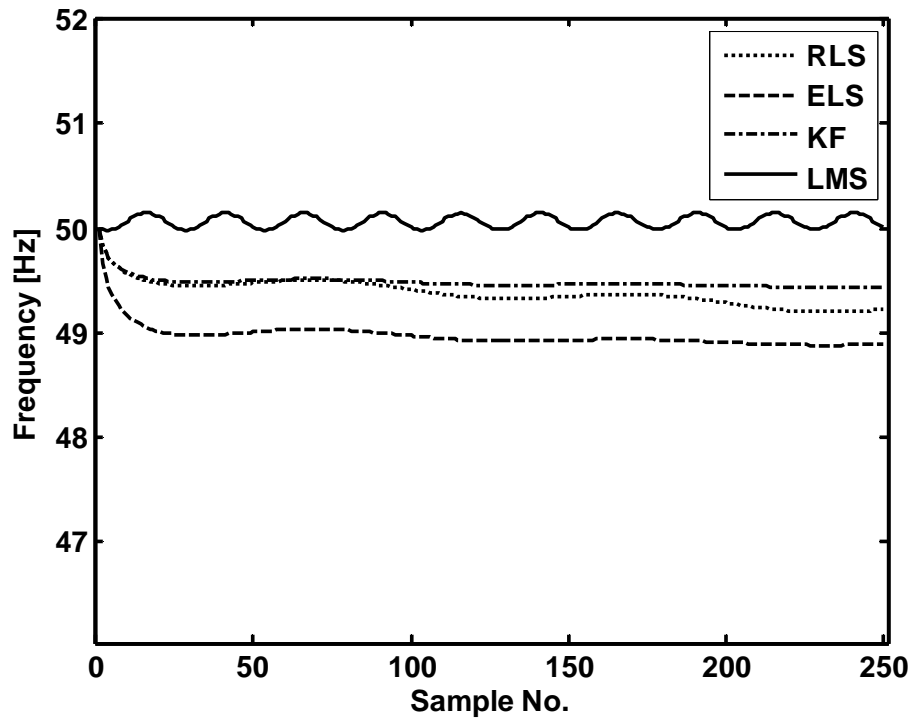
Fig.2.37 Estimation of frequency of real data using recursive methods
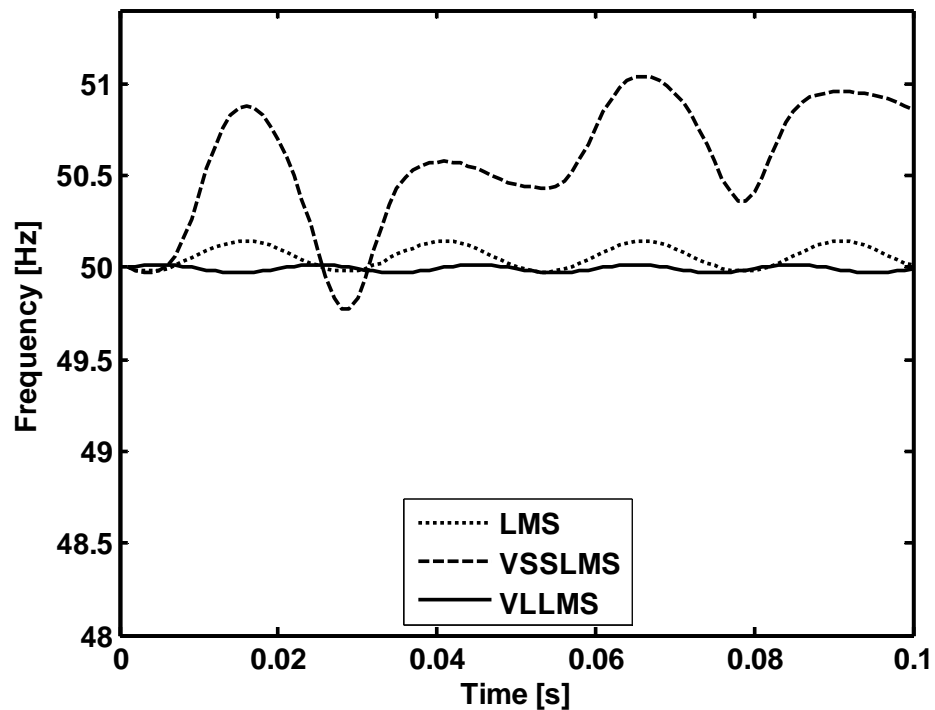
Fig. 2.38 VLLMS estimation performance of frequency of real data

Comparison of estimated frequency using LMS and its modified algorithms w.r.t. a 50 Hz constant frequency is shown in Fig. 2.38. Clearly it continues showing that VLLMS is better compared to the others.

2.8.2 Validation on real-time (Industrial Setup) data

Three phase voltage signals, generated at the terminals of the generators installed at the Captive Power Plant, National Aluminium Company (NALCO), India are collected at a sampling rate of 1 KHz. Figure 2.39 shows the schematic for the data collection set up that involves Voltage Transformers (VT) to facilitate the measurement. Voltage of 10.5 KV is generated at the terminals of the generator. The generated voltage is fed to 10.5KV/220KV Generator Transformer (GT). The output of GT is fed to bus bar. For acquiring digital voltage data, the generator is connected to 10.5KV/110KV VT. The output of VT is fed to Automatic Voltage Transducer (AVT) of input range is 0-15 KV and output range 4-20 mA. Current signal of mA range is fed to DDCMIS (Digital Distributed Control Monitory Information System).

DDCMIS provides digital data of Generator MW, MVA, pf, voltage and current. For our work, we obtained 3 phase digital voltage data from the output of DDCMIS. Fig. 2.40 shows the performance of the algorithms and is seen that proposed algorithm has superior performance in the estimation of frequency from the industrial data.
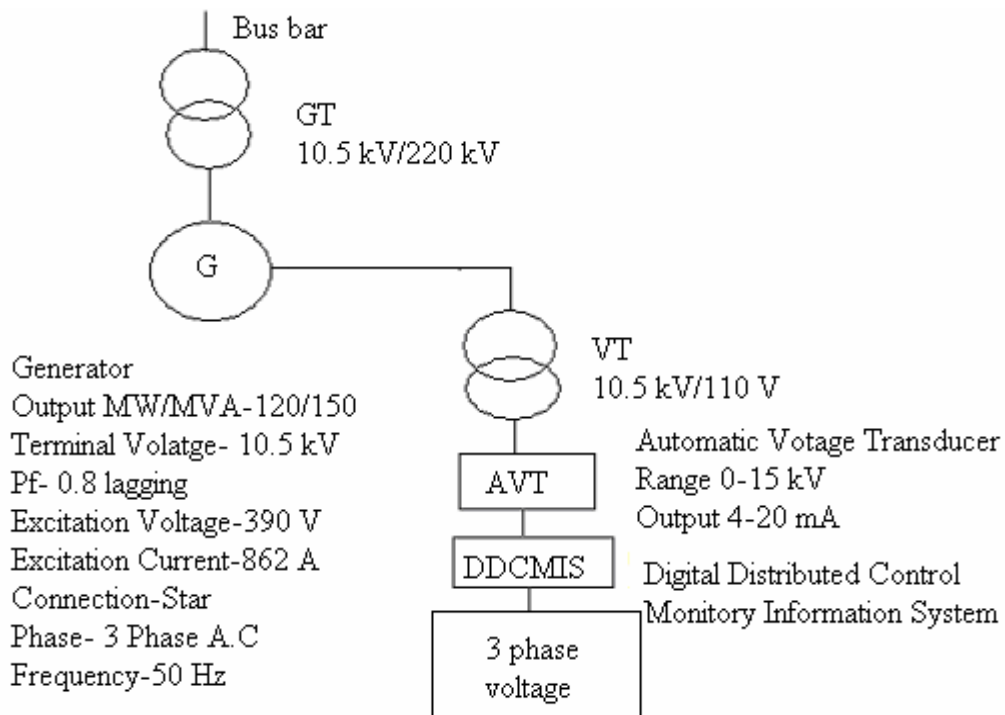
Fig. 2.39 Schematic diagram of collecting industrial data
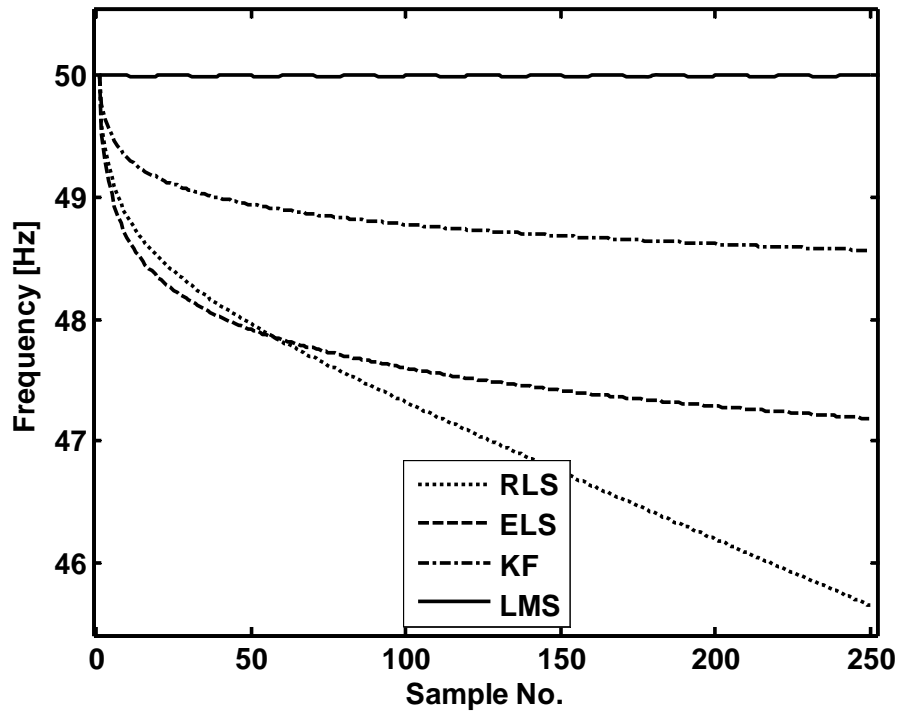
Fig.2.40 Estimation of frequency of industrial data using recursive methods
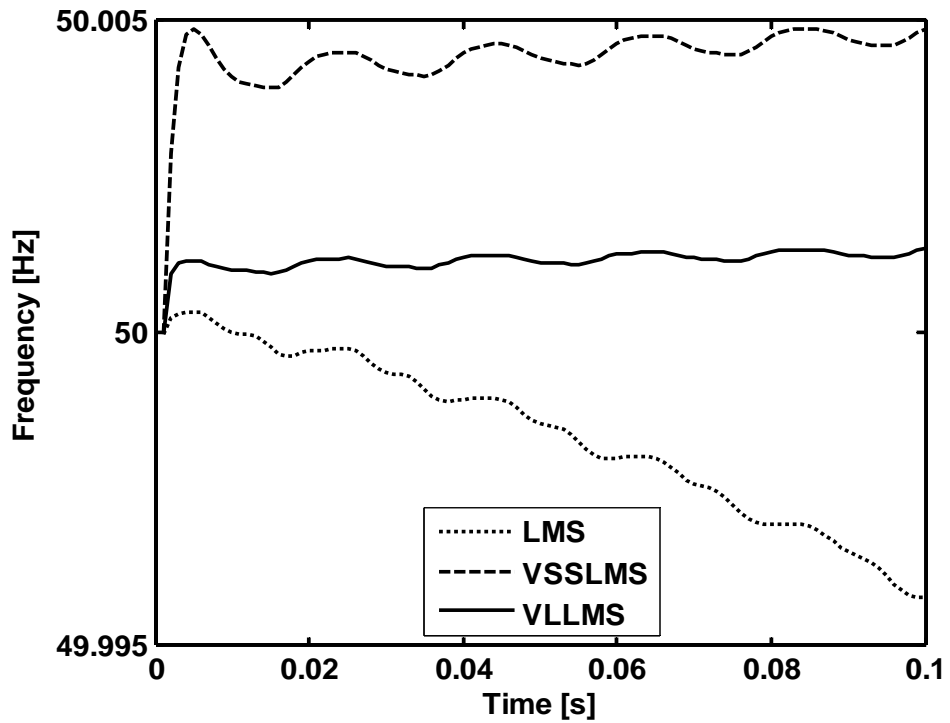
Fig.2.41 VLLMS estimation performance of frequency of industrial data

Fig. 2.41 shows the performance of using LMS and its modified algorithms and is seen that proposed algorithm i.e VLLMS has superior performance in the estimation of frequency from the industrial data.

2.9 Chapter Summary

This chapter mainly consists of two aspects. First section of this chapter presents the estimation of frequency of a power system signal by various recursive estimation techniques such as RLS, ELS, KF and LMS. However, initialization of covariance matrix is very important for RLS, ELS and KF algorithms because improper choice may lead to more computational time and more estimation error. LMS algorithm seems to be very complex due to the implementation of correlation matrix and proper choice of step size. From each case of simulation and experimental results both for single phase and three phase cases, it is concluded that LMS outperforms over other three algorithms. Second aspect of this chapter is proposition of an LMS based algorithm with variable leakage called VLLMS algorithm to estimate the frequency of power system. It has been shown that this algorithm is superior than other existing algorithms applied to the frequency estimation problem. Both simulation and experimental studies have been performed to study the efficacy of the proposed algorithm. Moreover, it has been observed that the proposed algorithm not only superior in minimizing the error but also superior in terms of convergence rate and computational aspect. Also, the variation of estimation error is minimum with respect to the SNR variations as compared to other existing algorithms.

Chapter -3

Development of Hybrid Algorithms for Power System Frequency Estimation

3.1 Introduction

Chapter 2 discusses frequency estimation of power system signals by using different signal processing techniques such as RLS, ELS, KF and LMS. In case of RLS, ELS and KF, initial choice of Co-Variance matrix and gain is difficult. LMS suffers from the problem of poor convergence rate as the adaptation step-size is fixed and estimation error is more. In order to obtain more accurate estimation, hybrid estimation algorithms by both signal processing and soft computing techniques are proposed in this chapter. The proposed hybrid estimation algorithms include RLS-Adaline (Recursive Least Square and Adaptive Linear Neural Network) and KF-Adaline (Kalman Filter Adaline) approaches to estimation of frequency of a power system. The inspiration of developing hybrid estimation algorithm evolved from good features of both Adaline and Recursive estimates. Previously, neural estimator was found to be an effective estimator [26, 75-76]. It consisted of an adaptive perceptron of neuron called Adaline. Since KF and RLS both are recursive in nature, online estimation is possible and KF can be used for both filtering and estimation, KF and RLS algorithms have been employed in the proposed hybrid algorithm for updating the weight in Adaline. Both RLS-Adaline and KF-Adaline estimators' track the power system signal in different cases such as signal corrupted with noise, in presence of harmonics and in presence of sub harmonics and inter harmonics.

Evolutionary Computation technique [65-66, 77-82] is a population based search algorithm; it works with a population of strings that represent different potential solutions. It enhances its search capability and the optima can be located more quickly when applied to complex optimization problems. An evolutionary computation technique called Bacterial Foraging Optimization (BFO) has been also exploited in this chapter for the development of

RLS-BFO and Adaline-BFO to power system frequency estimation. BFO is one of the recent bio-inspired computing used by many researchers in different areas of optimization. Mishra [69] applied BFO to estimate the harmonic components present in power system voltage/current waveforms. BFO rests on a simple principle of the foraging (food searching) behavior of E.Coli bacteria in human intestine. There are mainly four stages such as chemotaxis, swarming, reproduction and elimination and dispersal. In chemotactic stage, bacteria can move in a predefined direction or changes its direction of motion. In swarming, each bacterium provides signal to other bacterium to move together. In reproduction, healthiest bacteria split into two and less healthy bacteria die. In elimination and dispersal phase, a sudden unforeseen event occurs, which may drastically alter the smooth process of evolution and cause the elimination of the set of bacteria and/or disperse them to a new environment. Most ironically, instead of disturbing the usual chemo tactic growth of the set of bacteria, this unknown event may place a newer set of bacteria nearer to the food location.

Two combined approaches namely RLS-BFO and Adaline-BFO have been considered for the improvement in % age error of estimation, processing time of computation and estimation performance in different situations such as presence of harmonics, sub harmonics and inter harmonics in the signal as compared to BFO algorithm. The performances of frequency tracking of the proposed approaches are validated taking the data generated from laboratory setup as well as data collected from industry.

3.2 Hybrid Adaline Methods for Frequency estimation:

Fig. 3.1 shows the structure of hybrid Adaline estimation scheme. Firstly input (system structure matrix) is applied to Adaline structure. Output of Adaline (estimated signal) is then compared with the actual signal and the error so obtained is minimized by updating the weights of the Adaline using RLS/KF algorithm. In this section, frequency estimation using two new hybrid algorithms i.e RLS-Adaline and KF-Adaline methods are presented.
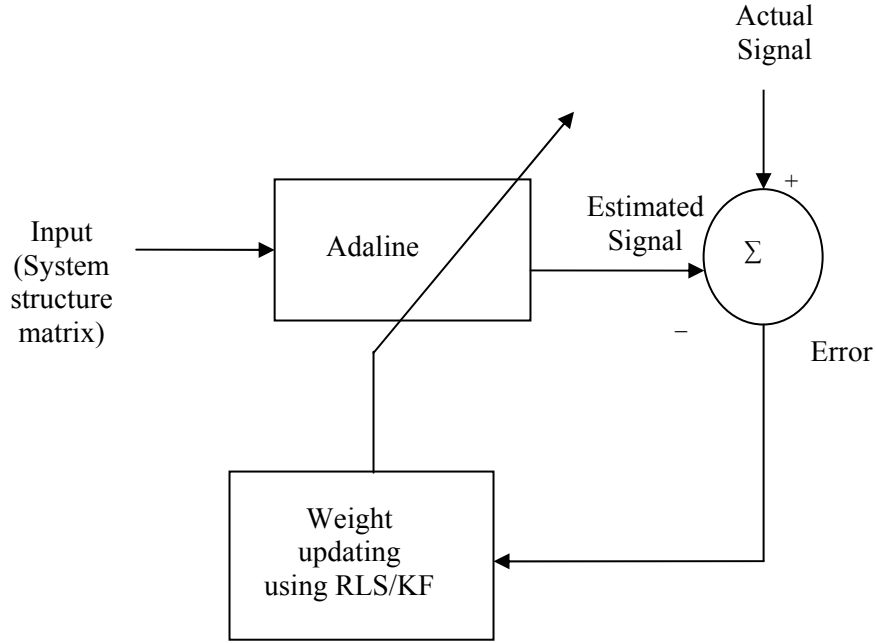
Fig. 3.1 Schematic of hybrid Adaline structure

3.2.1 Recursive Least Square-Adaptive Linear Neural Network (RLS-Adaline) approach:

From the discrete values of the three-phase voltage signal of a power system, a complex voltage vector is formed using the well-known $\alpha - \beta$ transformation [1, 13]. A non-linear state space formulation is then obtained for this complex signal and Recursive Least Square (RLS) approach is used to compute the true state of the model. As frequency is modeled as a state, the estimation of the state vector yields the unknown power system frequency. The discrete representation of three phase voltages of a power system may be expressed as follows

$$v_a(k) = V_m \cos(\omega kT + \phi) + \varepsilon_a(k)$$

$$v_b(k) = V_m \cos(\omega kT + \phi - \frac{2\pi}{3}) + \varepsilon_b(k) \tag{3.1}$$

$$v_c(k) = V_m \cos(\omega kT + \phi + \frac{2\pi}{3}) + \varepsilon_c(k)$$

where v_a, v_b and v_c are three phase voltage signals. V_m is the amplitude of the signal, ω is the angular frequency, $\varepsilon_a(k), \varepsilon_b(k), \varepsilon_c(k)$ are the noise terms, T is the sampling interval, k is

the sampling instant, ϕ is the phase of fundamental component. The complex form of signal derived from the three-phase voltages is obtained by $\alpha - \beta$ transform as mentioned below

$$v_\alpha(k) = \sqrt{\frac{2}{3}}(v_a(k) - 0.5v_b(k) - 0.5v_c(k))$$

$$v_\beta(k) = \sqrt{\frac{2}{3}}(0.866v_b(k) - 0.866v_c(k))$$

(3.2)

A complex voltage can be obtained from above equation as follows

$$v(k) = v_\alpha(k) + jv_\beta(k)$$
$$= Ae^{j(\omega k\Delta T + \phi)} + \varepsilon(k)$$

(3.3)

$$v(k) = v_\alpha(k) + jv_\beta(k) = \sqrt{\frac{3}{2}}V_m e^{j(\omega kT + \phi)}$$
$$= Ae^{j(\omega kT + \phi)} + \varepsilon(k)$$

(3.4)

where A is the amplitude of the signal and ε_k is the noise component.

Taking w_1 and w_2 as the state variables one can write

$$w_1(k) = e^{j\omega kT} = \cos k\omega T + j\sin k\omega T$$

(3.5)

$$w_2(k) = Ae^{j(\omega kT + \phi)}$$

(3.6)

$$W(k) = \begin{bmatrix} w_1(k) & w_2(k) \end{bmatrix}^T$$

The observation signal v_k can be modeled in a state space form as

$$\begin{bmatrix} w_1(k+1) \\ w_2(k+1) \end{bmatrix} = \begin{bmatrix} 1 & 0 \\ 0 & w_1(k) \end{bmatrix} \begin{bmatrix} w_1(k) \\ w_2(k) \end{bmatrix}$$

(3.7)

$$y(k) = v(k) = \begin{bmatrix} 0 & 1 \end{bmatrix} \begin{bmatrix} w_1(k) \\ w_2(k) \end{bmatrix} + \varepsilon(k)$$

(3.8)
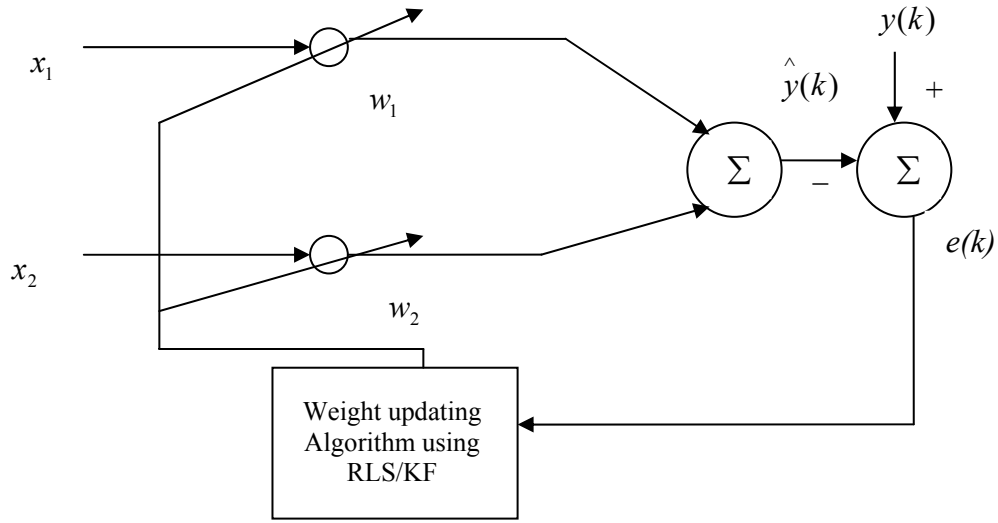
Fig.3.2 Block diagram of Hybrid-Adaline for frequency estimation

Fig.2 shows the block diagram of Adaline containing states, actual and estimated signal.

From equation (3.8)

$$X = \begin{bmatrix} x_1 & x_2 \end{bmatrix} = \begin{bmatrix} 0 & 1 \end{bmatrix} \tag{3.9}$$

Using equations (3.5) and (3.6) to (3.9), one gets

$$y(k) = XW(k) \tag{3.10}$$

RLS estimation technique can be applied to the power system estimation problem for which equation (3.8) is the appropriate representation (Regressor form).

$$\hat{W}(k) = \hat{W}(k-1) + K(k)\varepsilon(k) \tag{3.11}$$

where $\hat{W}(k) = $ current value of estimate

$\hat{W}(k-1) = $ Past value of estimate

$K(k) = $ Gain

The error in the measurement is given by

$$\varepsilon(k) = y(k) - X^T \hat{W}(k-1) \tag{3.12}$$

The gain K is updated using the following expression

$$K(k) = P(k-1)X[\lambda I + X^T P(k-1)X]^{-1} \tag{3.13}$$

where $P(k) =$ Error Covariance matrix

$\lambda(0 < \lambda < 1) =$ Forgetting factor

The covariance matrix updatation is as follows

$$P(k) = [I - K(k)X^T]P(k-1)/\lambda \tag{3.14}$$

Equations (3.9) to (3.12) are initialized at $k = 0$. The choice of initial covariance matrix $P(0)$ is large. Usually a value i.e $P = \alpha I$, where α is a large number and I is a square identity matrix is chosen. After the convergence of state vector is attained, the frequency is calculated from equation (3.5) as

$$\hat{W}_{11}(k) = w_1(k) = e^{j\omega kT}$$

$$\sin(\omega kT) = \text{Im}(\hat{W}_{11}(k))$$

$$\hat{f}_k = \frac{1}{2\pi T}(\sin^{-1} \text{Im}(\hat{W}_{11}(k))) \tag{3.15}$$

$\hat{f}$ is the estimated frequency of the signal

3.2.2 Kalman Filter-Adaptive Linear Neural Network (KF-Adaline) approach for frequency estimation:

The discretized voltage signal as described in 3.1(a) is considered. The equations (3.1) to (3.10) are taken into account.

Using the Kalman Filtering estimation technique to (3.10), the parameters are estimated using the formula given by

$$K(k) = \hat{P}(k/k-1)X^T(X\hat{P}(k/k-1)X^T + Q)^{-1} \tag{3.16}$$

where K is the Kalman gain, X is the observation vector, P is the covariance matrix, Q is the noise covariance of the signal.

The covariance matrix is related with Kalman gain with the following equation.

$$\hat{P}(k/k) = \hat{P}(k/k-1) - K(k)X\hat{P}(k/k-1) \tag{3.17}$$

The updated estimated state is related with previous state with the following equation.

$$\hat{W}(k/k) = \hat{W}(k/k-1) + K(k)(y(k) - X\hat{W}(k/k-1)) \tag{3.18}$$

After the final updatation of the state vector, the frequency is calculated from equation (3.15).

3.3 Results and Discussions (Frequency Estimation using RLS-Adaline and KF-Adaline)

3.3.1 Sinusoidal Signal in presence of noise

A 50 Hz signal of 1 p.u. amplitude and 0.5 p.u. phase angle with random noises is generated with a 1ms sampling interval. Table 3.1 shows the different values of parameters taken for two algorithms during both simulation and experimentation work.

Table-3.1
Parameters used in Algorithms (RLS-Adaline and KF-Adaline)

	δ	η	α_0	β	λ
RLS-Adaline	100	0.96	0.01	100	0.01
KF-Adaline	100	-	0.01	100	0.01

The performances of RLS-Adaline and KF-Adaline algorithms for SNRs of 20 dB, 30 dB and 40 dB are shown respectively in Figs. 3.3, 3.4 and 3.5. From these Figs., it is clear that with the increase in signal to noise ratio, there is expectedly more accuracy in the estimation. Further analysis is made considering the 40 dB SNR case as in the other cases; the errors using the existing algorithms are quite large. Fig. 3.6 shows MSE values using different methods. These figures show that the error is less (5.47×10^{-5}) in case of KF-Adaline algorithm.
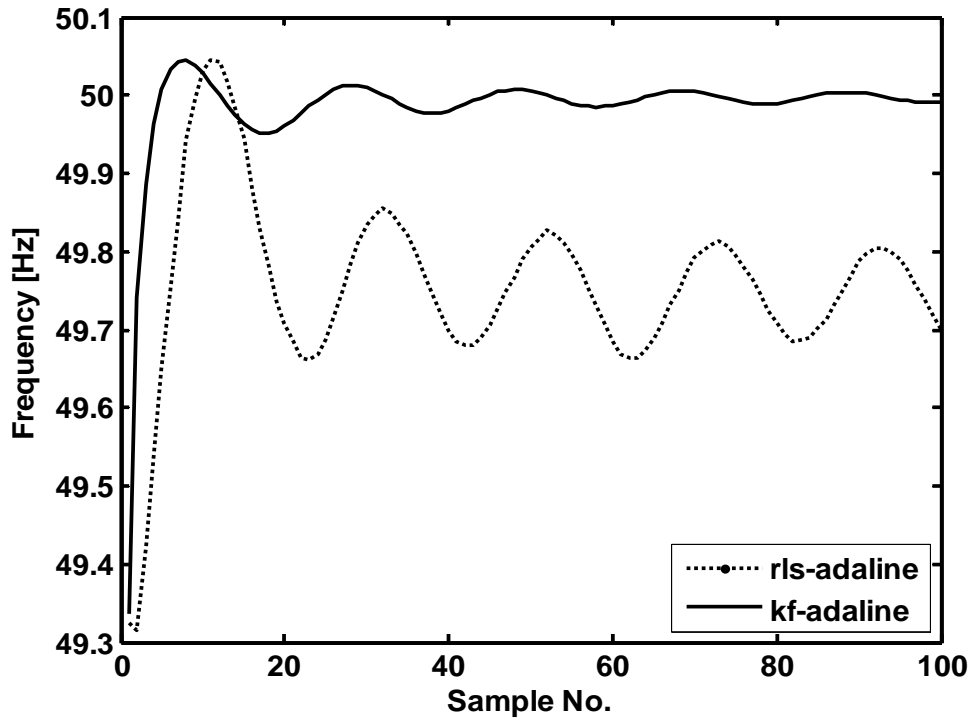
Fig.3.3 KF-Adaline estimation performance of frequency (SNR 20 dB)
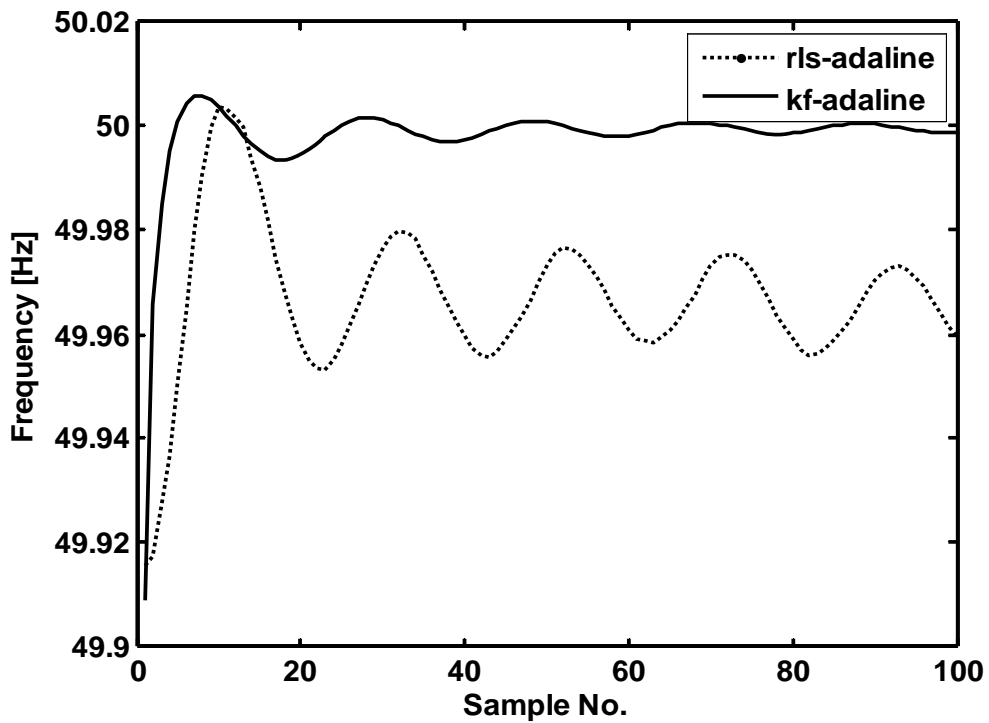
Fig.3.4 KF-Adaline estimation performance of frequency (SNR 30 dB)
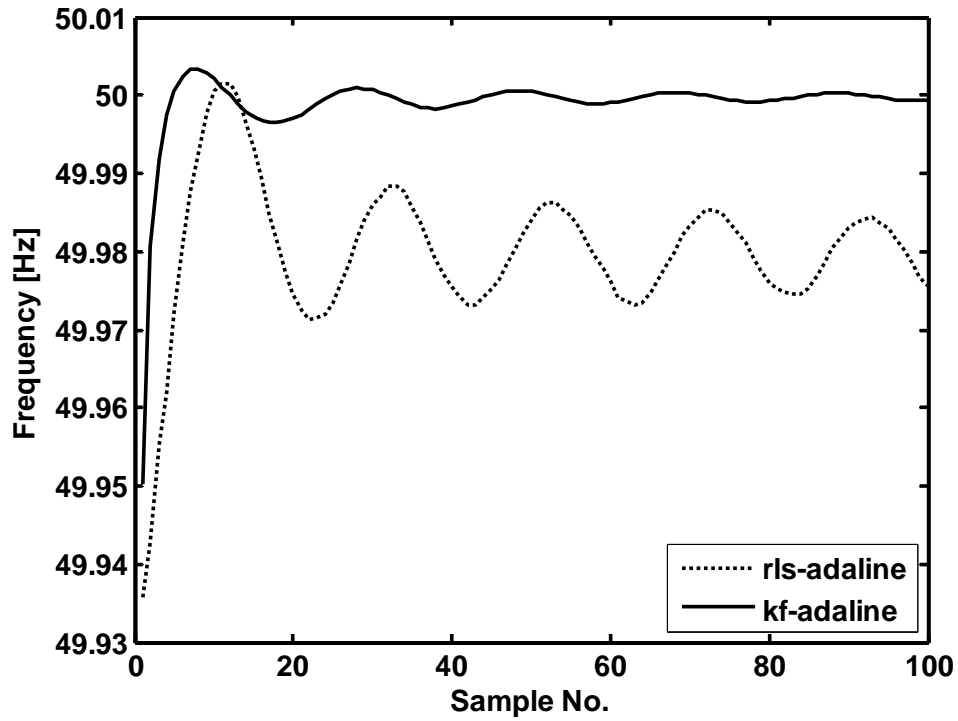
Fig.3.5 KF-Adaline estimation performance of frequency (SNR 40 dB)
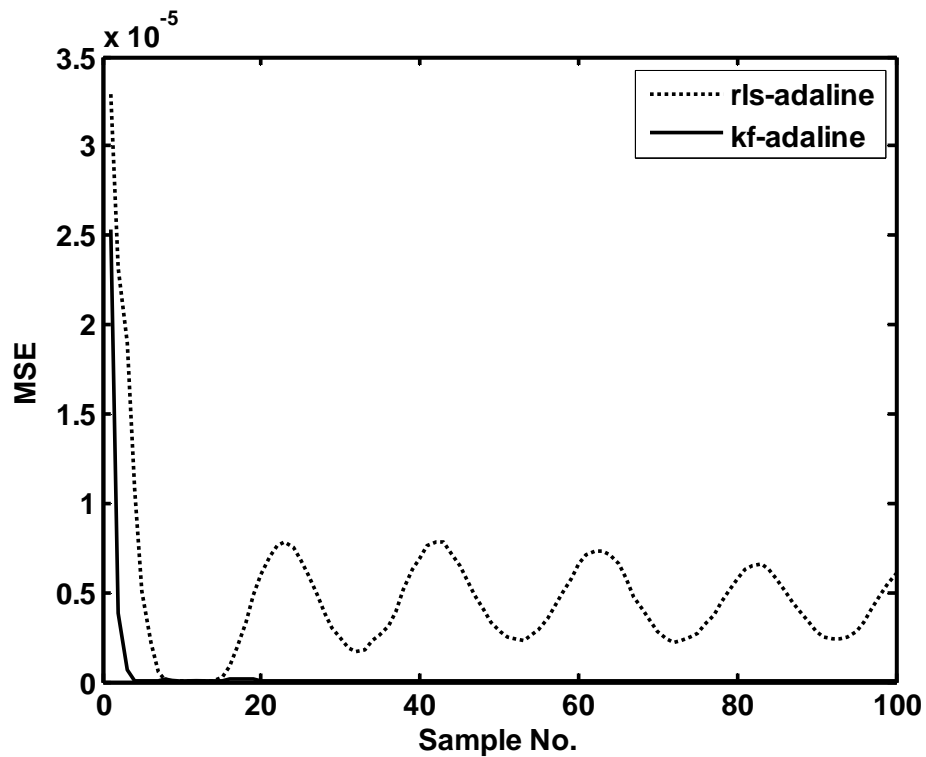
Fig. 3.6 MSE in the estimation of Frequency (RLS-Adaline and KF-Adaline)

3.3.2 Jump in frequency in the signal

The next case is considered to be the performance of the algorithm in presence of jump in frequency. For this, we consider that the frequency changes from 50 Hz to 49 Hz. Fig. 3.7, 3.8 and 3.9 show the estimation of frequency during sudden change in frequency at SNR of 20, 30 and 40 dB respectively. Both the algorithms (i.e RLS-Adaline and KF-Adaline) estimate frequency accurately but performance of KF-Adaline is little better (providing less estimation error i.e 0.113) than RLS-Adaline.
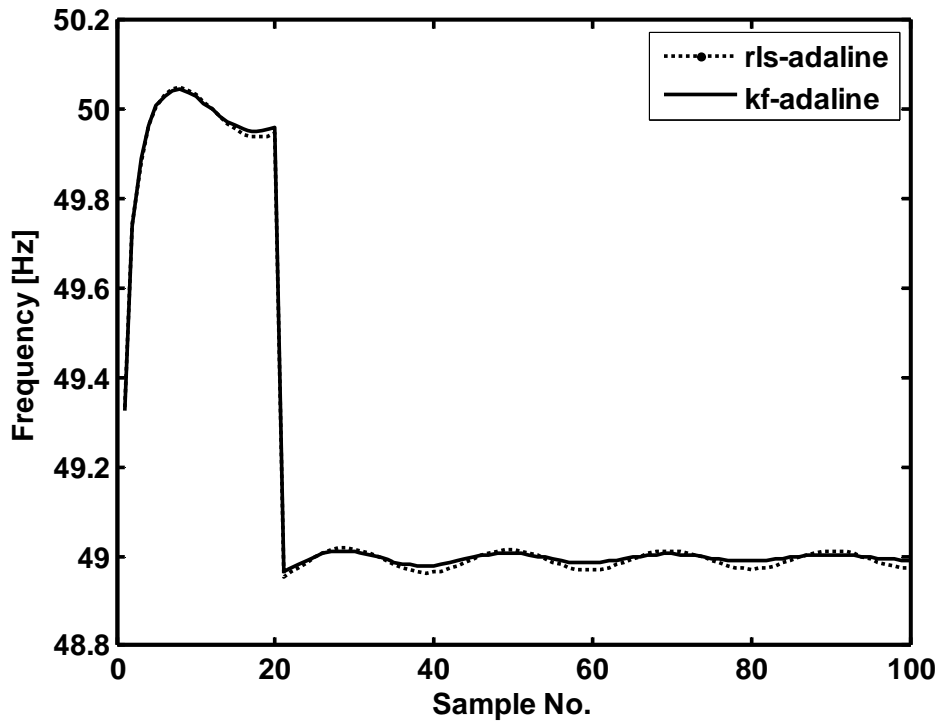
Fig. 3.7 KF-Adaline estimation performance of frequency during frequency jump (SNR 20 dB)
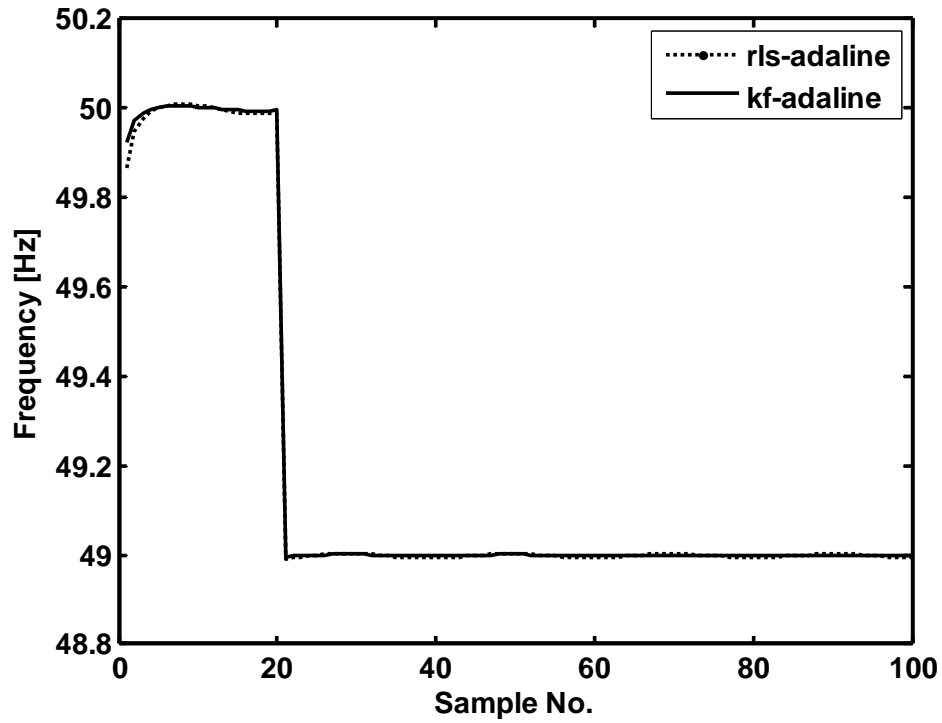
Fig. 3.8 KF-Adaline estimation performance of frequency during frequency jump (SNR 30 dB)
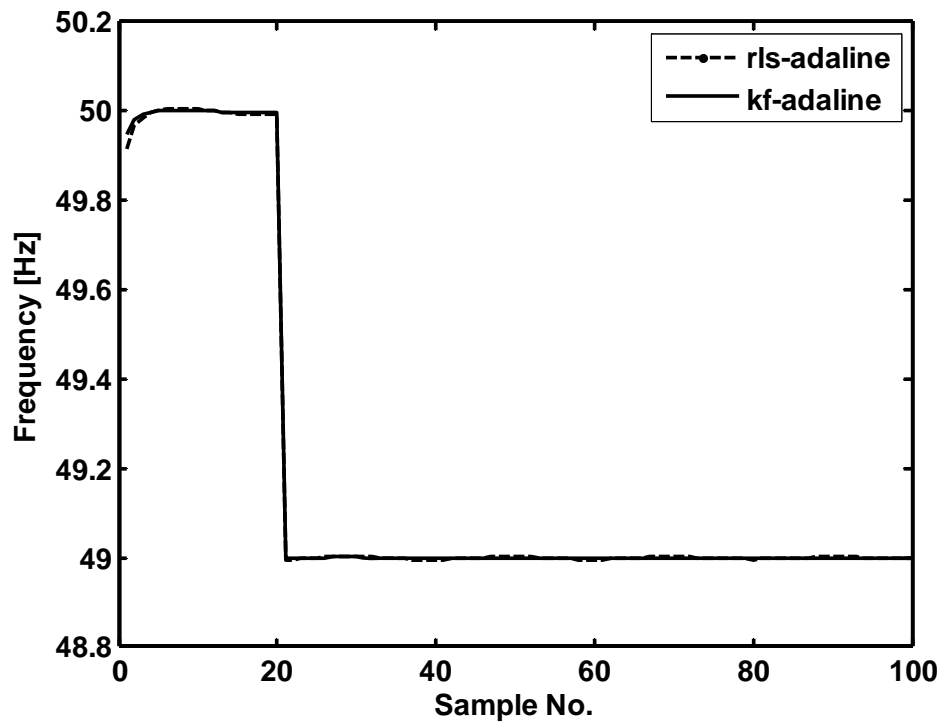
Fig. 3.9 KF-Adaline estimation performance of frequency during frequency jump (SNR 40 dB)

3.3.3 In the presence of Harmonics

Next we consider the problem of estimating fundamental frequency from signals having harmonics content in them. The common case of 3rd harmonic is considered. Fig. 3.10 shows the estimation of frequency using different algorithms from the signal with harmonics. It is verified from the above Fig. that a comparatively better performance (less estimation error i.e 0.1503) is obtained in case of KF-Adaline algorithm.
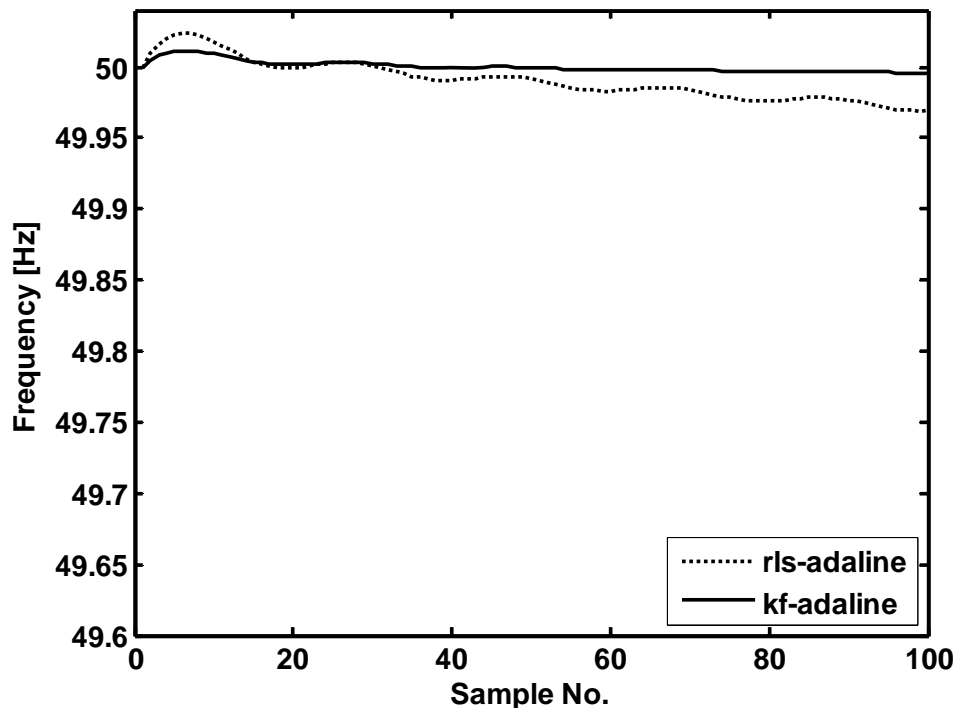
Fig. 3.10 KF-Adaline estimation performance of Frequency in presence of harmonics

3.3.4 In the presence of Sub Harmonics and Inter Harmonics

To evaluate the performance of the proposed algorithms (RLS-Adaline and KF-Adaline) in the estimation of frequency of signal in the presence of sub-harmonics and inter-harmonics, these sub and inter harmonics components are added into the original signal as given in equation (3.1). The frequency of sub-harmonic is 20 Hz, the amplitude is set as 0.5 p.u. and the phase is equal to 75 degrees. The frequency, amplitude and phase of the inter-harmonic is 140 Hz, 0.25 p.u. and 65 degrees respectively. Fig. 3.11 shows the

estimation of fundamental frequency in presence of sub-harmonics and inter-harmonics and is found that estimation is more accurate (less estimation error i.e. 0.163) in case of KF-Adaline algorithm than the RLS-Adaline.
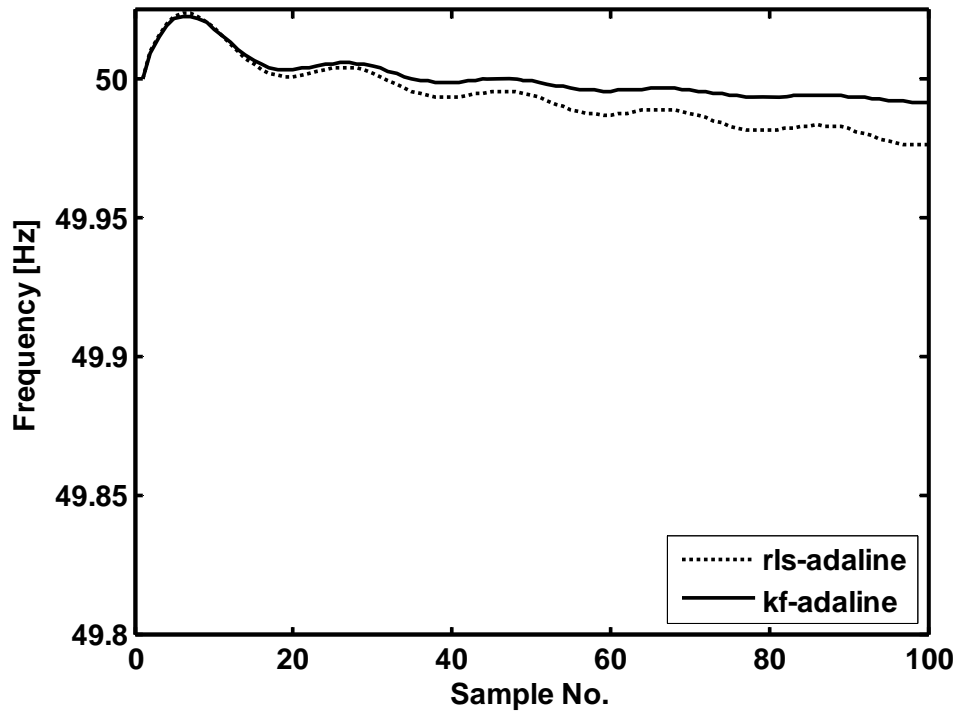
Fig. 3.11 KF-Adaline estimation performance of Frequency in presence of sub-harmonics and inter harmonics

3.4   Experimental Results

3.4.1 Validation on real-time (Laboratory Setup) data

To decide real-time application of the proposed RLS-Adaline and KF-Adaline algorithms applied for frequency estimation, datasets were obtained from the experiment conducted in the laboratory (Fig. 2.35 section 2.8.1). Fig. 3.12 shows the estimation of frequency of signal using both the algorithms from the real data obtained from the experiment. From this Fig. 3.12, it is found that the performance in estimation using KF-Adaline is better (less estimation error i.e. 0.1632) as compared to RLS-Adaline.

3.4.2 Validation on real-time (Industrial Setup) data

Apart from simulation and laboratory data, the efficacies of the proposed algorithm RLS-Adaline and KF-Adaline have been applied to data collected from an aluminium industry. The considered industrial setup is described in Fig. 2.39 (section 2.8.2). The estimated frequency of industrial data is shown in Fig. 3.13 and it is observed from the figure that the estimation using KF-Adaline is better (less estimation error i.e 0.1863) as compared to RLS-Adaline.
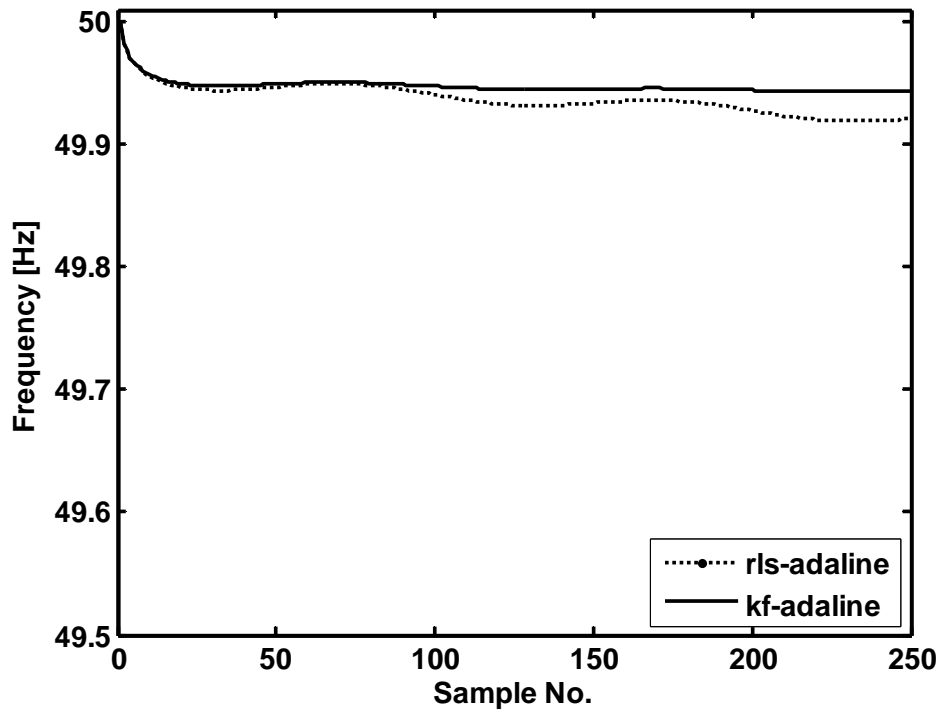
Fig. 3.12 KF-Adaline estimation performance of Frequency of real data
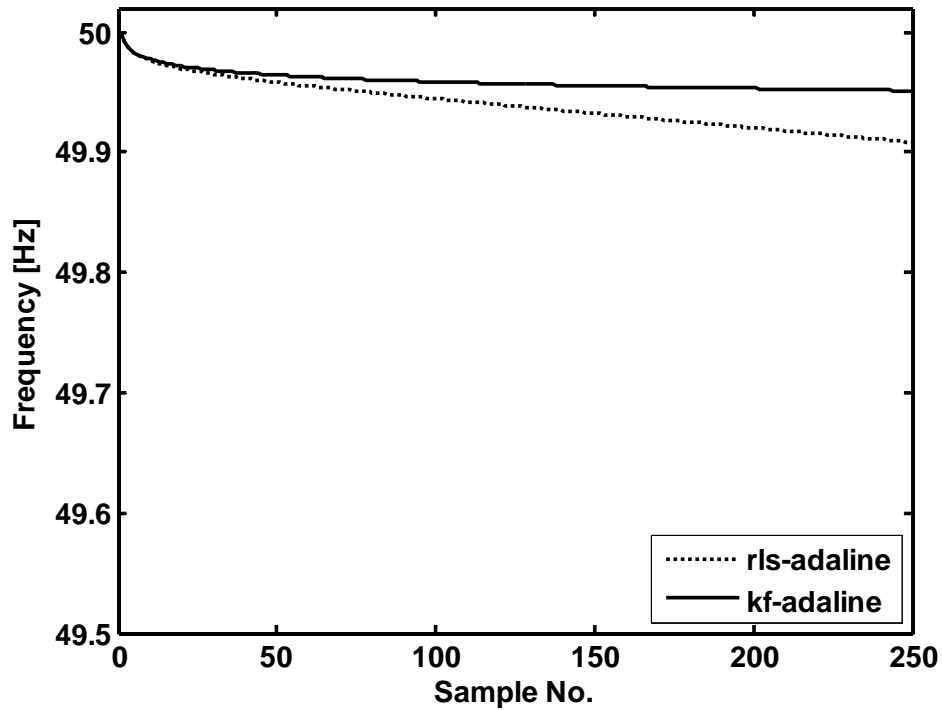
Fig. 3.13 KF-Adaline estimation performance of Frequency of industrial data

3.5 Hybrid BFO Methods for Frequency estimation
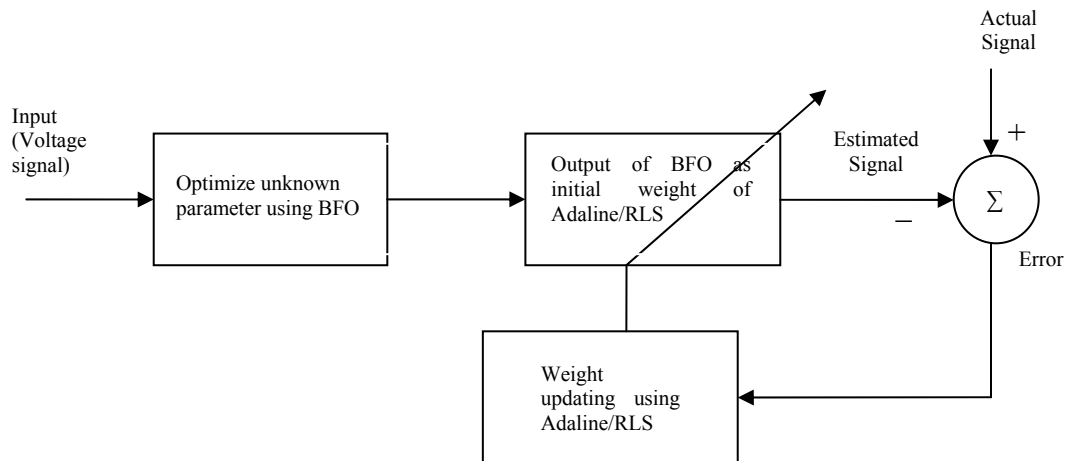
Fig. 3.14 Schematic of the estimation problem

Fig. 3.14 shows the structure of the estimation problem. First input signal is fed to BFO algorithm and unknown parameter vectors such as $W(k) = \begin{bmatrix} w_1(k) & w_2(k) \end{bmatrix}^T$ are

86

optimized using this algorithm. Then optimized output of BFO algorithm is taken as the initial value of weight of Adaline/ RLS algorithm. Output of Adaline/RLS (Estimated signal) is compared with the actual signal and the error obtained, is minimized by updating the weight of the Adaline/RLS. From the final updated weight of the Adaline/RLS, frequency of signal is estimated using (3.15).

3.5.1 Proposed RLS-BFO Combined Approach to Frequency Estimation

Same signal as described by (3.1) is considered. The steps from (3.1) to (3.10) are followed. Then parametric form of the signal such as $y(k) = XW(k)$ is taken. Where X is given by (3.9) and W is given by (3.8). The unknown parameter is optimized using BFO algorithm. The optimized output of BFO algorithm is taken as the initial values of unknown parameter (W) for estimation using RLS. The vector of unknown parameter can be updated using (3.11)-(3.14). After updating of unknown parameter vector, frequency of signal is estimated using (3.15)

Table: 3.2 Parameters of BFO

Name of parameters	Sample No.	No. of parameters to be optimized	Swimming length	No. of Chemotactic iterations	No. of reproduction steps	Max. no. of elimination dispersal events.	Probability of elimination and dispersal	cell-to-cell attractant repellant effect
Symbol	S	p	N_s	N_c	N_{re}	N_{ed}	P_{ed}	$d_{attract}, \omega_{attract},$ $h_{repellant}, \omega_{repellant}$

The proposed RLS-BFO algorithm is discussed below

1.Initialization of BFO Parameters

2. Elimination-dispersal loop: $l = l + 1$

3. Reproduction loop: $m = m + 1$

4. Chemo taxis loop: $n = n + 1$

a) For $i = 1,2....S$ Compute $J(i, n, m, l) = \sum_{t=1}^{N_s} \varepsilon^2(t) = \sum_{t=1}^{N_s} [y(t) - \hat{y}(t)]^2$

Let $J_{sw}(i, n, m, l) = J(i, n, m, l) + J_{cc}(x^i(n, m, l), P(n, m, l))$

$$J_{cc}(x, P(n, m, l)) = \sum_{i=1}^{S} J_{cc}^i(x, x^i(n, m, l)) = \sum_{i=1}^{S} \left[-d_{attract} \exp\left(-\omega_{attract} \sum_{m=1}^{P} (x_m - x^i{}_m)^2 \right) \right]$$

$$+ \sum_{i=1}^{S} \left[h_{repellant} \exp(-\omega_{repellant} \sum_{m=1}^{P} (x_m - x^i{}_m)^2 \right]$$

$J_{last} = J_{sw}(i, n, m, l)$

   End of for loop

b) For $i = 1,2....S$ take the tumbling / swimming decision

   • Tumble

   Generate a random vector $\Delta(i)$, on [-1, 1]

i) Update parameter

   $$x^i(n + 1, m, l) = x^i(n, m, l) + u \times C(i) \frac{\Delta(i)}{\sqrt{\Delta^T(i)\Delta(i)}}$$

ii) Compute: $J(i, n + 1, m, l)$

   $$J_{sw}(i, n+1, m, l) = J(i, n+1, m, l) + J_{cc}(x^i(n+1, m, l), P(n+1, m, l))$$

   • Swim

Let $nswim = 0$;(counter for swim length)

While $nswim < N_s$

Let $nswim = nswim + 1$

If $J_{sw}(i, n + 1, m, l) < J_{last}$ (if doing better),

  $J_{last} = J_{sw}(i, n + 1, m, l)$

$$x^i(n + 1, m, l) = x^i(n, m, l) + u \times C(i) \frac{\Delta(i)}{\sqrt{\Delta^T(i)\Delta(i)}}$$

Then $x^i(n+1, m, l)$ is used to compute the new $J(i, n + 1, m, l)$

Else $nswim = N_s$

This is the end of the while statement.

c) Go to the next sample $(i+1)$ if $i \neq S$ [i.e. go to b] to process the next sample.

d) If min (J) is less than the tolerance limit then break all the loops.

5. If $J < N_c$, go to 4, continue chemotaxis as life of bacteria is not over.

6. Reproduction

    a) For the given m and l, and for each i=1,2,3....S, let

$$J_{health} = \sum_{j=1}^{N_C+1} J_{sw}(i,n,m,l)$$ Sort parameter in ascending J_{health}

    b) $S_r = S/2$ parameters with highest J_{health} will be removed and other S_r no. of set of parameters with the best value split

7. If $m < N_{re}$ go to 3, start the next generation in the chemo tactic loop.

8. Elimination-dispersal

For i=1, 2...S, with P$_{ed}$, eliminate and disperse each set of parameters

9. If $l < N_{ed}$, go to 2; other wise end

10. Obtain optimized values for Weights (parameters)

11. Employ RLS for final updating of Weights using (3.11)-(3.14).

12. Estimate frequency of signal from updated Weights using (3.15)

3.5.2 Proposed Adaline-BFO Combined Approach to Frequency Estimation

The steps as described are followed till the unknown parameter is optimized using BFO algorithm. The optimized output of BFO algorithm is taken as the initial values of unknown parameter (W) for estimation using Adaline.

Fig.3.1 shows the block diagrammatic representation of the Adaline. Product of input signal and weight of the Adaline gives the estimated output and is compared with the desired output. The error obtained, is minimized by updating the weight of the Adaline.

The input to the Adaline from (3.9) is

$$X = \begin{bmatrix} x_1 & x_2 \end{bmatrix} = \begin{bmatrix} 0 & 1 \end{bmatrix}$$

where X is the system structure matrix and $y(k) = XW(k)$

The optimized output of the unknown parameter using BFO algorithm is taken as the initial values of the weight vector of Adaline (3.8) and is updated using a modified Widrow-Hoff delta rule as

$$W(k+1) = W(k) + \frac{\alpha e(k)S}{\lambda + X^T X} \tag{3.22}$$

where $S = SGN(X)$ $\tag{3.23}$

$$SGN(X_i) = \begin{cases} +1, X_i > 0 \\ -1, X_i < 0 \end{cases} \tag{3.24}$$

$i = 1,2,...,2N+2$
$0 < \alpha < 2$

The learning parameter α can be adapted using the following expression:

$$\alpha(k) = \frac{\alpha_0}{\left(1 + \dfrac{k}{\beta}\right)} \tag{3.25}$$

where α_0 is the initial learning rate and β is decaying rate constant. λ Is a small quantity and is usually chosen to make

$$\lambda + X^T X \neq 0$$

After updating of weight vector of the Adaline, Frequency of signal is estimated using (3.15)

Fig.3.15 desrcibes the flow chart of the proposed Adaline-BFO/RLS-BFO algorithm. In this figure, BFO is applied first and then output of BFO, which is taken as initial weight of the Adaline/RLS is then updated to minimize the error between the estimated and the desired output.
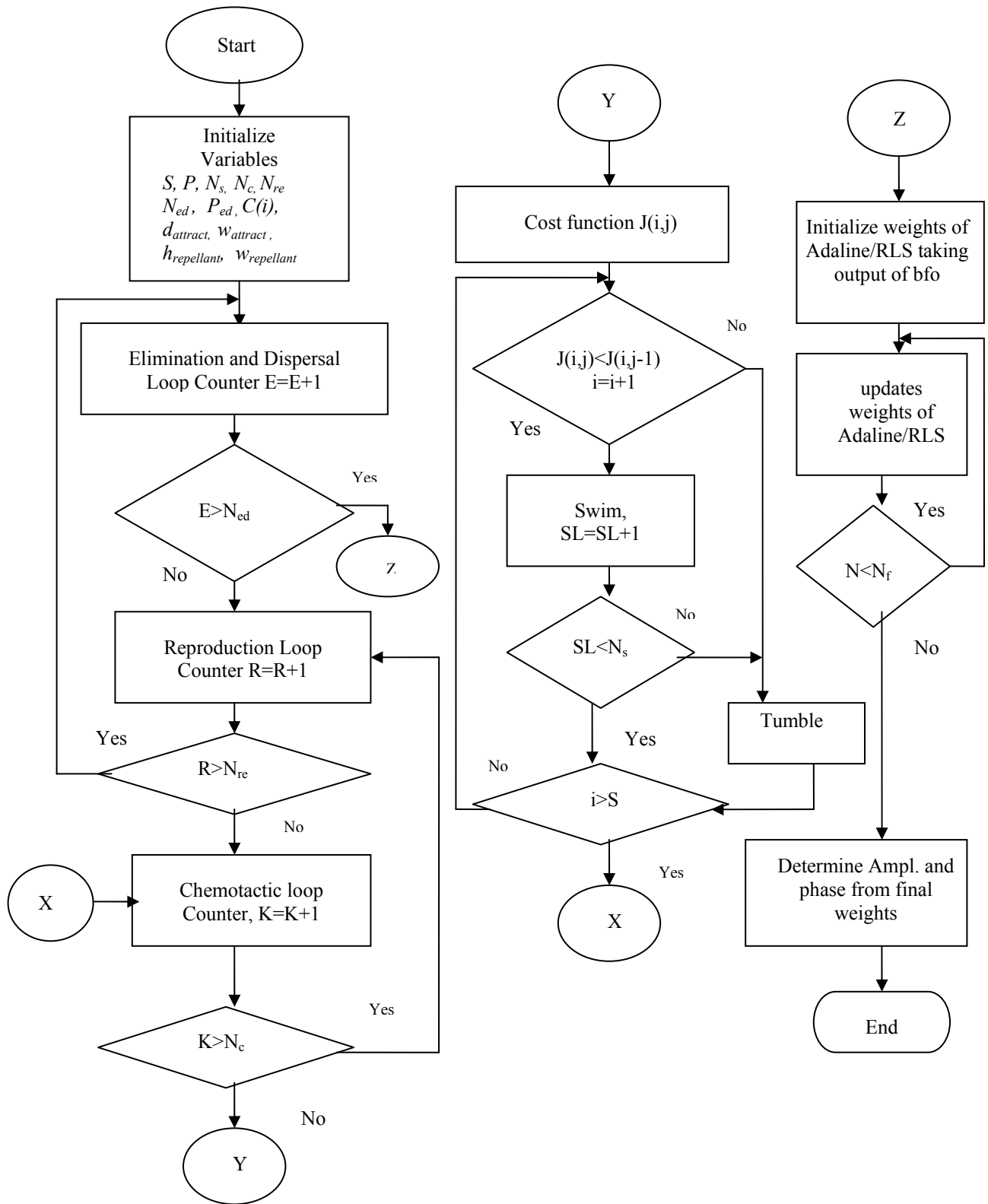
Fig. 3.15 Flow chart of the proposed Hybrid Algorithm

3.6 Results and Discussions (Frequency estimation using RLS-BFO and Adaline-BFO)

Table-3.3
Values of parameters used for simulation and experimental work (BFO, RLS-BFO and Adaline-BFO)

α_0	β	λ	S	p	N_s	N_c	N_{re}	N_{ed}	P_{ed}	$C(i)$	$d_{attract,}$	$w_{attract}$	$h_{repellant}$	$w_{repellant}$
0.01	100	0.01	100	2	3	3	7	7	0.25	0.001	0.05	0.3	0.05	10

3.6.1 Sinusoidal Signal in presence of noise

Table 3.3 shows the values of different parameters used in RLS-BFO and Adaline-BFO algorithms for the estimation of power system frequency.
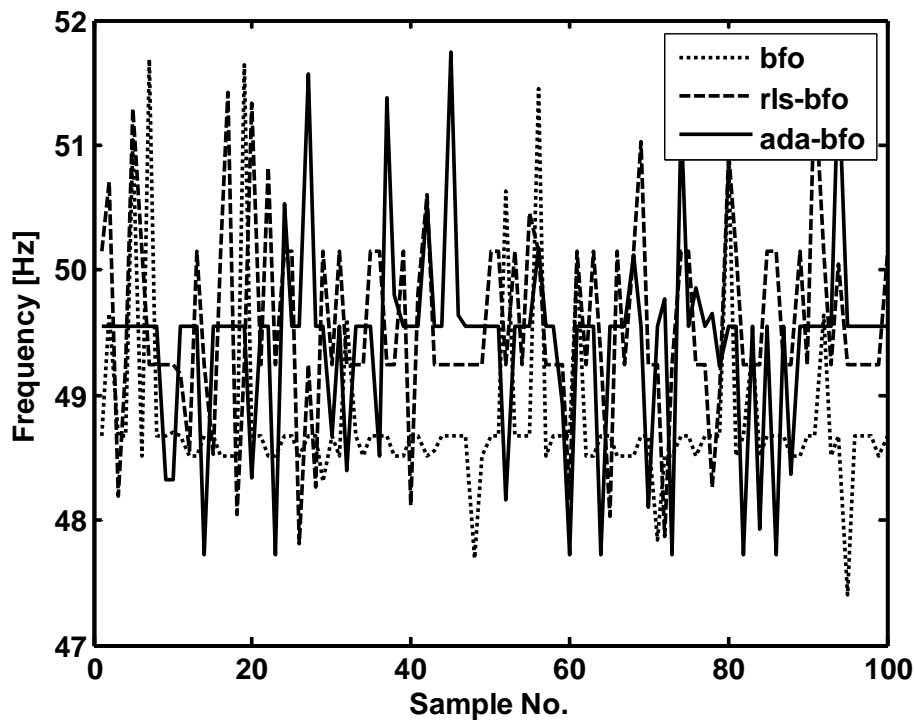
Fig. 3.16 Adaline-BFO estimation performance of Frequency (SNR 20 dB)
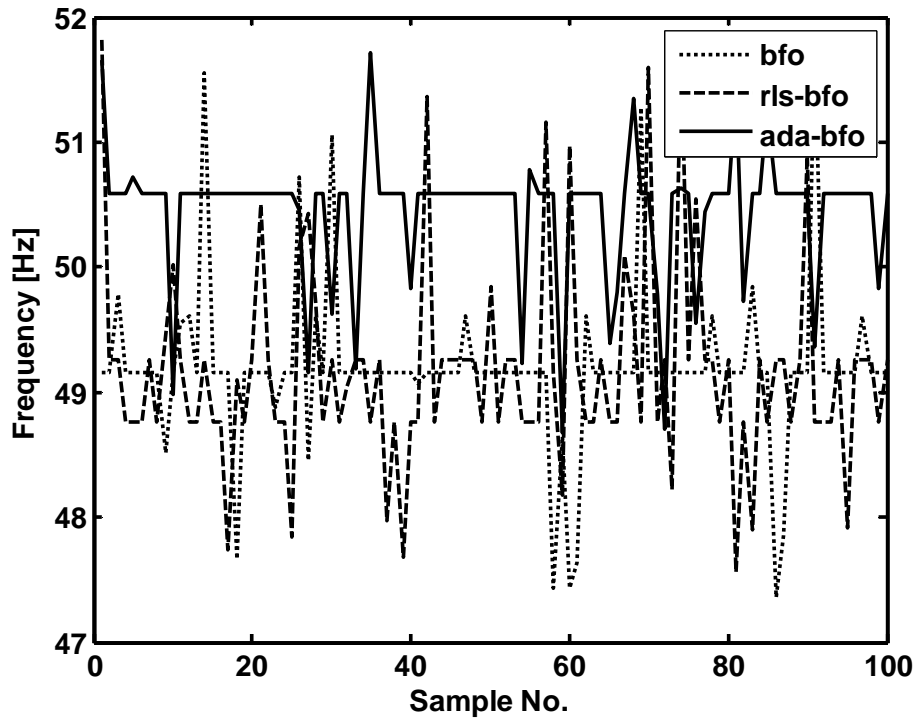
Fig. 3.17 Adaline-BFO estimation performance of Frequency (SNR 30 dB)
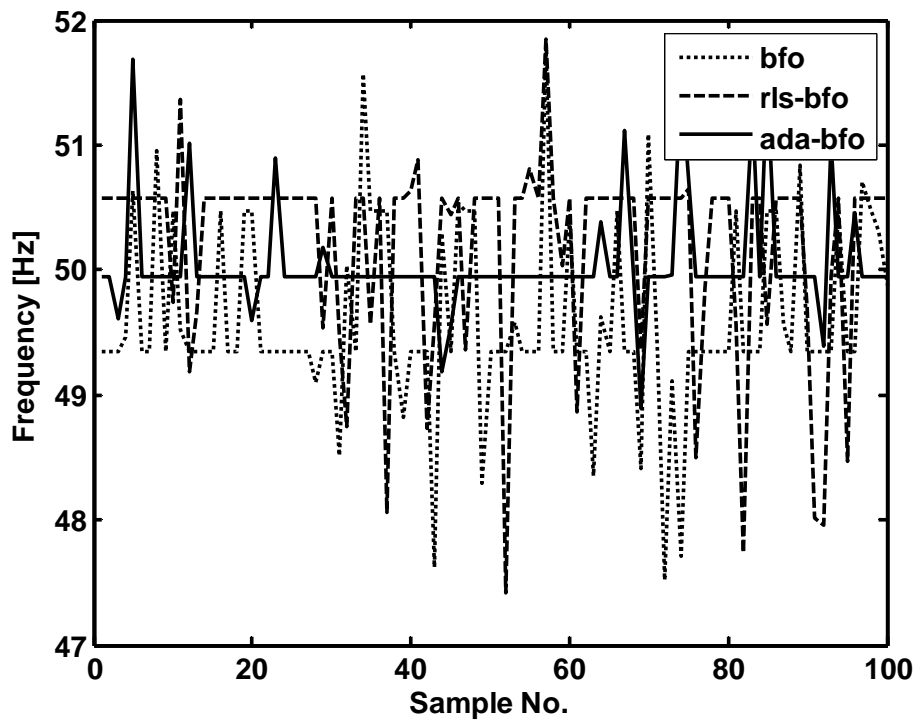
Fig. 3.18 Adaline-BFO estimation performance of Frequency (SNR 40 dB)
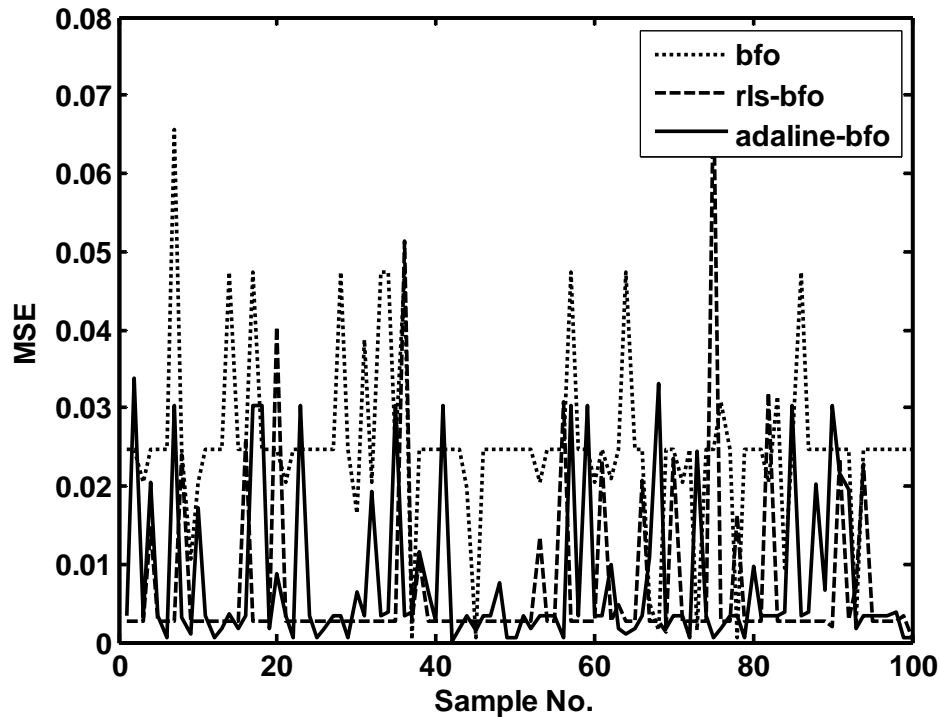
Fig. 3.19 Mean Square Error in the Estimation of Frequency of signal

Figs. 3.16-3.18 show a comparative estimation frequency of signal using BFO, RLS-BFO and Adaline-BFO algorithms at SNR of 20, 30 and 40 dB respectively. From these figures, it is verified that Adaline-BFO estimates more accurately (less estimation error i.e 0.0373 in case of Adaline-BFO at 40dB) compared to other two. Fig. 3.19 shows MSE in the estimation of signal using these three algorithms. MSE performance of Adaline-BFO is comparatively better (Adaline-BFO: 0.0081, RLS-BFO: 0.0129, BFO: 0.0168) as compared to other two.

3.6.2   In presence of Harmonics

The problem of estimating fundamental frequency from signals containing 3rd harmonics is considered. Fig. 3.20 shows the estimation of frequency using different algorithms from the signal with harmonics. It is found that a comparatively better performance(less estimation error i.e 0.0548) is obtained in case of Adaline-BFO algorithm as compared to other two.
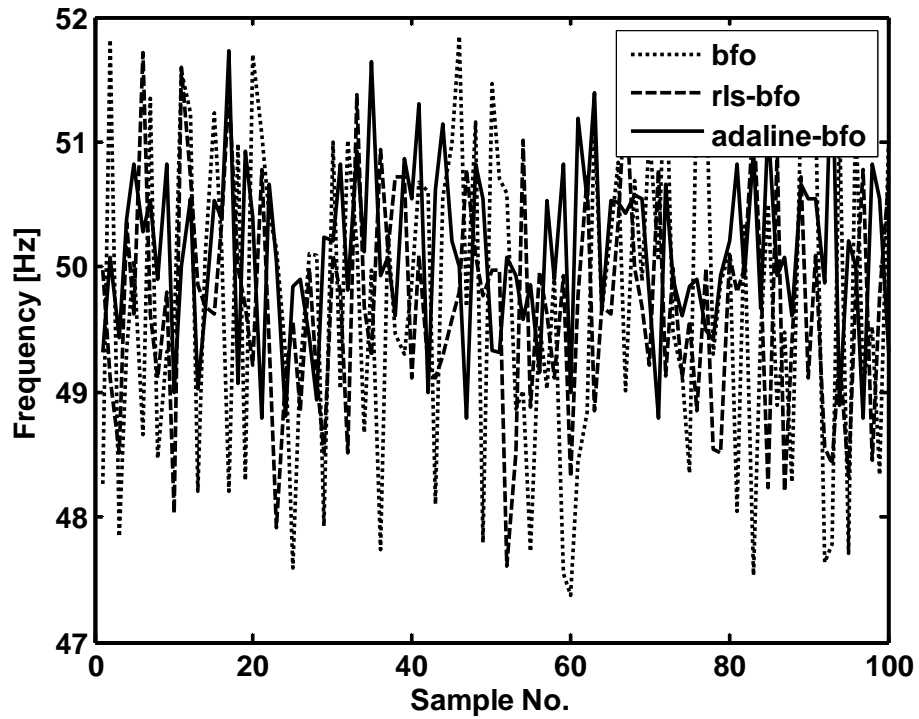
Fig. 3.20 Adaline-BFO estimation performance of Frequency in presence of harmonics

3.6.3 In the presence of Sub-harmonics and Inter-harmonics

For evaluation of the performance of the proposed algorithm in the estimation of frequency of signal in the presence of Sub-harmonics and inter-harmonics, these components are added into the original signal. The frequency of sub-harmonic is 20 Hz, the amplitude is set as 0.5 p.u. and the phase is equal to 75 degrees. The frequency, amplitude and phase of the inter-harmonic is 140 Hz, 0.25 p.u. and 65 degrees respectively.
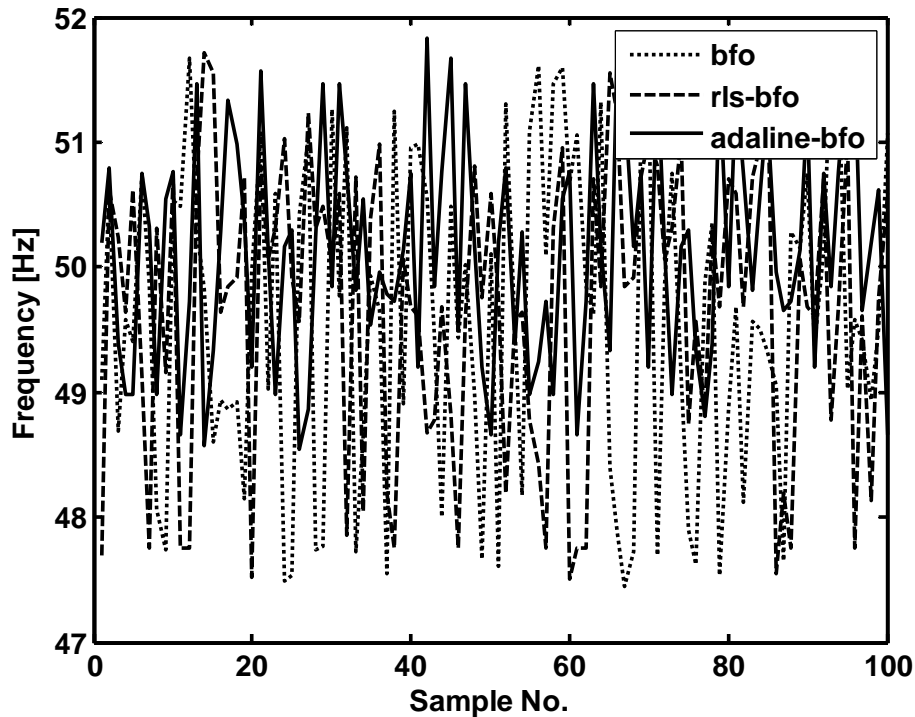
Fig. 3.21 Adaline-BFO estimation performance of Frequency in presence of sub and inter harmonics

Fig. 3.21 shows the estimation of fundamental frequency in presence of sub and inter-harmonics and is found that estimation is more accurate (i.e estimation error of 0.2859) in case of Adaline-BFO as compared to other two.

3.7 Experimental Results

3.7.1 Validation on real-time (Laboratory Setup) data

For real time application of the algorithms in estimating frequency in a power system, data i.e obtained in a laboratory environment from the supply on normal working day of the laboratory as per the experimental setup discussed in section 2.3(a) of fig. 2.19 is taken.
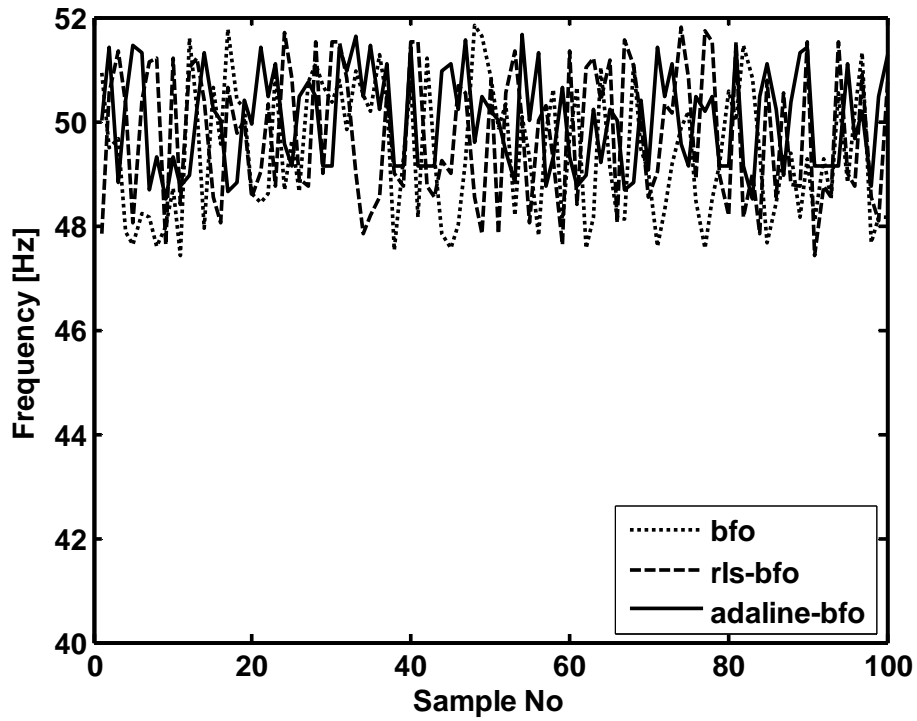
Fig. 3.22 Adaline-BFO estimation performance of Frequency of real data
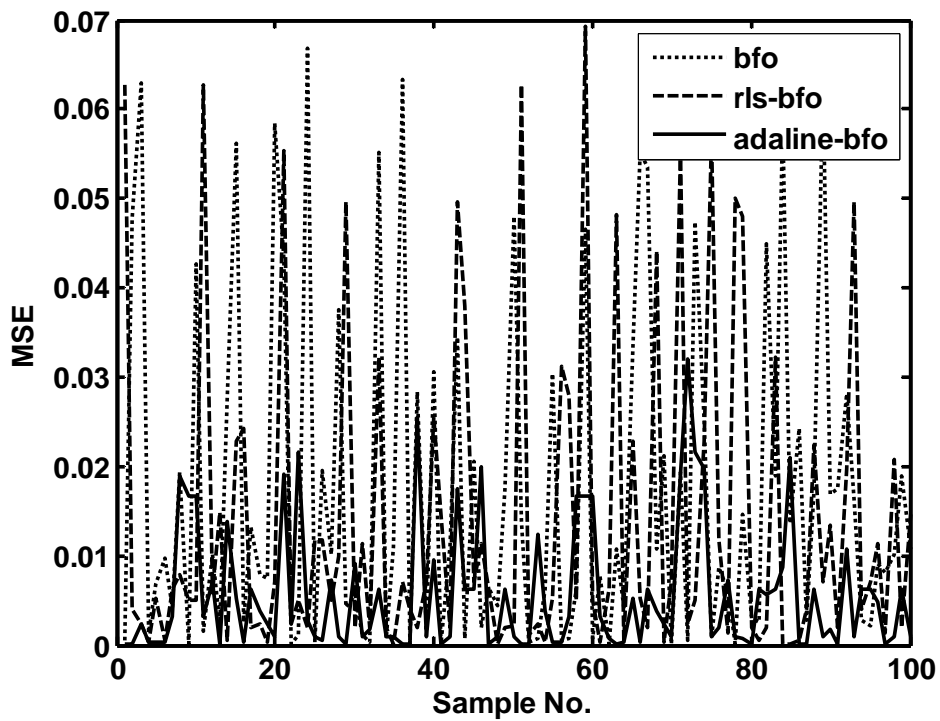
Fig. 3.23 Adaline-BFO estimation performance in MSE of Frequency of real data

Fig. 3.22 shows the estimation of frequency of signal using three algorithms on real data obtained from the experiment. Fig. 3.23 shows the MSE in the estimation of frequency of signal from the real data. From these Figs., it is found that Adaline-BFO provides an improved performance (less estimation error of 0.0956) as compared to other two.

3.7.2 Validation on real-time (Industrial setup) data
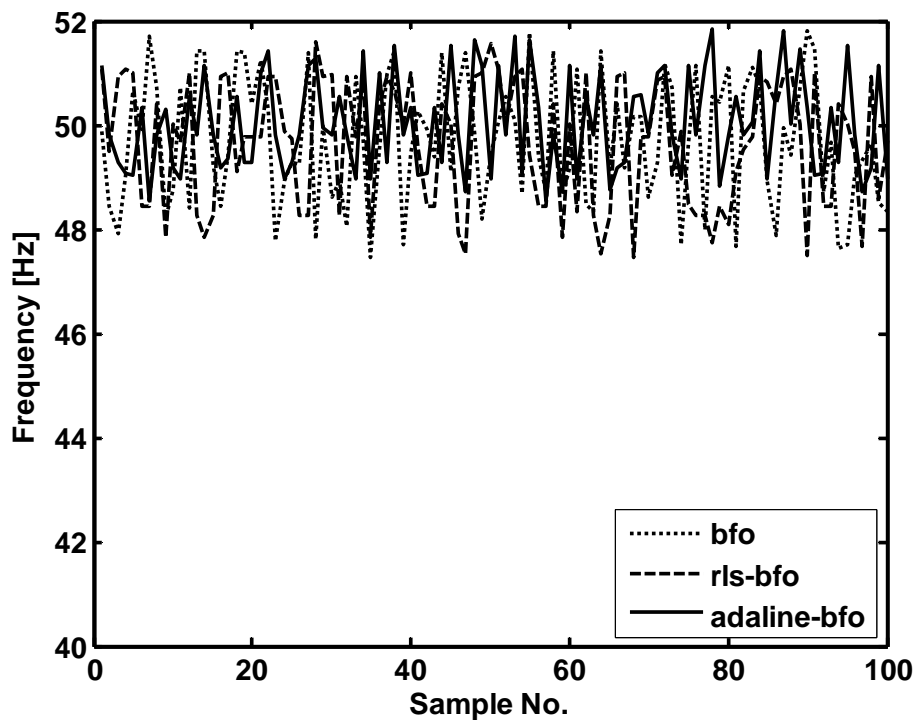
Fig. 3.24 Adaline-BFO estimation performance of Frequency of industrial data

For verification of algorithms with industrial data, data is collected from captive power plant of an aluminium industry as per the setup discussed in section 2.3(b) of Fig. 2.21. The estimated frequency of industrial data is shown in Fig. 3.24 and it is observed that the estimation using Adaline-BFO is better (less estimation error of 0.1246) as compared to RLS-BFO.

3.8 Chapter Summary

In this chapter, four new hybrid algorithms such as RLS-Adaline, KF-Adaline, RLS-BFO and Adaline-BFO are discussed. The performances of the first two proposed hybrid algorithms i.e RLS-Adaline and KF-Adaline are dependent on the initial choice of weight vector W and Covariance matrix P. By using an optimal choice of weight vector, faster convergence to the true value of signal parameter can be achieved. After the optimization of the weight vector, online tracking of frequency of signal can be carried out. Both the algorithms track the frequency of signal at different level of noises and different signal changing conditions but the performance of tracking using KF-Adaline is better than RLS-Adaline. The performances of the next two proposed hybrid BFO algorithms i.e RLS-BFO and Adaline-BFO are very dependent on the initial choice of maximum and minimum value of unknown parameters taken. In this work, we have taken maximum and minimum values as 10% deviation from their actual values. By using an optimal choice of parameters, faster convergence to the true value of signal parameter can be achieved. All the algorithms track the frequency of signals very well but the performance of tracking using Adaline-BFO is better compared to BFO and RLS-BFO algorithms.

Chapter-4

Power system Harmonics Estimation using Recursive Algorithms

4.1 Introduction

In an ac electrical power network, periodical distortions of current and voltage waveforms are unavoidable due to the increasing use of nonlinear and time varying devices. If a voltage or current waveform contains sinusoidal components other than the fundamental frequency, the waveform includes harmonics and the quality of power deteriorates due to presence of harmonics. The major components of causing harmonic pollution in industrial and commercial power systems are the increasing usage of non-linear loads such as diode, thyristor rectifiers, lighting equipments, uninterruptible power supplies (UPS), arc furnaces and adjustable speed motor drives etc. As a result harmonics, sub-harmonics and inter-harmonics are present in current and voltage waveforms. The main sources of inter-harmonics and sub-harmonics are electronics devices such as cycloconverters, which are used in wide range of applications such as rolling mill, linear motor drives and static VAR systems. Furthermore, arcing loads such as welders and arc furnaces are other sources of inter-harmonics. Both harmonics and inter-harmonics have quite negative impacts on power networks and customers. Negative effects of harmonics are increased I^2R losses, over voltage, unbalancing and mal-operations of the relays and saturation of transformer core. Thus, harmonic estimation is one of the critical and challenging issues while dealing with power system signals.

Recent literature [39-68] presents different techniques on power system harmonics estimation. In order to get the voltage and current frequency spectrum from discrete time samples, most frequency domain harmonic analysis algorithms are based on the Fast Fourier transform (FFT). However, FFT based technique suffers from leakage effect i.e an effect in the frequency analysis of finite length signals or finite length segments of infinite signals where it appears as if some energy has 'leaked' out of the original signal spectrum into other frequencies and its performance highly degrades while estimating inter and sub-harmonics,

including frequency deviations. Kalman Filter [37-39] is one of the robust algorithms for estimating the magnitudes of sinusoids of known frequencies embedded in an unknown measurement noise. But this algorithm [74] fails to track any dynamic changes of signal such as sudden changes in amplitude, phase or frequency of signal.

Recently, for more accuracy in estimation, Artificial Intelligence techniques such as fuzzy logic, neural network and evolutionary computations find extensive applications to harmonic estimation. Dash et al. [60] have used an algorithm based on an adaptive neural network, which was reported to track dynamic amplitude better as compared to the classical Kalman filtering approach. However, the initial choice of weight vector and learning parameters may affect the convergence characteristics of the neural network. Qidwai and Betayeb [65-66] use Genetic algorithm (GA), for this purpose. This method provides good results but main disadvantage is that is takes more time for convergence.

To overcome the problems faced in above mentioned techniques, EnKF algorithm for the estimation of harmonics is proposed. EnKF [53-55] is a recursive filter, which can be applied for problems with large number of variables. The Kalman Filter assumes all Probability density functions (pdfs) are Gaussian and use Bayesian update for change of mean and covariance matrix, maintenance of covariance matrix is computationally difficult due to its inverse operation for high dimensional systems. EnKF represents the distribution of system state by a collection of state vectors, known as ensemble and it replaces the covariance matrix by sample covariance, which is computed from the ensemble and is computationally feasible (due to lack of inverse operation) for high dimensional systems. Hence for accurate estimation of power system parameters such as amplitude, phase and frequency, Ensemble Kalman Filter (EnKF) algorithm may be a suitable candidate.

4.1.1 Causes and effects of integer and non-integer harmonics

Inter-harmonics are the components of frequency that are not integer multiples of the system fundamental frequency. Sub-harmonics are the inter-harmonics having frequency lower than the fundamental frequency. Both harmonics and inter-harmonics have quite negative impacts on power networks and customers. The customer produced harmonics are injected back into

the rest of the system. Thus harmonic pollution propagates all over the electrical distribution networks and undesired problems caused by the mis-operation of the electrical devices may occur. Subsequently, operation of electrical devices on the network may be adversely affected. Harmonics and inter-harmonics causes increase in heat of the transformers as a result, it draws high current magnitude. So saturation of transformer occurs and there is increase in eddy current loss. There will be the error in measurement of energy meter in networks and plants distorted by harmonics and inter-harmonics. There will also be loss in efficiency of turbo-generator due to its sub synchronous oscillation.

4.1.2 Causes and effects of decaying DC offset

Electrical signals may include harmonics and decaying dc offsets, especially in a transient state. The objective of estimation of dc offset is to remove these components [83-84] at the stage of signal processing so that error in analog-digital conversion may be minimized in the protection algorithm. Performance of DFT filter is also affected if the signal contains decaying dc component. These are of exponential type and mainly appear in current signals when short circuit occurs in electric power system. The initial value and time constant of this component depend on the time of short circuit (fault incipient angle) and on the X/R ratio of the circuit involved in the fault. When the signal analyzed includes an exponentially decaying, phase estimated using DFT has an error of up to 15%.

4.2 Harmonics Estimation Using Different Algorithms

4.2.1 Harmonics Estimation using Least Mean Square (LMS) algorithm

Let us assume the voltage or current waveforms of the known fundamental angular frequency ω as the sum of harmonics of unknown magnitudes and phases. The general form of the waveform is

$$y(t) = \sum_{n=1}^{N} A_n \sin(\omega_n t + \phi_n) + A_{dc} \exp(-\alpha_{dc} t) + \varepsilon(t) \tag{4.1}$$

where N is the number of harmonics. $\omega_n = n2\pi f_0$; f_0 is the fundamental frequency; $\varepsilon(t)$ is the additive noise; $A_{dc}\exp(-\alpha_{dc}t)$ is the dc offset decaying term.

After discretization of Eq. (4.1) with a sampling period, T one obtains the following expressions

$$y(k) = \sum_{n=1}^{N} A_n \sin(\omega_n kT + \phi_n) + A_{dc}\exp(-\alpha_{dc}kT) + \varepsilon(k) \tag{4.2}$$

Invoking Taylor series expansion of the dc decaying term, $A_{dc}\exp(-\alpha_{dc}t)$ and retaining only first two terms of the series yields

$$y_{dc} = A_{dc} - A_{dc}\alpha_{dc}kT \tag{4.3}$$

Using Eq. (4.3) in Eq. (4.2), $y(k)$ can be obtained as

$$y(k) = \sum_{n=1}^{N} A_n \sin(\omega_n kT + \phi_n) + A_{dc} - A_{dc}\alpha_{dc}kT + \varepsilon(k) \tag{4.4}$$

For estimation amplitudes and phases Eq.(4.4) can be rewritten as

$$y(k) = \sum_{n=1}^{N} [A_n \sin(\omega_n kT)\cos\phi_n + A_n \cos(\omega_n kT)\sin\phi_n] + A_{dc} - A_{dc}\alpha_{dc}kT + \varepsilon(k) \tag{4.5}$$

Eq. (4.5) can be rewritten in parametric form as follows

$$y(k) = H(k)X$$

$$H(k) = [\sin(\omega_1 kT) \quad \cos(\omega_1 kT) \quad ... \quad \sin(\omega_N kT) \quad \cos(\omega_N kT) \quad 1 \quad -kT]^T \tag{4.6}$$

The vector of unknown parameter

$$X(k) = [X_1(k) \quad X_2(k) \quad ... \quad X_{2N-1}(k) \quad X_{2N}(k) \quad X_{2N+1}(k) \quad X_{2N+2}(k)]^T \tag{4.7}$$

$$X = [A_1\cos(\phi_1) \quad A_1\sin(\phi_1) \quad ... \quad A_n\cos(\phi_n) \quad A_n\sin(\phi_n) \quad A_{dc} \quad A_{dc}\alpha_{dc}]^T \tag{4.8}$$

The LMS algorithm is applied to estimate the state. The algorithm minimizes the square of the error recursively by altering the unknown parameter X_k at each sampling instant using equation (4.9) given below

$$X_k = X_{k-1} + \mu_k e_k \hat{y_k} \tag{4.9}$$

where the error signal is

$$e_k = y_k - \hat{y_k}$$

The step size μ_k is varied for better convergence of the LMS algorithm in the presence of noise.

$$\mu_{k+1} = \lambda\mu_k + \gamma R_k^2 \tag{4.10}$$

where R_k represents the autocorrelation of e_k and e_{k-1}. It is computed as

$$R_k = \rho R_{k-1} + (1-\rho)e_k e_{k-1} \tag{4.11}$$

where ρ is an exponential weighting parameter and $0 < \rho < 1$, and $\lambda(0 < \lambda < 1)$ and $\gamma > 0$ control the convergence time.

After the updating of the vector of unknown parameter using LMS algorithm, amplitudes, phases of the fundamental and nth harmonic parameters and dc decaying parameters are derived as

$$A_n = \sqrt{\left(X_{2N}^2 + X_{2N-1}^2\right)} \tag{4.12}$$

$$\phi_n = \tan^{-1}\left(\frac{X_{2N}}{X_{2N-1}}\right) \tag{4.13}$$

$$A_{dc} = X_{2N+1} \tag{4.14}$$

$$\alpha_{dc} = \left(\frac{X_{2N+2}}{X_{2N+1}}\right) \tag{4.15}$$

4.2.2 Harmonics Estimation using RLS algorithm

The signal as described in section 4.2.1 is taken; the vector of unknown parameter X, as in (4.7) is updated using RLS as

X is updated using Recursive Least Square Algorithm as

$$\hat{X}(k+1) = \hat{X}(k) + K(k+1)e(k+1) \tag{4.16}$$

Error in measurement is

$$e(k+1) = y(k+1) - H(k+1)^T \hat{X}(k) \tag{4.17}$$

The gain K is related with covariance of parameter vector

$$K(k+1) = P(k)H(k+1)[1 + H(k+1)^T P(k)H(k+1)]^{-1} \tag{4.18}$$

The updated covariance of parameter vector using matrix inversion lemma

$$P(k+1) = [I - K(k+1)H(k+1)^T]P(k) \tag{4.19}$$

These equations are initialized by taking some initial values for the estimate at instants $t, \theta(t)$ and P. As the choice of initial covariance matrix is large it is taken as $P = \alpha I$, where α is a large number and I is a square identity matrix.

After the updating of the vector of unknown parameters using Recursive Least Square (RLS) algorithm, amplitudes, phases of the fundamental and nth harmonic parameters and dc decaying parameters can be derived using (4.12)-(4.15)

4.2.3 Harmonics Estimation using Recursive Least Mean Square (RLMS) algorithm

After the updating of the vector of unknown parameter using Recursive Least Square (RLS) algorithm, updated values of unknown parameters are taken as initial values of unknown for LMS algorithm. Then unknown parameters are updated using LMS algorithm.

4.2.4 Harmonics Estimation using Kalman Filter (KF) algorithm

The signal as described in section 4.2.1 is taken; the vector of unknown parameters X, as in (4.7) is updated using Kalman Filter algorithm as

$$G(k) = P(k/k-1)H(k)^T (H(k)P(k/k-1)H(k)^T + Q)^{-1} \tag{4.20}$$

G is the Kalman gain, H is the observation vector, P is the covariance matrix, Q is the noise covariance of the signal.

The covariance matrix is related with Kalman gain as given in the following equation.

$$P(k/k) = P(k/k-1) - G(k)H(k)P(k/k-1) \tag{4.21}$$

The updated estimated state vector is related with previous state vector as follows.

$$\hat{X}(k/k) = \hat{X}(k/k-1) + G(k)(y(k) - H(k)\hat{X}(k/k-1)) \tag{4.22}$$

After the updating of weight vector, amplitudes, phases of the fundamental and nth harmonic parameters and dc decaying parameters are found out using (4.12)-(4.15)

4.2.5 Harmonics Estimation using Ensemble Kalman Filter (EnKF) algorithm

The EnKF is a Monte Carlo approximation (useful for modeling with significant uncertainty in inputs) of the Kalman filter, which avoids evolving the covariance matrix of the probability density function (pdf) of the state vector x. In this case, the distribution is represented by a sample, which is called an ensemble

$$X = [x_1, x_2, \cdots, x_N]$$ (4.23)

X is an $n \times N$ matrix whose columns are the ensemble members, and it is called the prior ensemble. Ensemble members form a sample from the prior distribution. As every EnKF step ties ensemble members together so they are not independent. Signal data $y(t)$ is arranged as a $m \times N$ matrix

The vector of unknown parameter/ Ensemble as in (4.7) and (4.8) is given by

$$X(k) = [X_1(k) \quad X_2(k) \quad \dots \quad X_{2N-1}(k) \quad X_{2N}(k) \quad X_{2N+1}(k) \quad X_{2N+2}(k)]^T$$
$$X = [A_1 \cos(\phi_1) \quad A_1 \sin(\phi_1) \quad \dots \quad A_n \cos(\phi_n) \quad A_n \sin(\phi_n) \quad A_{dc} \quad A_{dc}\alpha_{dc}]^T$$

is updated using Ensemble Kalman Filtering as

The ensemble mean and covariance are

$$E(X) = \frac{1}{Q} \sum_{k=1}^{Q} X(k)$$ (4.24)

and $$C = \frac{GG^T}{Q-1}$$ (4.25)

where

$$G = X - E(X)$$ (4.26)

The updated ensemble is then given by

$$\hat{X} = X + CH^T (HCH^T + R)^{-1} (y - HX)$$ (4.27)

Where, columns of X represent a sample from the prior probability distribution and columns of $\hat{X}$ will form a sample from the posterior probability distribution. The EnKF is now obtained by replacing the state covariance P in Kalman gain matrix $K = PH^T (HPH^T + R)^{-1}$ by the

sample covariance C computed from the ensemble members (also called as ensemble covariance), where R is a covariance matrix, it is always positive semi definite and usually positive definite, so the inverse of above exists.

After the updating of the vector of unknown parameter using Ensemble Kalman Filtering algorithm, amplitudes, phases of the fundamental and nth harmonic parameters and dc decaying parameters are are found out using (4.12)-(4.15).

Description of EnKF algorithm based harmonics estimation

1. Initialize Amplitude, phase, frequency of fundamental and harmonics components, dc decaying components and ensemble vector

2. Generate a power system signal containing fundamental and higher order harmonics as per (4.28)

3. Discretize it and model in parametric form using (4.6)

4. Evaluate: Estimation error = Actual signal - Estimated signal (using initial ensemble in parametric form)

5. Find mean and covariance of ensemble using (4.24-4.26)

6. Update ensemble vector as per (4.27)

7. If final iteration is not reached, go to step 4

8. Estimate Amplitude, phase of fundamental and harmonic components and dc decaying components using (4.12)-(4.15).

4.3 Simulation Studies and Results

4.3.1 Static signal corrupted with random noise and decaying DC component

To evaluate the performance of the proposed algorithm in estimating harmonics amplitude and phase, Numerical experiments implemented in MATLAB have been performed. The power system signal used for the estimation, besides the fundamental frequency, contains higher harmonics of the 3rd, 5th, 7th, 11th and a slowly decaying DC component. This kind of signal is typical in industrial load comprising power electronic converters and arc furnaces [60].

$$y(t) = 1.5\sin(\omega t + 80^0) + 0.5\sin(3\omega t + 60^0) + 0.2\sin(5\omega t + 45^0) + 0.15\sin(7\omega t + 36^0)$$
$$+ 0.1\sin(11\omega t + 30^0) + 0.5\exp(-5t) + \varepsilon(t)$$

(4.28)

The signal is corrupted by random noise $\varepsilon(t) = 0.05randn$ of zero mean, normal distribution and unity variance.

Table 4.1 shows the different parameters used during simulation work

Table-4.1
Parameters used for simulation (RLS, LMS, KF, RLMS and EnKF)

Algorithms	R	δ	η	ρ	λ	γ	Initial μ	Initial W
RLS	-	100	0.96	-	-	-	-	-
LMS	-	-	-	0.99	0.97	0.001	0.001	0.018
KF	$100(I_{100\times100})$	100	-	-	-	-	-	-
RLMS	-	100	0.96	0.99	0.97	0.001	0.001	0.018
EnKF	$100(I_{100\times100})$	-	-	-	-	-	-	-
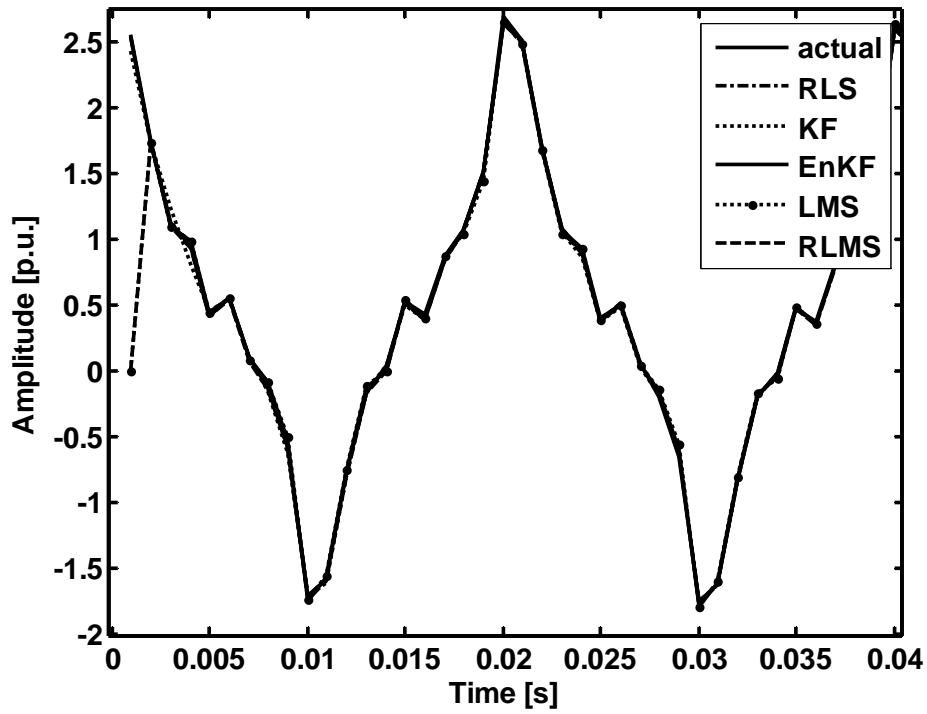
Fig.4.1 Actual and Estimated signal using RLS, KF, EnKF, LMS and RLMS
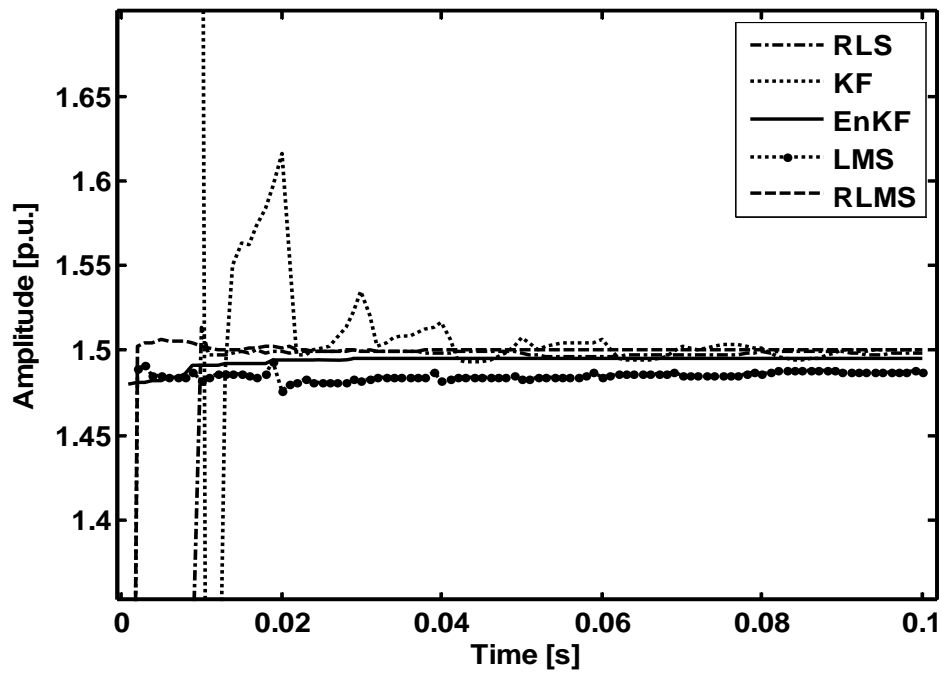
Fig.4.2 EnKF estimation performance of amplitude of fundamental component of signal
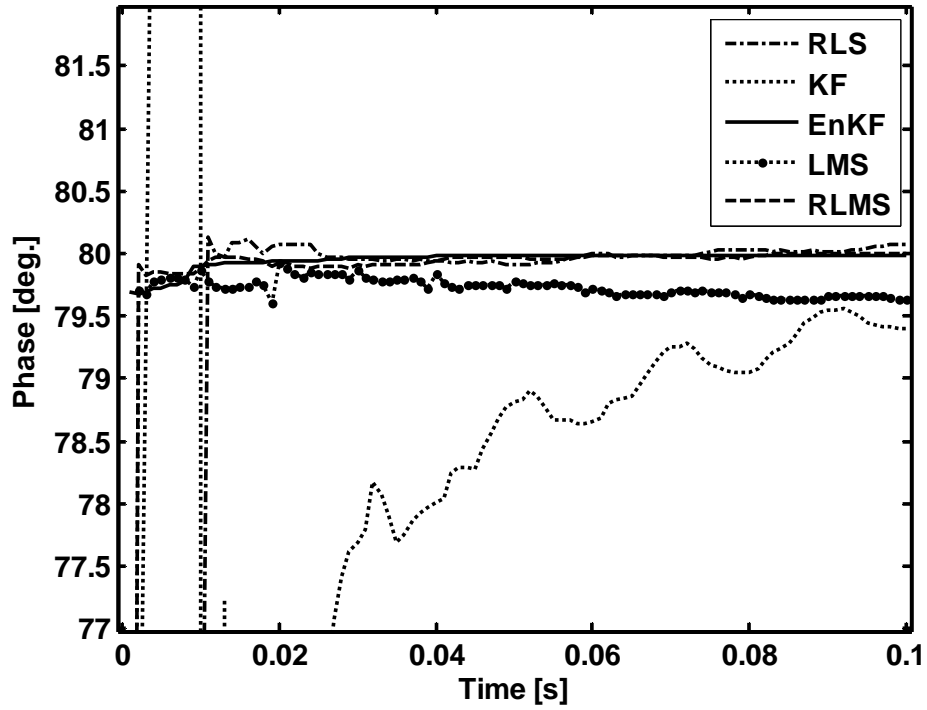
Fig.4.3 EnKF estimation performance of phase of fundamental component of signal
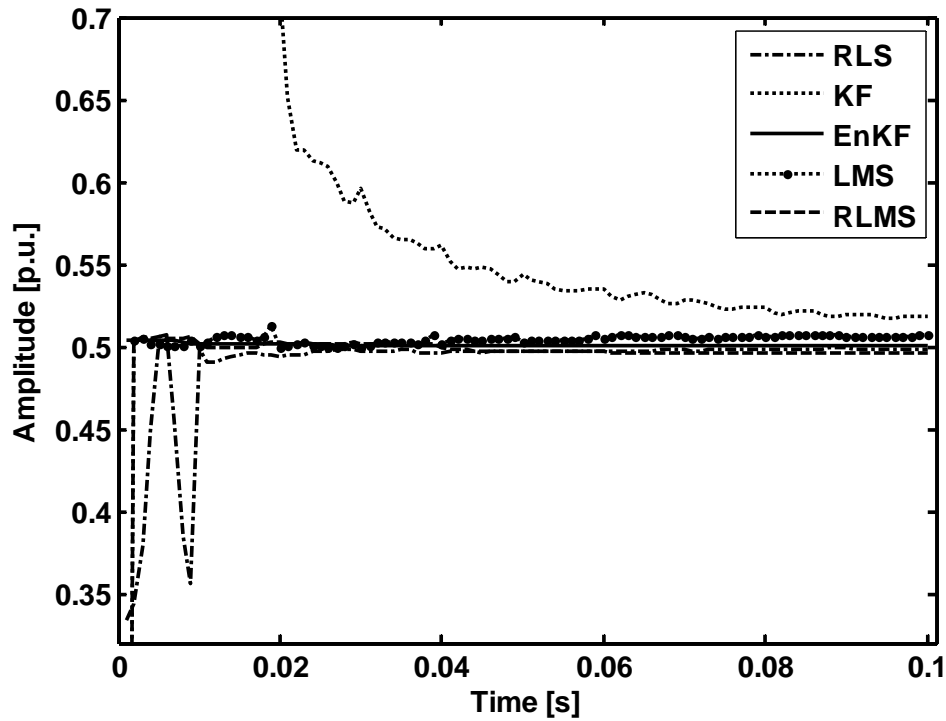
Fig.4.4 EnKF estimation performance of amplitude of 3rd harmonic component of signal
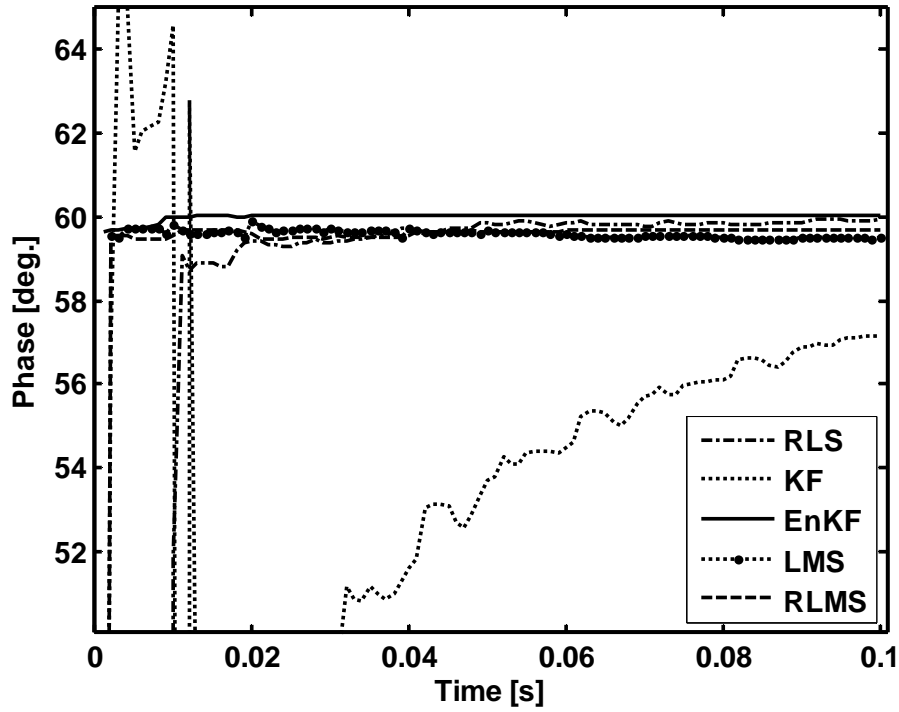
Fig.4.5 EnKF estimation performance of phase of 3rd harmonic component of signal
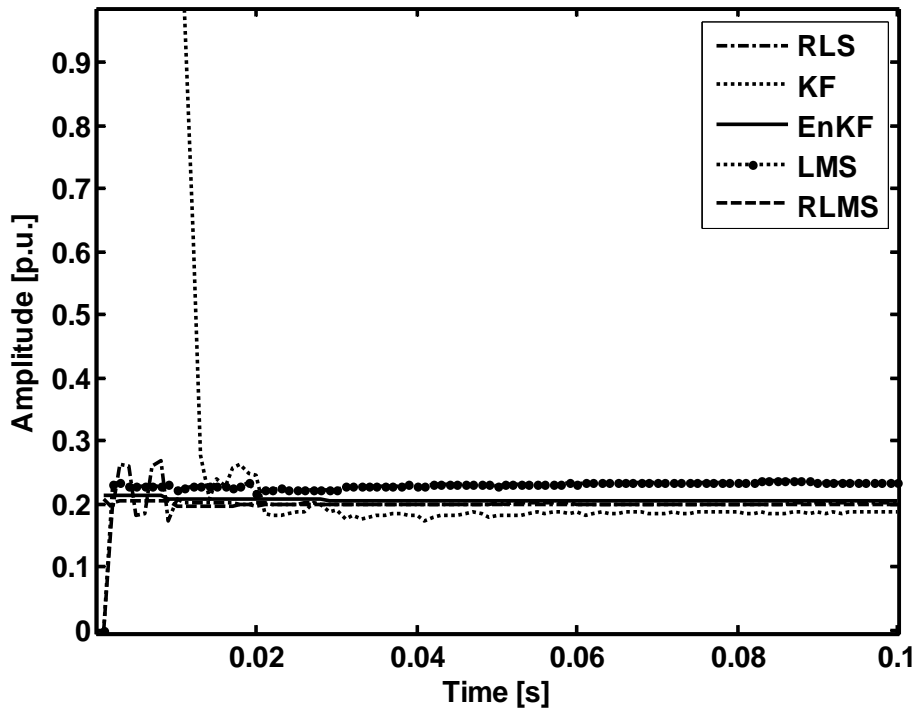
Fig.4.6 EnKF estimation performance of amplitude of 5th harmonic component of signal
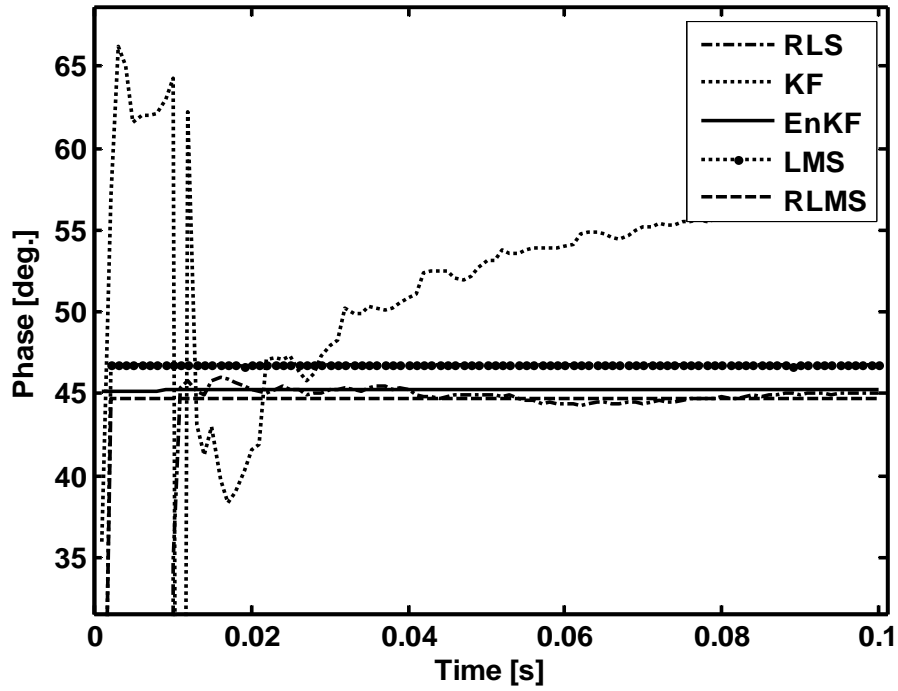
Fig.4.7 EnKF estimation performance of phase of 5th harmonic component of signal
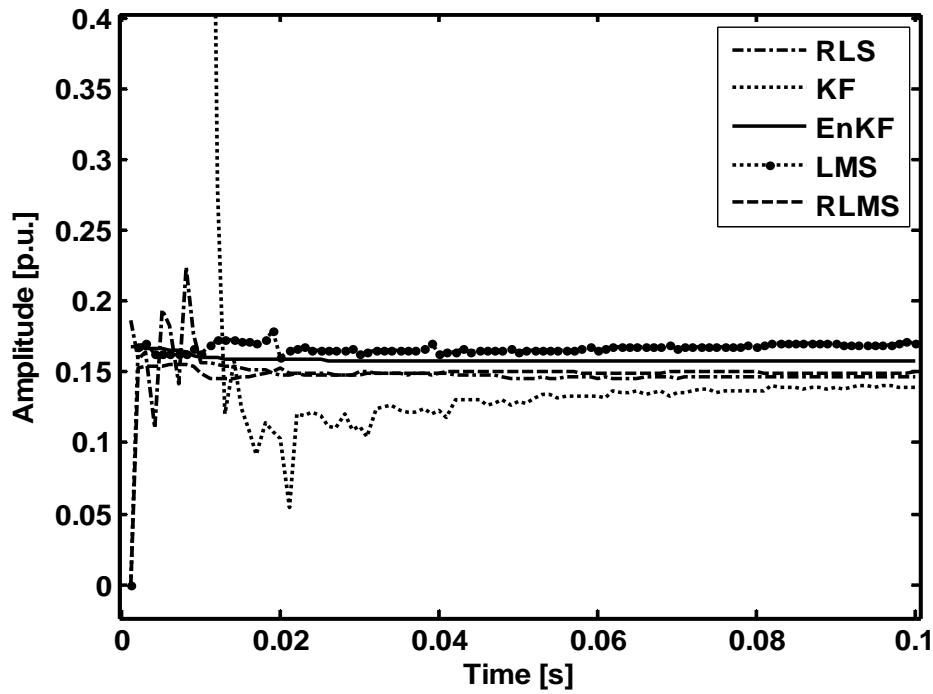
Fig.4.8 EnKF estimation performance of amplitude of 7th harmonic component of signal
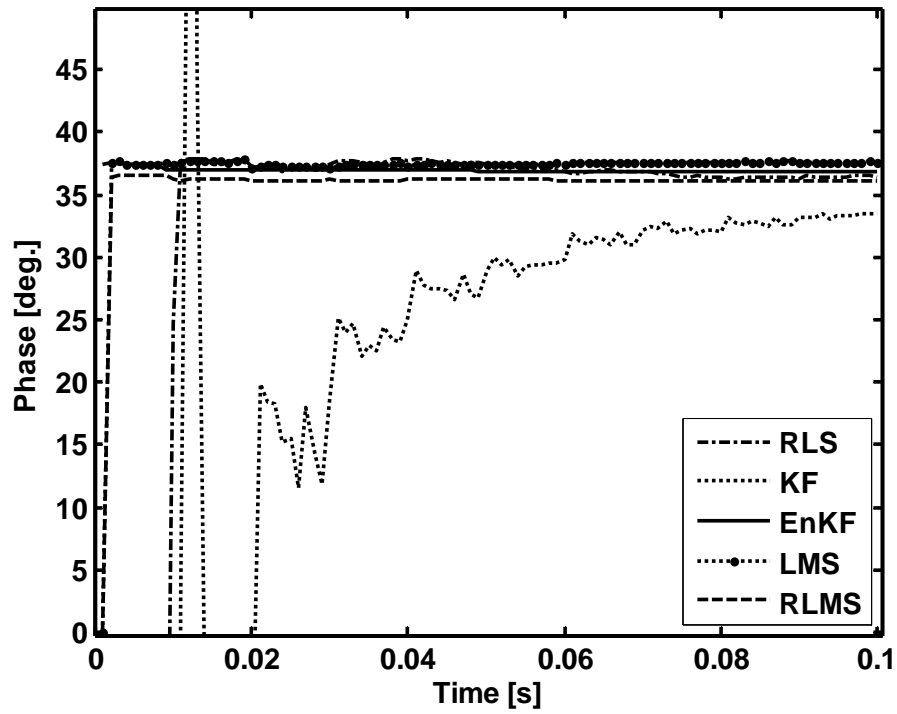
Fig.4.9. EnKF estimation performance of phase of 7th harmonic component of signal
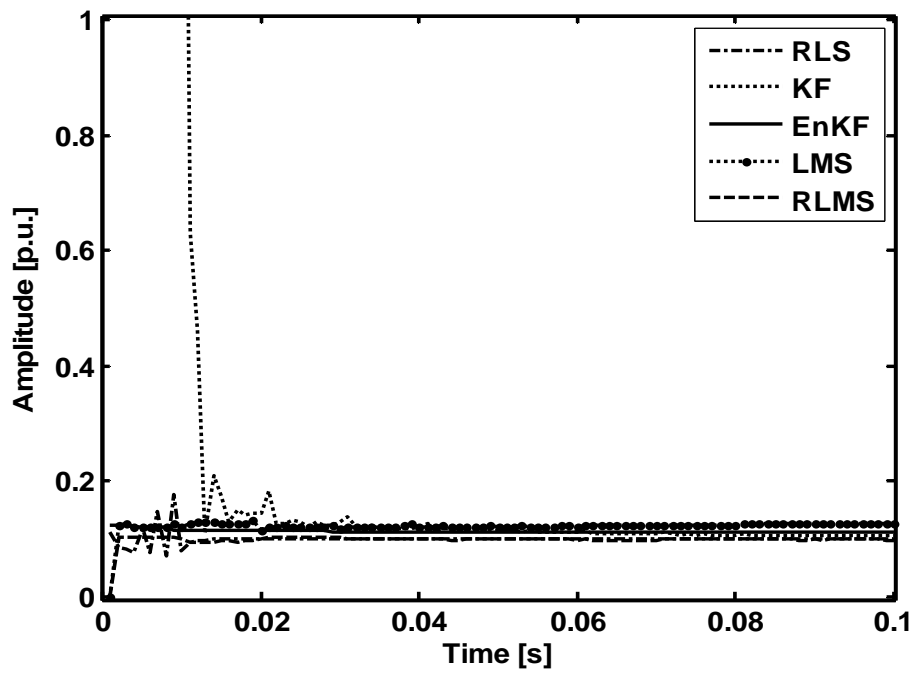
Fig.4.10. EnKF estimation performance of amplitude of 11th harmoniccomponent of signal
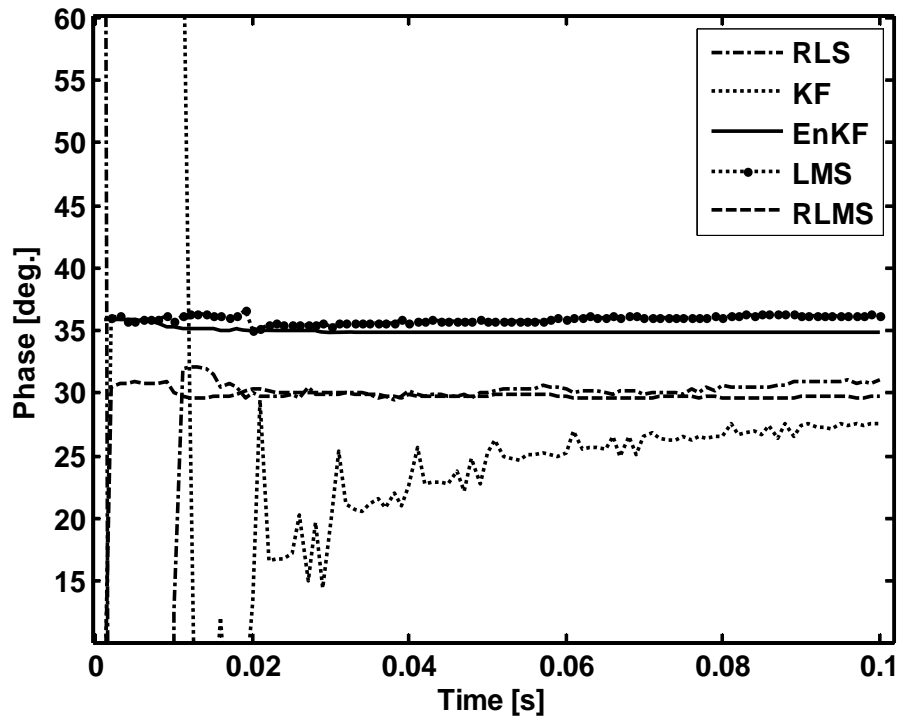
Fig.4.11 EnKF estimation performance of phase of 11th harmonic component of signal

Fig. 4.1 shows actual vs. estimated value of signal using five different algorithms. Actual vs estimated signal almost matches with each other with little deviation in case of KF algorithm. Fig. 4.2-4.11 show the tracking of fundamental, 3rd, 5th, 7th and 11th harmonics signal components in presence of random noise and decaying dc components using LMS, RLS, RLMS, KF and EnKF algorithms. KF, RLS and RLMS are tuned optimally by properly choosing the co-variance and noise variance matrices. In EnKF, the covariance matrix is replaced by sample covariance computed from ensemble. Using Kalman Filter results in oscillations in the estimated amplitude of fundamental and harmonics components in the presence of a distorted signal and noise. Time required to reach the actual values for the fundamental and harmonics components is 0.02 seconds or more on a 50 Hz system. Using RLS, the exact value of fundamental and harmonics components are obtained roughly in 0.01 sec. based on a 50 Hz waveform in presence of random noise and decaying dc components. In case of LMS and RLMS, the reference value is tracked within 0.0025 seconds. However, using EnKF, the reference value is tracked within less than 0.0025 seconds, which can be

marked in a zoomed figure. These results are quite significant in tracking steady-state fundamental and harmonics components of a power system over a period of 24 hours for the assessment of power quality and harmonics distortions.
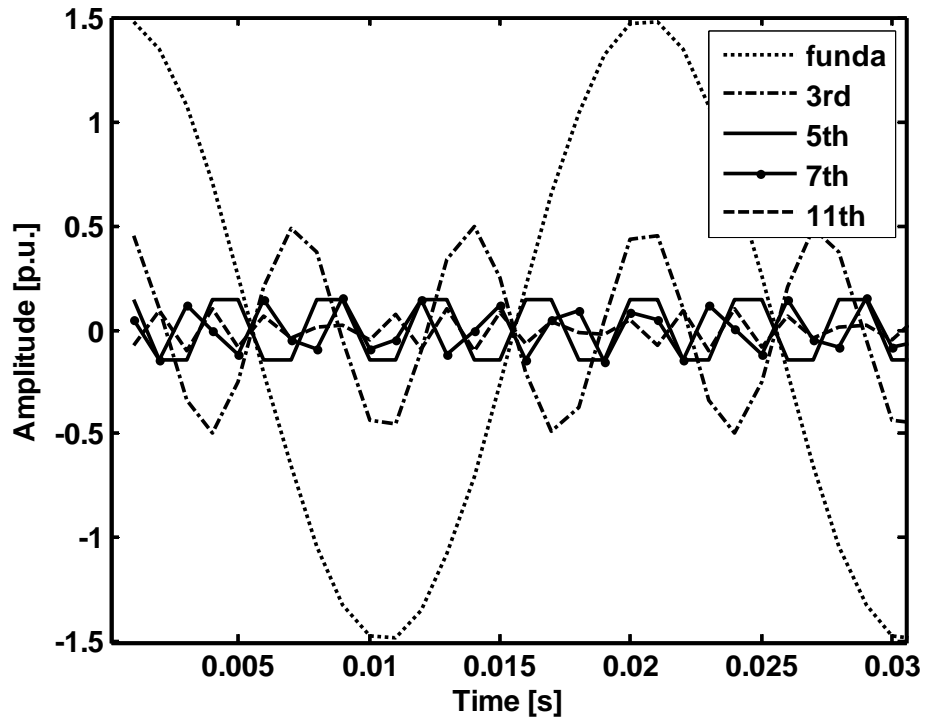
Fig. 4.12 Estimation of fundamental and harmonics components of signal (EnKF)
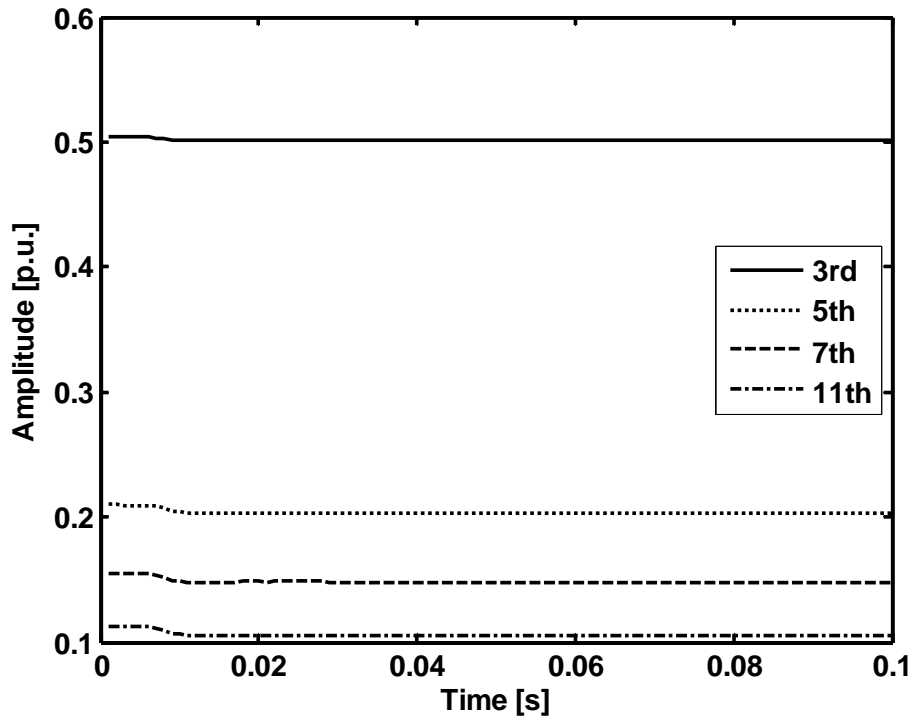
Fig.4.13 Estimation of amplitude of all harmonics component of signal using EnKF
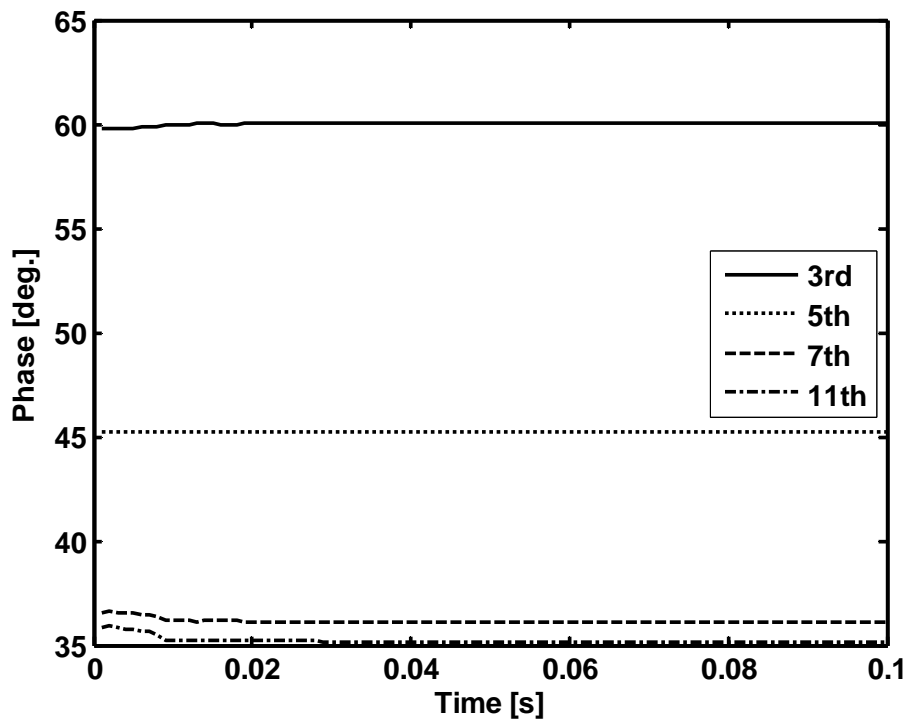
Fig.4.14 Estimation of phase of all harmonics component of signal using EnKF
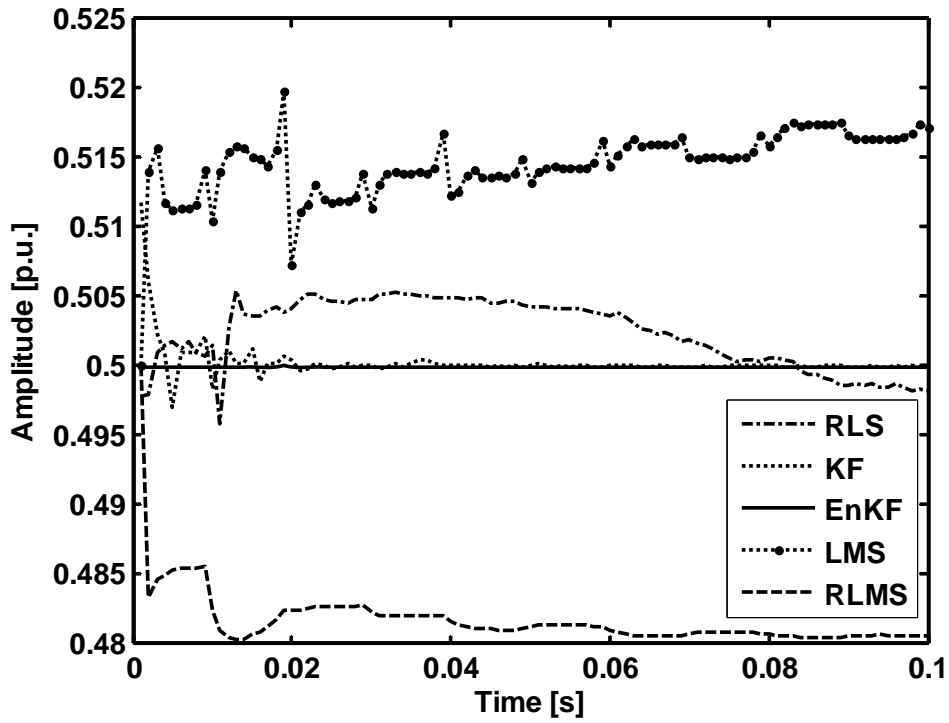
Fig.4.15 EnKF estimation performance of dc component of signal
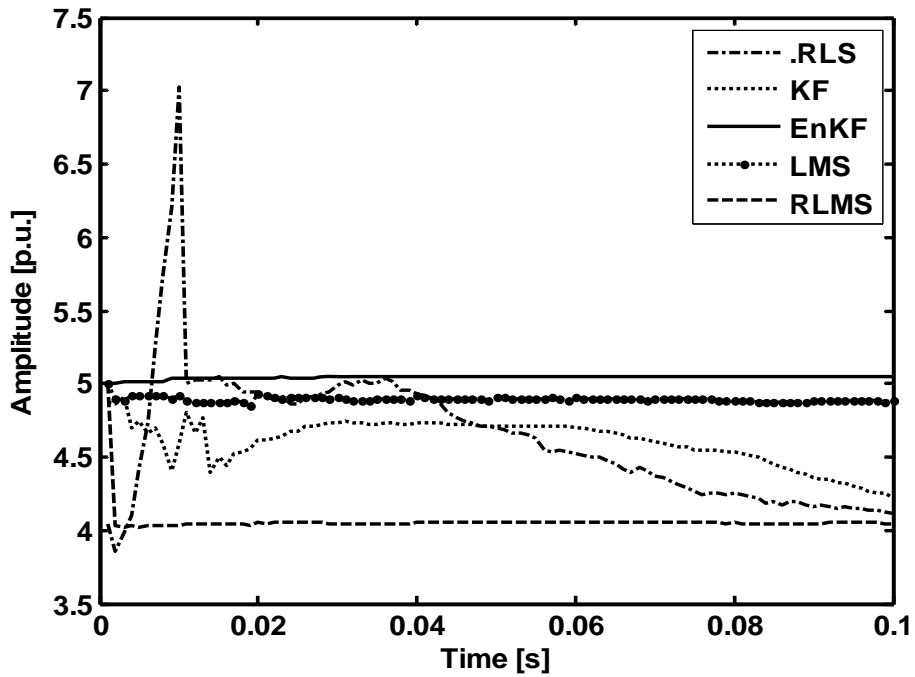
Fig.4.16 EnKF estimation performance of decaying dc offset of signal
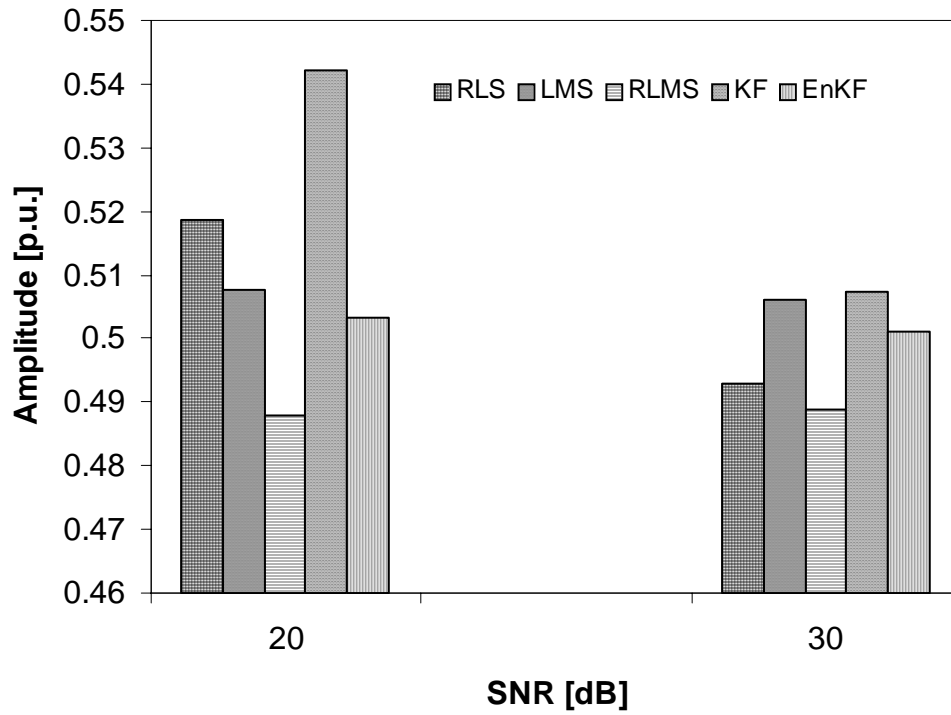
Fig. 4.17 Comparison of Estimation of amplitude of 3rd harmonic component of signal using bar chart
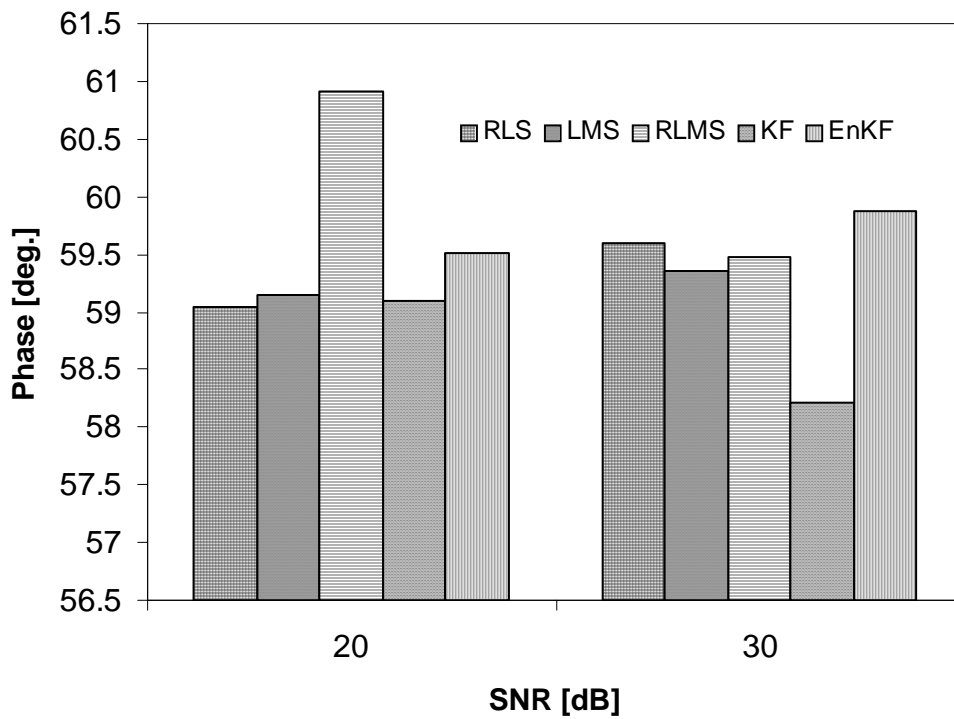
Fig. 4.18 Comparison of Estimation of phase of 3rd harmonic component of signal using bar chart
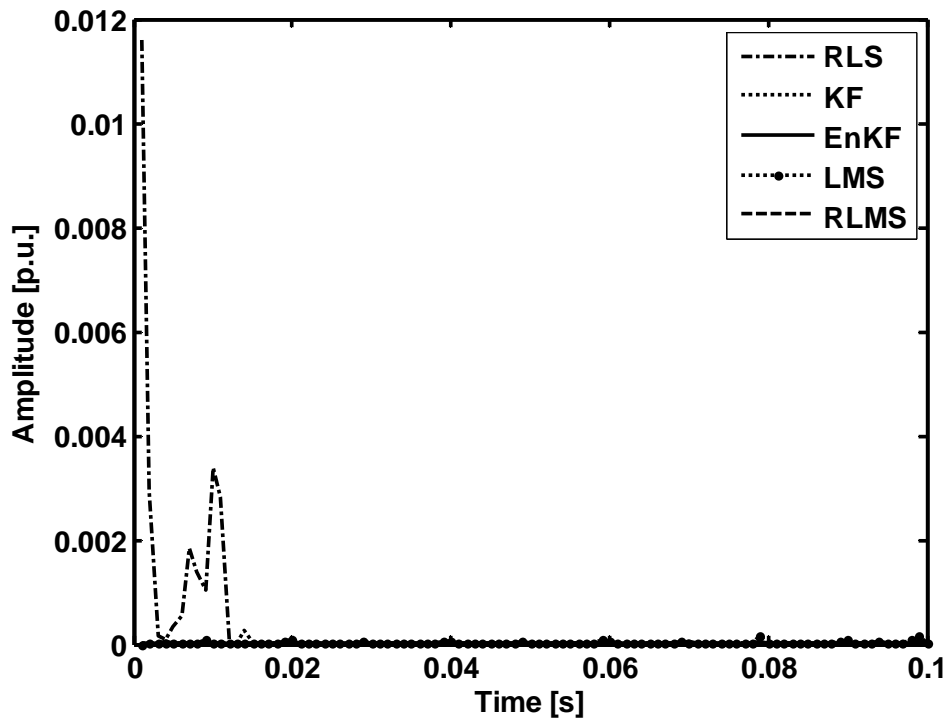
Fig.4.19. EnKF estimation performance of Mean Squared Error of signal

Fig. 4.12 shows the segregation of estimation of fundamental and all the harmonics of that signal using Ensemble Kalman Filter. From the figure, it is seen that highly accurate estimation is obtained in each case of estimation. Fig. 4.13 and 4.14 show the estimation of amplitude and phase of all harmonics components using EnKF. From the Figs., it is clear that EnKF accurately estimate the harmonics components in presence of noise and decaying dc-offsets. Fig. 4.15 and 4.26 show the estimation of dc component and decaying dc-offsets of signal using all the five algorithms with more accuracy in estimation using EnKF. Fig. 4.17 and 4.18 give a comparison of estimation of 3rd harmonic amplitude and phase of signal with 20 dB and 30 dB noises. From these two figs. concluded that estimation using EnKF is more accurate (amplitude 0.505 and phase 59.7-60 degrees) as compared to other four. Fig. 4.19 shows the comparison of MSE using the above five algorithms. From the figure, it is observed that MSE becomes zero after 0.015 seconds using KF algorithm but using LMS, RLS, RLMS and EnKF, the MSE becomes zero initially.

Table 4.2
Performance comparison of EnKF in presence of harmonics and d.c. offsets

Methods	Parameters	Fund-	3rd	5th	7th	11th	A_{dc}	α_{dc}	Comp. time (s)
Actual	f(Hz)	50	150	250	350	550	0. 5	5	
	A (V)	1.5	0.5	0.2	0.15	0.1			
	$\varphi(°)$	80	60	45	36	30			
DFT	A (V)	1.484	0.4852	0.1706	0.1535	0.0937	0.385	-	
	Deviation (%)	1.040	2.9507	14.682	2.3597	6.2761			
	$\varphi(°)$	80.57	60.30	47.098	34.354	25.300			
	Deviation (°)	0.570	0.3002	2.0985	1.646	4.6993			
LMS	A (V)	1.476	0.502	0.232	0.167	0.123	0. 512	4.8	0.348
	Deviation (%)	1.541	0.450	16.42	11.55	23.46			
	$\varphi(°)$	79.30	59.306	46.497	37.321	35.80			
	Deviation (°)	0.699	0.693	1.497	1.321	5.8			
RLS	A (V)	1.483	0.503	0.196	0.153	0.113	0. 504	4. 5	0.114
	Deviation (%)	1.131	0.76	1.795	2.530	13.829			
	$\varphi(°)$	78.57	58.381	42.908	34.189	32.682			
	Deviation (°)	1.506	1.618	2.091	1.810	2.682			
KF	A (V)	1.506	0.503	0.225	0.158	0.095	0. 503	4. 6	0.360
	Deviation (%)	0.453	0.681	12.69	5.717	4.922			
	$\varphi(°)$	80.25	59.839	46.827	34.464	34.994			
	Deviation (°)	0.253	0.161	1.827	1.535	4.994			
RLMS	A (V)	1.492	0.497	0.197	0.151	0.103	0.483	4. 1	1.418
	Deviation (%)	0.536	0.437	1.320	0.994	3.036			
	$\varphi(°)$	79.79	59.779	44.638	36.921	28.633			
	Deviation (°)	0.427	0.22	0.386	0.921	1.366			
EnKF	A (V)	1.498	0.501	0.200	0.151	0.0989	**0. 499**	**5.05**	**0.097**
	Deviation (%)	**0.113**	**0.191**	**0.198**	**0.909**	**1.088**			
	$\varphi(°)$	79.97	59.964	44.613	35.854	29.948			
	Deviation (°)	**0.028**	**0.035**	**0.361**	**0.145**	**0.051**			

Table 4.2 gives the simulation results obtained by the LMS, RLS, RLMS, KF and the proposed EnKF method.   Table shows that harmonics parameters obtained with the proposed approach exhibits the best estimation precision where the largest amplitude deviation is 1.0882% occurred at the 11th harmonics estimation and the largest phase angle deviation is 0.361^{0} occurred at the 5th harmonics estimation.

4.3.2 Estimation of harmonics in presence of amplitude drift

For considering the real time situations of a power system signal, abrupt change in amplitude of signal is taken into account in this section. Cases of 3rd and 5th harmonic component changes are considered. 3rd harmonic component of signal is allowed to change from 0.5 p.u. to 2 p.u. at 0.05 second and similarly 5th harmonic component is allowed to change from 0.2 p.u. to 1 p.u. at 0.05 second in the signal given in (4.28)
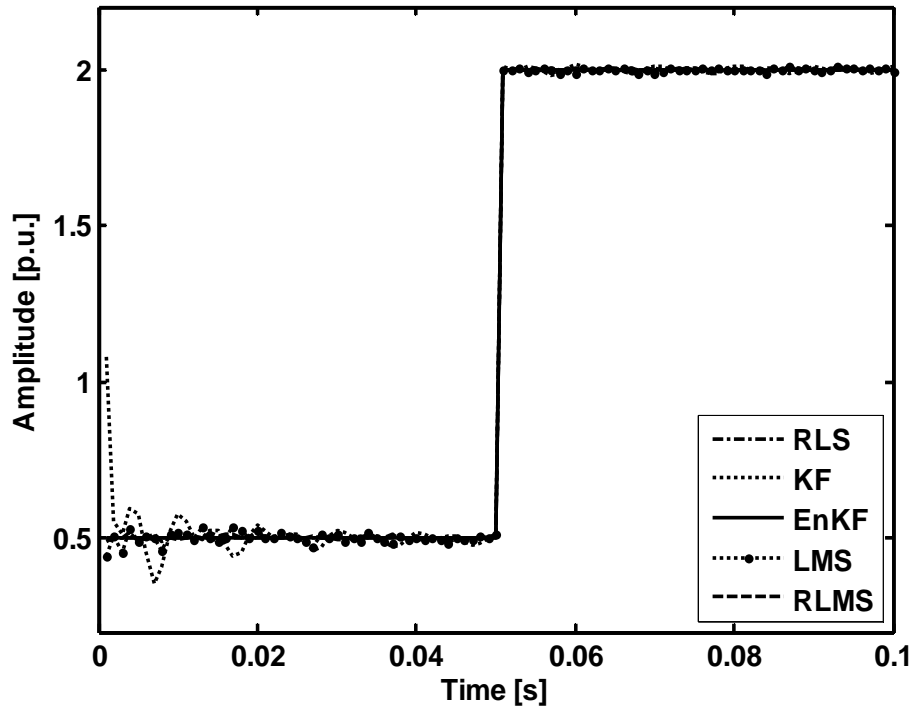
Fig.4.20. EnKF estimation performance of amplitude of 3rd harmonic component during amplitude drift
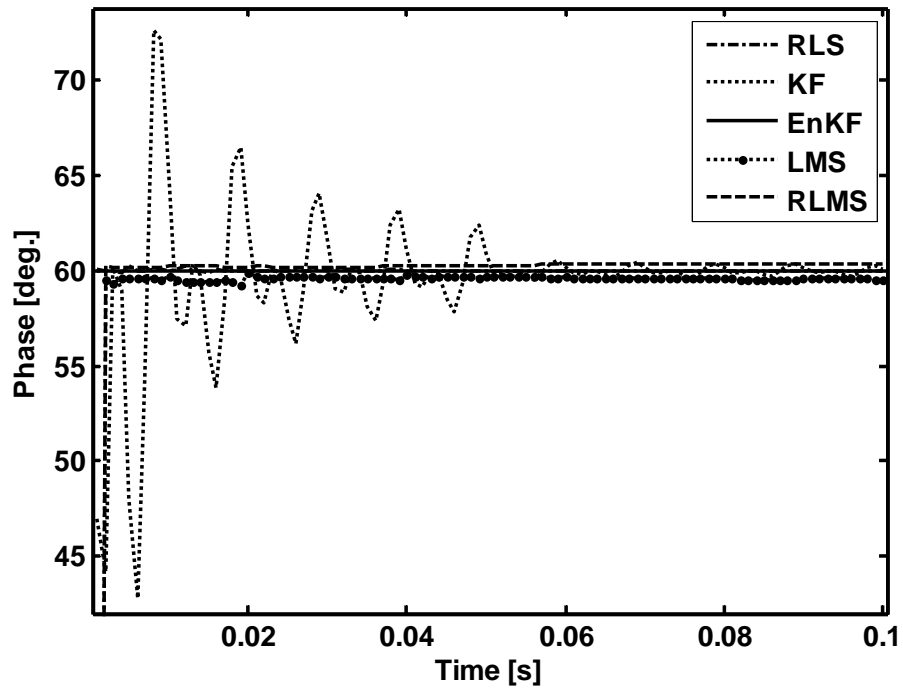
Fig.4.21. EnKF estimation performance of phase of 3rd harmonics component during amplitude drift
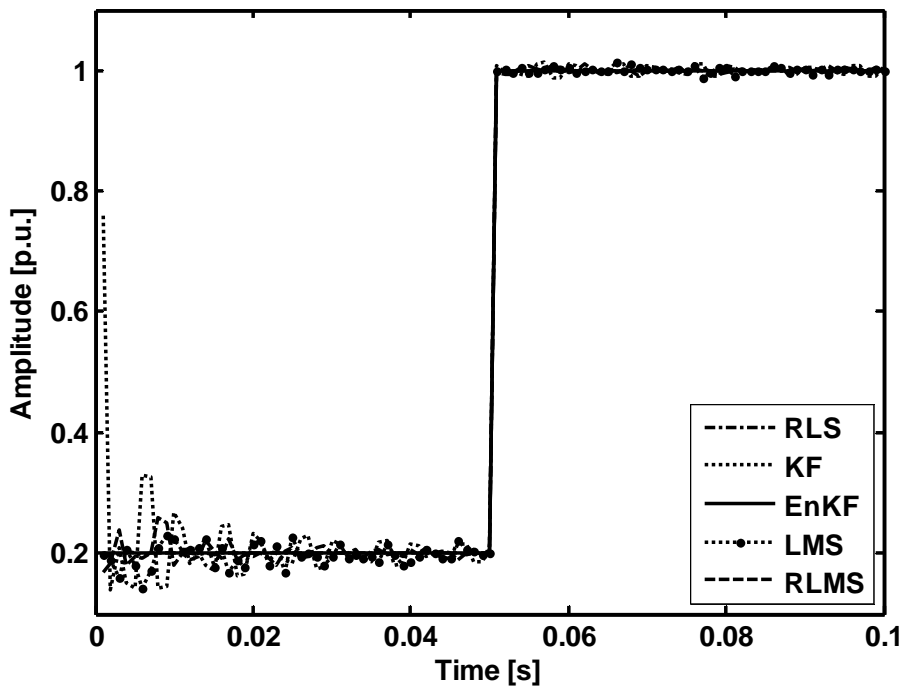
Fig.4.22. EnKF estimation performance of amplitude of 5th harmonics component during amplitude drift
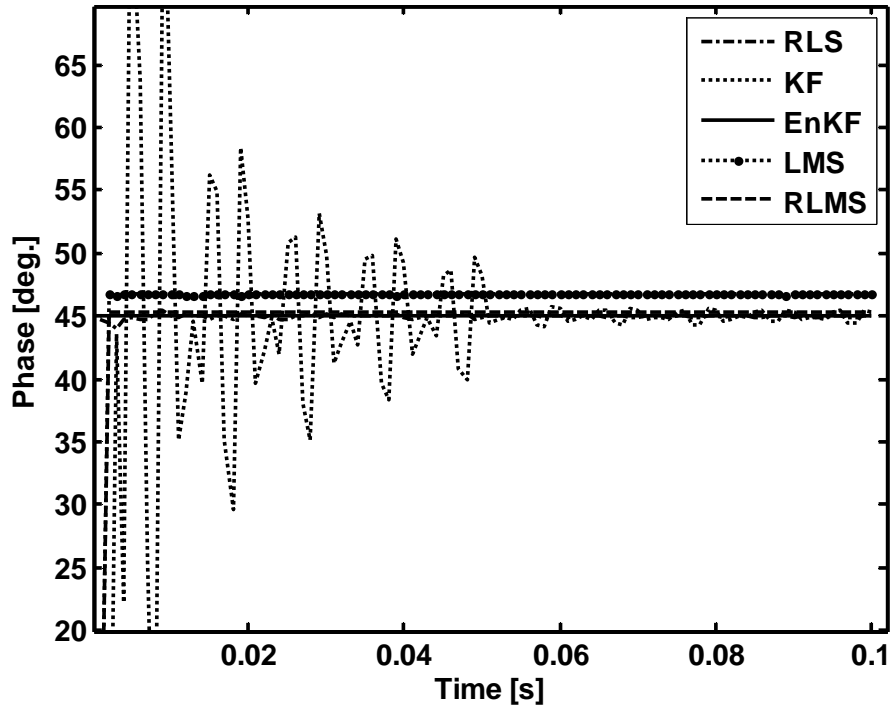
Fig.4.23. EnKF estimation performance of phase of 5th harmonic component during amplitude drift

Fig. 4.20-4.23 show the estimation of 3rd and 5th harmonics amplitudes and phases using the above five algorithms. It is observed that all algorithms track the change in amplitude from 0.5 to 2.0 p.u. in 3rd harmonics case and 0.2 to 1.0 p.u. in 5th harmonics case with oscillations in estimation using KF. But regarding the estimation of phase in two cases, it is same to that of that of the case of without amplitude drift as discussed earlier.

4.3.3 Effect of frequency drift on harmonics estimation

Effects of frequency drift on the estimation are also considered in presence of random noise. Here, it is assumed that a large value of frequency drift $\Delta f = 1.0$ Hz at 0.05 sec., restored to original frequency of 50 Hz at 0.07 sec.
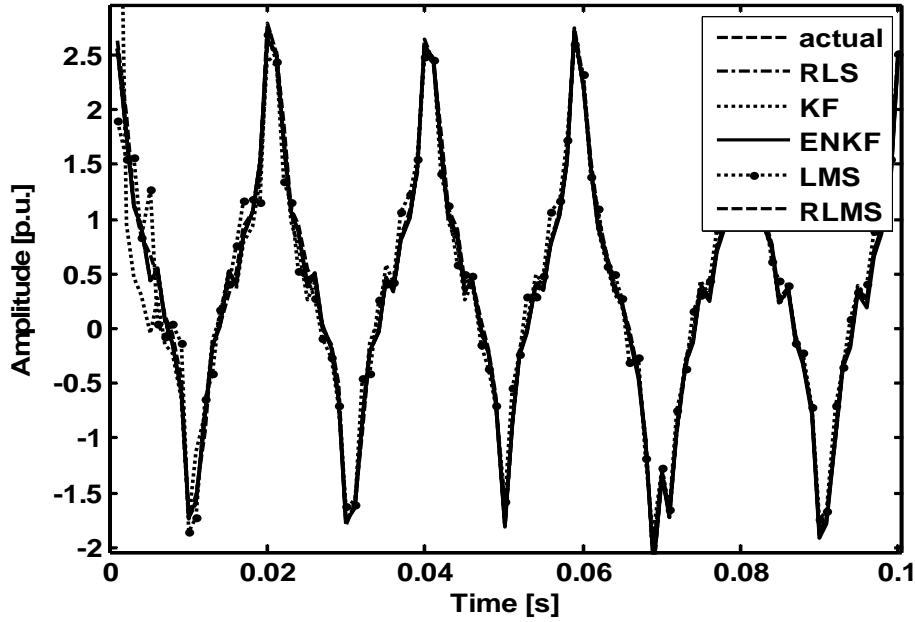
Fig.4.24. EnKF estimation performance of signal during frequency drift

From Fig. 4.24 it is found that the estimated signal during frequency change almost matches with actual in all cases having deviation in the estimation using KF algorithm during initial 0.01 sec. of signal and more accurate estimation (estimated signal matches with actual) using EnKF algorithm. But for small drift i.e. 0.1Hz or less, there may be no change in the waveform of signal.

4.3.4 Harmonics estimation of signal in presence of inter and sub-harmonics

To evaluate the performance of the proposed algorithm in the estimation of a signal in the presence of sub-harmonics and inter-harmonics, a sub-harmonic and two inter-harmonics components are added to the original signal as given in (4.28). The frequency of sub-harmonic is 20 Hz, the amplitude is set to be 0.5 p.u. and the phase is equal to 75 degrees. The frequency, amplitude and phase of one of the inter-harmonics are 130 Hz, 0.25p.u. and 65 degrees respectively. The frequency, amplitude and phase of the other inter-harmonic are 180 Hz, 0.35p.u. and 10 degrees respectively.

124
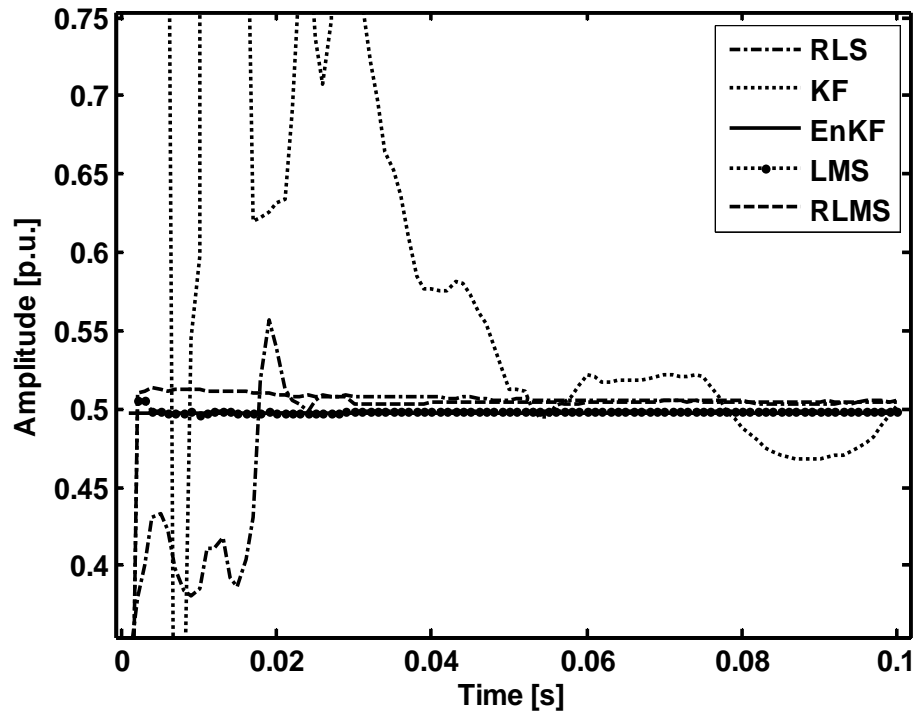
Fig.4.25. EnKF estimation performance of sub-harmonics having amplitude 0.5 p.u.
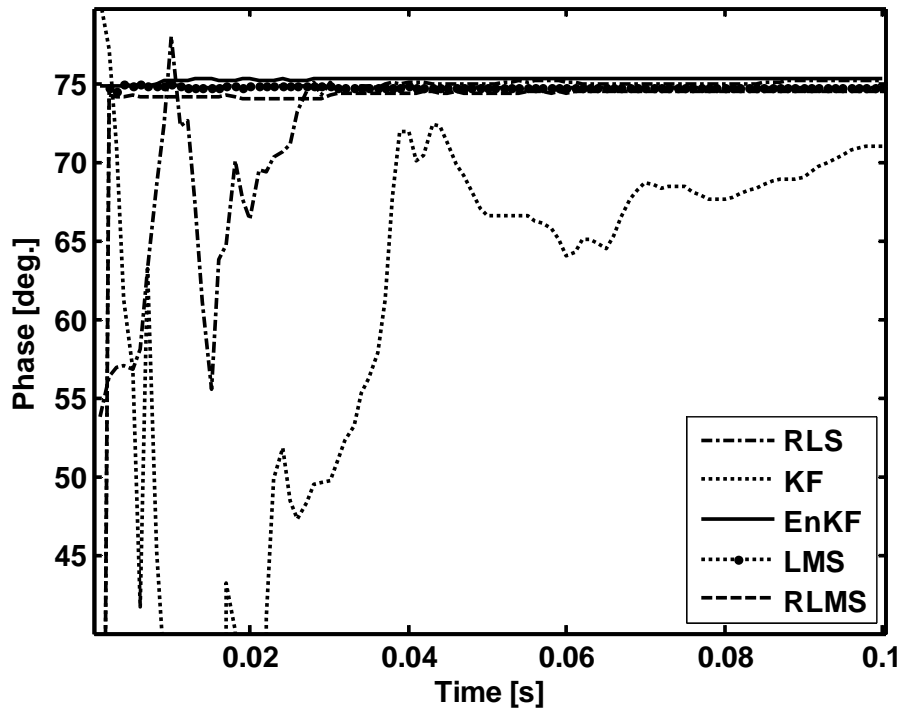
Fig.4.26. EnKF estimation performance of sub-harmonics having phase 75^0
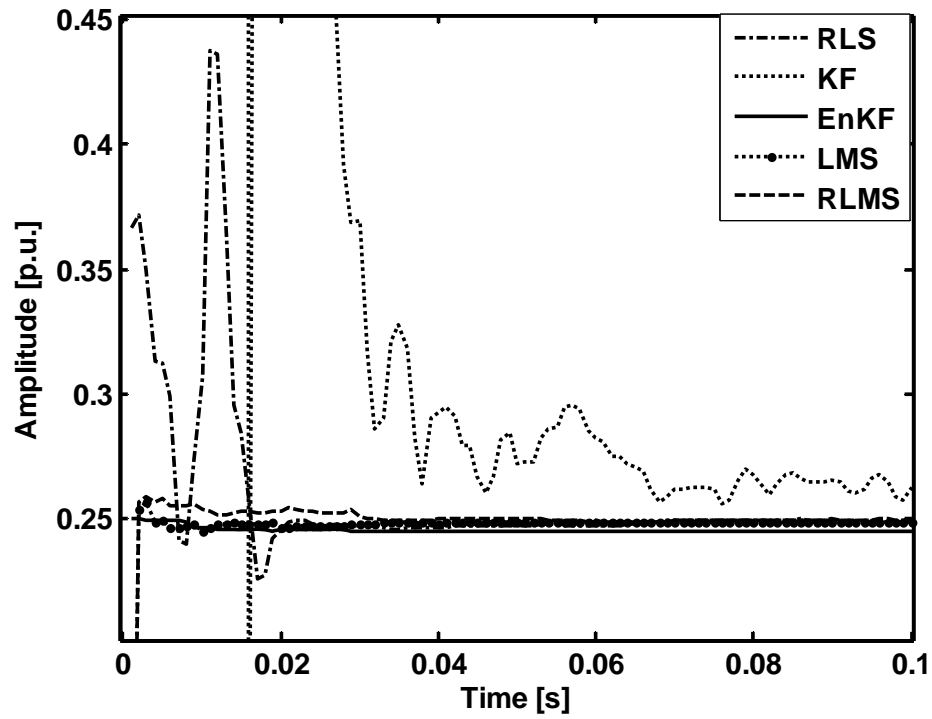
Fig.4.27. EnKF estimation performance of inter-harmonics having amplitude 0.25 p.u.
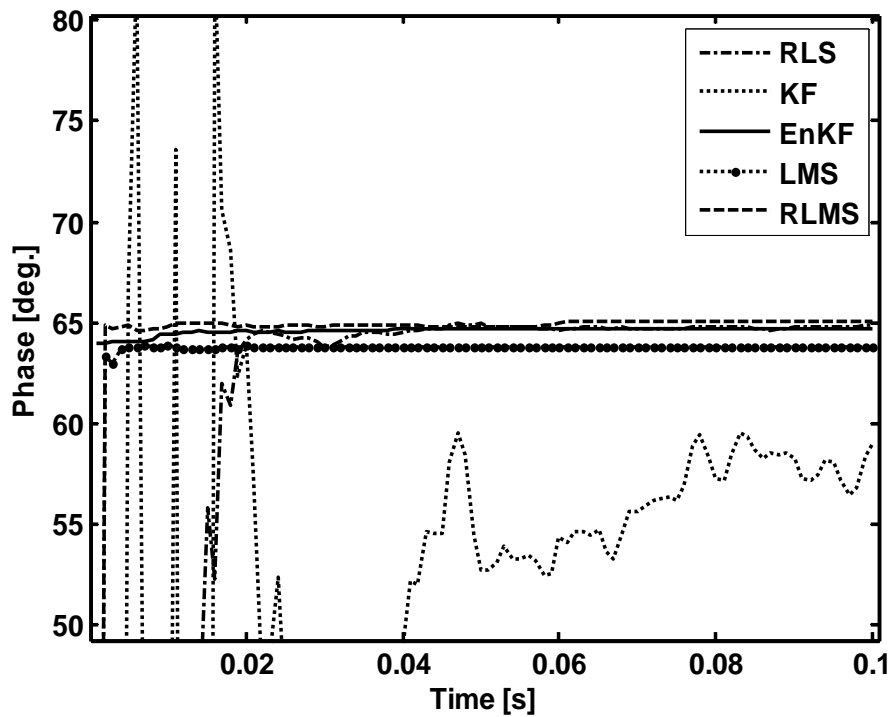
Fig.4.28. EnKF estimation performance of inter-harmonics having phase 65^0
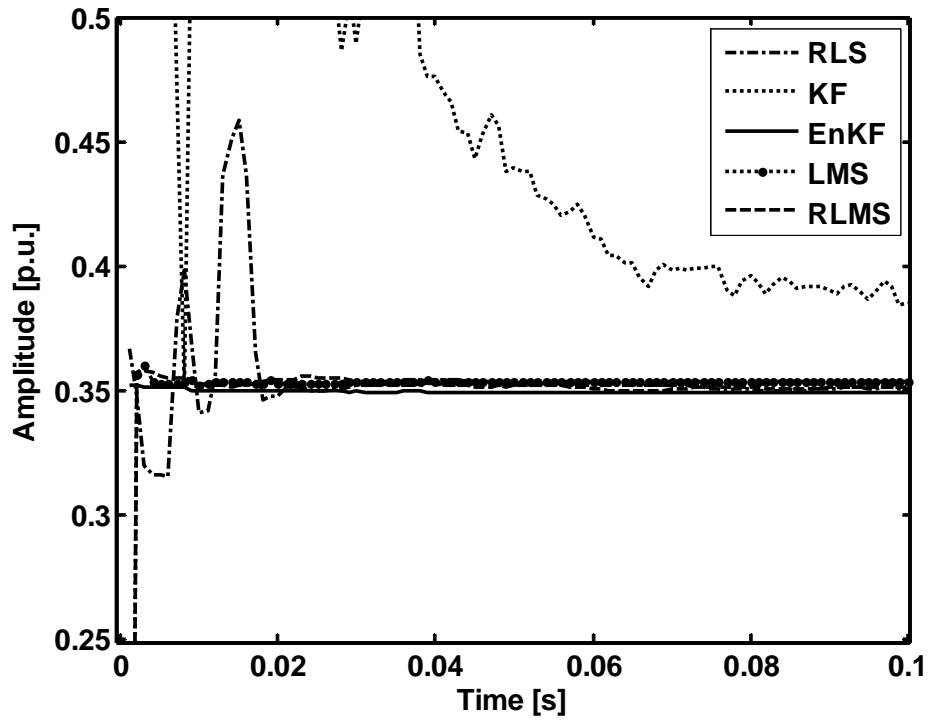
Fig.4.29. EnKF estimation performance of inter-harmonics having amplitude 0.35 p.u.
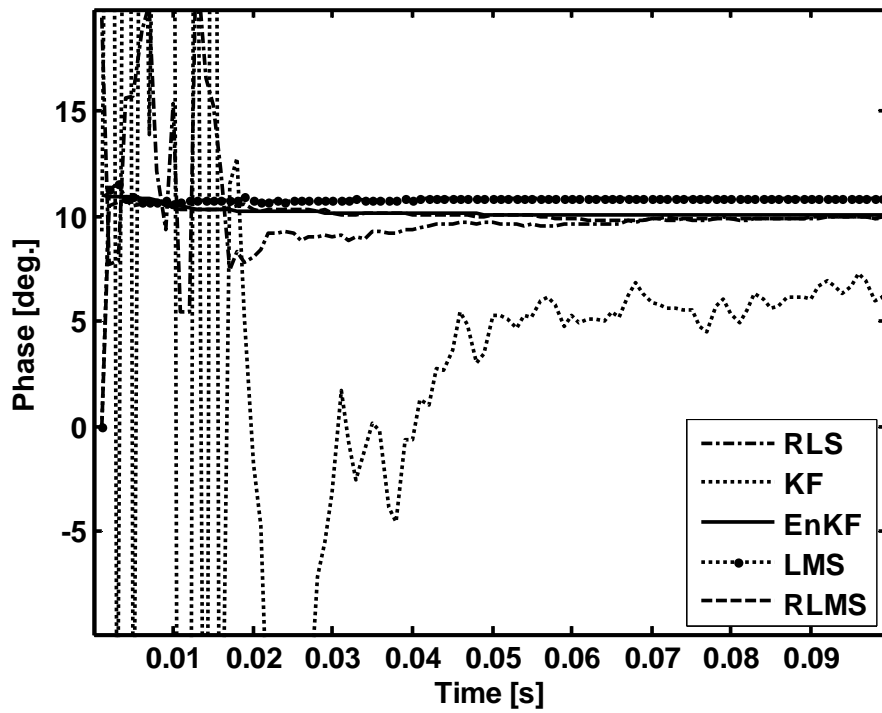
Fig.4.30. EnKF estimation performance of inter-harmonics having phase 10^0

Fig. 4.25-4.30 show the estimation of amplitudes and phases of a sub-harmonic and two inter-harmonics. The time required to track the actual values for the sub-harmonics and inter-harmonics components using KF algorithm is 0.04 second or more. Using RLS, time required to track the actual value is 0.02 second or more. LMS and RLMS track the actual value within 0.0025 second. But using EnKF, the estimation is accurate with very less tracking time i.e less than 0.0025sec.

Table 4.3 gives the estimation results of power system signal having two inter harmonics and one sub-harmonic component using DFT, LMS, RLS, KF, RLMS and EnKF algorithms. This table shows that the performance of estimation using EnKF is the best (less % age in deviation in estimation of amplitude, less deviation is estimation of phase, less amount of computational time) as compared to other five methods. The largest amplitude deviation is 0.349% occurred at 11th harmonic estimation and the largest phase angle deviation is 0.4321^{0} occurred at 7th harmonic estimation.

Table 4.3
Performance comparison of EnKF in presence of inter-harmonicsand sub-harmonics

Methods	Param-	Sub	Fund-	3rd	Inter1	Inter2	5th	7th	11th
Actual	f(Hz)	20	50	150	180	230	250	350	550
	A (V)	0.5	1.5	0.5	0.25	0.35	0.2	0.15	0.1
	φ(°)	75	80	60	65	10	45	36	30
DFT	A (V)	0.5102	1.5083	0.4719	0.2401	0.3434	0.201	0.1720	0.0969
	Deviation (%)	5.1297	0.5521	5.6245	3.9713	1.8814	0.849	14.662	3.0767
	φ(°)	72.027	79.847	57.551	62.410	11.149	41.009	38.786	21.863
	Deviation (°)	2.9723	0.153	2.449	2.5895	1.1495	3.990	2.7861	8.1364
LMS	A (V)	0.4955	1.4771	0.5025	0.2481	0.3513	0.2331	0.1676	0.1237
	Deviation (%)	1.878	1.527	0.5007	0.7568	0.3844	16.553	11.725	23.7136
	φ(°)	74.423	79.294	59.298	63.565	10.979	46.495	37.333	35.8216
	Deviation (°)	0.5764	0.7053	0.7016	1.435	0.9793	1.495	1.3339	5.8216
RLS	A (V)	0.490	1.483	0.494	0.263	0.354	0.228	0.155	0.0995
	Deviation (%)	2.942	1.085	1.072	5.534	1.177	14.273	3.946	0.5361
	φ(°)	73.351	78.111	58.086	61.894	11.49	46.793	34.858	34.541
	Deviation (°)	1.648	1.888	1.913	3.105	1.49	1.797	1.1419	4.541
KF	A (V)	0.492	1.496	0.503	0.254	0.358	0.205	0.161	0.117
	Deviation (%)	1.508	0.240	0.657	1.859	2.322	2.957	7.918	17.222
	φ(°)	75.353	80.244	59.613	64.218	8.680	42.204	37.109	35.316
	Deviation (°)	0.353	0.244	0.386	0.782	1.319	2.792	1.109	5.316
RLMS	A (V)	0.4971	1.4925	0.4975	0.246	0.3510	0.201	0.146	0.1010
	Deviation (%)	0.5842	0.5015	0.5021	1.509	0.2729	0.813	3.141	1.0081
	φ(°)	74.432	79.548	59.677	64.559	10.405	43.454	35.566	32.446
	Deviation (°)	0.5678	0.451	0.322	0.440	0.405	1.54	0.433	2.446
EnKF	A (V)	0.5051	1.497	0.501	0.2500	0.3505	0.1997	0.1499	0.1003
	Deviation (%)	**0.0203**	**0.167**	**0. 313**	**0.0098**	**0.1410**	**0.1747**	**0.0917**	**0. 349**
	φ(°)	75.311	79.888	59.853	64.782	10.219	44.952	35.567	29.883
	Deviation (°)	**0.311**	**0.111**	**0.1462**	**0.2178**	**0.219**	**0.048**	**0.4321**	**0.1164**

The performance index ε, used to evaluate the quality of estimates

$$\varepsilon = \frac{\sum\limits_{k=1}^{N}(y(k) - y(\hat{k}))^2}{\sum\limits_{k=1}^{N} y(k)^2} \times 100 \tag{4.29}$$

where $y(k)$ and $y(\hat{k})$ are actual and estimated signal respectively. In this case the significance of the performance index ε is that it provides the accuracy of the estimation algorithm. Less the value of ε, means more accuracy of estimation and vice versa.

Table 4.4
Comparison of Performance Index of different methods   (RLS, LMS, KF, RLMS and EnKF)

SNR	LMS	RLS	KF	RLMS	EnKF
No noise	6.2583	0.0583	0.0197	4.5163	7.6×10^{-4}
40 dB	7.8445	0.0636	0.04	4. 5550	0.0041
20 dB	8.0444	0.8921	0.6477	5.2386	0.4272
10 dB	14.3639	5.253	12.710	11.8722	4.323
0 dB	23.9864	46.286	35.483	27.407	17.0657

The performance indices of all the five algorithms are given in Table 4.4. From which it can be seen that EnKF achieves a significant improvements in terms of reducing error for harmonics estimation in comparison to four other algorithms

4.3.5 Harmonic Estimation of a Dynamic Signal

To examine the performance of EnKF algorithm in tracking harmonics and its robustness in rejecting noise, a time-varying signal of the form as given below is considered

$$y(t) = \{1.5 + a_1(t)\}\sin(\omega_0 t + 80^0) + \{0.5 + a_3(t)\}\sin(3\omega_0 t + 60^0)$$
$$+ \{0.2 + a_5(t)\}\sin(5\omega_0 t + 45^0) + \varepsilon(t) \tag{4.30}$$

is used where the amplitude modulating parameters $a_1(t), a_2(t)$ and $a_3(t)$ are

$$a_1 = 0.15 \sin 2\pi f_1 t + 0.05 \sin 2\pi f_5 t \tag{4.31}$$

$$a_3 = 0.05 \sin 2\pi f_3 t + 0.02 \sin 2\pi f_5 t \qquad (4.32)$$

$$a_5 = 0.025 \sin 2\pi f_1 t + 0.005 \sin 2\pi f_5 t \qquad (4.33)$$

$f_1 = 1.0 \, \text{Hz}$. $f_3 = 3.0 \, \text{Hz}$. $f_5 = 6.0 \, \text{Hz}$. In the above example, the random noise $\varepsilon(t)$ has a normal distribution of zero mean, unity variance and amplitude of $0.05 randn$.
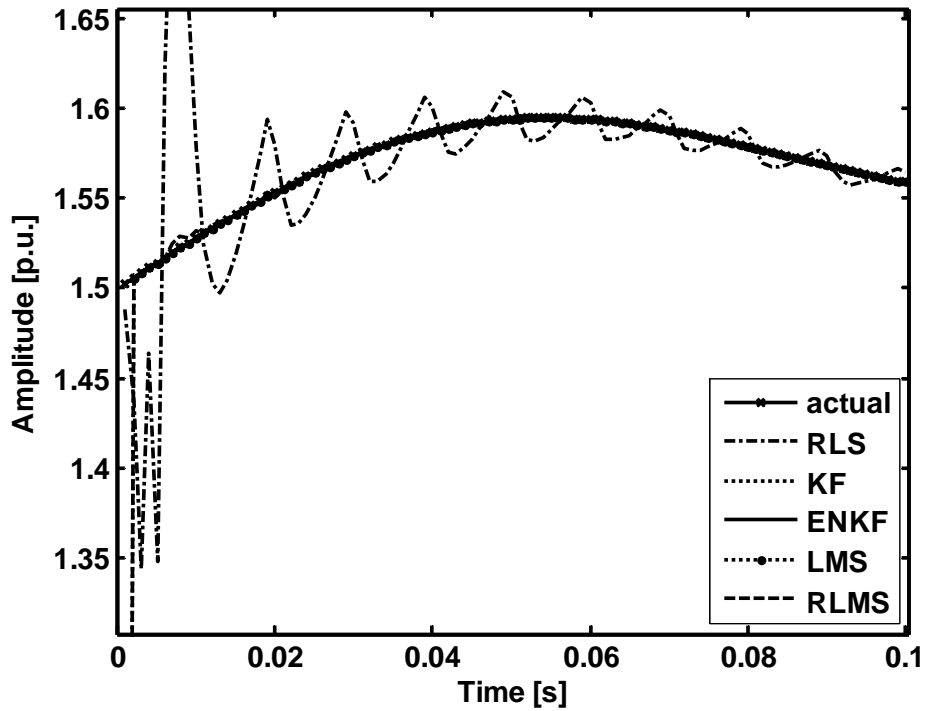
Fig.4.31 EnKF estimation performance of amplitude of fundamental component of dynamic signal
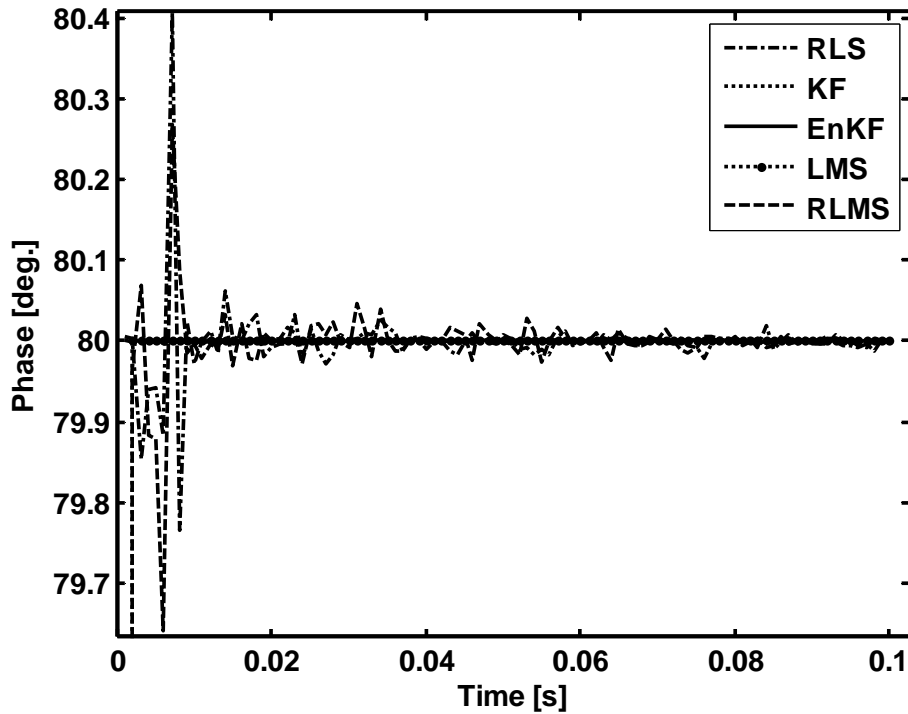
Fig.4.32 EnKF estimation performance of phase of fundamental component of dynamic signal
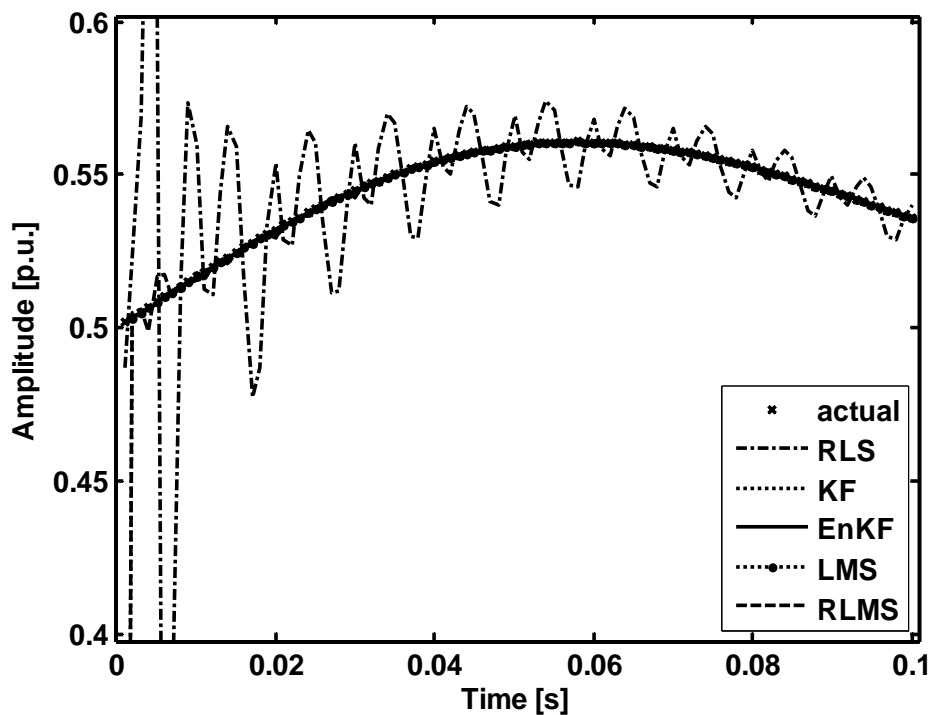
Fig.4.33 EnKF estimation performance of amplitude of 3rd harmonic component of dynamic signal
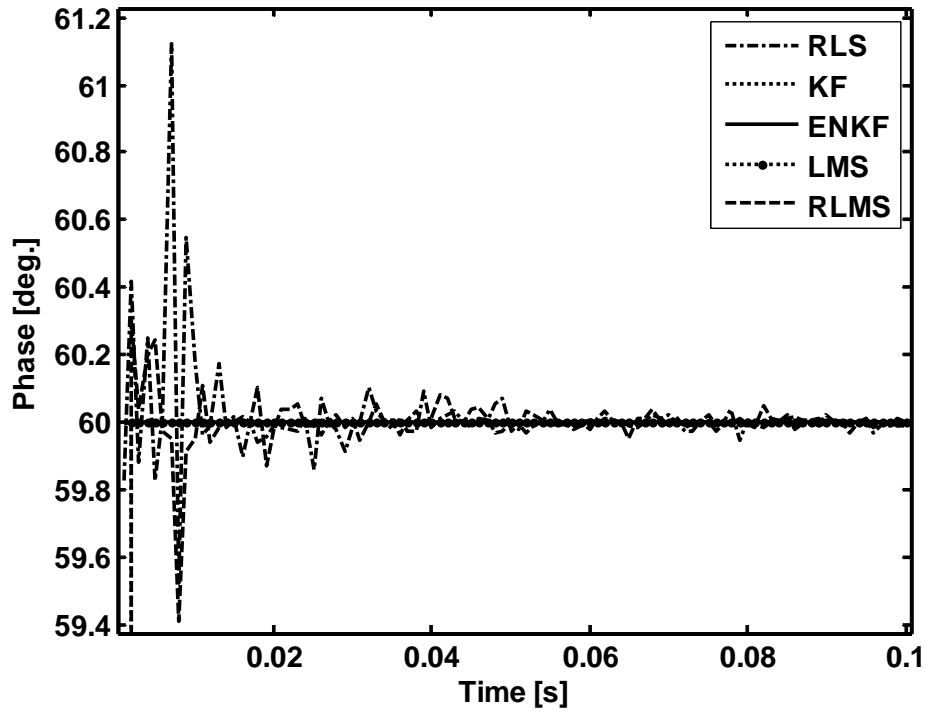
Fig.4.34 EnKF estimation performance of phase of 3rd harmonics component of dynamic signal
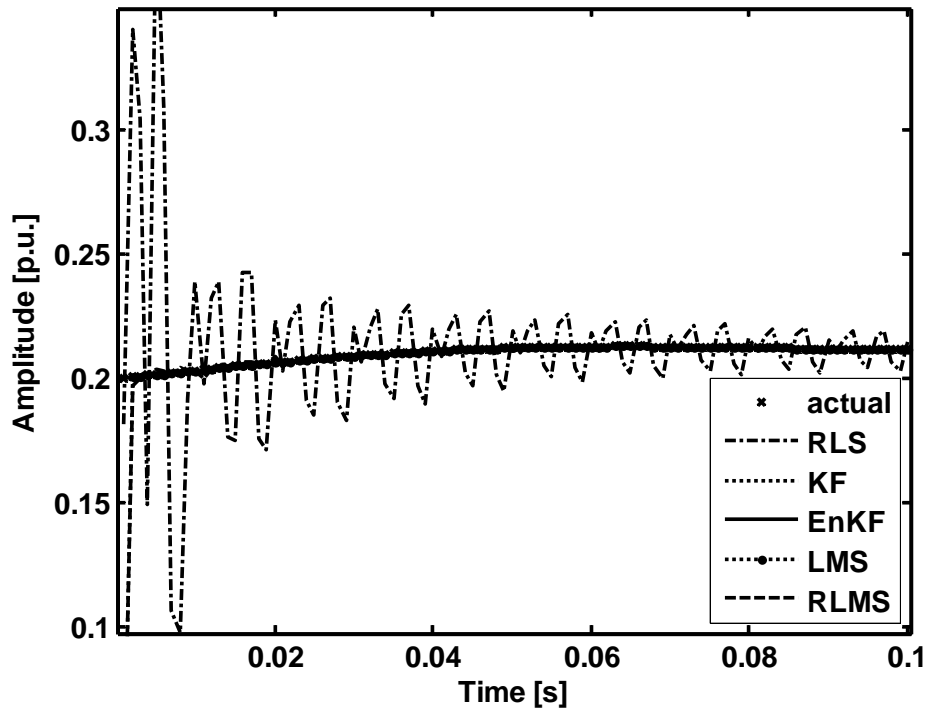
Fig.4.35 EnKF estimation performance of amplitude of 5th harmonic component of dynamic signal
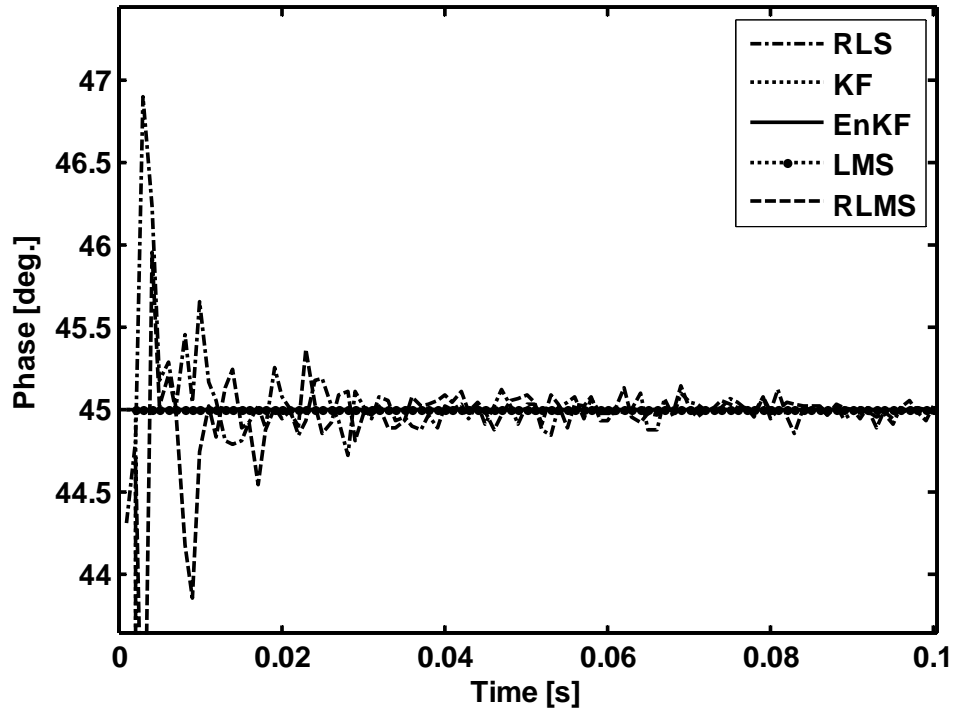
Fig.4.36 EnKF estimation performance of phase of 5th harmonics component of dynamic signal

The estimation of time varying fundamental, 3rd and 5th harmonics signal in the presence of random noise is shown in Fig. 4.31-4.36. It is observed that there is more deviation in estimation using KF but using other four algorithms, the estimated value closely matches with the actual with more accurate estimation using EnKF algorithm.

Table- 4.5
Performance comparison of EnKF for Dynamic Signal

Methods	Param-	Fund-	3rd	5th
Actual	f(Hz)	50	150	250
	A (V)	1.5701	0.5447	0.2101
	φ(°)	80	60	45
LMS	A (V)	1.5628	0.5424	0.2091
	Deviation (%)	0.4731	0.4730	0.4095
	φ(°)	79.5999	59.7005	44.7744
	Deviation (°)	0.4001	0.2995	0.2256
RLS	A (V)	1.5701	0.5447	0.2101
	Deviation (%)	0.0119	0.0432	0.0162
	φ(°)	79.9975	59.987	44.9615
	Deviation (°)	0.0025	0.013	0.0385
KF	A (V)	1.5701	0.5447	0.2101
	Deviation (%)	0.0119	0.0432	0.0157
	φ(°)	80	60.0001	45.0003
	Deviation (°)	2.57×10^{-5}	5.316×10^{-5}	2.615×10^{-4}
RLMS	A (V)	1.5629	0.5423	0.2091
	Deviation (%)	0.4650	0.4856	0.4716
	φ(°)	79.6063	59.6928	44.7805
	Deviation (°)	0.3937	0.3072	0.2195
EnKF	A (V)	1.57	0.5447	0.2101
	Deviation (%)	**0.007**	**0.0432**	**0.0032**
	φ(°)	80	60	45
	Deviation (°)	**2.57×10^{-5}**	**4.5×10^{-5}**	**5.812×10^{-7}**

Table 4.5 gives the simulation results of the dynamic signal as given by (4.29). This table shows that for the dynamic signal estimation, all the methods discussed in this thesis give accurate estimation but the accuracy using EnKF is better(least % deviation in amplitudes least deviations in phase angles) as compared to other four methods.

4.3.6 Harmonics tracking in faulted power systems

The proposed EnKF method is applied to track time varying harmonics components of a transmission system during L-G fault condition as given in (4.37). A single line to ground fault on the A phase of a transmission line was simulated using SIMULINK. A fault resistance of 0.001 Ω is assumed between the A-phase and ground. The measurements are sampled using a sampling frequency of 5 kHz.
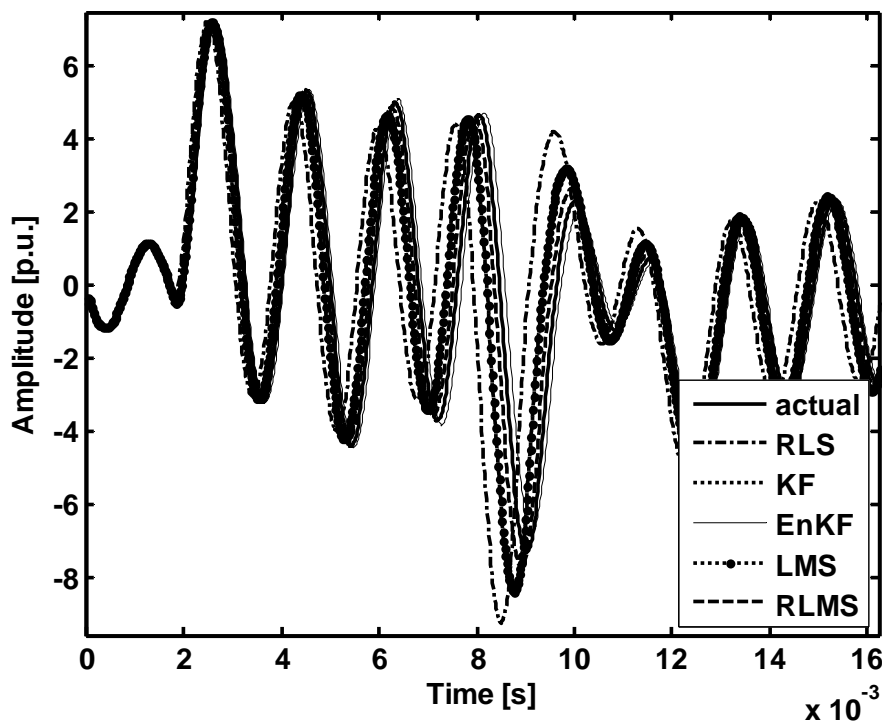
Fig. 4.37 EnKF estimation performance of signal for the fault current data

From Fig.4.37, it is seen that the estimation using EnKF closely matches with actual fault signal as compared to other four methods. Table 4.6 shows the comparison of

performance indices of five algorithms for the case of estimation of fault data. EnKF shows better performance on estimation compared to other four methods.

Table 4.6
Comparison of Performance Indices of estimation of different methods (RLS, LMS, KF, RLMS and EnKF) on L-G fault data

Parameter	LMS	RLS	KF	RLMS	EnKF
ε	7. 1629	6.1075	3. 3452	5.	1.1254

4.4 Experimental Studies and Results

For real time application of the algorithms in estimating harmonics in a power system, data i.e obtained in a laboratory environment from the supply on normal working day of the laboratory as per the experimental setup discussed in section 2.8.1 of Fig. 2.35 is taken.
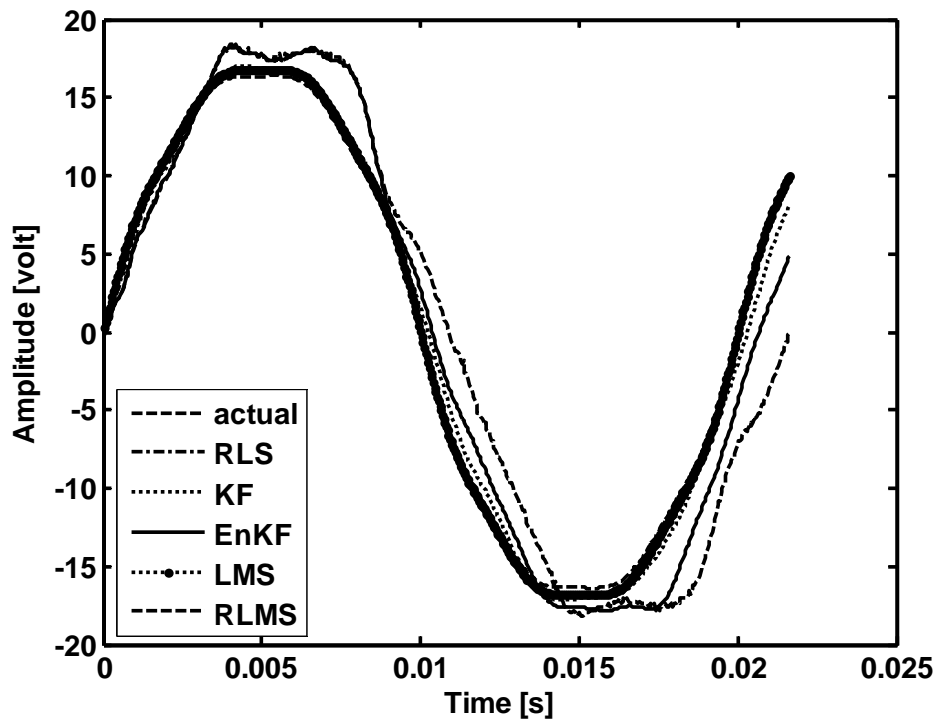
Fig. 4.38 EnKF estimation performance of signal from experimental data

Table 4.7
Comparison of Performance Index of Experimental Data   (RLS, LMS, KF, RLMS and EnKF)

Parameter	LMS	RLS	KF	RLMS	EnKF
ε	4.6169	2.4985	7.4718	2. 5653	0.1156

Fig. 4.38 shows the estimation of signal using above five algorithms from the data obtained from the laboratory experiment. In the figure, the estimated waveform approaches the actual over the cycle. The performance index (to evaluate the quality of estimates) of estimation is calculated for the five algorithms and the results are given in Table 4.6. EnKF yeilds the more accurate estimation result (since it has smallest performance index (around 0.11%)), which is acceptable. From Fig. 4.39, the estimated waveform is very close to the real one in first half cycle and small deviation is there in second half cycle. Hence, the obtained results are satisfactory for the application with real data.

The proposed EnKF estimation algorithm is developed to overcome the estimation problems in high dimensional system, because in that case the maintenance of covariance matrix in Kalman Filter is computationally not feasible (due to its inverse operation for high dimensional systems). EnKF replaces the covariance matrix by the sample covariance derived from ensemble and ensemble is operated as if a random sample. Since large matrix multiplication for evaluating the covariance matrix is absent in case of EnKF, so computational time required is less in case of EnKF. In case of highly nonlinear dynamics, Kalman Filtering approach fails in propagating the error covariance but this proposed approach can be applicable for highly uncertain and nonlinear system. In case of Kalman Filter the sample points are chosen deterministically, but in case of EnKF, the number of ensemble required is heuristic. So one of the critical issues of discussion is the accuracy of state estimation as a function of ensemble size.

4.5 Chapter Summary

In this chapter, a new algorithm called EnKF for accurate estimation of amplitudes and phases of the harmonics contained in a voltage or current waveform for power quality monitoring is presented. Several computer simulation tests have been conducted to estimate harmonics in a power system signal corrupted with noise and decaying dc components to assess the speed of convergence and tracking accuracy of the Ensemble Kalman Filtering algorithm. The proposed EnKF based harmonic estimation algorithm estimates amplitude and phase of the harmonics accurately during amplitude and frequency drift of the signal. EnKF algorithm can be used to estimate the inter-harmonics and sub-harmonics and the estimation accuracy is found to be satisfactory. Also this algorithm estimates accurately the signal in L-G fault condition. From the results presented in section 4.5 of this chapter it is clear that excellent estimation accuracy (in terms of % age deviation in amplitude, deviation in phase angle and computational time) and convergence speed is achieved by using EnKF algorithm in comparison to other five algorithms (DFT, RLS, LMS, RLMS and KF). The efficacy of the proposed EnKF algorithm is also validated using laboratory test data.

Chapter-5

Harmonics Estimation Using Hybrid Algorithms

5.1 Introduction

Harmonics estimation of power system signals using different signal processing techniques such as RLS, LMS, RLMS, KF and EnKF are discussed in chapter 4. With a view to achieve further improvement in % error in estimation, processing time, performance in presence of inter and sub-harmonic components and reduction in tracking time, hybrid estimation algorithms involving signal processing and soft computing techniques are used in this chapter. The chapter first presents combined RLS-Adaline (Recursive Least Square and Adaptive Linear Neural Network) and KF-Adaline (Kalman Filter Adaline) approaches for the estimation of harmonic components of distorted signals. Kalman Filter and RLS carry out the weight updating in Adaline. The estimators' track the signal corrupted with noise and decaying DC components very accurately. Adaptive tracking of harmonic components of a power system can easily be done using these algorithms. The proposed approaches are tested both for static and dynamic signal. These approaches are also able to track the harmonics components in presence of inter and sub harmonics.

Exploiting good features of optimization, using Genetic Algorithm (GA), power system harmonics estimation was proposed in [65] using GA. In the above GA based harmonic estimation scheme, phases are estimated using GA, subsequently amplitudes of signal is estimated by using Least Square method. It has been observed that the time of convergence is improved using combined LS and GA approach to harmonics estimation. But there is some poor performance exhibited by GA-LS approach. These deficiencies are degradation in efficiency in case of highly correlated parameters and premature convergence of the GA.

Two new algorithms such as RLS-BFO and Adaline-BFO, for the estimation of both the phases and amplitudes of integral harmonics, sub-harmonics and inter-harmonics as well as their deviations has been proposed in this chapter. Above two combined approaches have been proposed for achieving improvement in % error in estimation of signal, processing time and performance in presence of change in amplitude and phase angle of harmonic components.

The tracking performances of the proposed approaches are validated taking the data generated from laboratory setup. There is an improvement in convergence and processing time on using these algorithms.

5.2 Hybrid Adaline approaches for Harmonics estimation:

5.2.1 RLS- Adaline based Harmonics Estimation

Consider the signal described in (4.1) in chapter 4. Discretizing this using (4.2) and then rewriting it, one obtains (4.5). The signal given in (4.5) can be written in parametric form as

$$y(k) = X(k)W \tag{5.1}$$

where $X(k)$ is the observation matrix and the parameter vector W are defined in eq.(5.2) and (5.3) respectively.

$$X(k) = [\sin(\omega_1 kT) \quad \cos(\omega_1 kT) \quad ... \quad \sin(\omega_N kT) \quad \cos(\omega_N kT) \quad 1 \quad -kT]^T \tag{5.2}$$

The weight vector of the Adaline

$$W(k) = [W_1(k) \quad W_2(k) \quad ... \quad W_{2N-1}(k) \quad W_{2N}(k) \quad W_{2N+1}(k) \quad W_{2N+2}(k)]^T \tag{5.3}$$

Fig. 5.1 shows the block diagram of RLS-Adaline structure of implementation for the estimation of power system harmonics. $X_1, X_2, X_3...X_n$ are the inputs to Adaline. After multiplication of the input with the weight vector gives the estimated output $\hat{y}(k)$.

Reference output $y(k)$ is compared with the estimated output $\hat{y}(k)$ and the error so obtained is minimized by updating the weights of the Adaline using RLS algorithm.
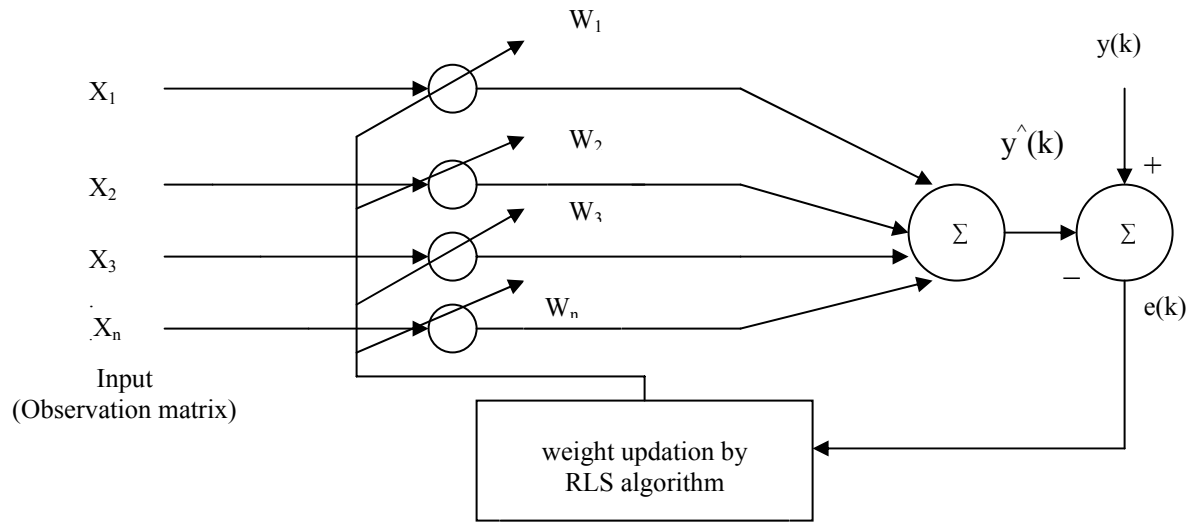
Fig.5.1 Structure of RLS-Adaline

The weight vector of the Adaline is updated using RLS algorithm as

$$\hat{W}(k+1) = \hat{W}(k) + K(k+1)e(k+1) \tag{5.4}$$

Error in measurement is given by

$$e(k+1) = y(k+1) - x(k+1)^T \hat{W}(k) \tag{5.5}$$

The gain K is related with the covariance of parameter vector as follows

$$K(k+1) = P(k)x(k+1)[1 + x(k+1)^T P(k)x(k+1)]^{-1} \tag{5.6}$$

The updated covariance of parameter vector using matrix inversion lemma is given as

$$P(k+1) = [I - K(k+1)x(k+1)^T]P(k) \tag{5.7}$$

After the updating the weight vector using RLS algorithm, amplitudes, phases of the fundamental and nth harmonic parameters and dc decaying parameters can be derived as follows

$$A_n = \sqrt{\left(W_{2N}^2 + W_{2N-1}^2\right)} \tag{5.8}$$

$$\phi_n = \tan^{-1}\left(\frac{W_{2N}}{W_{2N-1}}\right) \tag{5.9}$$

$$A_{dc} = W_{2N+1} \tag{5.10}$$

$$\alpha_{dc} = \left(\frac{W_{2N+2}}{W_{2N+1}}\right) \tag{5.11}$$

Because

$$W = [A_1 \cos(\phi_1) \quad A_1 \sin(\phi_1) \quad ... \quad A_n \cos(\phi_n) \quad A_n \sin(\phi_n) \quad A_{dc} \quad A_{dc}\alpha_{dc}]^T \tag{5.12}$$

5.2.2 KF- Adaline based Harmonics Estimation

As described in Fig. 5.1, Fig. 5.2 shows the structure of KF-Adaline for power system harmonics estimation. Only difference is here the weights of the Adaline are updated using Kalman Filter algorithm.
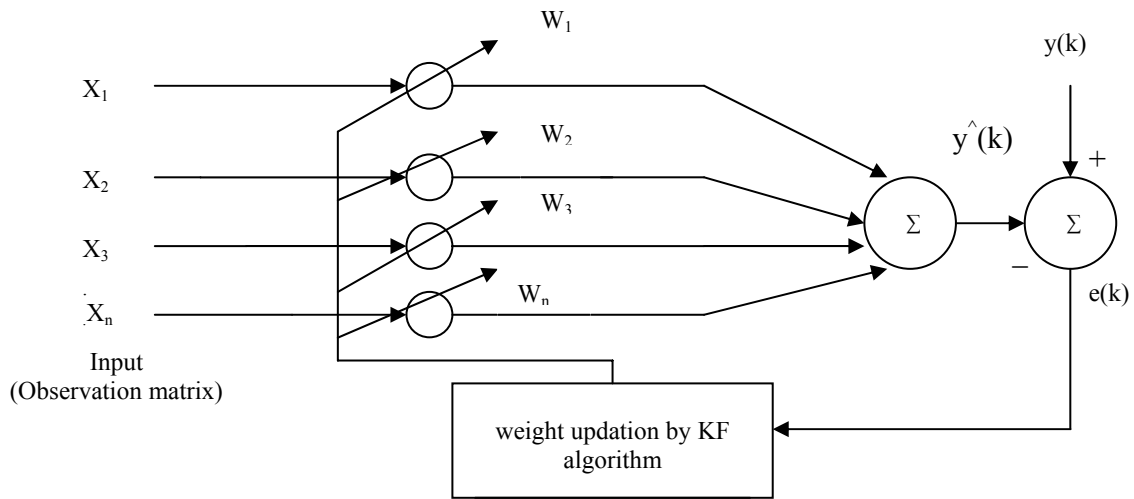
Fig.5.2 Structure of KF-Adaline

The signal as described in section 5.2.a is taken; the weight vector of Adaline as in (5.3) is updated using Kalman Filter algorithm as

$$G(k) = P(k/k-1)x(k)^T(x(k)P(k/k-1)x(k)^T + Q)^{-1} \tag{5.13}$$

G is the Kalman gain, x is the observation vector, P is the covariance matrix, Q is the noise covariance of the signal.

So the covariance matrix is related with Kalman gain with the following equation.

$$P(k/k) = P(k/k-1) - G(k)x(k)P(k/k-1) \tag{5.14}$$

The updated estimated state is related with previous state with the following equation.

$$\hat{W}(k/k) = \hat{W}(k/k-1) + G(k)(y(k) - x(k)\hat{W}(k/k-1)) \tag{5.15}$$

After the updating of weight vector using KF algorithm, amplitudes, phases of the fundamental and nth harmonic parameters and dc decaying parameters are estimated using (5.8) – (5.11)

5.3 Simulation Results

5.3.1 Static signal corrupted with random noise and decaying DC component

The power system signal used for the estimation, besides the fundamental frequency, contains higher harmonics of the 3rd, 5th, 7th, 11th and a slowly decaying DC component. This kind of signal is typical in industrial load comprising power electronic converters and arc furnaces. The signal as given in (4.28) of chapter- 4 is considered. The values of different parameters of two hybrid algorithms are taken as per the data given in Table 3.1 of chapter-3. The estimation results of fundamental as well as harmonic components of amplitudes and phases of the signal using two hybrid algorithms are presented next.
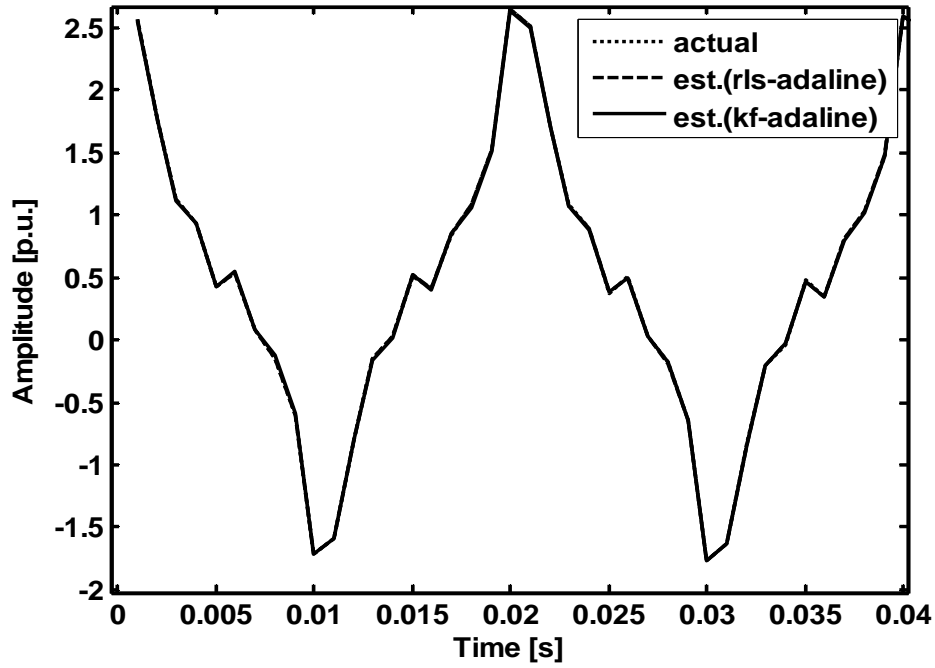
Fig.5.3 Comparison of Actual and Estimated values of synthetic signal (RLS-Adaline and KF-Adaline)
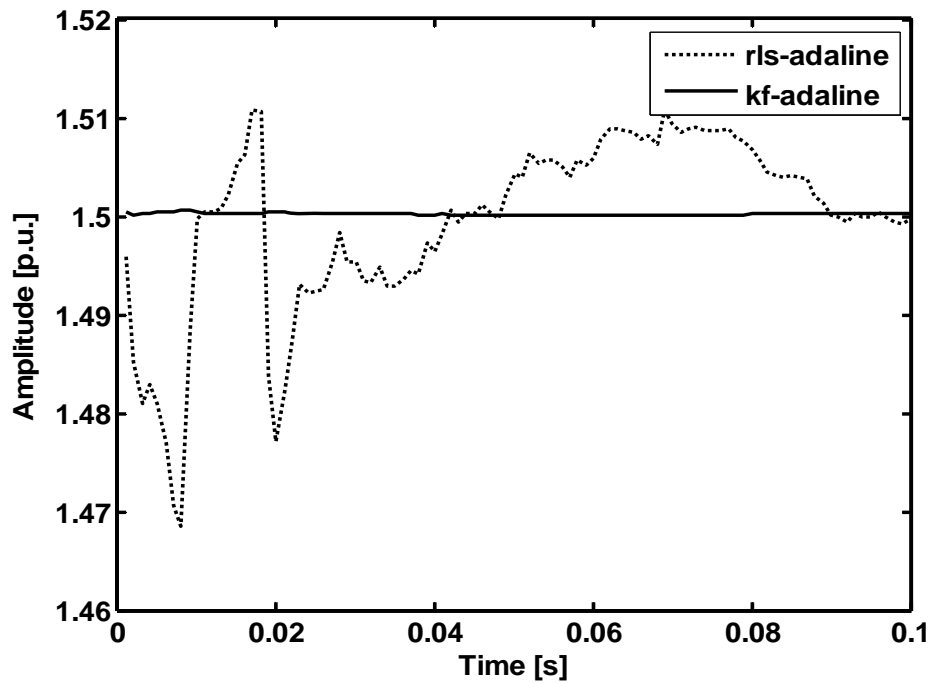
Fig.5.4 KF-Adaline estimation performance of amplitude of fundamental component of signal
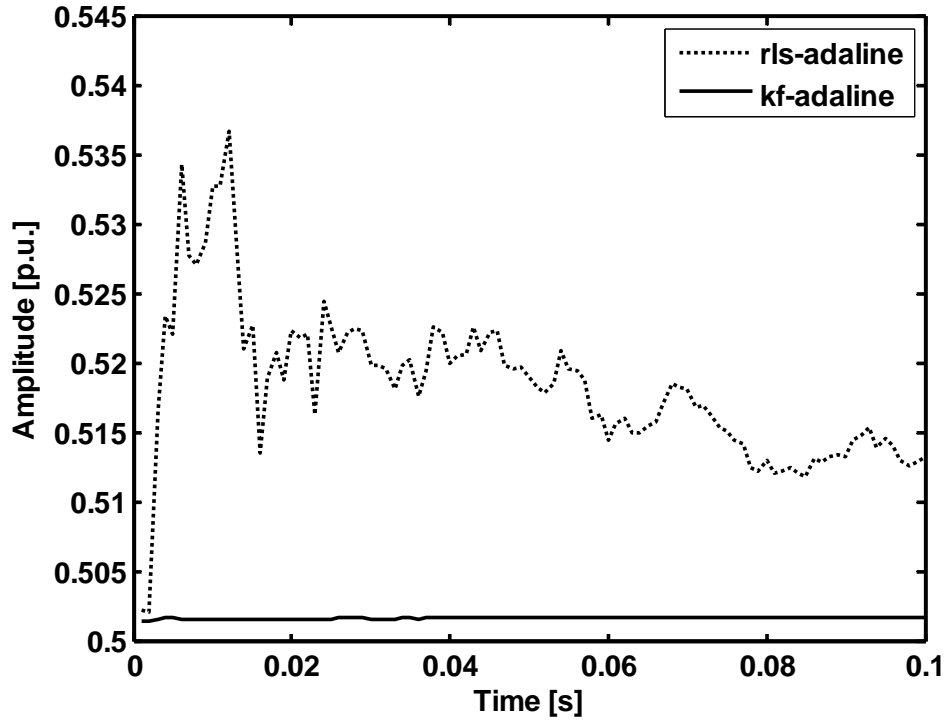
Fig. 5.5 KF-Adaline estimation performance of amplitude of 3rd harmonic component of signal
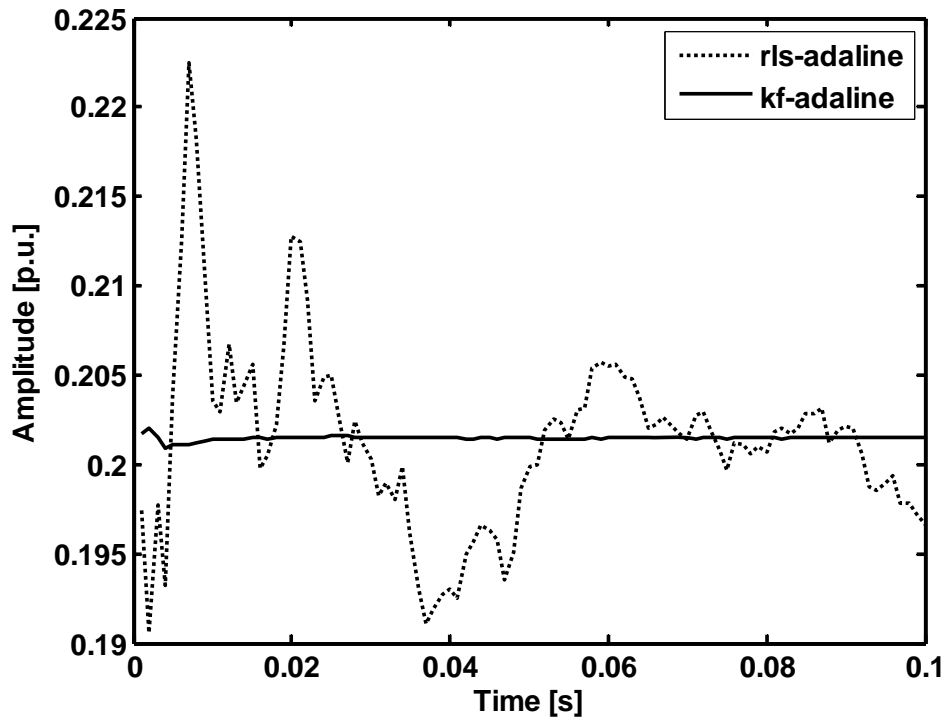
Fig. 5.6 KF-Adaline estimation performance of amplitude of 5th harmonic component of signal
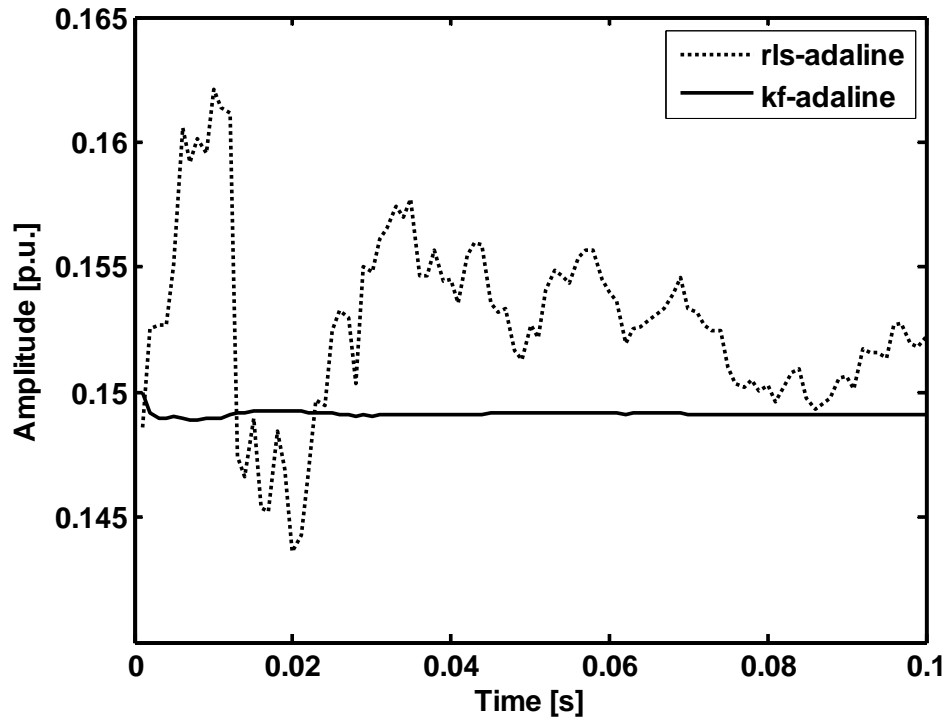
Fig. 5.7 KF-Adaline estimation performance of amplitude of 7th harmonic component of signal
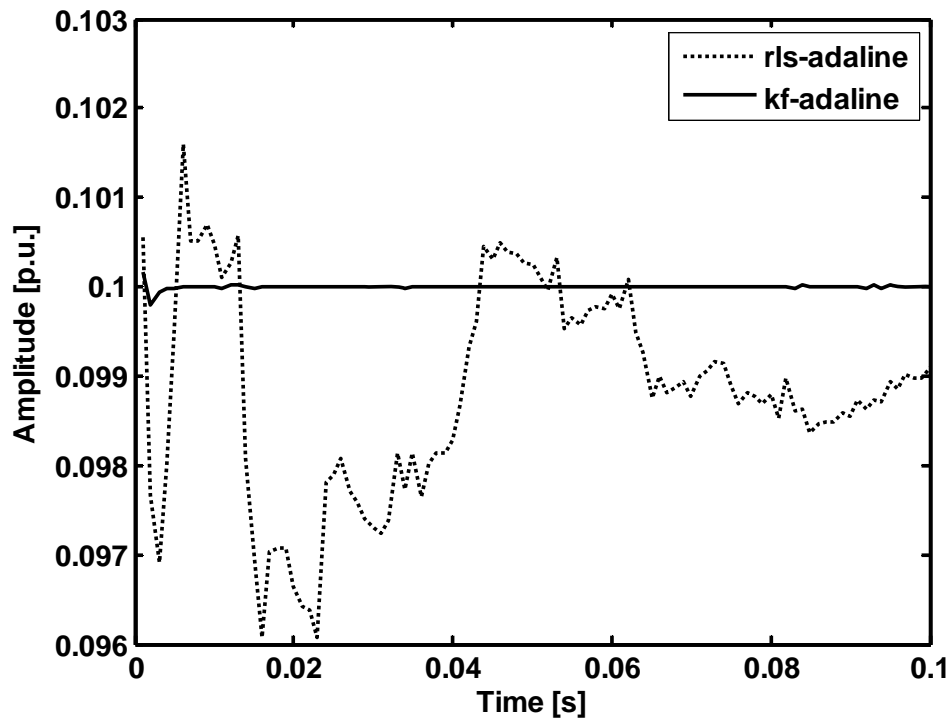
Fig. 5.8 KF-Adaline estimation performance of amplitude of 11th harmonic component of signal
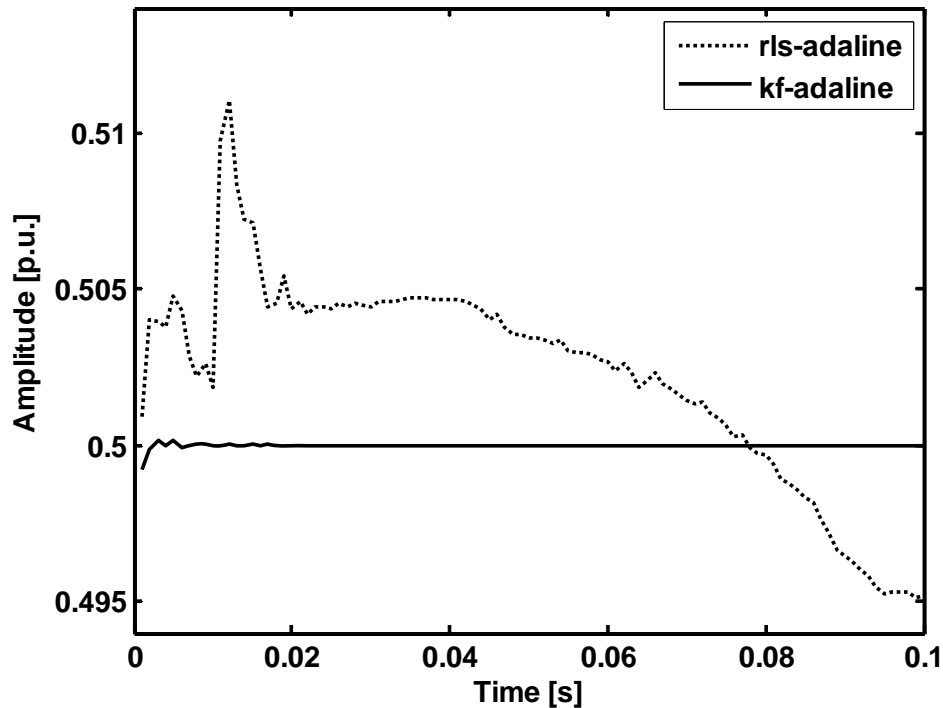
Fig. 5.9 KF-Adaline estimation performance of dc component of signal

Fig. 5.3 shows the comparison of actual and estimated signal obtained by using RLS-Adaline and KF-Adaline algorithms. It is seen from the above Fig. that actual signal and estimated signal closely match with each other in both of estimation algorithms. Fig. 5.4 shows the comparative estimation of fundamental amplitude of the signal using both RLS-Adaline and KF-Adaline methods. In case of RLS-Adaline, estimated amplitude oscillates between 1.47 p.u. to 1.51p.u. but KF-Adaline estimates fundamental amplitude as 1.5 p.u. Fig. 5.5 provides a comparative estimation of third harmonic component of the considered signal using the above two methods. In the estimation using RLS-Adaline, during first few initial times period estimation is 0.535 p.u. after that it settles around 0.515 p.u. KF-Adaline estimates third harmonics amplitude as 0.502 p.u. Fig.5.6 shows the estimated result of 5th harmonic amplitude using both the algorithms. RLS-adaline estimates 5th harmonics amplitude between 0.19 to 0.22 p.u., having more oscillations during initial time period. But the estimated value of fifth harmonic component using KF-Adaline is 0.202 p.u. Fig. 5.7 gives the estimated result of 7th harmonic component of signal using the two algorithms. RLS-Adaline estimates it around 0.155 p.u. but

oscillation varies from 0.145 to 0.16 p.u. KF-Adaline estimates 7th harmonic component as 0.149 p.u., which is more accurate. Fig. 5.8 provides a comparative estimation of 11th harmonic component of signal using both the algorithms. RLS-Adaline estimates it between 0.09 to 0.13 p.u. with its oscillations around 0.11 p.u. but KF-Adaline estimates it as 0.101 p.u. Fig. 5.9 shows the comparative estimation of dc component of signal using both the algorithms. Estimated value of signal using KF-Adaline is 0.496 p.u. but its value, using RLS-Adaline varies from 0.492 to 0.525 p.u. and it settles at 0.495 p.u. So we found that the estimation using KF-Adaline is more accurate compared to RLS-Adaline.

Fig.5.10 KF-Adaline estimation performance of phase of fundamental component of signal

Fig.5.11 KF-Adaline estimation performance of phase of 3rd harmonic component of signal

Fig.5.12 KF-Adaline estimation performance of phase of 5th harmonic component of signal

Fig.5.13 KF-Adaline estimation performance of phase of 7th harmonic component of signal

Fig.5.14 KF-Adaline estimation performance of phase of 11th harmonic component of signal

Fig.5.15 KF-Adaline estimation performance of MSE of static signal

Figures 5.10-5.14 show the tracking performances of the fundamental, 3rd, 5th, 7th and 11th harmonic component of signal in presence of random noise and decaying DC component using RLS-Adaline and KF-Adaline methods. In the above estimation process, KF-Adaline is tuned optimally by properly choosing the covariance and noise covariance matrices. The time required for trapping the fundamental and harmonic is approximately 0.02 sec. (20 samples) for RLS-Adaline method but KF-Adaline traps the fundamental and harmonic components initially with more correct estimation. Fig.5.15 shows the comparative estimation of Mean Square Error (MSE) of signal using the two algorithms. From the figure, it is found that, MSE performance in case of KF-Adaline is comparatively better than RLS-Adaline method.

5.3.2 Estimation of harmonics in presence of amplitude drift
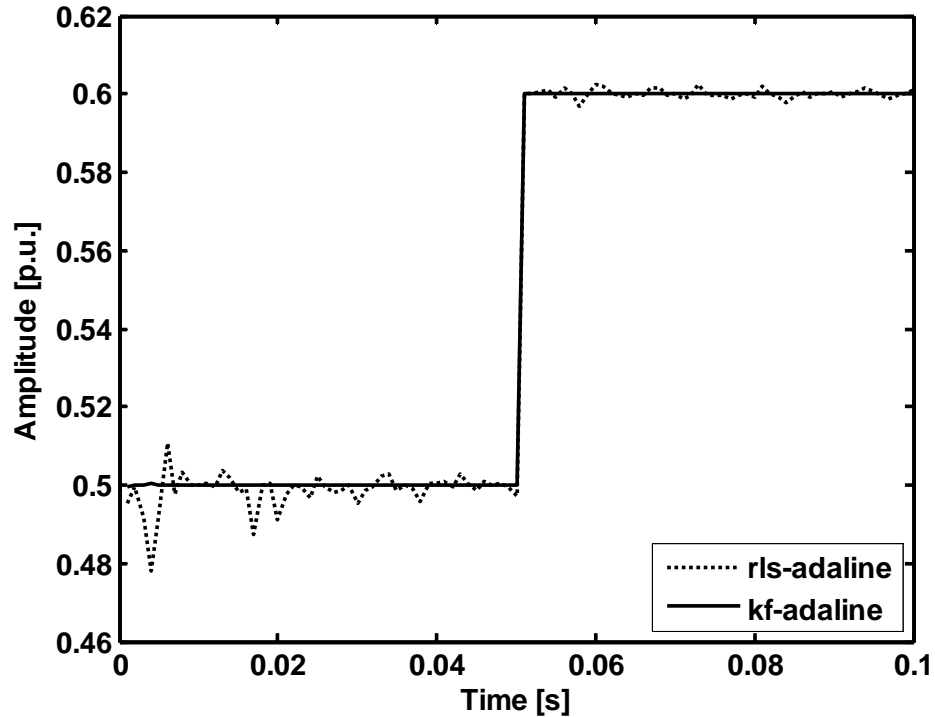
Fig. 5.16 KF-Adaline estimation performance of 3rd harmonic component of signal during amplitude change

Fig.5.16 shows the tracking of 3rd harmonic component of signal, when its amplitude suddenly changes from 0.5 p.u. to 0.6 p.u. at 0.05 sec. From the figure 5.15, it is seen that both the methods track the 3rd harmonic component but tracking by KF-Adaline is comparatively better.

Table 5.1 gives the harmonic estimations obtained by the RLS-Adaline, KF-Adaline methods. In contrast, the final harmonics parameters obtained with the proposed approach exhibit the best estimation precision where the largest amplitude deviation is 1.0928% occurred at the 3rd harmonics estimation and the largest phase angle deviation is 2.4829^{0} occurred at the 11th harmonics estimation also the computational time required using KF-Adaline is less compared to RLS-Adaline.

Table 5.1
Performance comparison of RLS-Adaline and KF-Adaline in presence of harmonics

Methods	Param-	Fund-	3rd	5th	7th	11th	Compu. time (sec.)
Actual	f(Hz)	50	150	250	350	550	
	A (V)	1.5	0.5	0.2	0.15	0.1	
	$\varphi(°)$	80	60	45	36	30	
RLS-Adaline	A (V)	1.4808	0.5070	0.1972	0.1458	0.1018	0.3575
	Deviation (%)	1.2807	1.3985	1.3822	2.7884	1.7560	
	$\varphi(°)$	78.5142	58.4516	43.118	34.8884	34.4097	
	Deviation (°)	1.4858	1.5484	1.882	1.1116	4.4097	
KF-Adaline	A (V)	1.4996	0.5055	0.1999	0.1490	0.0991	**0.0827**
	Deviation (%)	**0.0284**	**1.0928**	**0.0621**	**0.6897**	**0.9189**	
	$\varphi(°)$	80.2181	59.6455	43.8172	35.4725	32.4829	
	Deviation (°)	**0.2181**	**0.3545**	**1.1828**	**0.5275**	**2.4829**	

5.3.3 Harmonics Estimation of Signal in presence of Inter and Sub-Harmonics

To evaluate the performance of the proposed algorithm in the estimation of a signal in the presence of sub-harmonics and inter-harmonics, a sub-harmonic and two inter-harmonics components are added to the original signal. The frequency of sub-harmonic is 20 Hz, the amplitude is set to be 0.505 p.u. and the phase is equal to 75 degrees. The frequency, amplitude and phase of one of the inter-harmonic is 130 Hz, 0.25p.u. and 65 degrees respectively. The frequency, amplitude and phase of the other inter-harmonic is 180 Hz, 0.35p.u. and 10 degrees respectively.

Fig.5.17 KF-Adaline estimation performance of amplitude of sub-harmonic component of signal
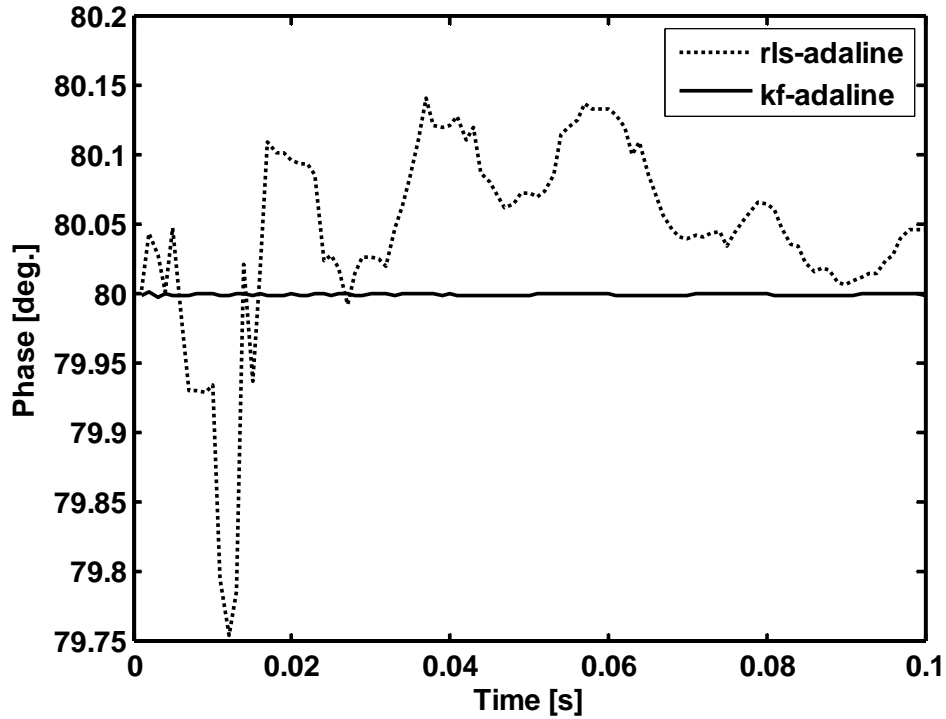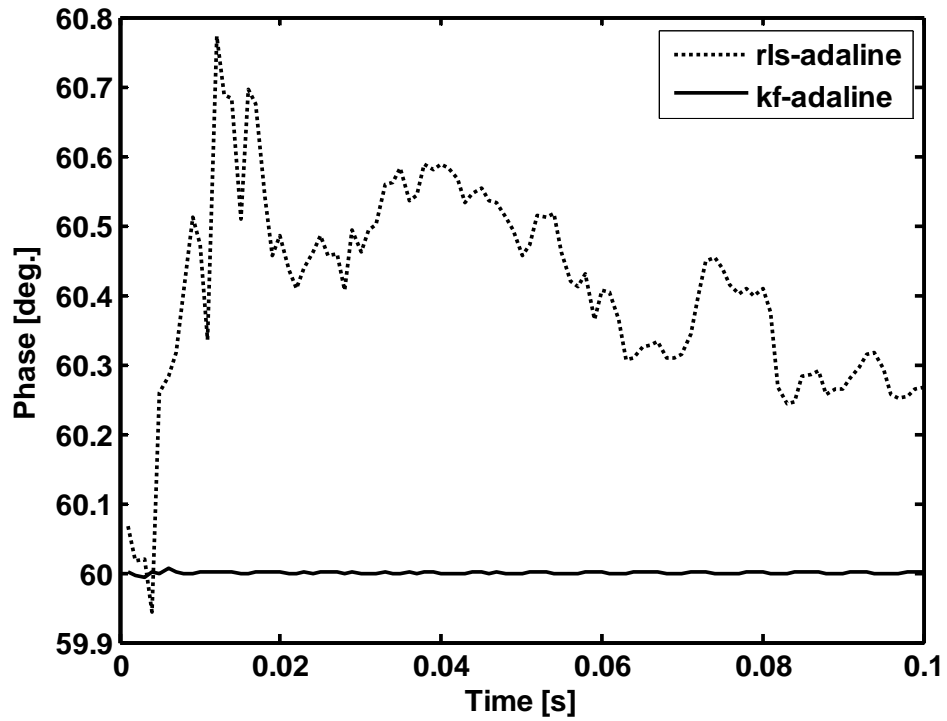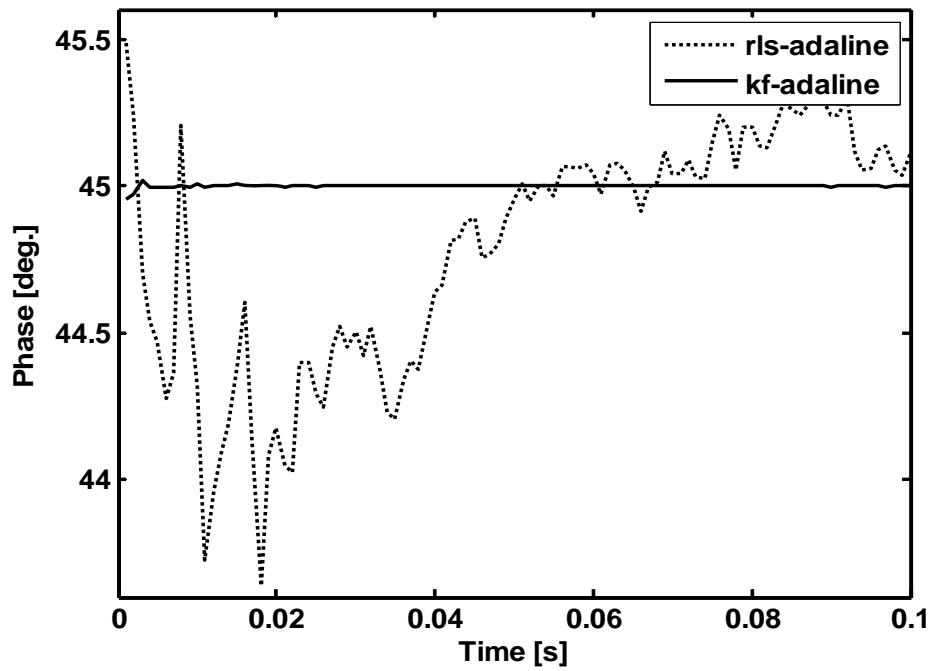

Fig.5.18 KF-Adaline estimation performance of phase of sub-harmonic component of signal
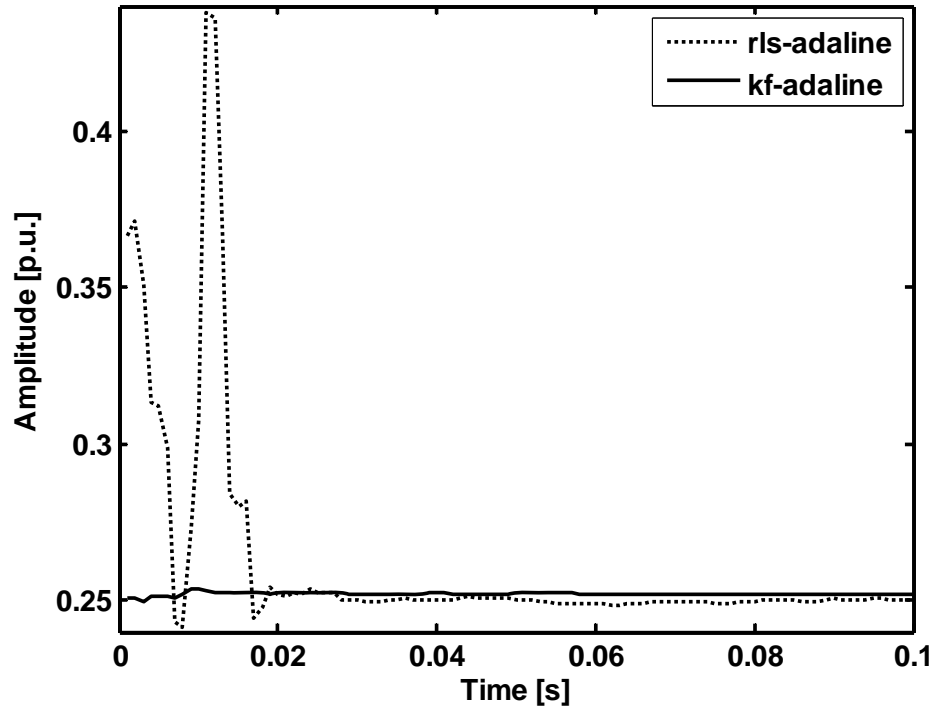
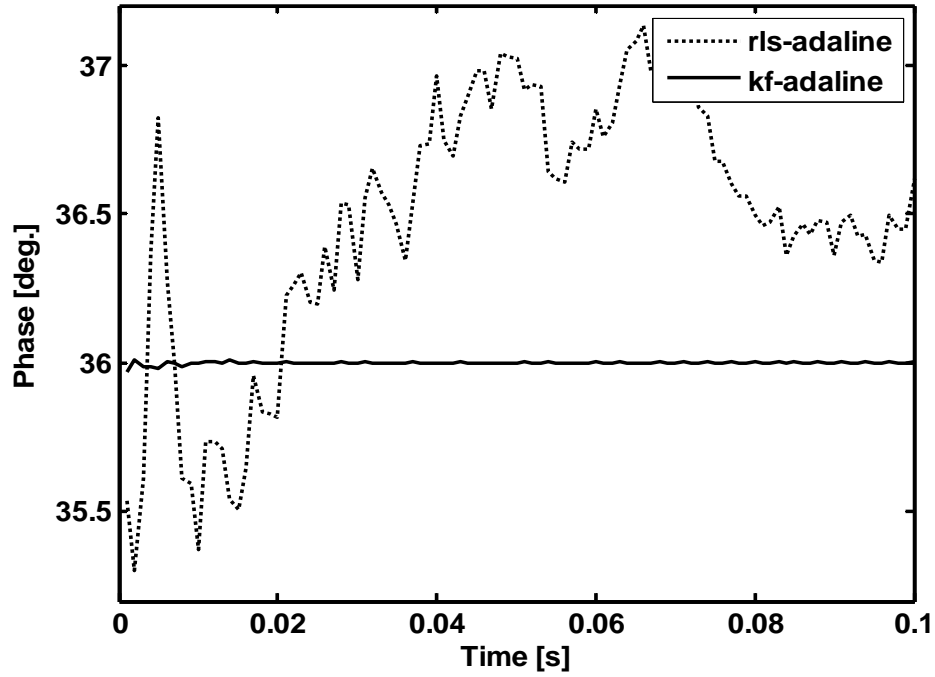Fig.5.19 KF-Adaline estimation performance of amplitude of inter-harmonic1 of signal
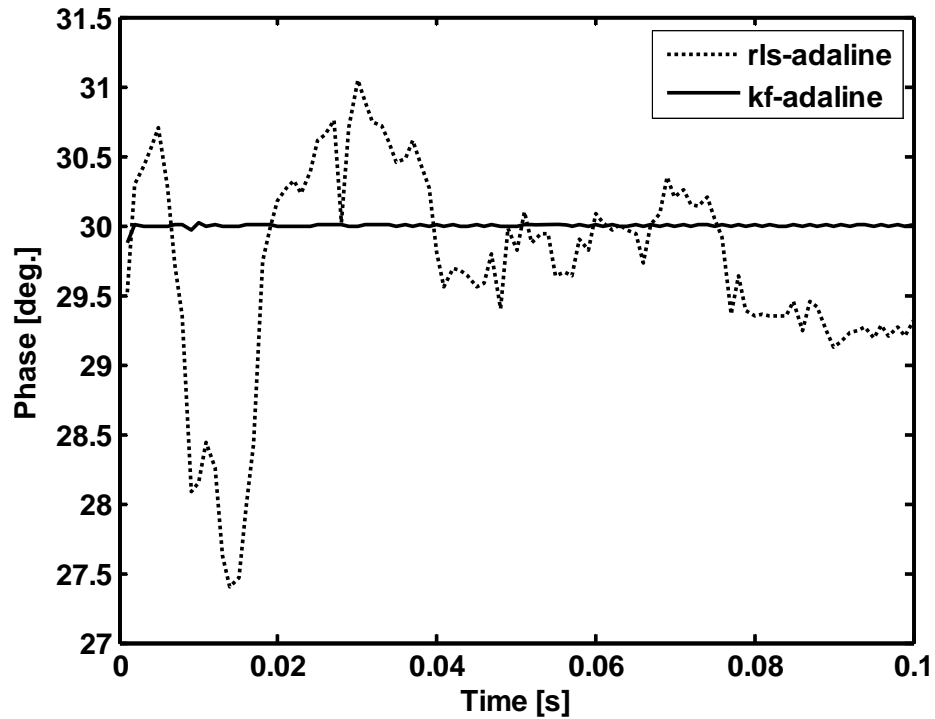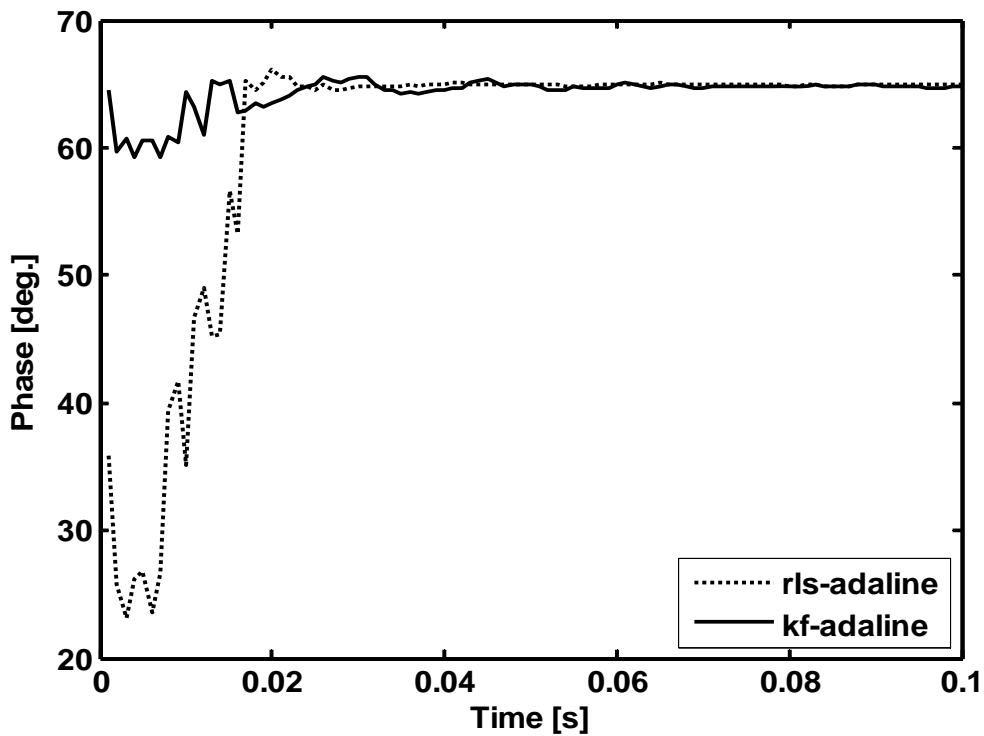

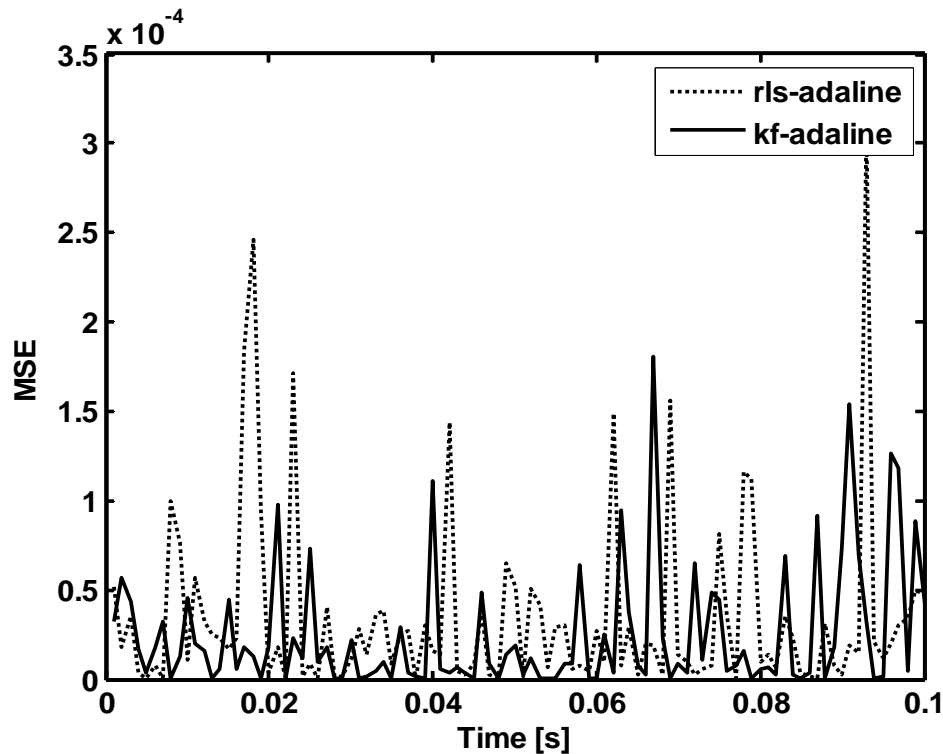Fig.5.20 KF-Adaline estimation performance of phase of inter-harmonic1 of signal
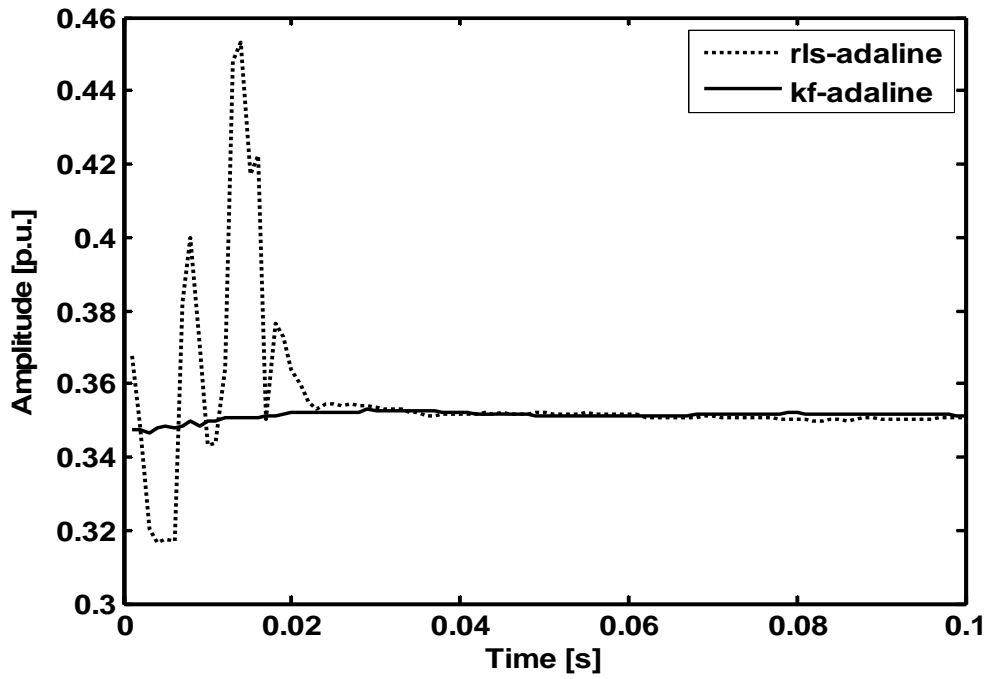
Fig.5.21 KF-Adaline estimation performance of amplitude of inter-harmonic2 of signal
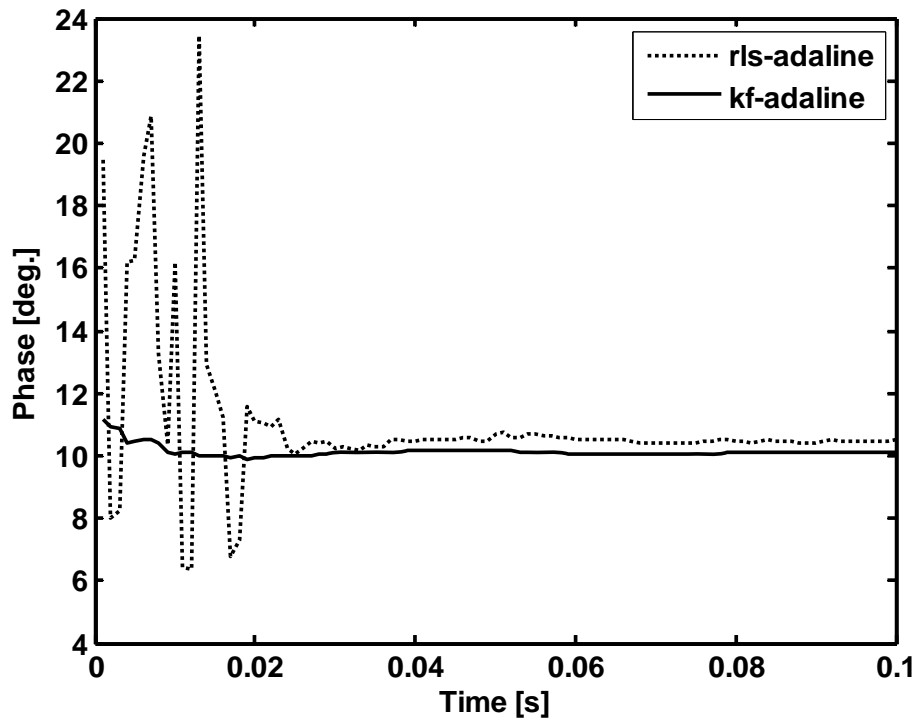
Fig.5.22 KF-Adaline estimation performance of phase of inter-harmonic2 of signal

Figures 5.17-5.22 show the estimation of amplitudes and phases of a sub-harmonic and two inter-harmonics. The time required to reach the reference values for the sub-harmonics and inter-harmonics components is 0.02 sec. using KF-Adaline algorithm. Using RLS-Adaline, time required to reach the reference value is 0.03 sec.

Table 5.2 gives the simulation results of the signal having two inter harmonics and one sub-harmonic component using RLS-Adaline and KF-Adaline methods. It shows that as a whole the performance of estimation using KF-Adaline is better as compared to RLS-Adaline. The largest amplitude deviation is 8.4476% occurred at 11th harmonics estimation and the largest phase angle deviation is 4.0501^0 occurred at 11th harmonics estimation.

Table 5.2
Performance comparison of RLS-Adaline and KF-Adaline with inter and sub-Harmonics

Methods	Paramete-	Sub	Funda-	3rd	Inter1	Inter2	5th	7th	11th
Actual	f(Hz)	20	50	150	180	230	250	350	550
	A (V)	0.5	1.5	0.5	0.25	0.35	0.2	0.15	0.1
	φ(°)	75	80	60	65	10	45	36	30
RLS-Adaline	A (V)	0.49	1.484	0.491	0.264	0.351	0.203	0.154	0.1
	Deviation (%)	2.836	1.019	1.651	5.689	0.346	1.559	3.274	0.401
	φ(°)	73.10	78.113	57.80	61.51	11.35	41.77	38.15	39.141
	Deviation (°)	1.898	1.886	2.196	3.489	1.35	3.227	2.151	9.141
KF-Adaline	A (V)	0.494	1.5	0.5	0.253	0.361	0.204	0.143	0.091
	Deviation (%)	1.063	0.046	0.12	1.51	3.168	2.039	4.119	8.447
	φ(°)	75.11	80.245	59.939	65.206	8.927	42.92	34.97	34.05
	Deviation (°)	0.114	0.245	0.06	0.206	1.097	2.074	1.022	4.05

In the simulation studies the performance index ε is given by

$$\varepsilon = \frac{\sum_{k=1}^{N}(y(k) - y(\hat{k}))^2}{\sum_{k=1}^{N} y(k)^2} \times 100 \tag{5.16}$$

where $y(k)$ and $y(\hat{k})$ are actual and estimated signal respectively. In this case the significance of the performance index ε is that it provides the accuracy of the estimation algorithm. Less the value of ε, means more accuracy of estimation and vice versa.

Table 5.3
Comparison of Performance Indices (RLS-Adaline and KF-Adaline)

SNR	RLS-Adaline	KF-Adaline
No noise	0.0583	0.0197
40 dB	0.0636	0.04
20 dB	0.8921	0.6477
10 dB	12.710	5.253

The estimation results of RLS-Adaline and KF-Adaline are given in Table 5.3. From which it can be seen that KF-Adaline achieves a significant improvements in terms of reducing error for harmonics estimation in comparison to RLS-Adaline.

5.3.4 Harmonic Estimation of a Dynamic Signal

To examine the performance of RLS-Adaline algorithm in tracking harmonics and its robustness in rejecting noise, a time-varying signal of the form (4.30) of chapter 4 is used. The variations of fundamental, 3rd and 5th harmonics components of signal w.r.t time are given in (4.31)-(4.33).

Where $f_1 = 1.0\,\text{Hz}$ $f_3 = 3.0\,\text{Hz}.$ $f_5 = 6.0\,\text{Hz}.$
And random noise $\mu(t)$ is same as in the case of static signal.
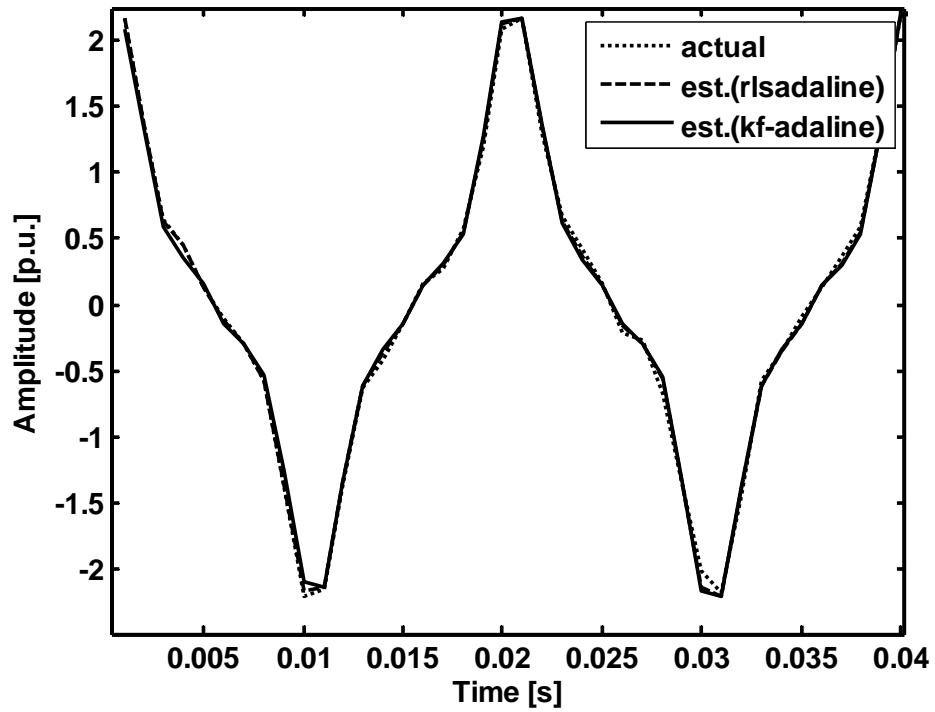
Fig.5.23 Comparison of actual and estimated wave forms of dynamic signal (RLS-Adaline and KF-Adaline).
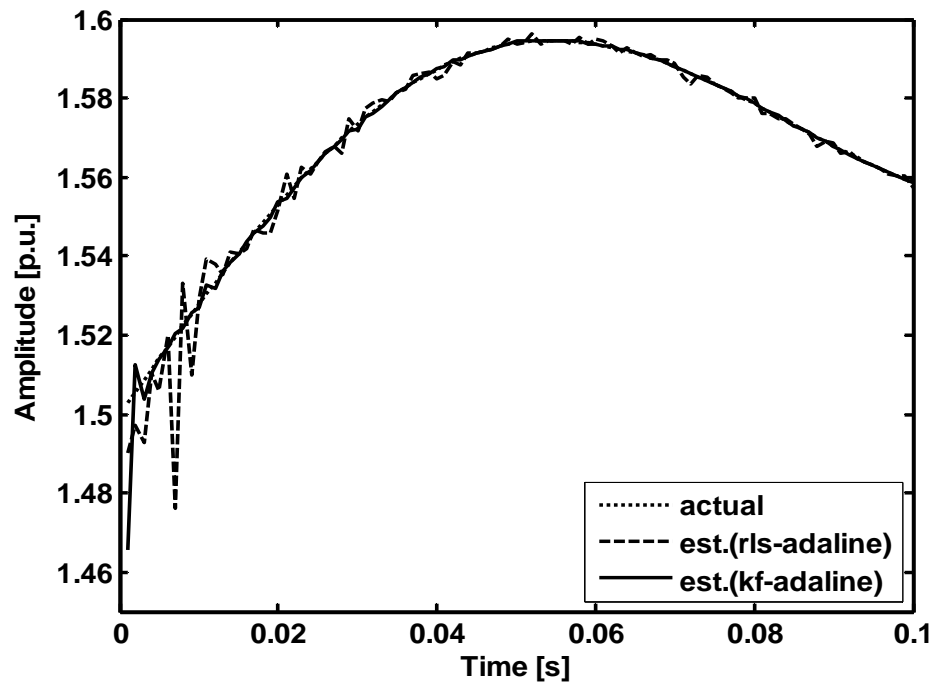
Fig.5.24 KF-Adaline estimation performance of amplitude of fundamental component of dynamic signal
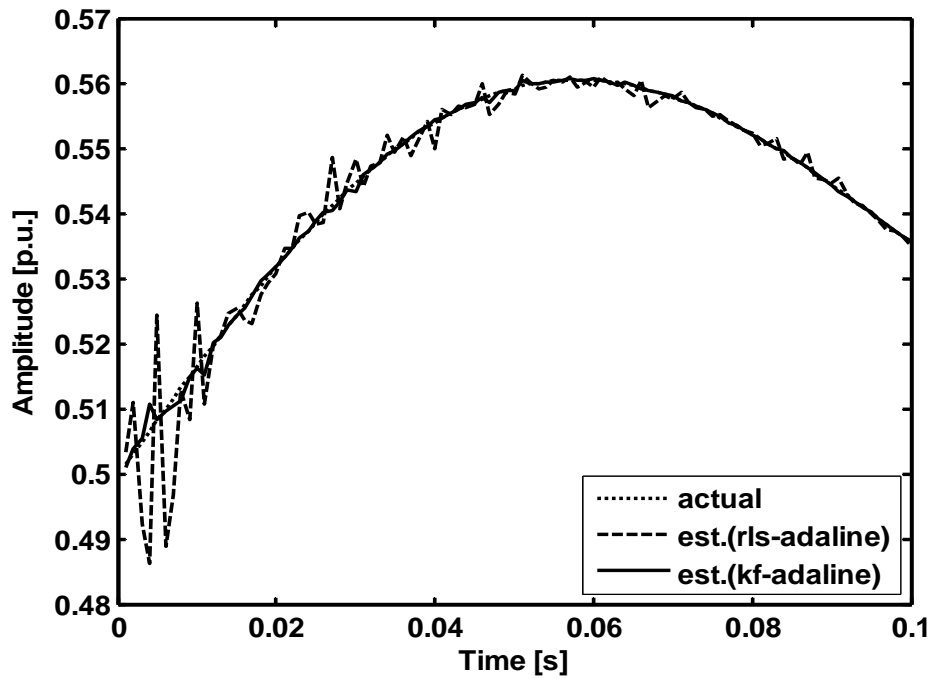
Fig.5.25 KF-Adaline estimation performance of amplitude of third harmonic component
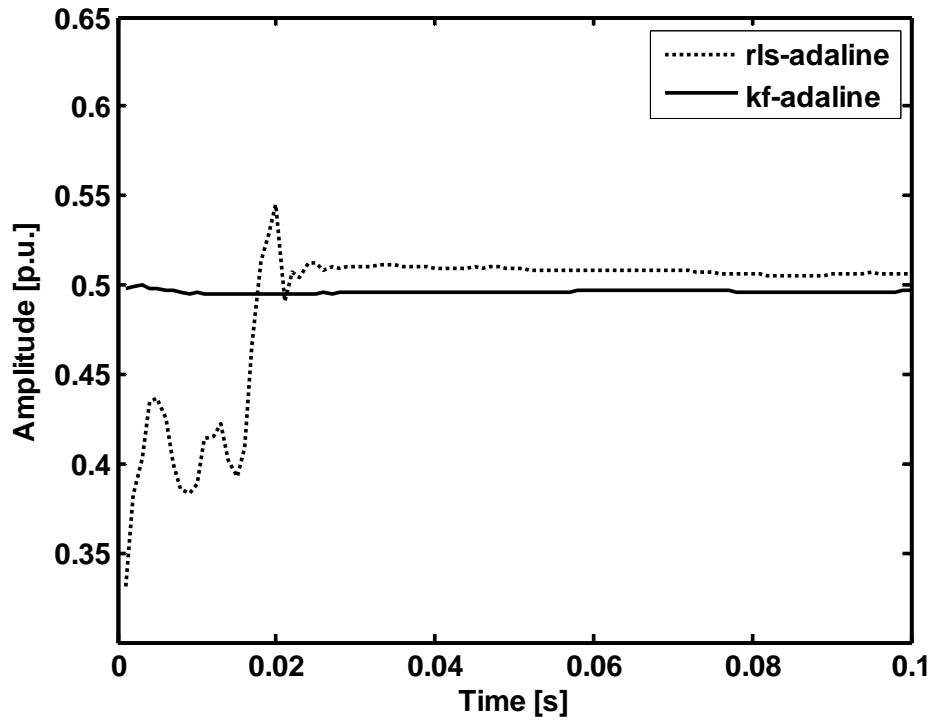of dynamic signal
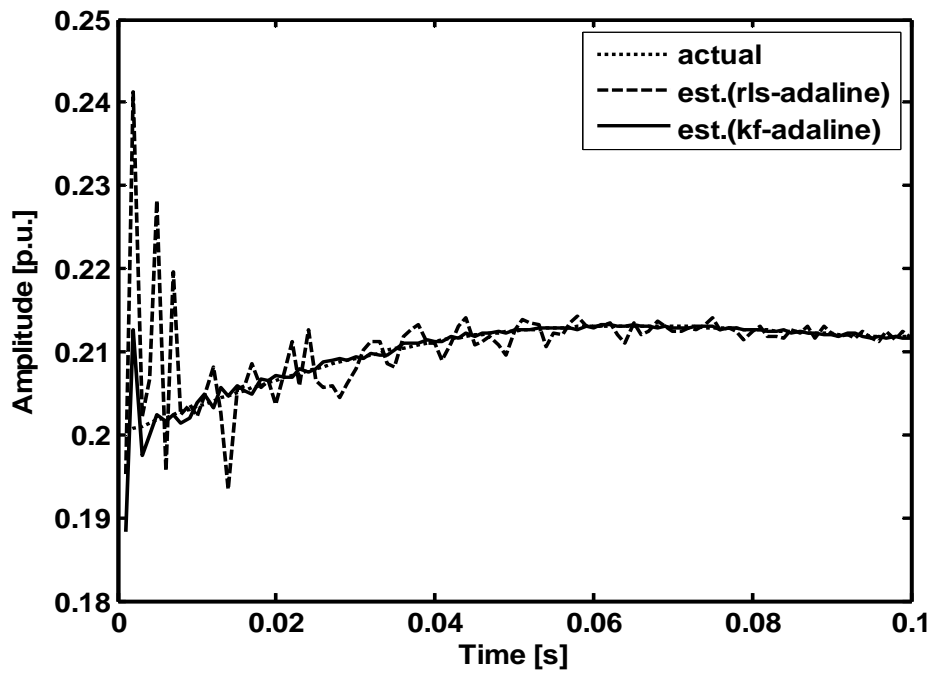
Fig.5.26 KF-Adaline estimation performance of amplitude of fifth harmonic component
of dynamic signal

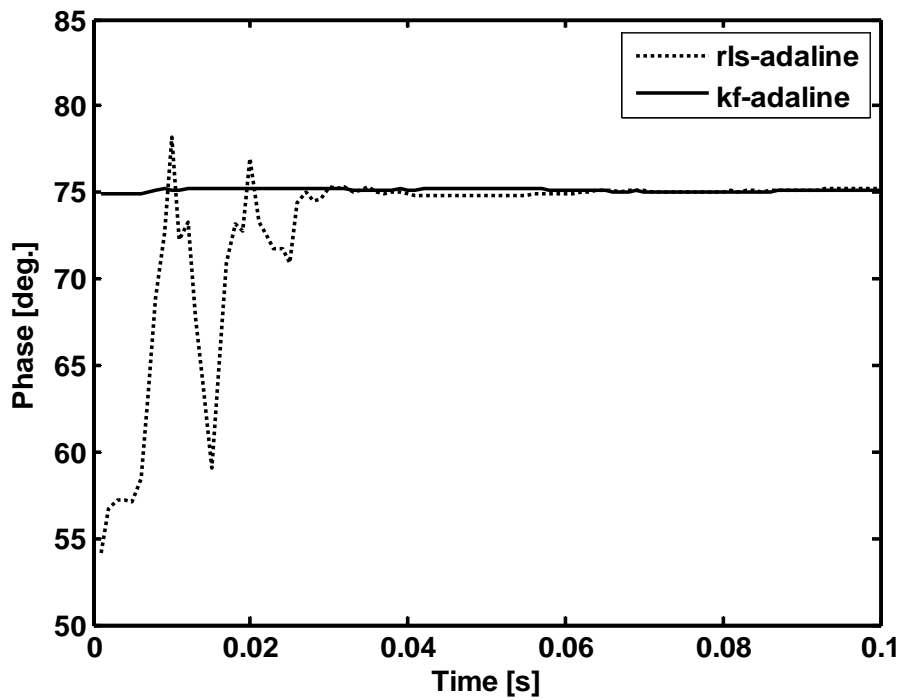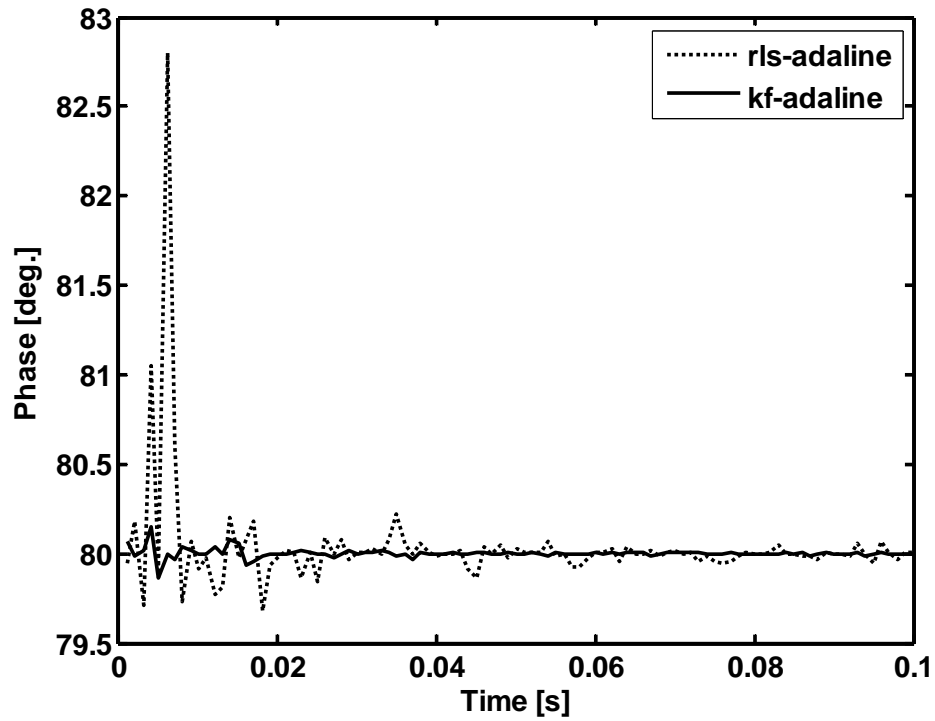Fig.5.27 KF-Adaline estimation performance of phase of fundamental component of dynamic signal
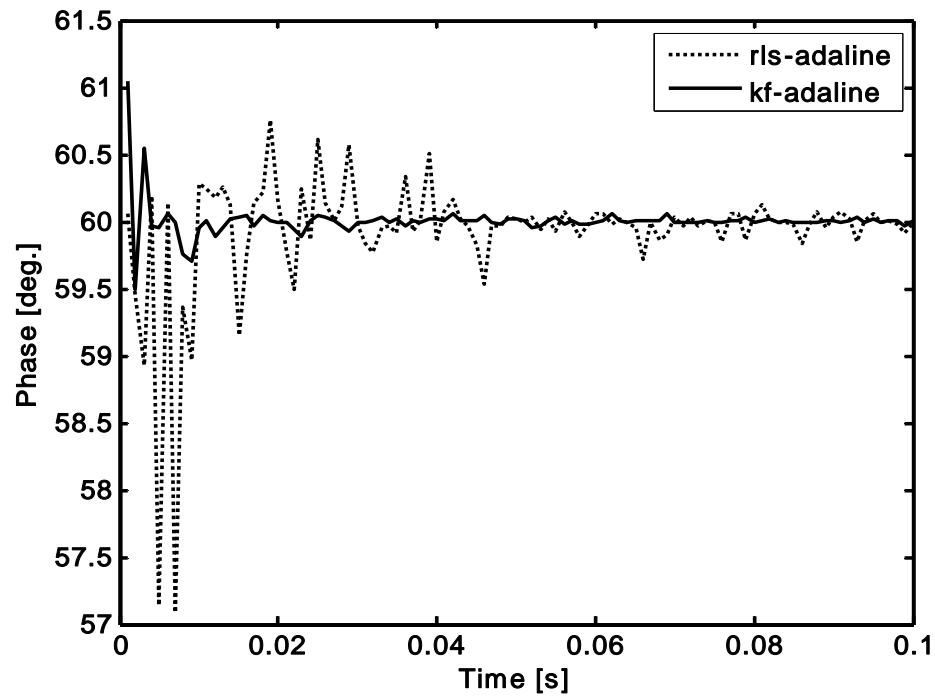
Fig.5.28 KF-Adaline estimation performance of phase of third harmonic component of dynamic signal
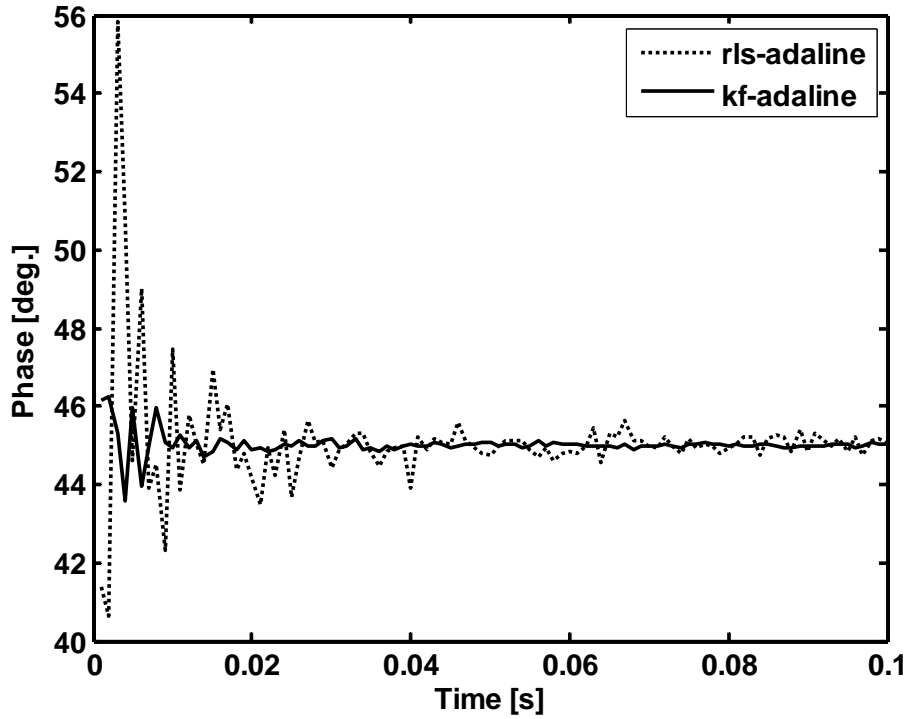
Fig.5.29 KF-Adaline estimation performance of phase of fifth harmonic component of dynamic signal
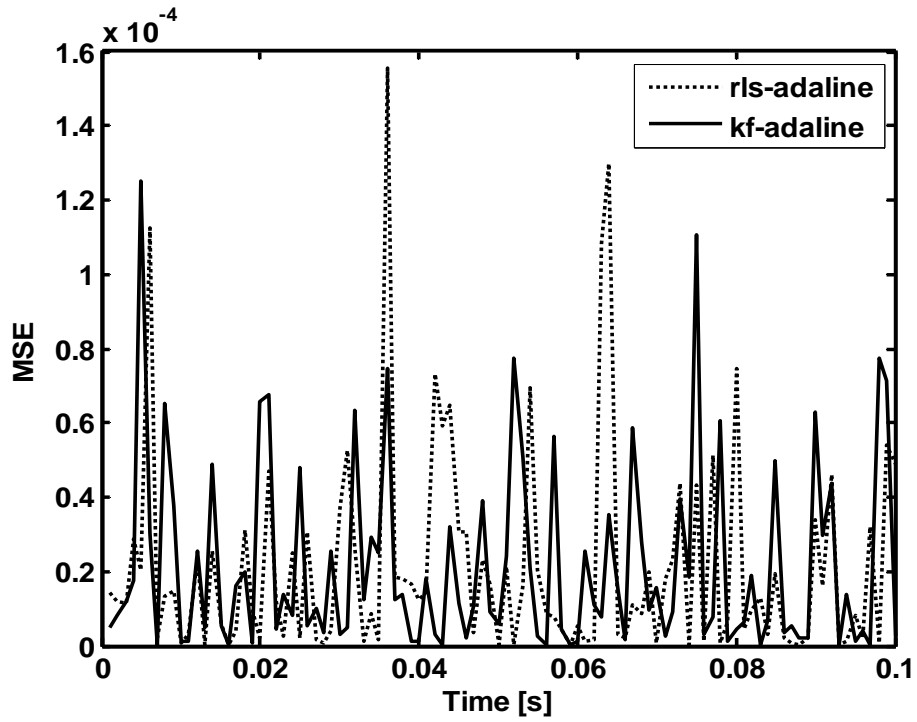
Fig.5.30 KF-Adaline estimation performance of MSE of dynamic signal

Fig.5.23 shows the actual vs. estimated value of signal using RLS-Adaline and KF-Adaline algorithms. In both the cases actual and estimated value closely matches with each other. Fig. 5.24-5.26 show the tracking of fundamental, 3rd and 5th harmonic component of amplitude of a dynamic signal using both RLS-Adaline and KF-Adaline methods. In all the three cases RLS-Adaline provides oscillatory estimation but KF-Adaline provides more accurate and consistent performance. Figs 5.27-5.29 show the tracking of fundamental, 3rd and 5th harmonic components of phases of a dynamic signal using both the methods. Both the methods estimates correctly but KF-Adaline performance is better having negligible oscillations. Fig.5.30 provides a comparative performance of Mean Square Error (MSE) of signal. KF-Adaline performance is slightly better in MSE analysis

Table 5.4
Performance comparison of RLS-Adaline and KF-Adaline for Dynamics Signal

Methods	Parameters	Fundamental	3rd	5th	Computational time (seconds)
Actual	f(Hz)	50	150	250	
	A (V)	1.5701	0.5447	0.2101	
	φ(°)	80	60	45	
RLS-Adaline	A (V)	1.5699	0.5447	0.2101	1.233
	Deviation (%)	0.0242	0.0435	0.0021	
	φ(°)	79.9942	60.0037	44.9651	
	Deviation (°)	0.0058	0.0037	0.0349	
KF-Adaline	A (V)	1.5701	0.5447	0.2101	0.878
	Deviation (%)	0.0117	0.0427	0.0151	
	φ(°)	80	59.9999	44.9996	
	Deviation (°)	4.44×10^{-6}	7.51×10^{-5}	3.65×10^{-4}	

Table 5.4 gives the simulation results of the dynamic signal. Table shows that for the dynamic signal estimation, both the methods discussed in this chapter give accurate

estimation but the accuracy using KF-Adaline is slightly better as compared to RLS-Adaline method.

5.4 Experimental Studies and Results

For real time application of the algorithms in estimating harmonics in a power system, data i.e obtained in a laboratory environment on running a DG set on normal working day of the laboratory as per the experimental setup discussed in section 4.4 of chapter 4 is taken. Fig. 5.31 shows the estimation of signal using both the algorithms from the real data obtained from the experiment. From this Fig., it is concluded that the estimated waveform is very close to the real one in first half cycle and small deviation is there in second half cycle. Hence the obtained results are satisfactory for the application with experimental data.
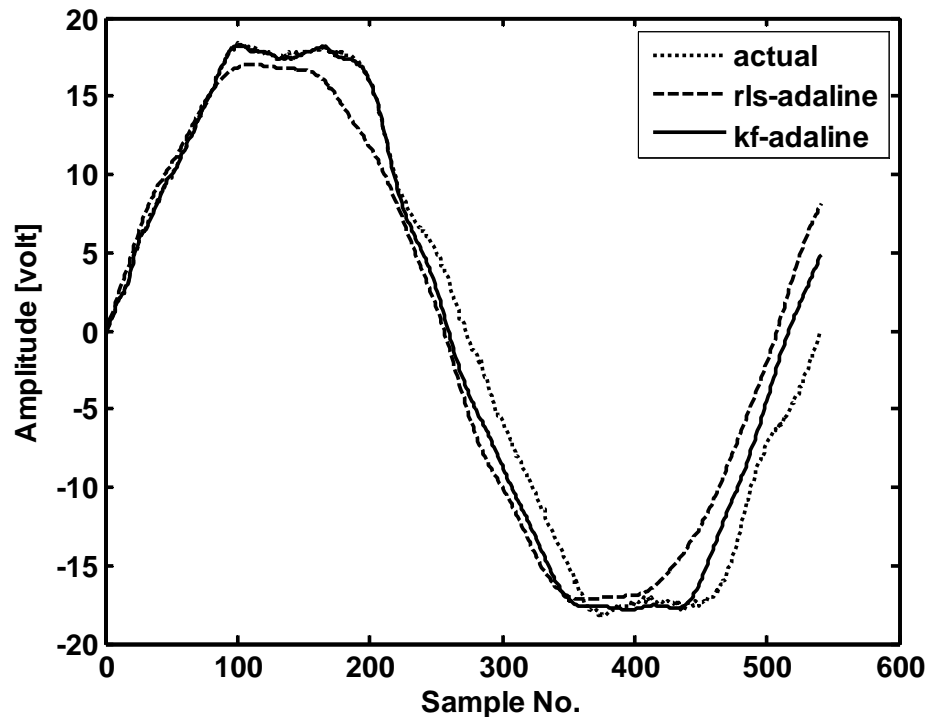
Fig. 5.31 KF-Adaline estimation performance of signal from real data

Table 5.5
Comparison of Performance Index of Experimental Data (RLS-Adaline and KF-Adaline)

Parameter	RLS-Adaline	KF-Adaline
ε	7.4718	2.4985

   For the purpose of estimation, the performance index is calculated for the two algorithms based on equation (5.21) and the results are given in Table 5.5. In this case KF-Adaline obtains the most accurate estimation result since it has less performance index (around 2.5%), which is acceptable.

5.5 Hybrid BFO Methods for Harmonics estimation

   The Schematic as described in section 3.2.2 and Fig. 3.14 for frequency estimation is used for harmonics estimation. First input signal is fed to BFO algorithm and unknown parameters are optimized using this algorithm. Then optimized output of BFO algorithm is taken as the initial value of weight of Adaline/ RLS algorithm. Output of Adaline/RLS is compared with the desired output and the error obtained, is minimized by updating the weight of the Adaline/RLS. From the final updated weight of the Adaline/RLS, amplitudes and phases of the fundamental and harmonics components are determined.

5.5.1 Proposed RLS-BFO Combined Approach to Harmonic Estimation

   Same signal as described by (4.1) is considered. The steps from (4.1) to (4.5) are followed. Then parametric form of the signal such as $y(t) = H(t)X$ is taken. Where $H(t)$ is given by (4.6) and X is given by (4.7) and (4.8). The optimized output of the unknown parameter using BFO algorithm is taken as the initial values of unknown parameter (X) for estimation using RLS. The vector of unknown parameter can be updated using (4.16)-(4.19). After updating of unknown parameter vector, amplitudes, phases of the

fundamental and nth harmonic parameters and dc decaying parameters are estimated using equations (4.12)-(4.15).

5.5.2 Proposed Adaline-BFO Combined Approach to Harmonics Estimation

The general form of the waveform of (4.1) of previous chapter is taken. The waveform is discretized as per (4.2). It is then rewritten as (4.5), on approximating decaying term using first two terms of Taylor series expansion.

The signal (4.5) in parametric form may be written as

$$y(k) = X(k)W \tag{5.17}$$

The equation (5.1)) gives an idea of using an adaptive linear combiner comprising a neural network called 'Adaline' to estimate the components of the harmonics. Fig.5.1 of previous chapter shows the block diagrammatic representation of the Adaline. Product of input signal and weight of the Adaline gives the estimated output and is compared with the desired output. The error obtained, is minimized by updating the weight of the Adaline.

The input to the Adaline is

$$X(k) = [\sin(\omega_1 kT) \quad \cos(\omega_1 kT) \quad ... \quad \sin(\omega_N kT) \quad \cos(\omega_N kT) \quad 1 \quad -kT]^T$$

The weight vector of the Adaline

$$W(k) = [W_1(k) \quad W_2(k) \quad ... \quad W_{2N-1}(k) \quad W_{2N}(k) \quad W_{2N+1}(k) \quad W_{2N+2}(k)]^T$$

The optimized output of the unknown parameter using BFO algorithm is taken as the initial values of the weight vector of Adaline and is updated using a modified Widrow-Hoff delta rule as

$$W(k+1) = W(k) + \frac{\alpha e(k)U}{\lambda + X^T(k)X(k)} \tag{5.18}$$

where $U = SGN(X(k))$ \qquad\qquad (5.19)

$$SGN(X_i) = \begin{cases} +1, X_i > 0 \\ -1, X_i < 0 \end{cases} \tag{5.20}$$

$$i = 1,2,...,2N + 2$$

$$0 < \alpha < 2$$

The learning parameter α can be adapted using the following expression:

$$\alpha(k) = \frac{\alpha_0}{\left(1 + \dfrac{k}{\beta}\right)} \tag{5.21}$$

where α_0 is the initial learning rate and β is decaying rate constant. λ Is a small quantity and is usually chosen to make

$$\lambda + X^T(k)X(k) \neq 0$$

After updating of weight vector of the Adaline, amplitudes and phases of the fundamental and nth harmonic parameters and dc decaying parameters are estimated using (5.8)-(5.11).

where

$$W = [A_1 \cos(\phi_1) \quad A_1 \sin(\phi_1) \quad ... \quad A_n \cos(\phi_n) \quad A_n \sin(\phi_n) \quad A_{dc} \quad A_{dc}\alpha_{dc}]^T$$

Flow chart as described in Fig. 3.15 is also used for the estimation of harmonics in a power system signal.

5.6 Simulation Results and Discussions

5.6.1 Static signal corrupted with random noise and decaying DC component.

The power system signal corrupted with random noise and decaying DC component is taken. The signal used for the estimation, besides the fundamental frequency, contains higher harmonics of the 3rd, 5th, 7th, 11th and a slowly decaying DC component. This kind of signal is typical in industrial load comprising power electronic converters and arc furnaces. The signal as in (4.26) of previous chapter is taken. The signal is corrupted by random noise $\mu(t) = 0.01rand(t)$ having normal distribution with zero mean and unity variance. In the simulation work, in harmonics estimation, the

168

values of different parameters taken during both simulation and experimentation work are given in Table 5.6. The no. of parameters to be optimized, $p=12$ (without inter and sub-harmonics case), $p=18$ (with inter and sub-harmonics case) are taken.

Table-5.6
Values of parameters used for simulation and experimental work (BFO, RLS-BFO and Adaline-BFO)

α_0	β	λ	S	p	N_s	N_c	N_{re}	N_{ed}	P_{ed}	$C(i)$	$d_{attract,}$	$w_{attract}$	$h_{repellant}$	$w_{repellant}$
0.01	100	0.01	100	12, 18	3	5	10	10	0.25	0.001	0.05	0.3	0.05	10
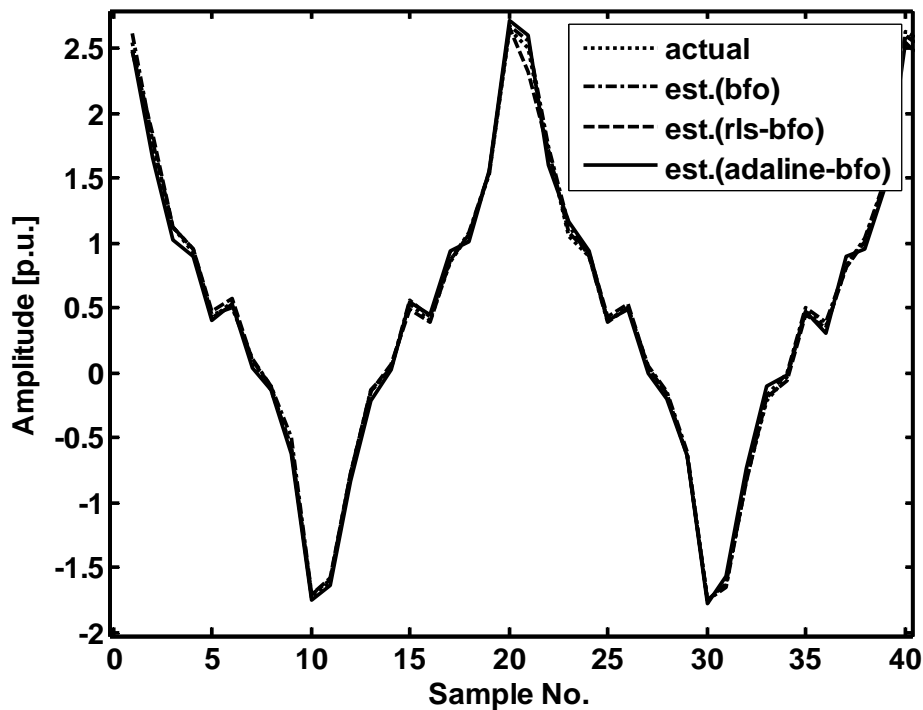
Fig. 5.32 Comparison of Actual vs. Estimated output of signal (40 dB) (BFO, RLS-BFO and Adaline-BFO)
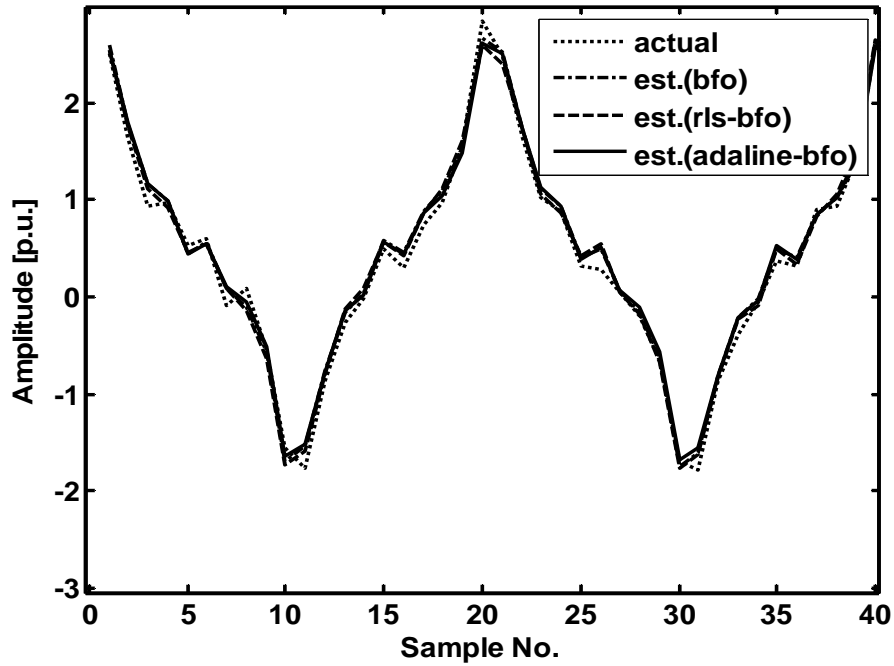
Fig. 5.33 Actual vs. Estimated output of signal (20 dB) (BFO, RLS-BFO and Adaline-BFO)
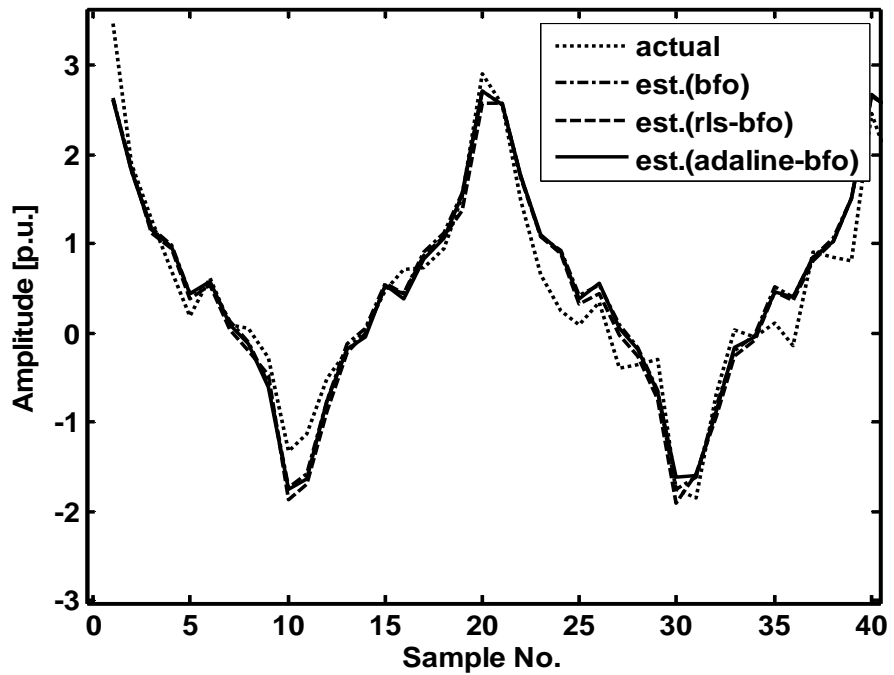
Fig. 5.34 Actual vs. Estimated output of signal (10 dB) (BFO, RLS-BFO and Adaline-BFO)

Figures 5.32-5.34 compares actual and estimated value of signal using three algorithms with SNR values of 40, 20 and 10 dB respectively .It is seen that at 40 dB SNR value the estimated value closely matches with the actual value but as SNR value of signal decreases, there is more deviations of estimated value from actual value
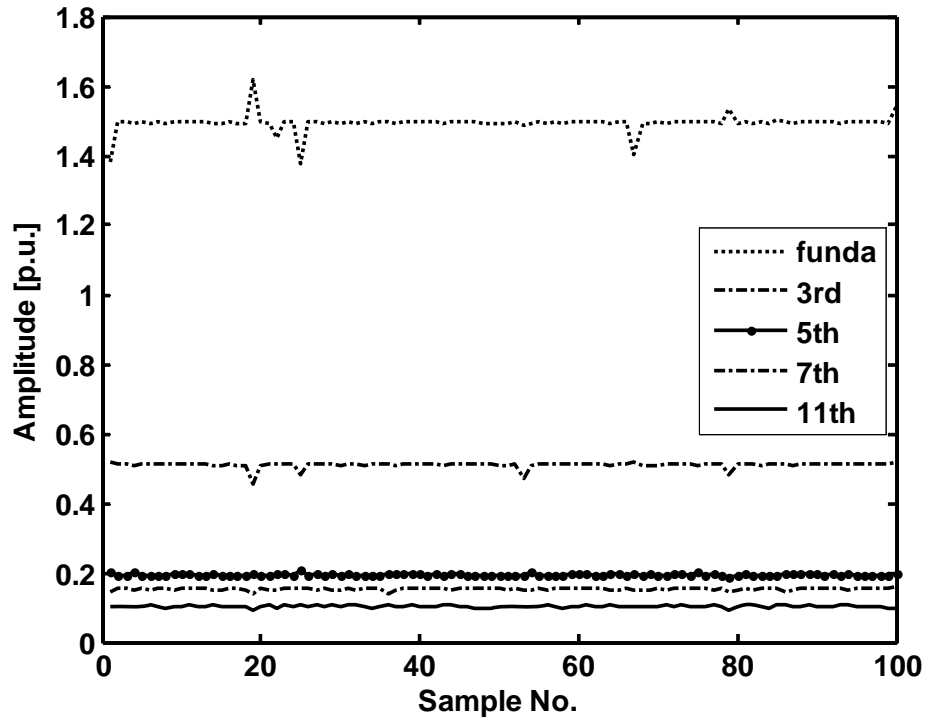
Fig. 5.35 Estimation of Amplitude of Fundamental and Harmonics components of signal using RLS-BFO
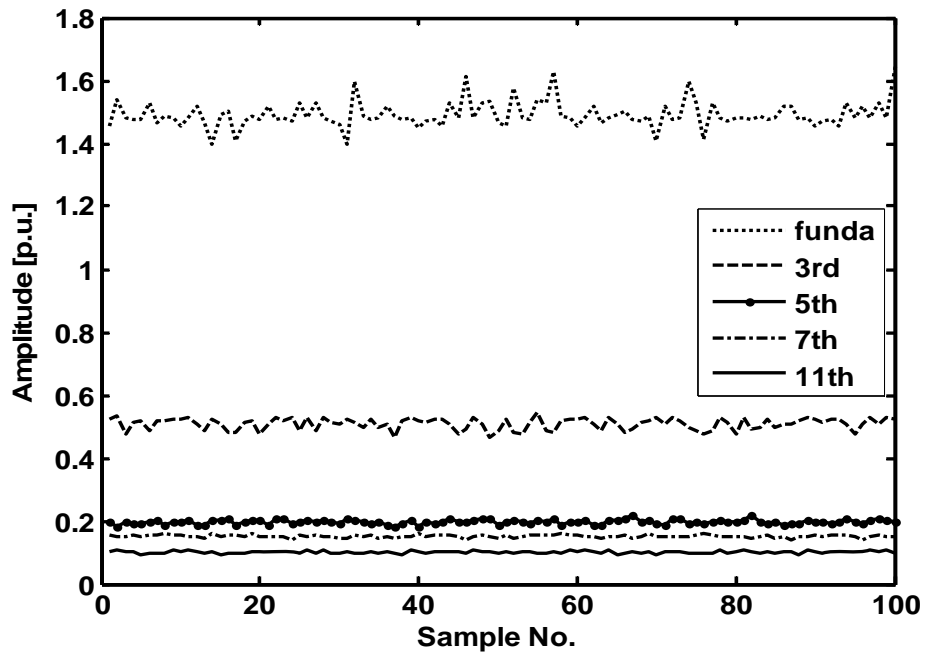
Fig.5.36 Estimation of Amplitude of Fundamental and Harmonics components of signal using Adaline-BFO
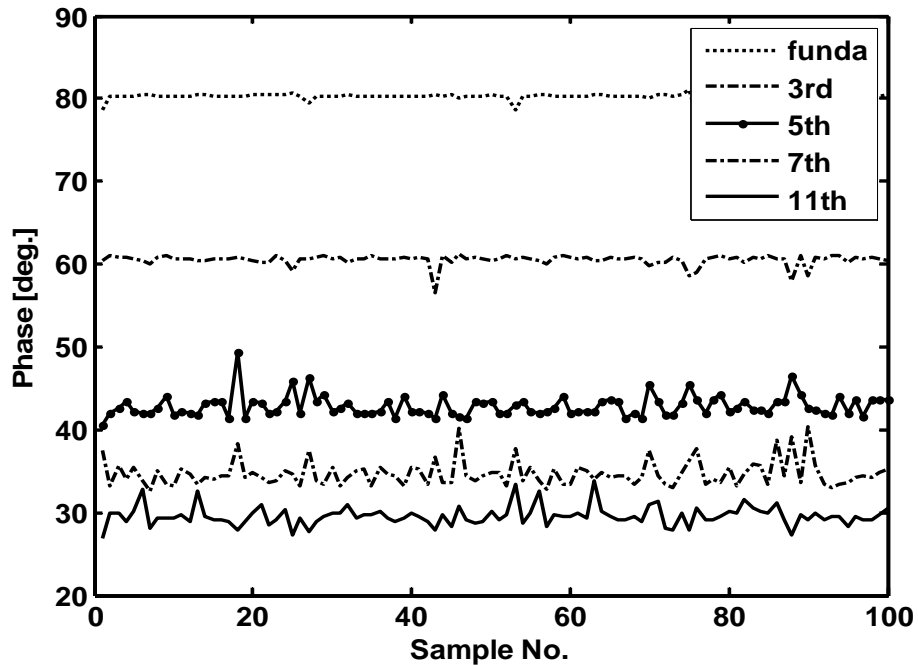
Fig. 5.37 Estimation of phase of Fundamental and Harmonic Components of signal using RLS-BFO
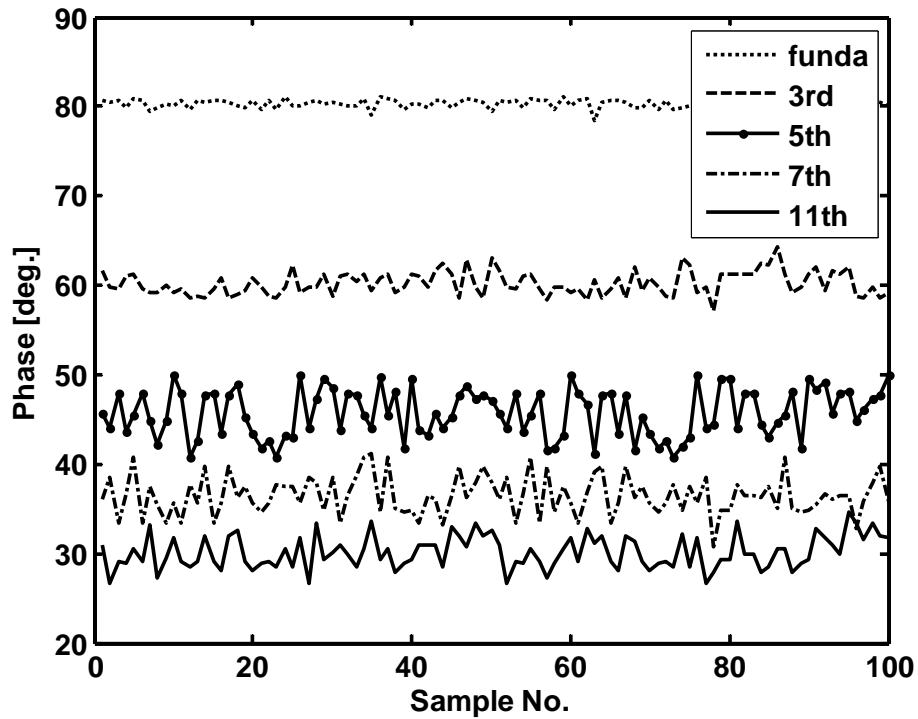
Fig. 5.38 Estimation of Phase of Fundamental and Harmonics Components of signal
using Adaline-BFO
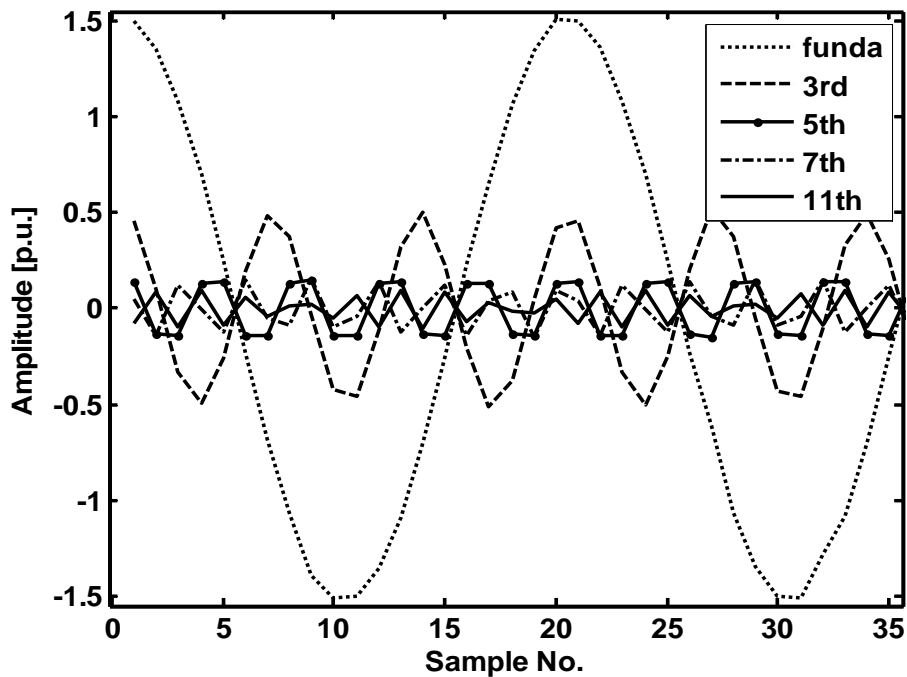
Fig. 5.39 Estimation of signal having fundamental and all the harmonics using RLS-BFO
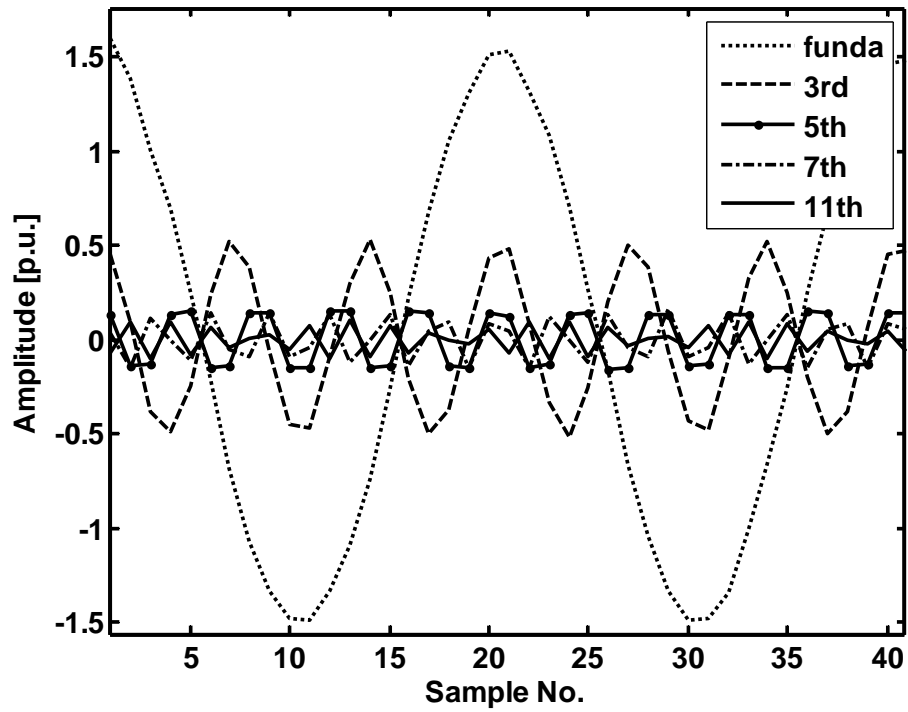
Fig. 5.40 Estimation of signal having fundamental and all the harmonics using Adaline-BFO
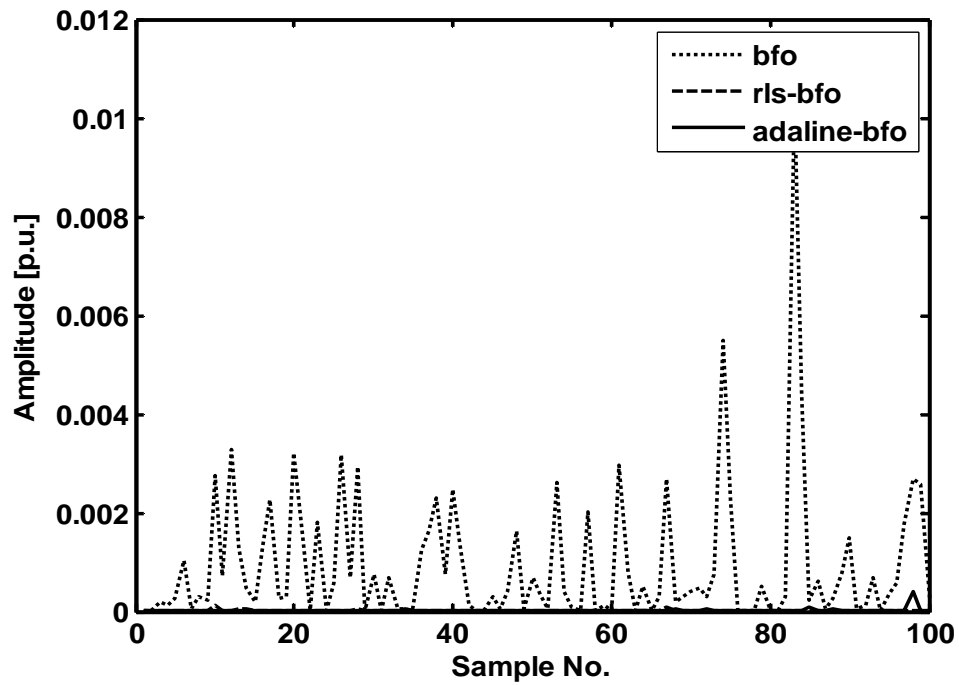
Fig. 5.41 Adaline-BFO estimation performance of MSE of signal

Figs. 5.35 and 5.36 estimate amplitudes of fundamental as well as harmonic components contained in the signal using RLS-BFO and Adaline-BFO algorithms respectively. Figs. 5.37 and 5.38 show the estimation of phases of fundamental and harmonic components using RLS-BFO and Adaline-BFO respectively. From these four figs., we come to conclude that both the algorithms track the fundamental as well as harmonic components accurately. Fig. 5.39 and 5.40 separately estimates fundamental and harmonic components contained in the signal using RLS-BFO and Adaline-BFO respectively. Fig.5.41 shows the comparative estimation of Mean Square Error (MSE) of signal using the two algorithms. From the figure, it is found that, MSE performance in case of Adaline-BFO and RLS-BFO is comparatively better than BFO
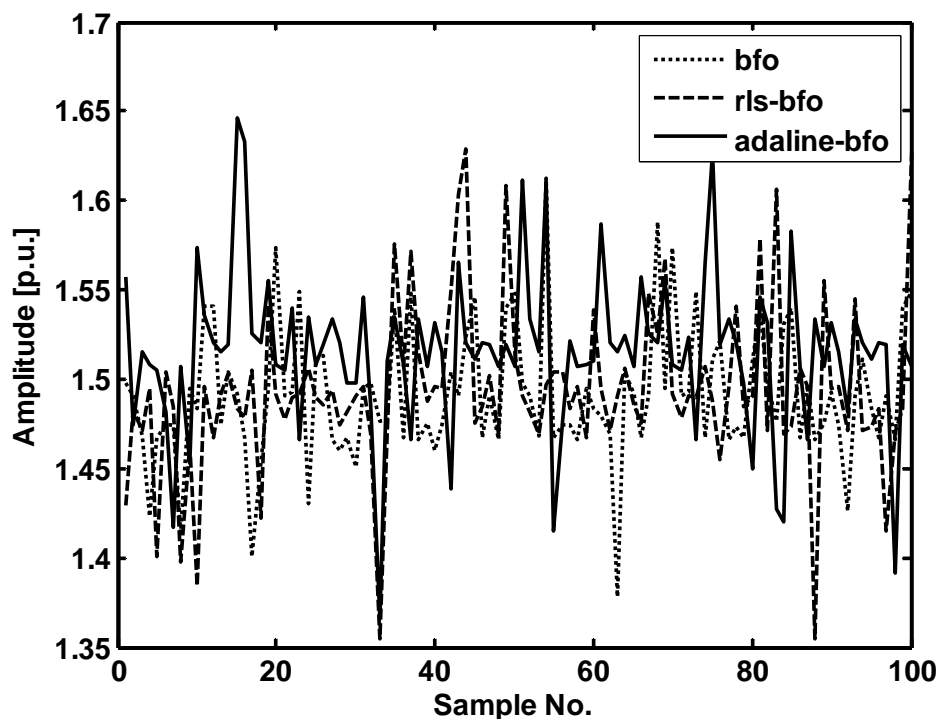
Fig. 5.42 Comparison of Estimation of amplitude of Fundamental component of signal
(BFO, RLS-BFO and Adaline-BFO)
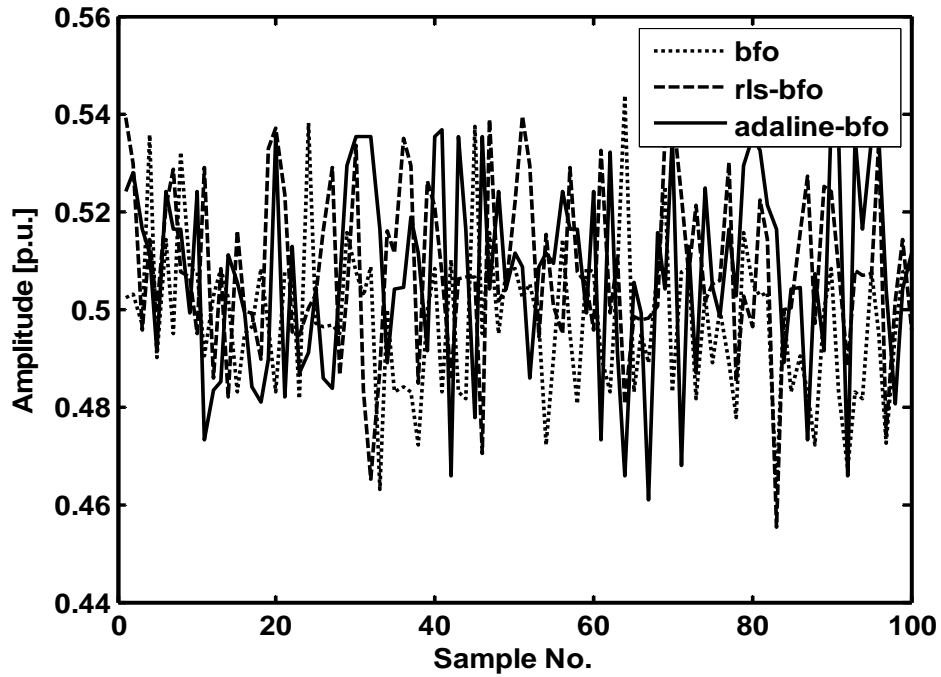
Fig. 5.43 Comparison of Estimation of amplitude of 3rd Harmonic component of Signal (BFO, RLS-BFO and Adaline-BFO)
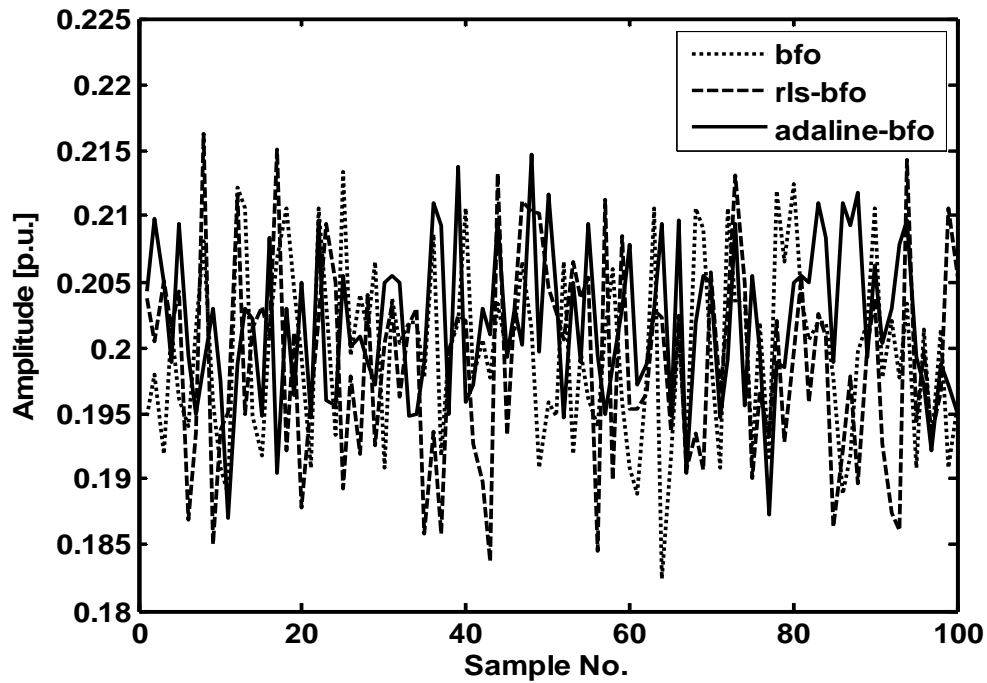
Fig. 5.44 Comparison of Estimation of amplitude of 5th Harmonic component of Signal (BFO, RLS-BFO and Adaline-BFO)
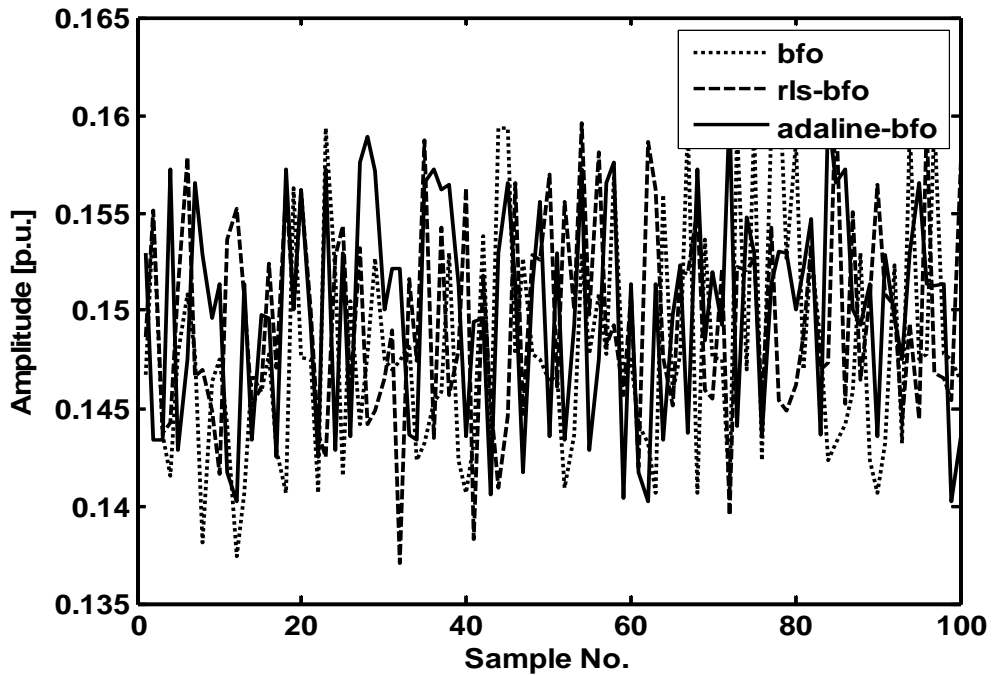
Fig. 5.45 Comparison of Estimation of amplitude of 7th Harmonic component of Signal (BFO, RLS-BFO and Adaline-BFO)
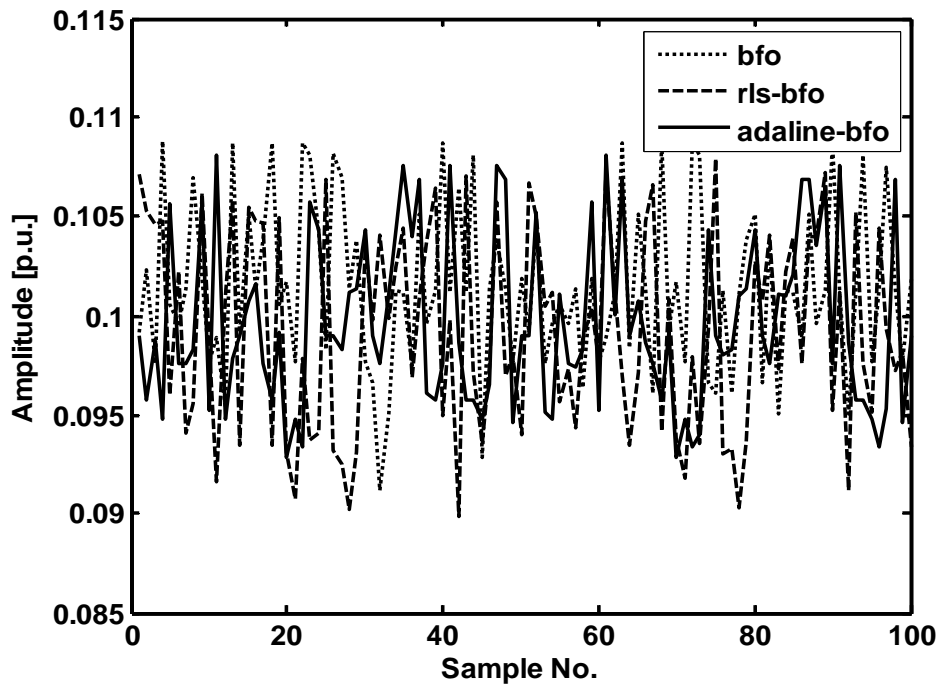
Fig. 5.46 Comparison of Estimation amplitude of 11th Harmonic component of Signal (BFO, RLS-BFO and Adaline-BFO)

Figs. 5.42-5.46 show a comparison of estimation of amplitudes of fundamental, 3rd, 5th, 7th and 11th harmonics components of signal respectively using BFO, RLS-BFO and Adaline-BFO algorithms. From these figures, it is verified that Adaline-BFO estimates fundamental as well as harmonic components more accurately compared to other two.
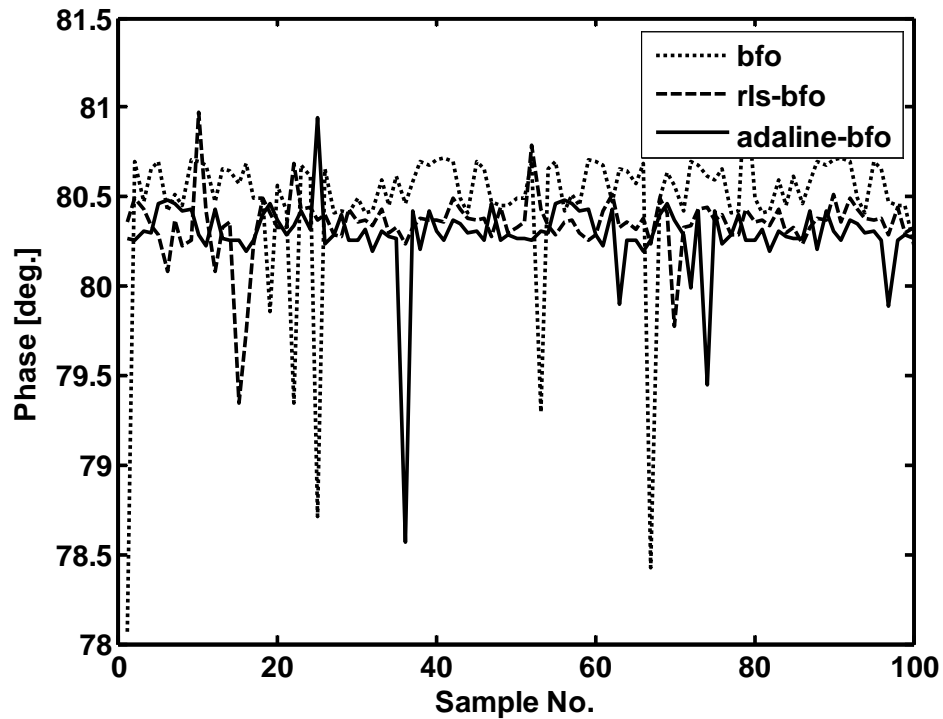
Fig. 5.47 Comparison of Estimation of phase of Fundamental component of Signal
(BFO, RLS-BFO and Adaline-BFO)
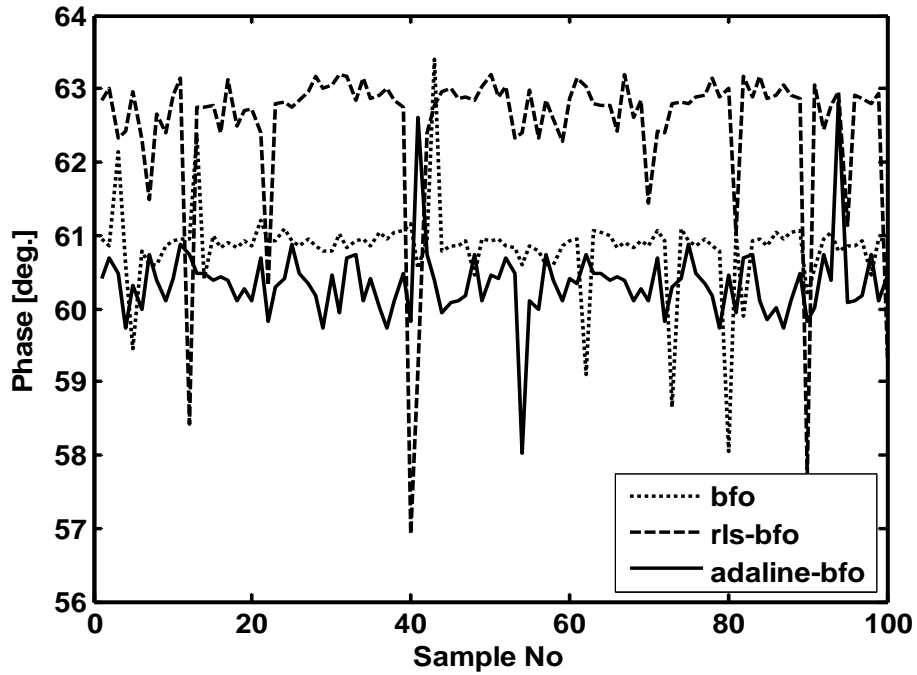
Fig. 5.48 Comparison of Estimation of phase of 3rd Harmonic component of Signal (BFO, RLS-BFO and Adaline-BFO)
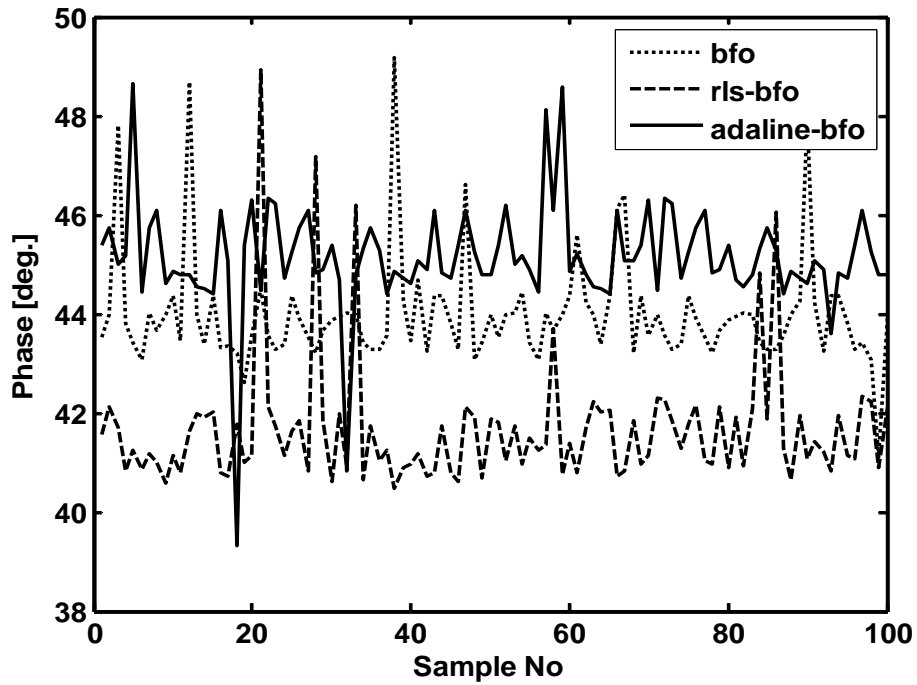
Fig. 5.49 Comparison of Estimation of phase of 5th Harmonic component of Signal (BFO, RLS-BFO and Adaline-BFO)
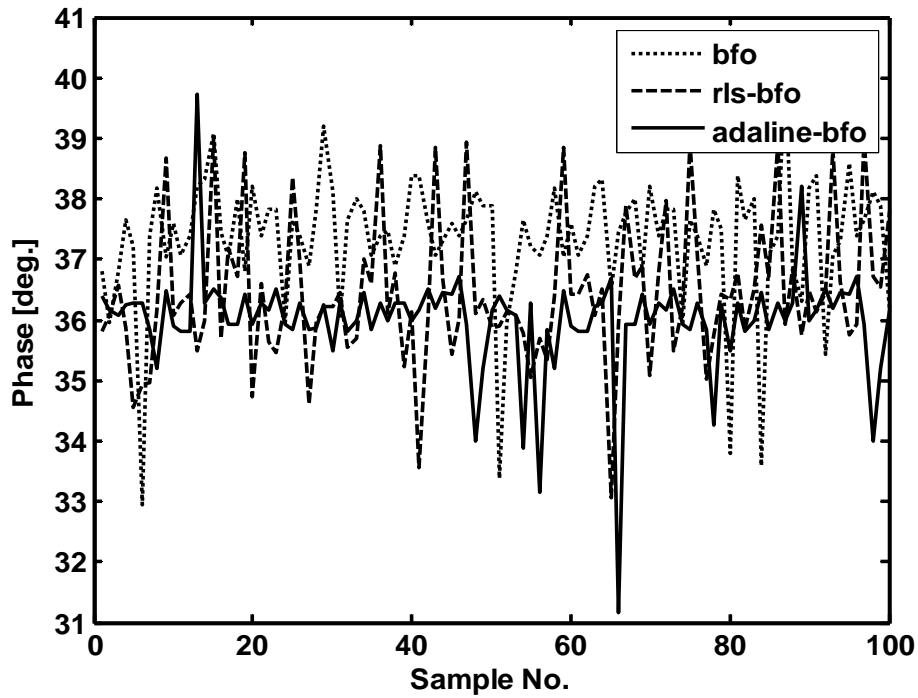
Fig. 5.50 Comparison of Estimation of phase of 7th Harmonic component of Signal
(BFO, RLS-BFO and Adaline-BFO)
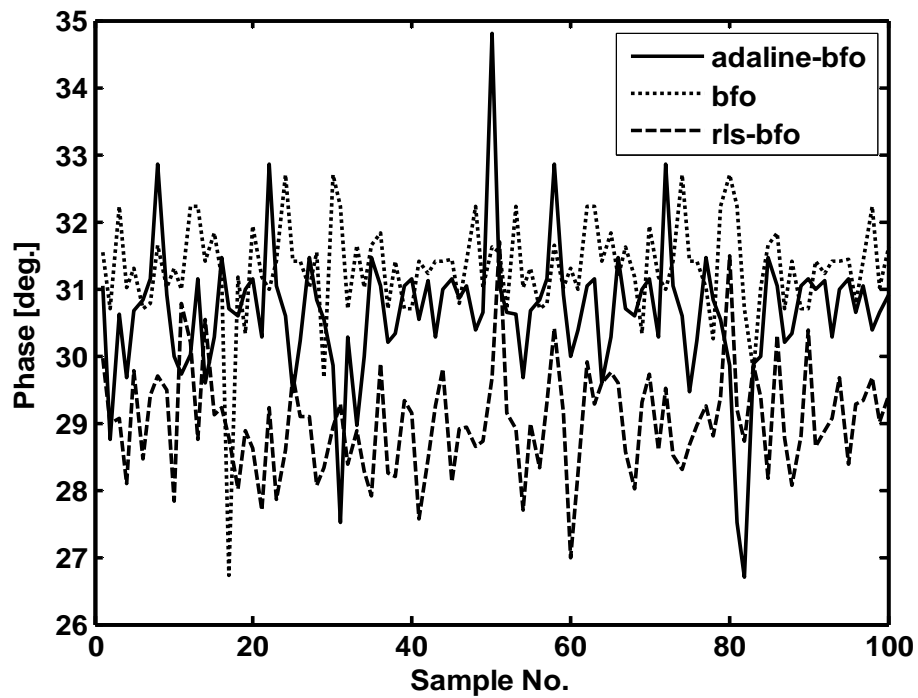
Fig. 5.51 Comparison of Estimation of phase of 11th Harmonics component of Signal
(BFO, RLS-BFO and Adaline-BFO)

Figures 5.47-5.51 show a comparative estimation of phases of fundamental, 3rd, 5th, 7th and 11th harmonics components signal respectively using BFO, RLS-BFO and Adaline-BFO algorithms. Adaline-BFO also gives more correct estimation compared to other two in these figures.

Table 5.5 gives the simulation results obtained by using the BFO, RLS-BFO and Adaline-BFO algorithms. The harmonic parameters obtained with Adaline-BFO exhibit the best estimation precision where the largest amplitude deviation is 1.746% occurred at the 11th harmonics estimation and the largest phase angle deviation is 0.8516^0 occurred at the 7th harmonics estimation.

Table-5.7
Performance Comparison of BFO, RLS-BFO and Adaline-BFO in presence of noise and d.c. offsets

Methods	Param-	Fund-	3rd	5th	7th	11th	Comp. time (sec.)
Actual	f(Hz)	50	150	250	350	550	
	A (V)	1.5	0.5	0.2	0.15	0.1	
	φ(°)	80	60	45	36	30	
BFO	A (V)	1.4878	0.5108	0.1945	0.1556	0.1034	10. 931
	Deviation (%)	0.8147	2.1631	2.7267	3.7389	3.4202	
	φ(°)	80.4732	57.9005	45.8235	34.5606	29.127	
	Deviation (°)	0.4732	2.0995	0.8235	1.4394	0.873	
RLS-BFO	A (V)	1.4942	0.4986	0.2019	0.1526	0.0977	9. 546
	Deviation (%)	0.384	0.2857	0.9607	1.7609	2.3218	
	φ(°)	80.3468	58.5461	45.6977	34.8079	30.1675	
	Deviation (°)	0.3468	1.4539	0.6977	1.1921	0.1675	
Adaline-BFO	A (V)	1.5042	0.4986	0.2018	0.1507	0.0986	9.345
	Deviation (%)	0.2777	0.2857	0.9021	0.4369	1.746	
	φ(°)	80.2338	59.3487	45.1327	36.8516	29.9361	
	Deviation (°)	0.2338	0.6513	0.1327	0.8516	0.0639	

5.6.2 Harmonics Estimation of signal in presence of inter and sub-harmonics

To evaluate the performance of the Adaline-BFO algorithm in the estimation of a signal in the presence of sub-harmonics and inter-harmonics, a sub-harmonic and two inter-harmonics components are added to the original signal. The frequency of sub-harmonic is 20 Hz, the amplitude is set to be 0.505 p.u. and the phase is equal to 75 degrees. The frequency, amplitude and phase of one of the inter-harmonic is 130 Hz, 0.25p.u. and 65 degrees respectively. The frequency, amplitude and phase of the other inter-harmonic is 180 Hz, 0.35p.u. and 20 degrees respectively.
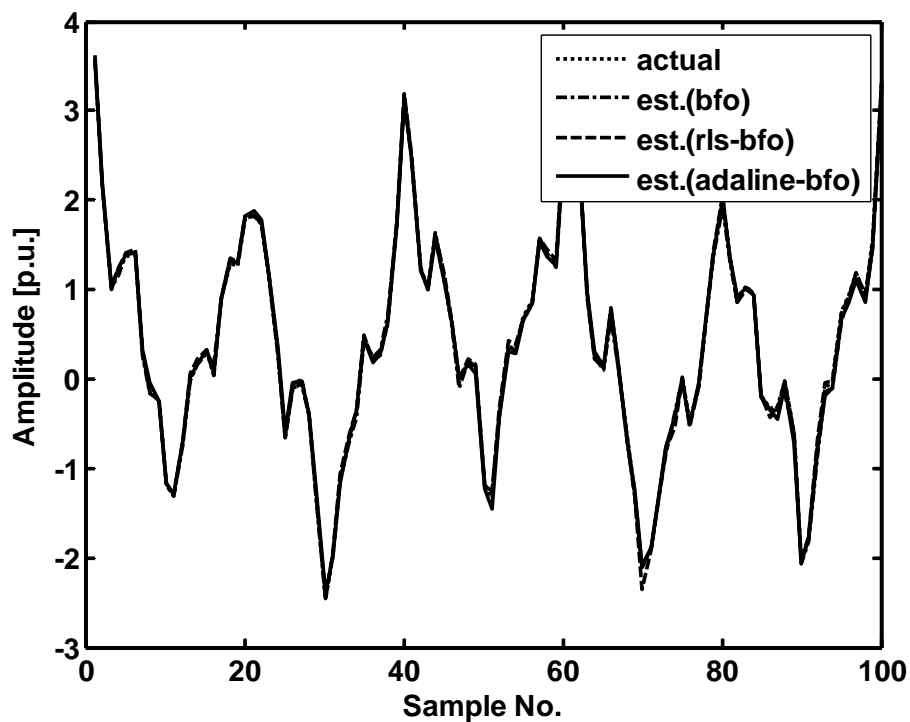
Fig. 5.52 Comparison of Actual vs. Estimated signal in presence of sub-harmonic and inter-harmonics (BFO, RLS-BFO and Adaline-BFO)
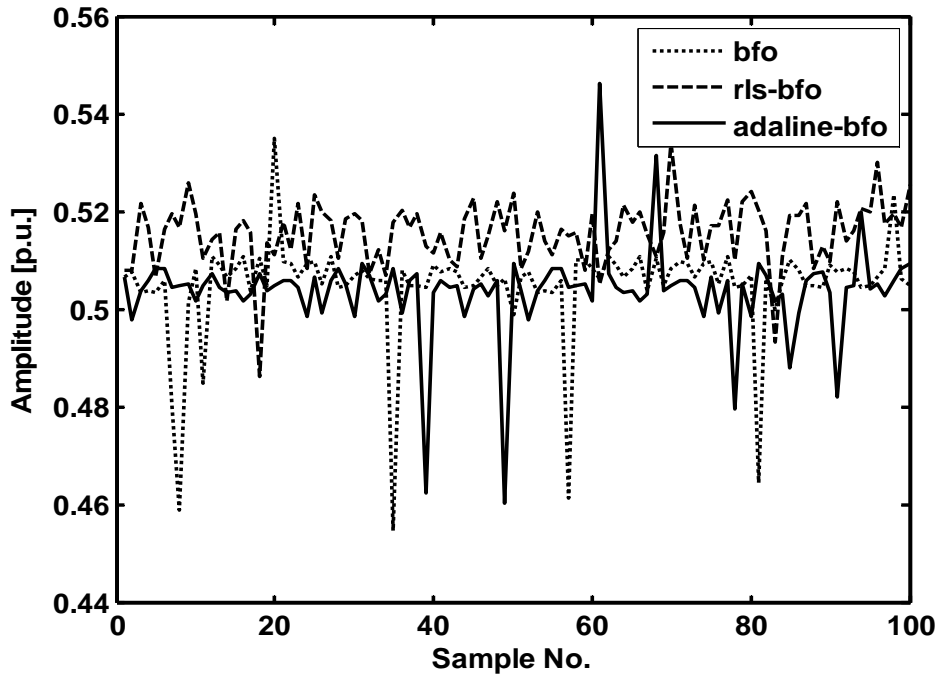
Fig. 5.53 Adaline-BFO estimation performance of amplitude of sub-harmonic component of signal
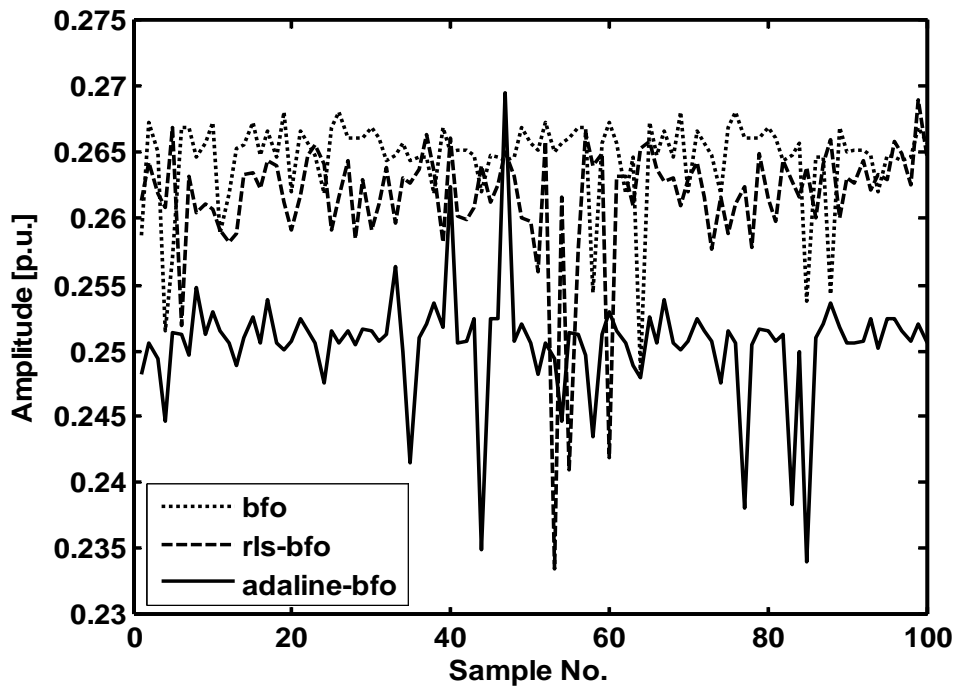
Fig.5.54 Adaline-BFO estimation performance of amplitude of inter-harmonic1

component of signal
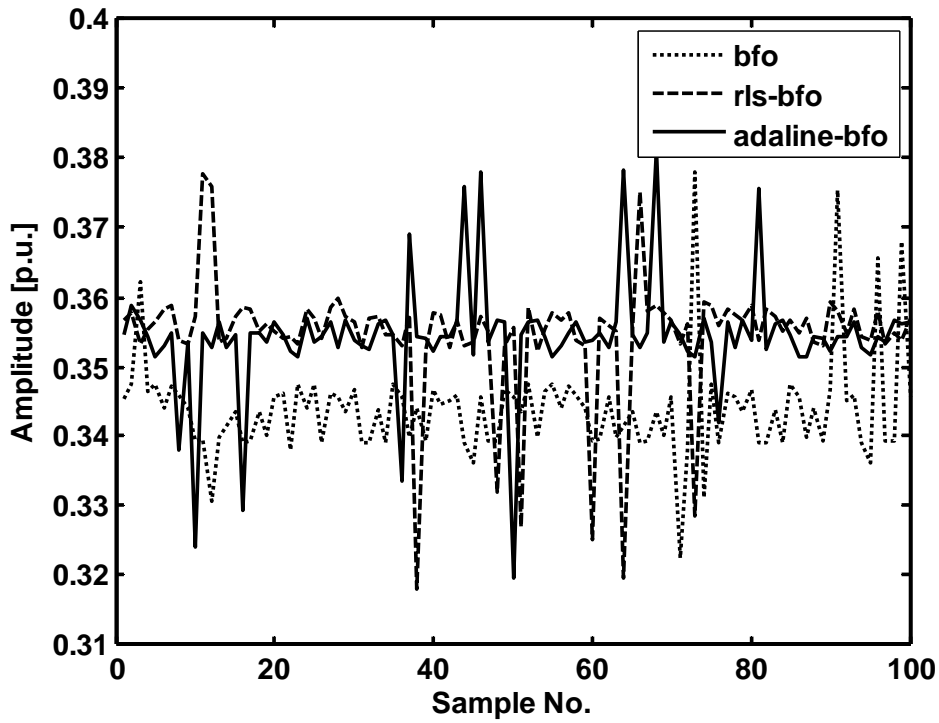
Fig. 5.55 Adaline-BFO estimation performance of amplitude of inter-harmonic2 component of signal
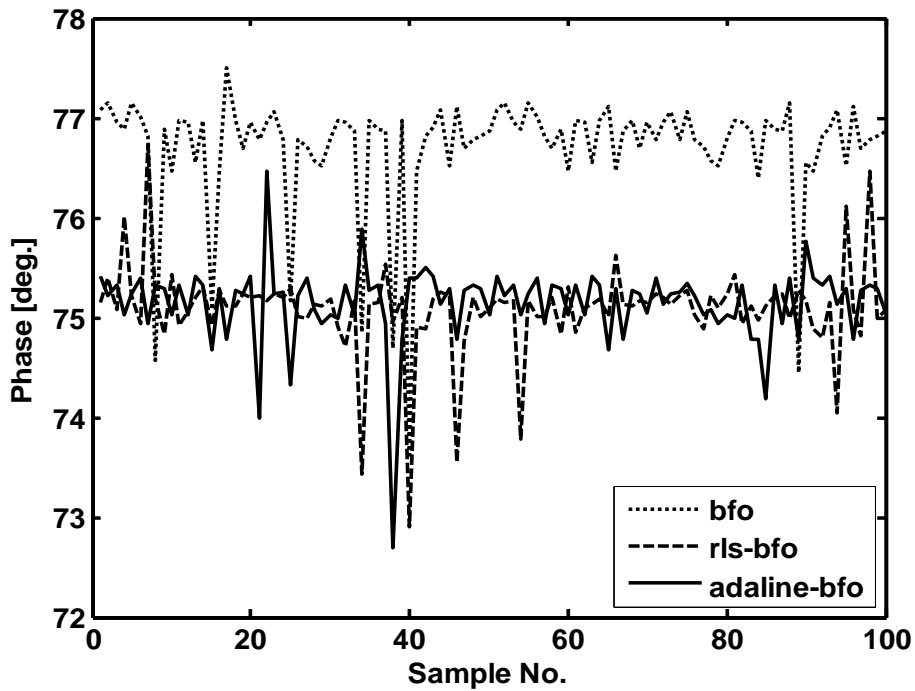
Fig. 5.56 Adaline-BFO estimation performance of phase of sub-harmonic component of signal

184
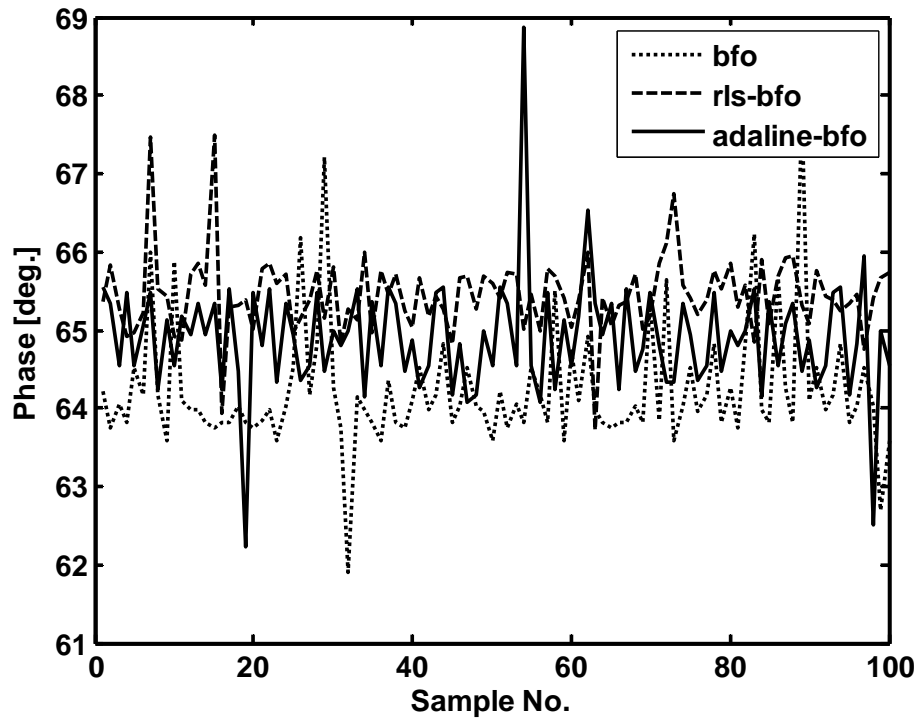
Fig. 5.57 Adaline-BFO estimation performance of phase of inter-harmonic1 component of signal
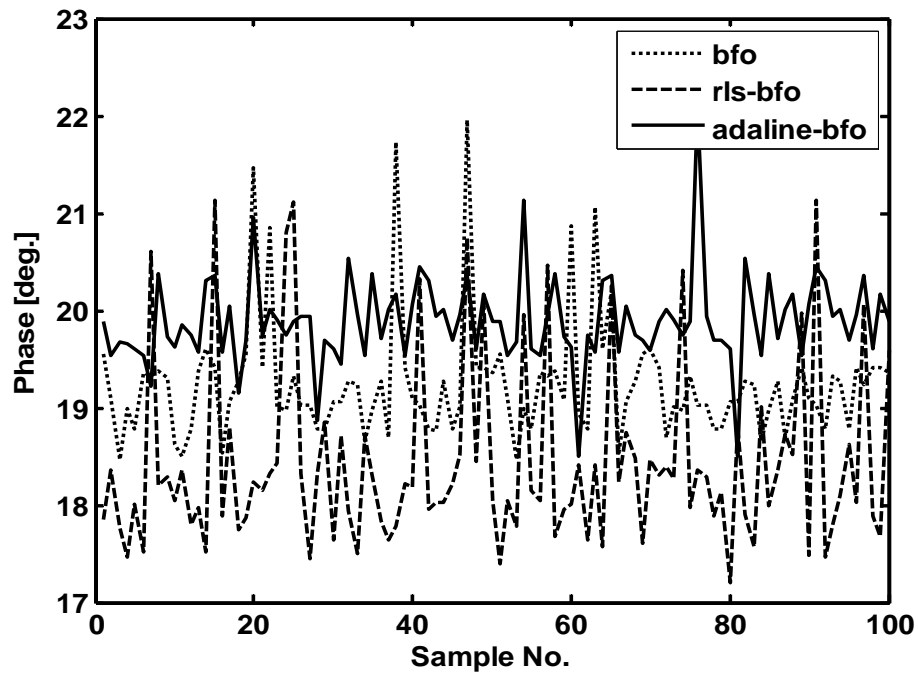
Fig. 5.58 Adaline-BFO estimation performance of phase of inter-harmonic2 component of signal

Fig. 5.52 shows the comparative estimation of actual and estimated signal using the three algorithms. In this case estimated signal of three algorithms are more or less match with the true value. Fig. 5.53-5.58 show the estimation of amplitudes and phases of a sub-harmonic and two inter-harmonics using the three algorithms. Using Adaline-BFO, the estimation is very perfect with most of the sample converge towards the reference value in each case of estimation.

Table-5.8
Comparison of BFO, RLS-BFO and Adaline-BFO in presence of Inter and Sub-Harmonics

Methods	Parameters	Sub	Fund-	3rd	Inter1	Inter2	5th	7th	11th	Compu. time (s)
Actual	f(Hz)	20	50	150	180	230	250	350	550	
	A (V)	0.505	1.5	0.5	0.25	0.35	0.2	0.15	0.1	
	$\varphi(°)$	75	80	60	65	20	45	36	30	
BFO	A (V)	0.525	1.478	0.487	0.266	0.372	0. 205	0.146	0. 101	13.833
	Deviation (%)	3.995	1.410	2.457	6.557	6.529	2. 576	2.417	1. 55	
	$\varphi(°)$	74.48	79.83	61.231	63.99	19.688	47. 698	36.73	29.392	
	Deviation (°)	0.514	0.163	1.231	1.009	0.311	2.698	0.736	0.607	
RLS-BFO	A (V)	0.511	1.508	0.492	0.258	0.363	0.201	0.152	0.101	12.837
	Deviation (%)	1.190	0.571	1.588	3.237	3. 965	0.785	1.425	1.48	
	$\varphi(°)$	74.81	79.91	59.076	65.34	19.723	46. 278	35.38	30.43	
	Deviation (°)	0.183	0.085	0.924	0.344	0.276	1. 278	0.618	0.433	
Adaline-BFO	A (V)	0.507	1.502	0.495	0.249	0.339	0. 200	0.147	0.100	12.669
	Deviation (%)	0.494	0.195	0.956	0.204	2.875	0. 454	1.414	0.802	
	$\varphi(°)$	80.11	80.06	60.06	65.19	19.867	45.95	36.44	30.064	
	Deviation (°)	0.117	0.064	0.065	0.190	0.132	0.959	0.447	0.064	

Table-5.6 gives the simulation results of the signal having two inter harmonics and one sub-harmonic component, using BFO and RLS-BFO and Adaline-BFO algorithms. It shows that as a whole the performance of estimation using Adaline-BFO is better as compared to other two. The largest amplitude deviation is 2.875% occurred at 230 Hz inter-harmonic estimation and the largest phase angle deviation is 1.9593^0 occurred at 5th harmonics estimation.

In the simulation studies the performance index ε is estimated by

$$\varepsilon = \frac{\sum_{k=1}^{N}(y(k) - y(\hat{k}))^2}{\sum_{k=1}^{N}y(k)^2} \times 100$$

where $y(k)$ and $y(\hat{k})$ are actual and estimated signal respectively. In this case the significance of the performance index ε is that it provides the accuracy of the estimation algorithm. Less the value of ε, means more accuracy of estimation and vice versa.

Table-5.9
Comparison of Performance Index (BFO, RLS-BFO and Adaline-BFO)

SNR	BFO	RLS-BFO	Adaline-BFO
No noise	0.1178	0.0870	0.0640
40 dB	0.1381	0.0923	0.0720
20 dB	0.8073	0.7870	0.6834
10 dB	5.2549	4.5482	4.4051
0 dB	45.4871	32.8243	31.9521

The estimation results of BFO, RLS-BFO and the Adaline-BFO scheme are given in Table 6.3, from which it can be seen that Adaline-BFO achieves a significant improvements in terms of reducing error for harmonics estimation in comparison to BFO and RLS-BFO.

5.7 Experimental Studies and Results

Real-time voltage data generation was accomplished in a laboratory environment from the mains supply as described in experimental setup in section 2.3.1 in chapter 2. Fig. 5.59 shows the estimation of signal using all the three algorithms from the real data obtained from the experiment. From Fig. 5.59, it is clear that the estimated waveform follows the real waveform over one cycle.
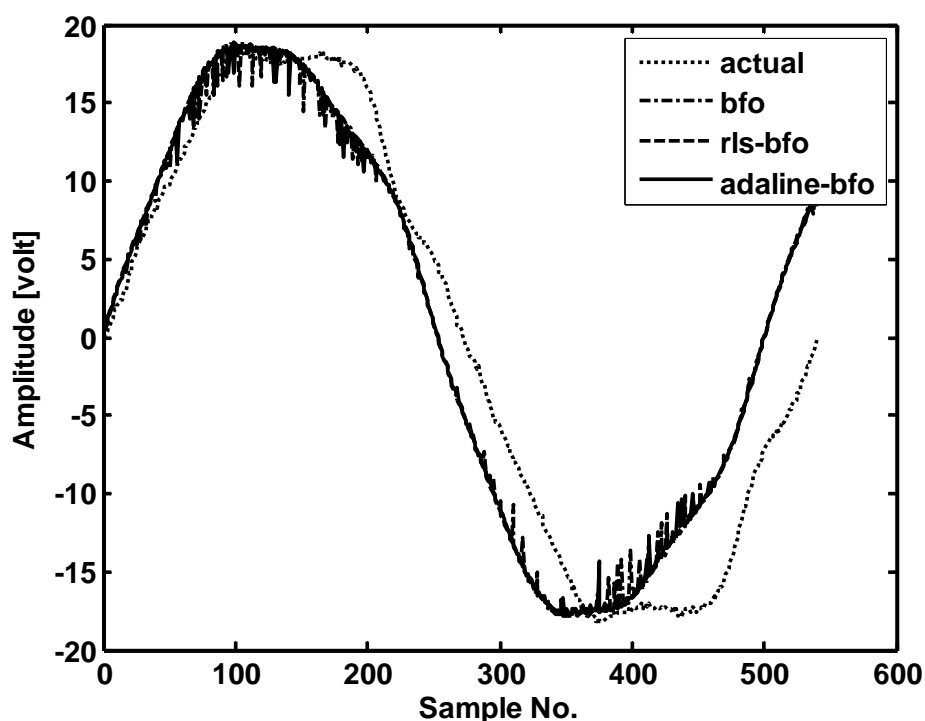
Fig. 5.59 Adaline-BFO estimation performance of signal from real data

Table-5.10
Comparison of Performance Index on estimation of Experimental Data

Parameter	BFO	RLS-BFO	Adaline-BFO
ε	11.0512	10.9613	10.6253

The performance index of estimation of real data is calculated for the three algorithms and the results are given in Table-5.8. In this case Adaline-BFO obtains the most accurate estimation result. Hence the obtained results are satisfactory for the application with real data.

5.8 Chapter Summary

In this chapter, four new hybrid algorithms such as RLS-Adaline, KF-Adaline, RLS-BFO and Adaline-BFO applied to harmonics estimation have been described . The performances RLS-Adaline and KF-Adaline are dependent on the initial choice of weight vector W and Covariance matrix P. By using an optimal choice of weight vector, faster convergence to the true value of signal parameter can be achieved. After the optimization of the weight vector, online tracking of the changes in amplitudes and phases of the fundamental and harmonic components in presence of noise and decaying dc components can be carried out. Both the algorithms track the fundamental and harmonic signals very well for both static and dynamic signal but the performance of tracking using KF-Adaline is better than RLS-Adaline. The performances of the two proposed hybrid BFO algorithms i.e RLS-BFO and Adaline-BFO are dependent on the initial choice of maximum and minimum values of unknown parameters taken. In this work, we have taken maximum and minimum values as 10% deviation from their actual values. By using an optimal choice of parameters, faster convergence to the true value of signal parameter can be achieved. All the algorithms track the fundamental as well as harmonics components of signals very well but the tracking performance using Adaline-BFO is better compared to BFO and RLS-BFO algorithms.

Chapter-6

Hybrid Active Power Filter Design

6.1. Introduction

In chapters 4 and 5 different signal processing and hybrid techniques applied to power system harmonics estimation are discussed. After estimation of the harmonic components in the power system, the design of Hybrid Active Power Filter is discussed in this chapter for elimination of these. It may be noted that passive filters were conventionally used to reduce harmonics in power system whilst capacitor banks brings improvement in power factor of AC loads. However, passive filters are incapable of filtering in the highly transient conditions, where the distortion present in a system is highly unpredictable [85-87]. The major drawbacks of passive filters are their large size, fixed compensation and resonance phenomena. Since the conventional passive filter is not able to provide a complete elimination, recently some Active Power Filters (APFs) have been widely used for the compensation of harmonics in electric power system. Shunt active power filter operates on the principle of injecting harmonic current into the power system with the same magnitudes as the harmonics current generated by a nonlinear load but with 180^0 phase shift [87-90]. A controlled voltage source inverter is required to generate the compensating currents [91-92]. Active power filters are able to damp harmonics resonance between the passive filter and source impedance. But use of only active filter is a very expensive solution as it requires comparatively high power converter ratings. Taking into account the advantages of passive and active filters, hybrid power filters [94-95] are designed. They are capable of controlling the voltage variations and distortions as well as suppression of harmonics. These hybrid filters [98-104] have a wide range of spectrum, ranging from those available in the market to those under research and development. They are based on cutting-edge power electronics technology

which includes power conversion circuits, semiconductor devices, analog/digital signal processing, voltage/current sensors, and control theory.

In active and hybrid power filters [94-97], a number of control strategies such as Hysteresis and sliding mode control techniques may be used to regulate the current produced by the voltage source inverter. But in those cases frequency is variable [93]. Hence, there may be difficulty in the design as well as in the control of noise level. PWM control technique [85] can eliminate these problems but signal can be altered due to dynamic response of current feedback loop, thereby reducing the ability of signal to compensate fast current transitions.

In this thesis, to achieve more accurate estimation, a combination of signal processing and soft computing technique is proposed for frequency and harmonics estimation. This chapter describes combined KF-Adaline (Kalman Filter Adaline) approach to estimation of harmonics content of power system signal. The neural estimator is based on the use of an adaptive perceptron comprising a linear adaptive neuron called Adaline. Kalman Filter has been employed in the proposed hybrid algorithm for updating the weight in Adaline. Performances of KF-Adaline have been compared with only KF and Adaline algorithms. After estimation of harmonics with the proposed algorithm, a modified PWM control technique is applied to HAPF for harmonics compensation in distorted power signals. The modified PWM control technique is based on comparing simultaneously a triangular high frequency carrier signal with a controlling signal and its 180^0 out of phase signal. The simulated results of this hybrid power filter using modified PWM technique are compared with the active and passive filter. The performance of HAPF is also verified uaing experimental studies on a laboratory prototype.

6.2 Classification of Harmonics Filters

6.2.1 Passive Harmonic Filters

Passive harmonic filters consisting of inductors, capacitors and/or resistors can be classified into tuned filters and high-pass filters. They are connected in parallel with nonlinear loads such as power converters, ac electric arc furnaces, and so on.

(a)   (b)
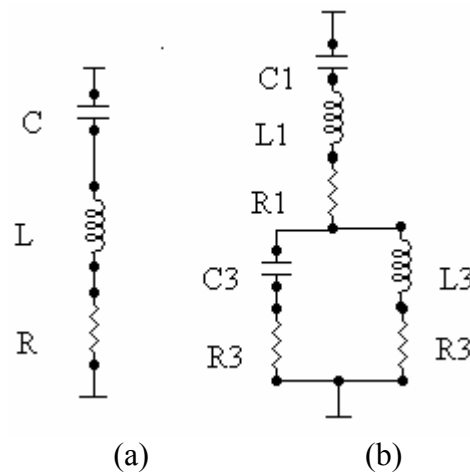
Fig. 6.1 Passive tuned filters (a) Single tuned. (b) Double tuned.

(a)   (b)   (c)
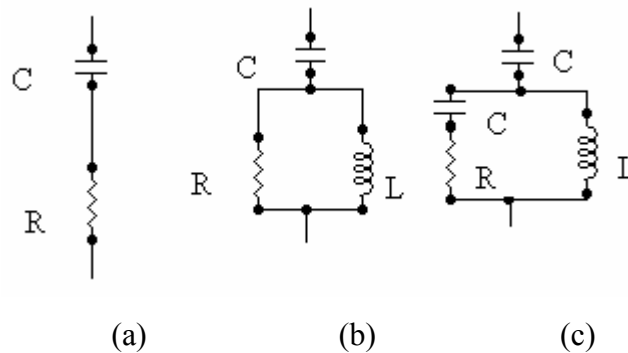
Fig. 6.2 Passive high-pass filters. (a) First order (b) Second order (c) Third order

Figs. 6.1 and 6.2 show circuit configurations of the passive filters on a per-phase base. Out of them, the combination of four single-tuned filters tuned to the 5th, 7th, 11th, and 13th harmonic frequencies and a second-order high-pass filter tuned around the 17th harmonic frequency are widely used in a high-power three-phase thyristor rectifier[86]. The main objective of providing a passive filter to a nonlinear load is to provide low-

impedance paths for specific harmonic frequencies, thereby resulting in absorbing the dominant harmonic currents flowing out of the load. Though a second-order high-pass filter provides good filtering performance in a wide frequency range, it produces higher fundamental-frequency loss compared to a single-tuned filter. In case of inductive loads, power factor correction to some extent is carried out by a Passive harmonic filter.

Harmonic series and/or parallel resonances between the passive filter and the power system impedance may occur at a lower frequency than each tuned frequency. A passive filter may sink some specific harmonic currents from other nonlinear loads. Due to this, a passive filter may become overloaded and ineffective. Before installing a careful consideration should be made taking into account the harmonics resonance and overloading effect.

6.2.2 Active Harmonic Filters

So far as circuit configurations are concerned, Active filters can be classified into shunt active filters and series active filters. But, shunt active filters are preferred to series active filters in terms of design and function.
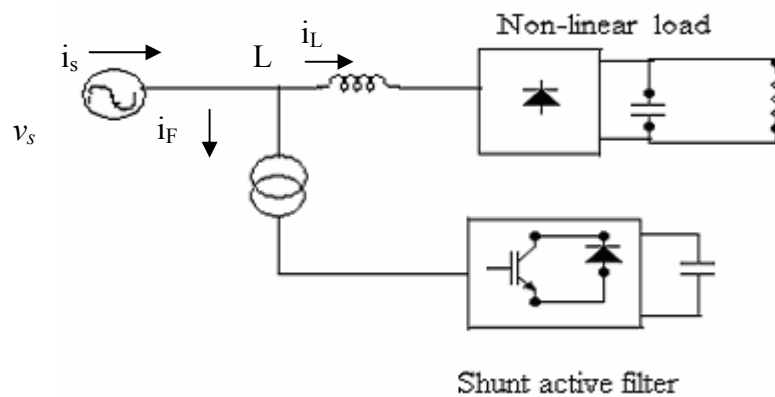
Fig. 6.3 Single-phase or three-phase shunt active filter

Fig. 6.3 shows a system configuration of a single-phase or three-phase shunt active filter for harmonic "current" filtering of a single-phase or three-phase diode rectifier with a capacitive dc load. Active filters are generally connected in parallel with the harmonic-

producing load with or without a transformer. The active filter can be controlled by extracting harmonic current from the detected load current by drawing the compensating current from the utility supply voltage, so as to cancel out the harmonic current. The function of an ac inductor that is installed at the ac side of the diode rectifier is to operate the active filter stably and properly.
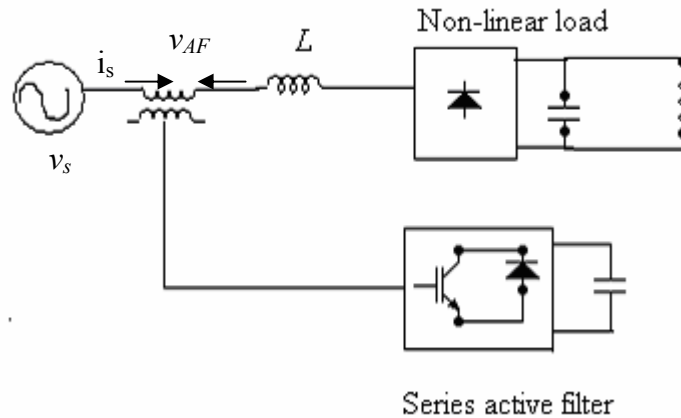
Fig. 6.4 Single-phase or three-phase series active filter.

Fig. 6.4 shows the system configuration of a single-phase or three-phase series active filter for harmonic "voltage" filtering of a single-phase or three-phase diode rectifier with a capacitive load. The series active filter is connected in series with the supply voltage through a three-phase transformer or three single-phase transformers. Like the shunt active filter, the series active filter is controlled on extracting the harmonic current from the detected supply current by means of digital signal processing or by applying the compensating voltage across the primary of the transformer, which results in significantly reducing the supply harmonic current when the feedback gain is set to be high.

6.2.3 Hybrid Harmonic Filters
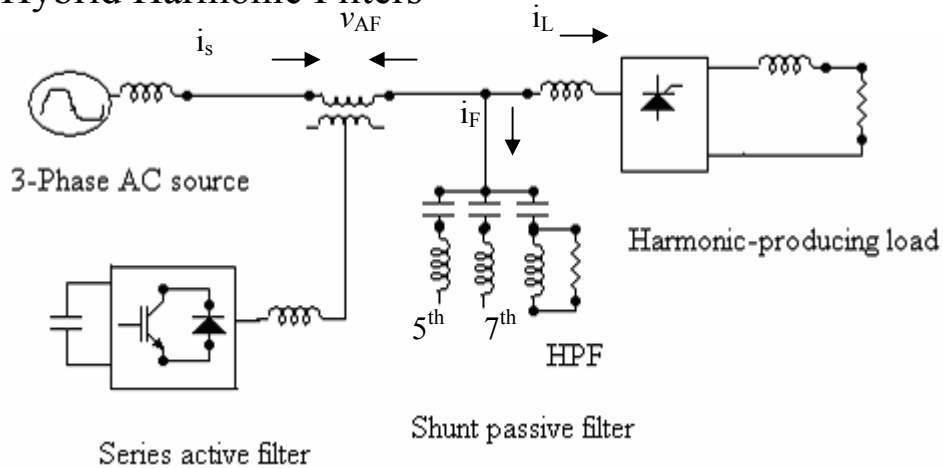
Fig. 6.5 Combination of a series active filter and a shunt passive filter
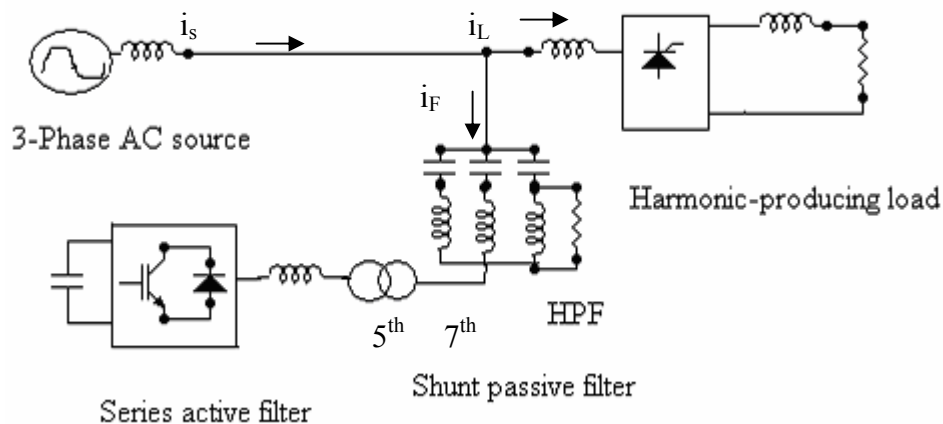
Fig. 6.6 Series connection of an active filter and a passive filter

Figs. 6.5 [94-95] and 6.6 [96-97] show the simplified circuit diagrams of the hybrid filters. The idea of the two hybrid filters motivates power electronics researchers/engineers for development of various hybrid active filters, focusing on their practical uses [98-104]. The two hybrid filters (Fig. 6.7 and Fig. 6.8) are based on combinations of an active filter, a three-phase transformer (or three single-phase transformers), and a passive filter containing two single-tuned filters to the fifth- and seventh-harmonic frequencies and a second-order high-pass filter tuned around the 11th harmonic frequency. These hybrid filters may be slightly different in circuit configuration but they are almost the same in operating principle and filtering performance. Such type

of combination with the passive filter makes it possible to significantly reduce the rating of the active filter. Active filter not only compensates the harmonic currents produced by the thyristor rectifier but also achieves "harmonic isolation" between the supply and the load [94-95]. As a result, harmonic resonance effect and flow of harmonic current in the supply is restricted.

6.3. Description of the studied system

Figure 6.7 shows the system under study where a non-linear load (rectifier load) is connected across an a.c supply. Due to the presence of nonlinear load, with the introduction of harmonics, source current waveform becomes distorted. The main objective of this work is to mitigate the harmonic content of the source current signal.
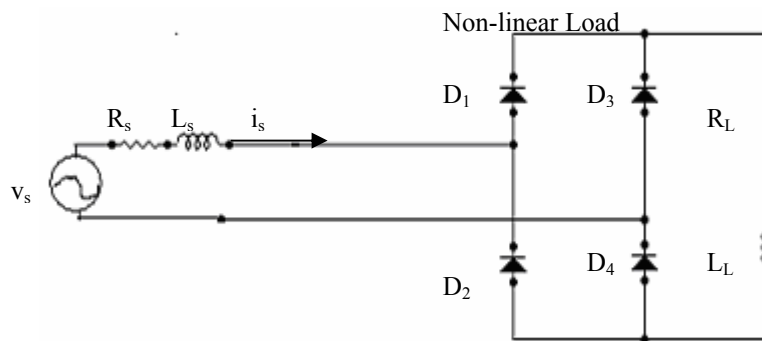
Fig.6.7 Studied system

6.4. KF-Adaline algorithm for harmonic estimation

KF-Adaline based algorithm for harmonics estimation as discussed in 5.2.2 is applied here for estimation of different order of the harmonics content at different cases of source current signal i.e without using filter, with passive filter, with active filter and with HAPF.

6.5. Proposed HAPF Method of Harmonics Filtering

Proposed single phase HAPF as shown in Fig. 6.8 consists of a full-bridge voltage-source inverter, a DC side capacitor C_{dc}, an inductor L_c and a transformer. The primary winding of the transformer is connected to AC mains and secondary is connected to PWM inverter. The inductance through which the inverter is connected to power supply network firstly acts as a controller of the active filter current and secondly acts as a first order passive filter attenuating the high frequency ripples generated by the inverter. The filter acts as a current source, which cancels the current type harmonics and supplies the necessary reactive energy needed by the non-linear load. A single phase diode bridge rectifier feeding R-L circuit acts as a non-linear load.
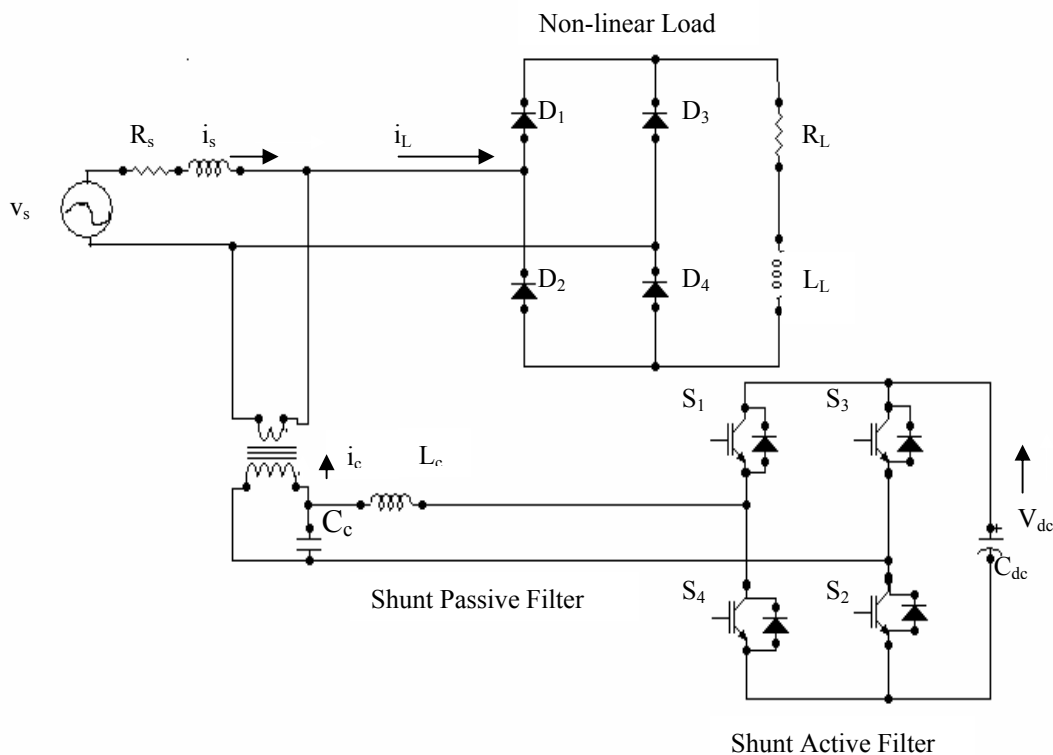
Fig.6.8 Single phase shunt hybrid power filter

Performance of an active power filter is greatly influenced by the method used for extracting the current reference. The demodulation method of the single-phase circuits is

197

used to obtain current reference. In the indirect current control strategy, the switching signals for HAPF devices are obtained by comparing the fundamental active source current that constitutes the reference (i_s^*) and sensed (i_s) source current.

Refering to Fig. 6.7, the current of the non-linear load is given by

$$i_L(\theta_s) = \sum_{k=1}^{\infty} I_{Lk} \sin(k\theta_s - \phi_k) = I_{L1} \sin(\theta_s - \phi_1) + \sum_{k=2}^{\infty} I_{Lk} \sin(k\theta_s - \phi_k) \qquad (6.1)$$

The fundamental component i_{Lf} and the harmonic components i_{Lk} of the load current i_L are given as follows:

$$i_{Lf} = I_{L1} \sin(\theta_s - \phi_1) \qquad (6.2)$$

$$i_{Lk} = \sum_{k=2}^{\infty} I_{Lk} \sin(k\theta_s - \phi_k) \qquad (6.3)$$

Again, the fundamental current is divided into two currents:

The fundamental active current, $i_{Lfa} = I_{L1} \cos\phi_1 \sin\theta_s$

The fundamental reactive current, $i_{Lfr} = I_{L1} \sin\phi_1 \cos\theta_s$

The objective of the work is to eliminate harmonics. Therefore, the reference current of the active filter i_s^* is equal to fundamental active current i_{Lfa}

$$i_s^* = i_{Lfa} = i_L - (i_{Lk} + i_{Lfr}) \qquad (6.4)$$

For simplifying the filtering of the load current, i_{Lk}, fundamental component is transformed into DC component by multiplying both sides of Eq. (6.1) by $\sin\theta_s$.

$$i_L(\theta_s)\sin\theta_s = I_{l1} \sin(\theta_s - \phi_1)\sin\theta_s + \sum_{k=2}^{\infty} I_{Lk} \sin(k\theta_s - \phi_h)\sin\theta_s$$

$$= \frac{I_{L1}}{2}\cos\phi_1 - \frac{I_{L1}}{2}\cos(2\theta_s - \phi_1) + \sin\theta_s \sum_{k=2}^{\infty} I_{Lk} \sin(k\theta_s - \phi_k) \qquad (6.5)$$

Eq. (6.5) shows the presence of DC component and the AC components of which the minimum frequency is equal to twice the frequency of the network. So a low pass filter with a low cut-off frequency is used to prevent the high frequency component entering the output. The filtered output current is given by

$$(i_L \sin \theta_s)_{filtered} = \frac{I_{L1}}{2} \cos \phi_1$$

The error between the reference value $\overset{*}{V}_{dc}$ and the sensed feedback value V_{dc} is passed through a PI controller giving a signal which is added to $2i_{Lf}$, that gives peak value of the reference current. For reconstituting the fundamental active current, peak value is multiplied by $\sin \theta_s$. The block diagram of the proposed control algorithm with active filter is shown in Fig.6.9
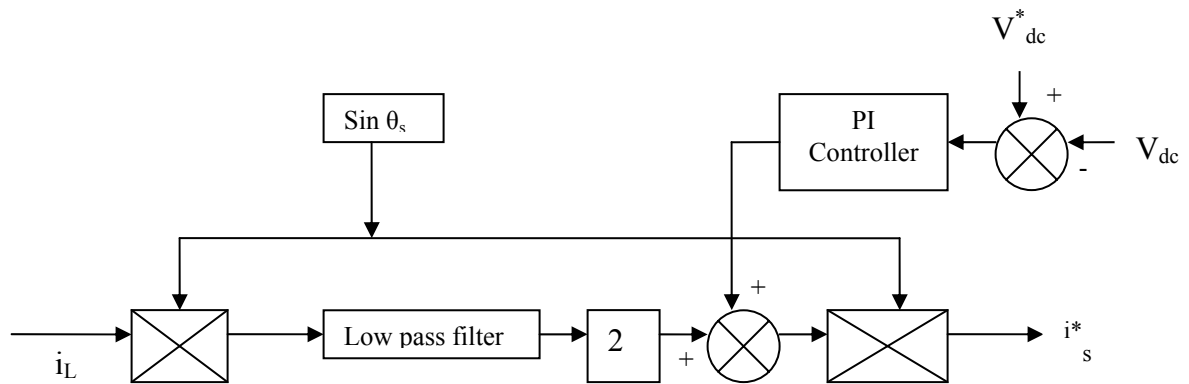
Fig. 6.9 Proposed indirect current control algorithm of active power filter system

6.5.1. Generation of Gating Signals

The operation of the switches of the inverter can be controlled by using PWM techniques. There are different methods of PWM techniques such as single PWM, multiple PWM and sinusoidal PWM techniques. Control of the switches for modified PWM technique requires comparing simultaneously a triangular high frequency carrier signal with a slow varying regulation signal and its 180^0 out of phase signal. In this technique, two reference signals are required for comparing the triangular signal to obtain pulses that are required to operate the switches as shown in Fig. 1. Basic idea to produce switching signals using modified PWM Technique is shown in Fig. 6.10.
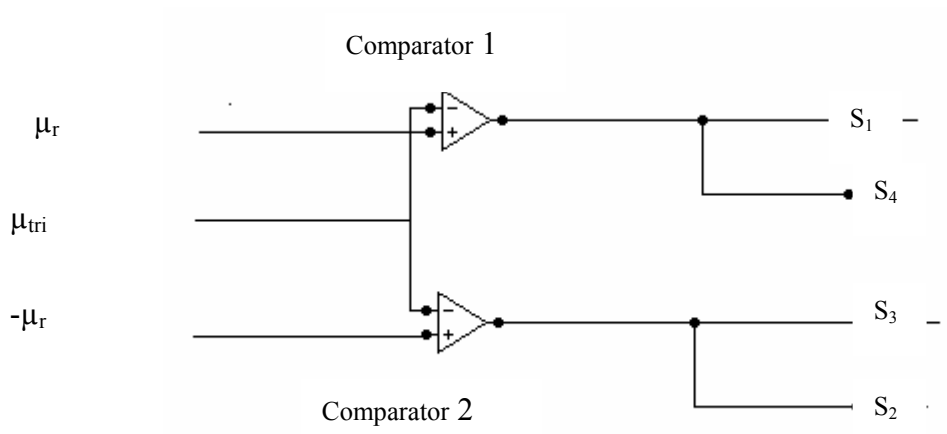
Comparator 1

Fig. 6.10 Modified PWM generator

The current reference i_s^*, obtained from the Modified PWM control algorithm is compared with the sensed signal i_s. The error obtained is fed to a current controller with limiter at its output. The signal obtained from the controller and its 180^0 out of phase is compared with a high frequency triangular wave, generating the gating signal as shown in Fig.6.11. Accordingly, the corresponding IGBT^s will be made on or off number of times over the cycle. Hence, the output current of the PWM inverter can be controlled by means of proposed control strategies which will be useful for elimination of source harmonics present due to the non-linear load. In addition, simulated waveforms before and after filtering can be analyzed by using KF-Adaline algorithm for detailed estimation of harmonics present in the signal.
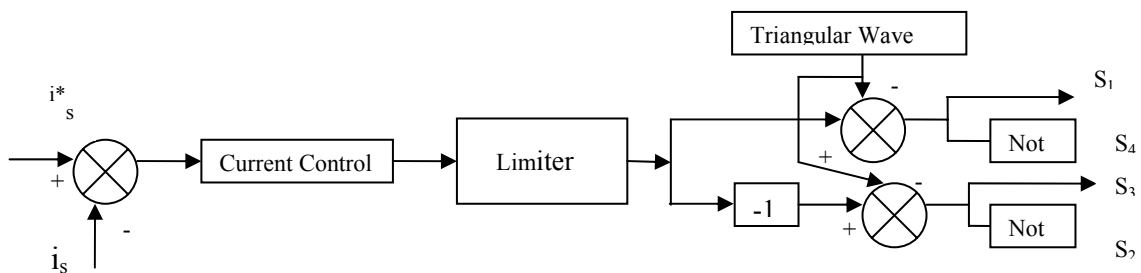
Fig. 6.11 Principle of generation of gating signals

6.6 Results and Discussion

In order to validate the accuracy of the Shunt Hybrid Power Filter with the proposed Modified PWM control algorithm, the system described in section 3 has been modeled and simulated using MATLAB/SIMULINK. The objective of the simulation is to examine the superiority in performance of HAPF as compared to Passive as well as Active Power Filter applied to the studied system. The system parameters used in these simulations are given in Table 6.1

Table 6.1 System Parameters for different types of Filter

Line voltage and frequency	$v_s = 120$ V (rms), $f_s = 60$ Hz
Line Impedance	$R_s = 0.1\Omega$, $L_s = 1\,\text{mH}$
Voltage source type of non-linear load impedance	$R_L = 3\Omega$, $L_L = 10\,\text{mH}$
Shunt passive power filter parameter	$L_c = 0.1\,\text{mH}$, $C_c = 7\,\mu\text{F}$
Shunt active power filter parameter	$V_{dc} = 350$ V and $C_{dc} = 1000\,\mu\text{F}$

6.6.1 Simulation results with passive filter

The load current i_L, shunt passive filter current i_c, supply current i_s and supply voltage v_s are shown in Fig 6.12. The harmonics spectra of the supply current without and with shunt passive filter are shown in Figs. 6.13 and 6.14 respectively. The Total Harmonics Distortion (THD) is reduced from 19.46% before compensation to 8.75% after compensation
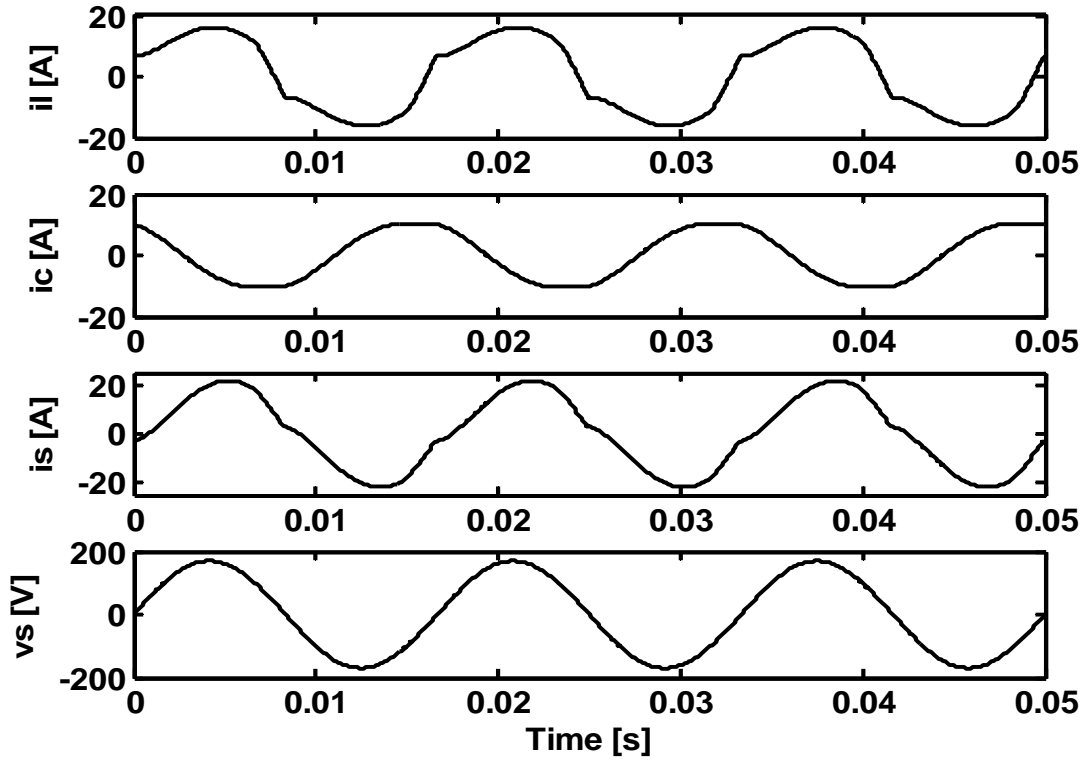
Fig. 6.12 Simulated waveforms with a shunt passive power filter
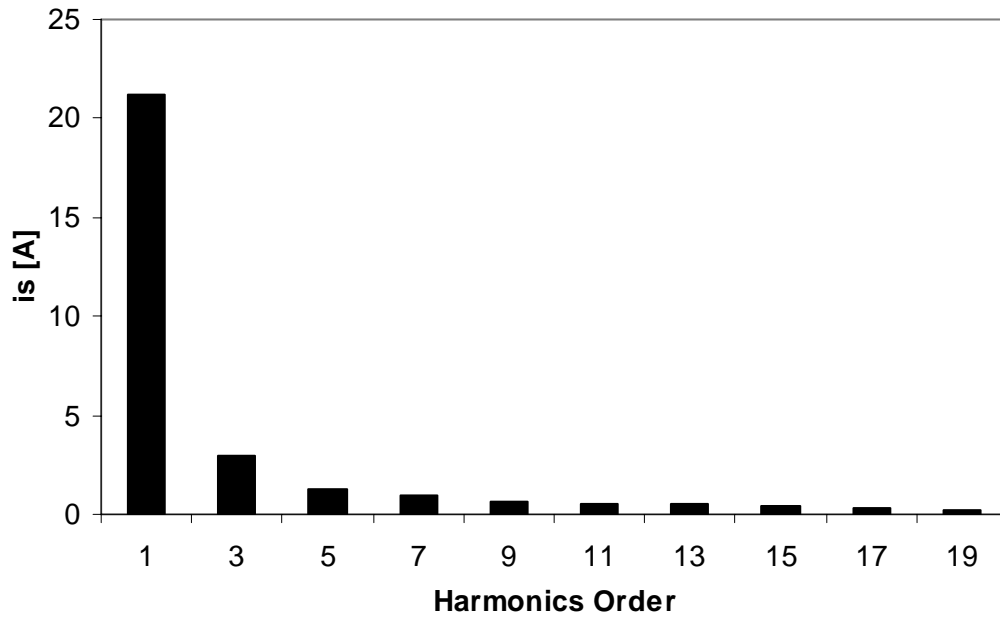
Fig.6.13 Source current spectrum without using filter
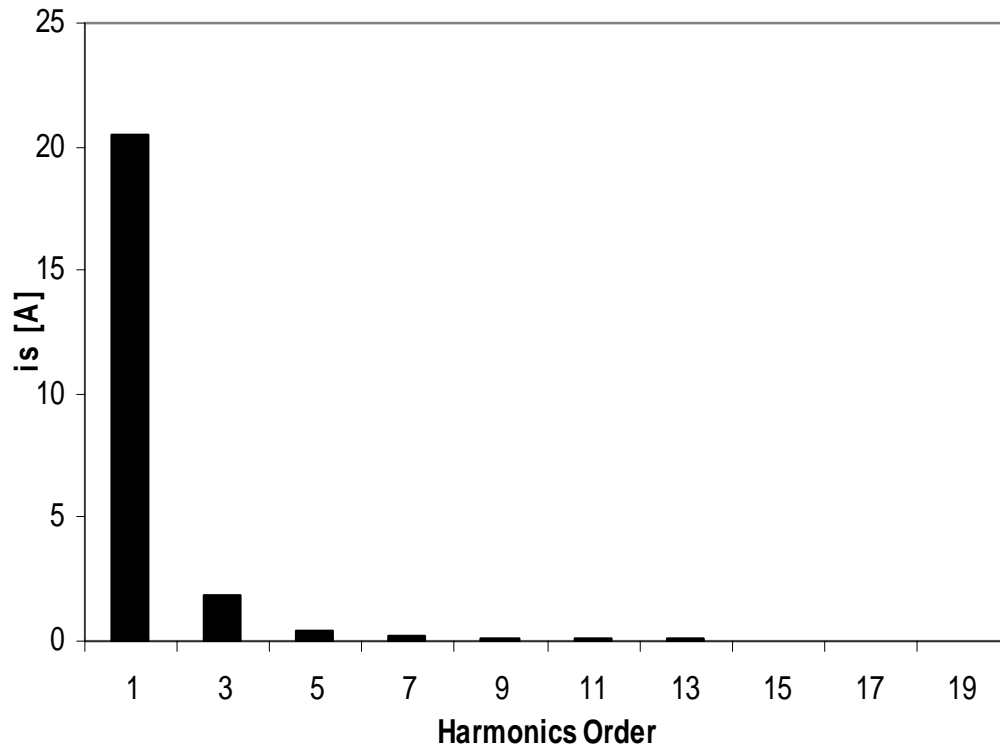
Fig.6.14 Source current spectrum using passive filter

6.6.2 Simulation Results with Active Power Filter (APF)

Fig.6.15 shows the load current i_L, shunt active filter current i_c, supply current i_s and supply voltage v_s of a nonlinear load connected to AC mains. It is observed that the steady state waveforms are close to fully compensated harmonics of source current. The harmonic spectrum of the source current using active power filter is shown in Fig. 6.16. The total harmonics distortion of the source current is reduced from 19.46 % before compensation to 4.67% after compensation.
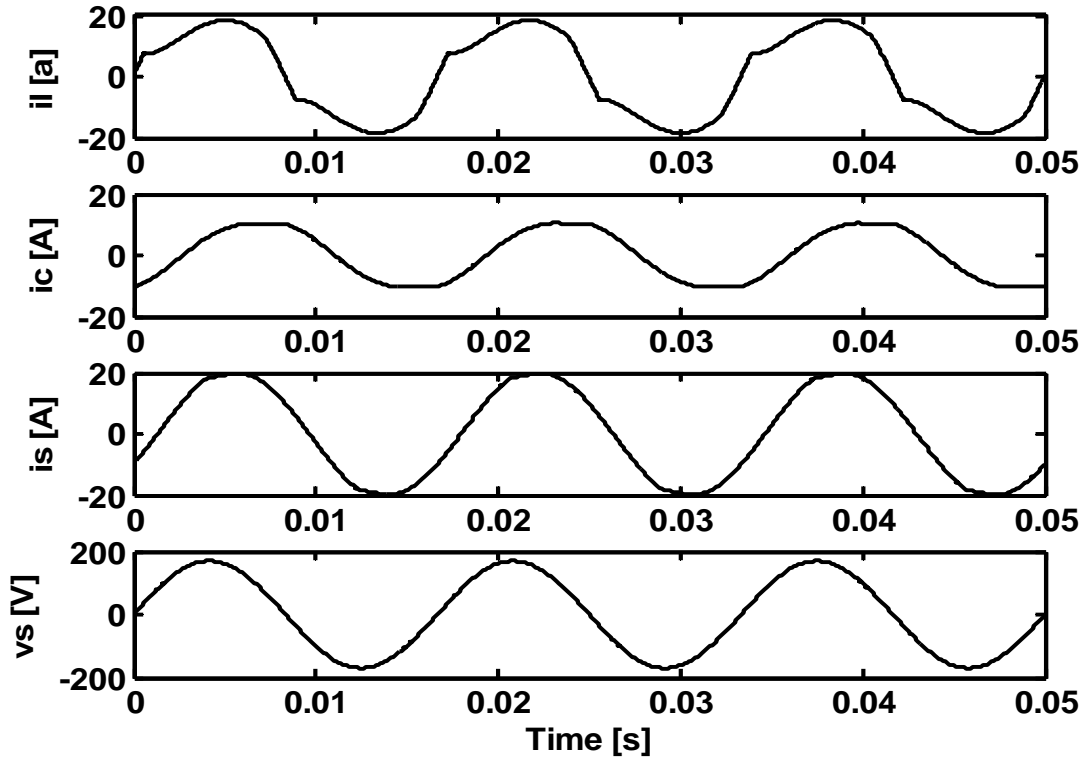
Fig. 6.15 Simulated waveforms with a shunt active power filter
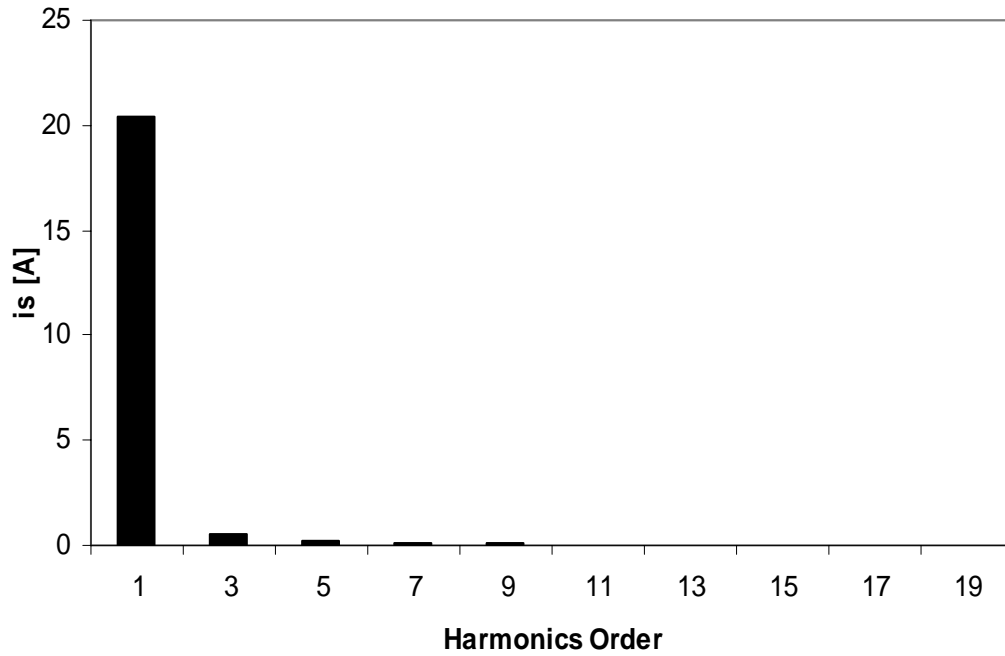
Fig.6.16 Source current spectrum using active filter

6.6.3 Simulation results with HAPF

The load current i_L, shunt passive filter current i_c, supply current i_s and supply voltage v_s are shown in Figure 6.17. The harmonic spectrum of the source current is shown in Figure 6.18. The total harmonic distortion (THD) is reduced from 19.2% before compensation to 1.82% after compensation.
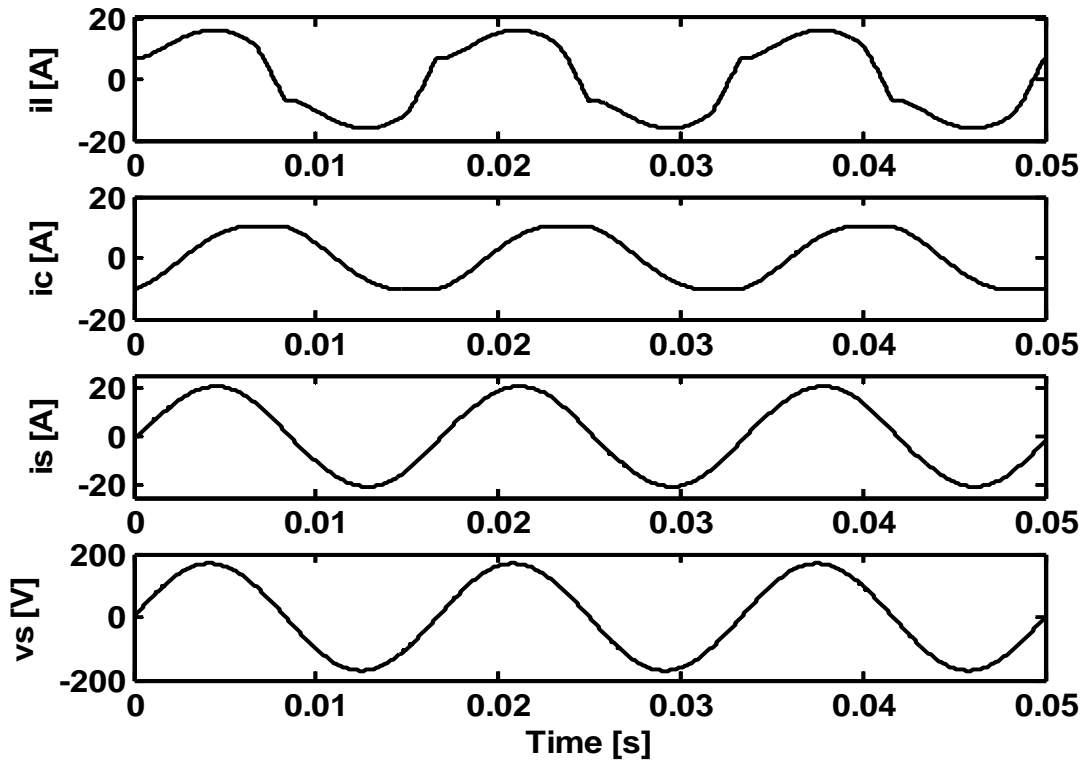
Fig. 6.17 Simulated waveforms with HAPF
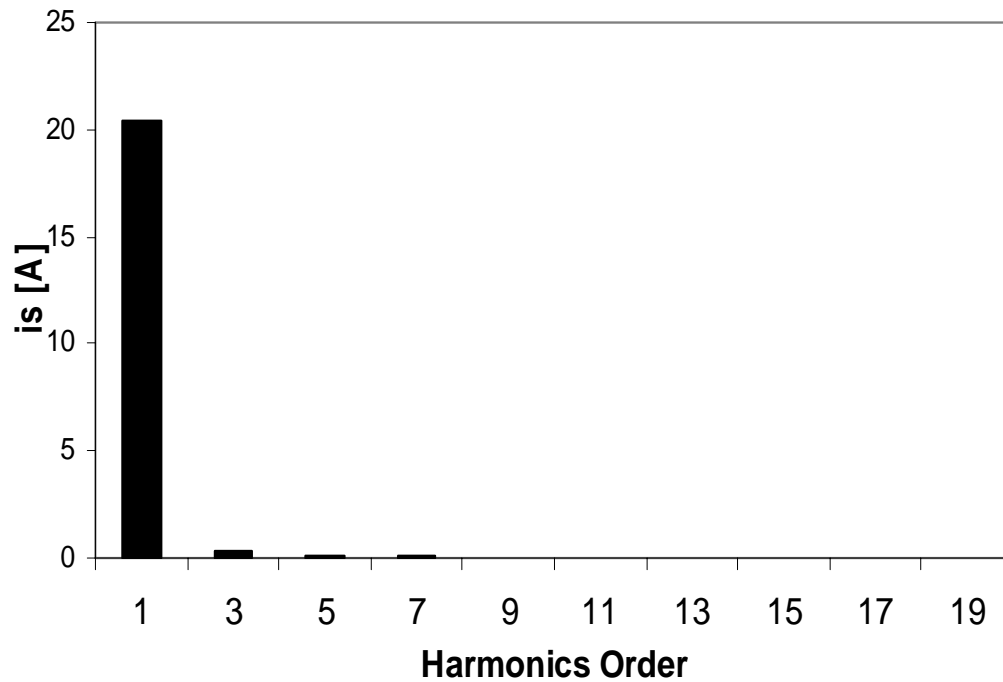
Fig. 6.18 Source current spectrum using hybrid filter

6.6.4 Harmonics Estimation results using KF-Adaline Algorithm

KF-Adaline Method of Estimation of Harmonics has been discussed in section 3. Here we have taken the simulated waveforms of the proposed model by using the MATLAB-SIMULINK. The data obtained from the distorted signal has been fed into the MATLAB program for detailed analysis (like THD, each harmonics contents and LOH etc.) of those distorted signals before and after filtering. Table 6.2 shows the values of different parameters used in different algorithms in both simulation and experimentation work.

Table-6.2
Parameters used in Algorithms (KF, Adaline and KF-Adaline)

	δ	α_0	β	λ
KF	100	-	-	-
Adaline	-	0.01	100	0.01
KF-Adaline	100	0.01	100	0.01

Figs. 6.19 to 6.23 show the comparison of estimation of 3rd, 5th, 7th, 9th and 11th harmonics components of source current signal for without filtering and passive, active and hybrid filtering cases. From these four figures, it is found that in case of hybrid filter, harmonics components are minimized in all cases of estimation. Figure 6.24 shows the comparison of MSE in the estimation of signal in different cases and it is found that MSE is also minimized in case of Hybrid filter. Comparison of performances of estimation for passive, active and HAPF cases using KF, Adaline and KF-Adaline method are shown in figures 6.25, 6.26 and 6.27 respectively. From these figures, it is found that KF-Adaline outperforms over KF and Adaline in estimation of harmonics and HAPF outperforms over active and passive filters in elimination of harmonics.
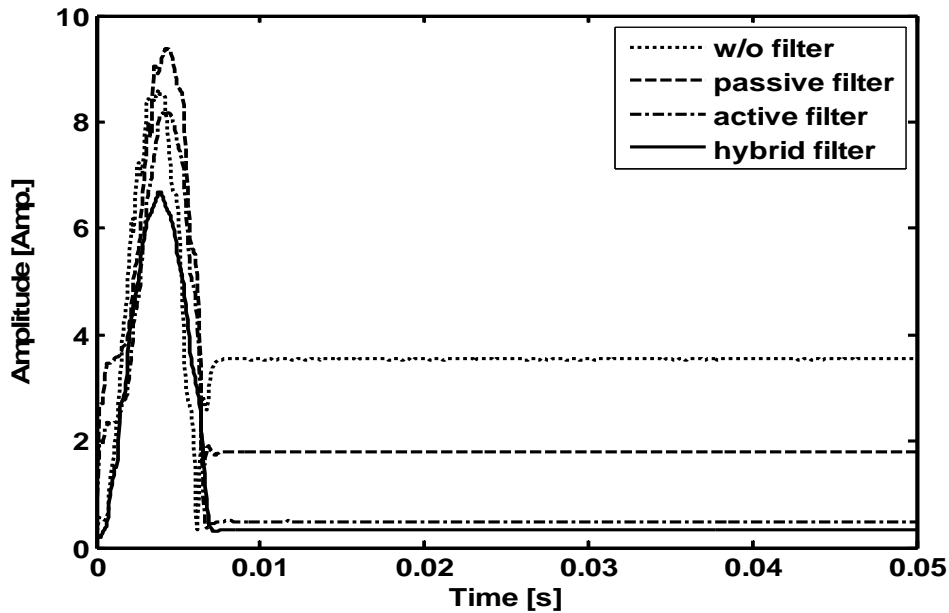
Fig.6.19 Performance comparison of hybrid filter for 3rd harmonic signal
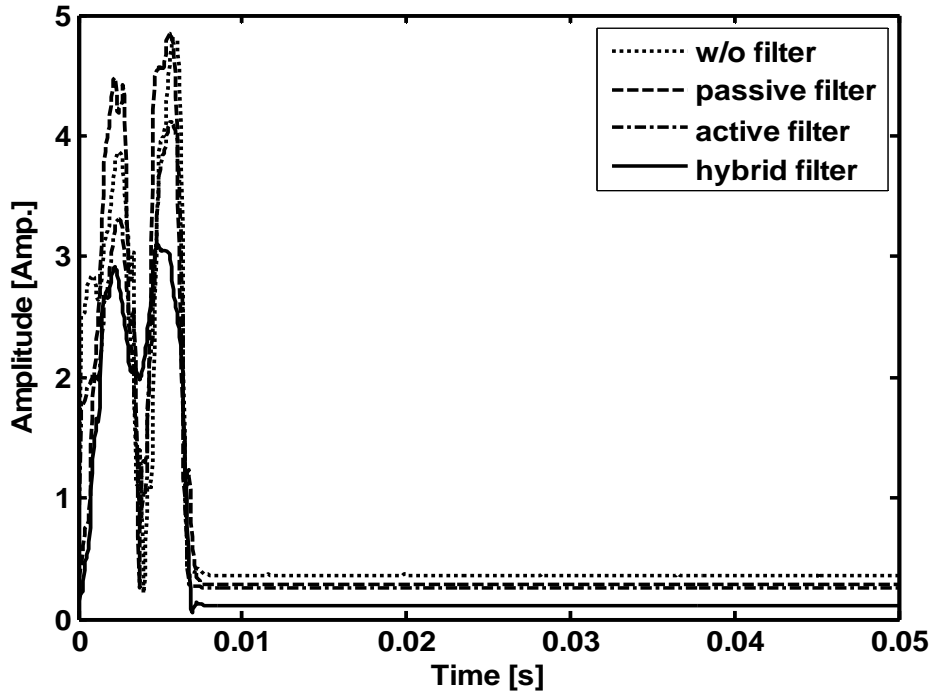
Fig.6.20 Performance comparison of hybrid filter for 5th harmonic signal
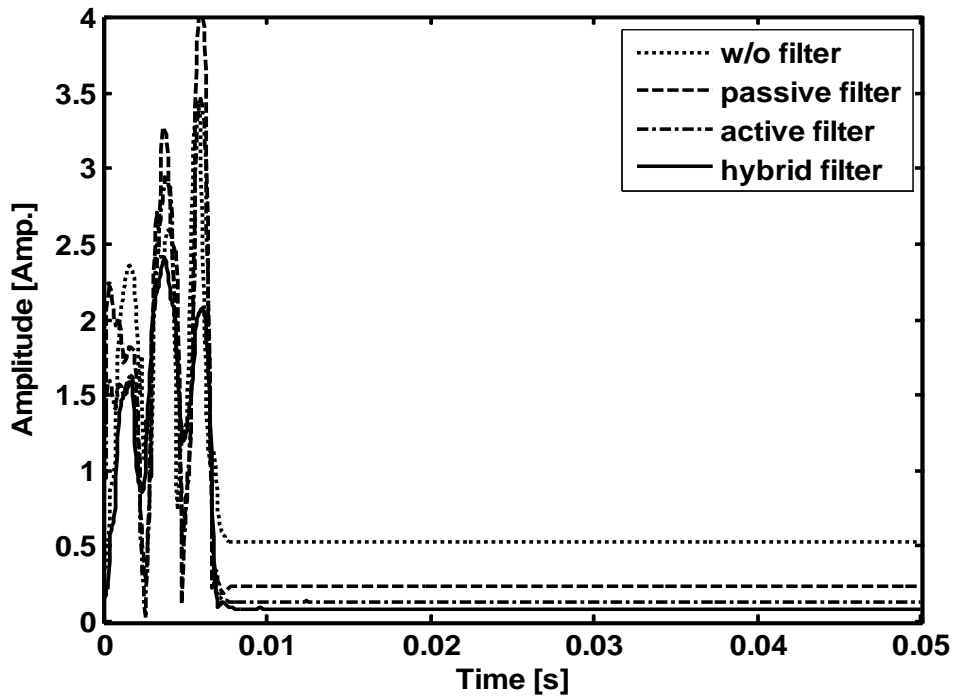
Fig.6.21 Performance comparison of hybrid filter for 7th harmonic signal
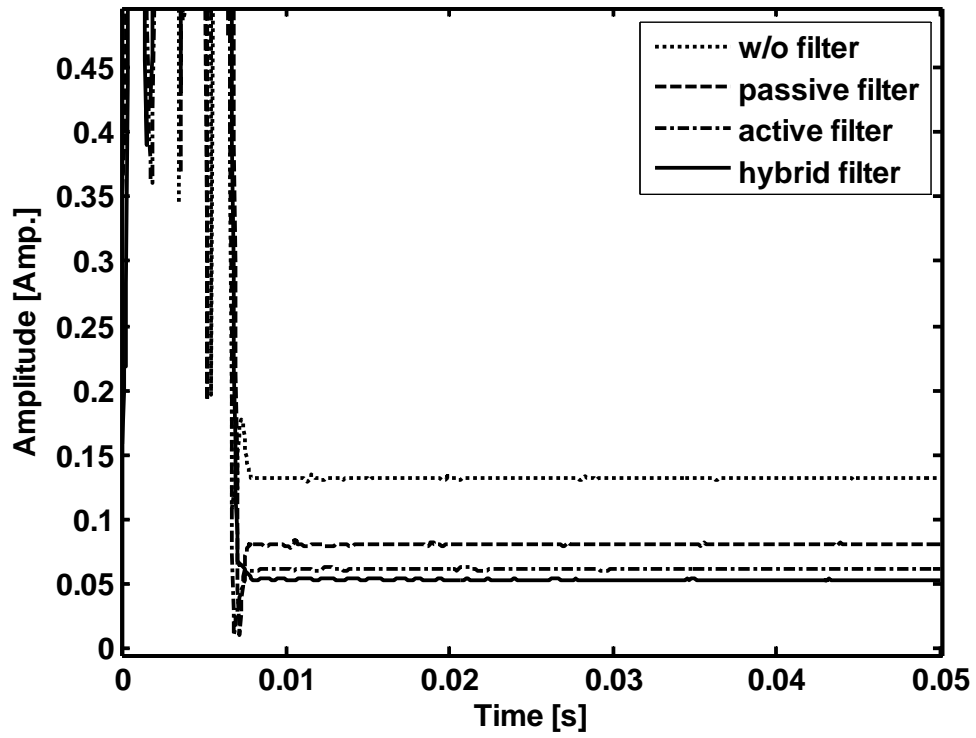
Fig.6.22 Performance comparison of hybrid filter for 9th harmonic signal
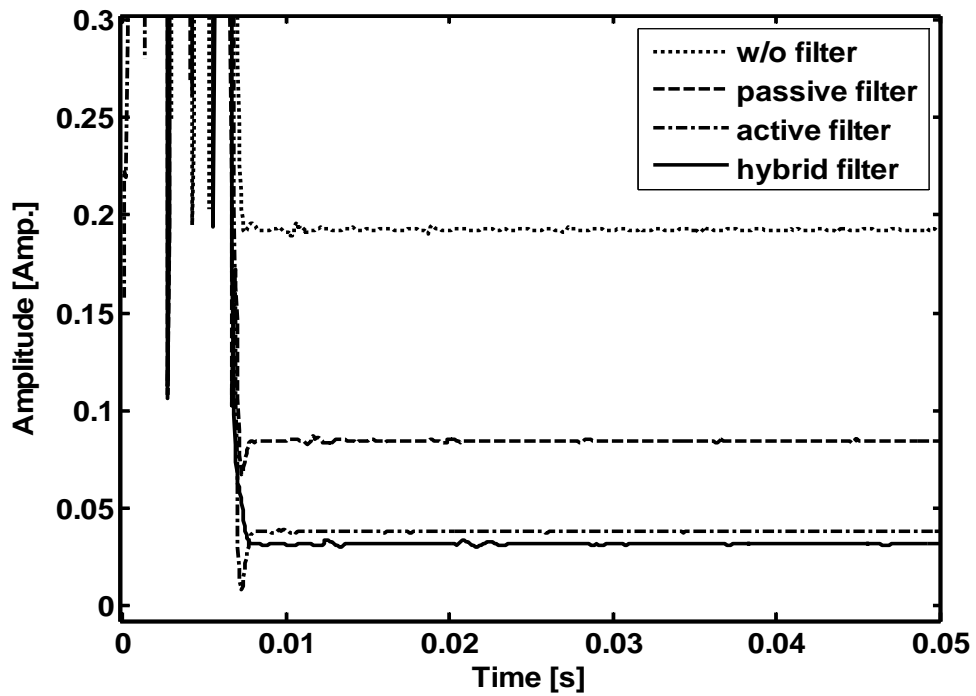
Fig.6.23 Performance comparison of hybrid filter for 11th harmonic signal
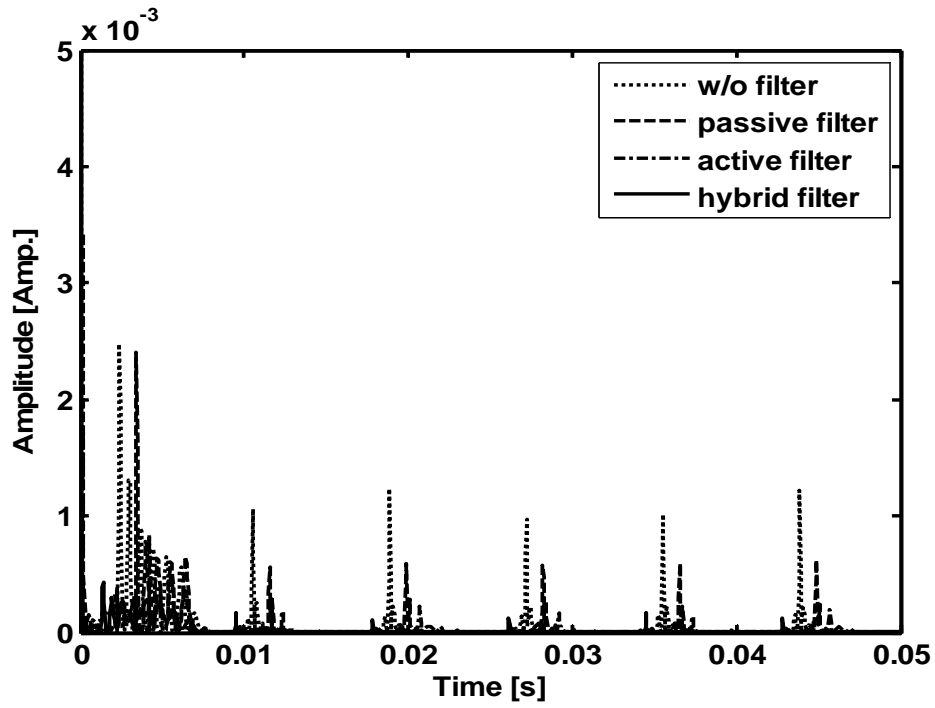
Fig.6.24 Performance comparison of hybrid filter for MSE of signal
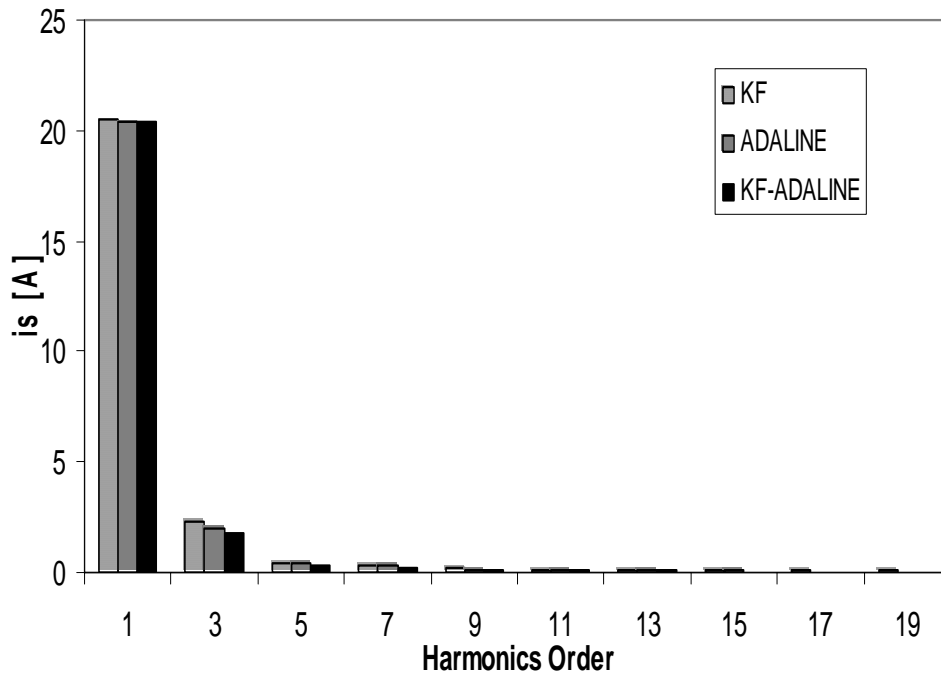
Fig.6.25 Comparison of source current spectrum of Passive Filter using different methods
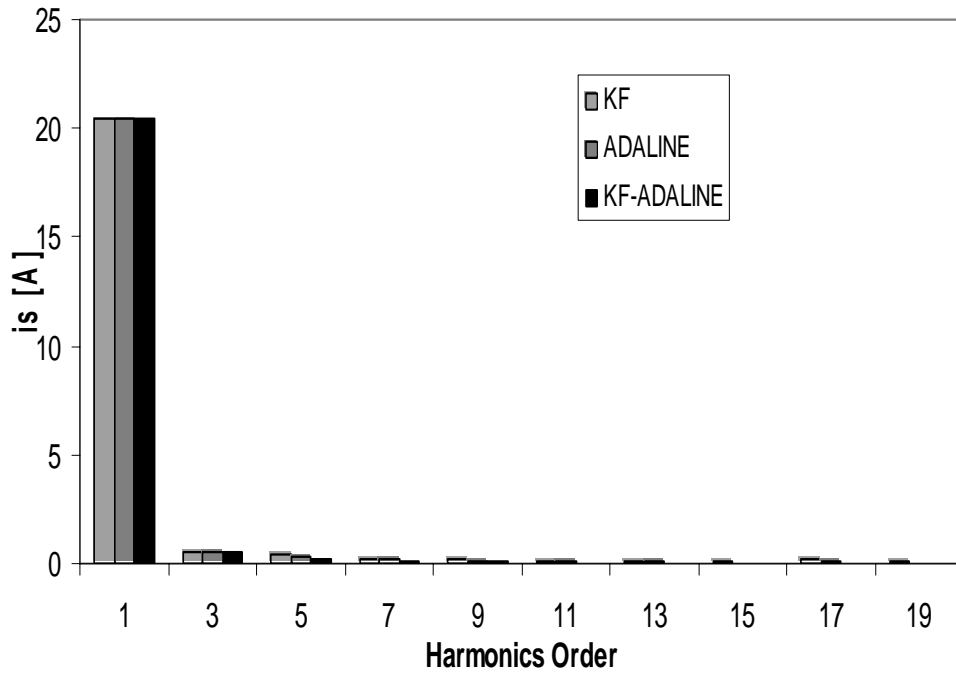
Fig.6.26 Comparison of source current spectrum of Active Filter using different methods
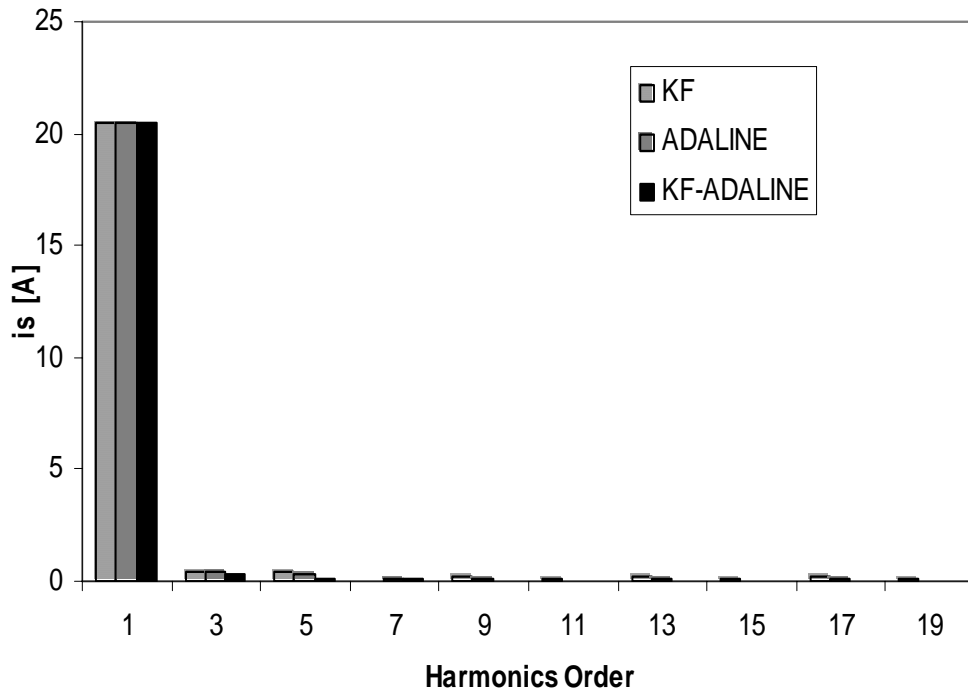
Fig.6.27 Comparison of source current spectrum of HAPF using different methods

Table 6.3 shows the comparative assessment of different estimation and harmonics elimination techniques. On comparing the actual values of harmonics obtained from SIMULINK, it is found that more accuracy in estimation is found using KF-Adaline method and more amounts of harmonics is eliminated using HAPF.

Table 6.3 Comparison of Estimation and Elimination Techniques

Har-order	Passive Filter				Active Filter				HAPF			
	Actual Values	KF	Ada.	KF-Ada.	Actual Values	KF	Ada.	KF-Ada.	Actual Values	KF	Ada.	KF-Ada
1	20.44	20.45	20.43	20.443	20.44	20.47	20.44	20.447	20.44	20.47	20.44	20.441
3	1.81	2.3	2	1.805	0.49	0.55	0.52	0.486	0.33	0.4	0.45	0.332
5	0.37	0.45	0.42	0.364	0.26	0.4	0.32	0.256	0.10	0.4	0.3	0.110
7	0.23	0.3	0.27	0.234	0.13	0.2	0.18	0.131	0.08	0.02	0.08	0.082
9	0.13	0.2	0.15	0.131	0.06	0.18	0.1	0.061	0.05	0.21	0.1	0.06
11	0.08	0.13	0.1	0.084	0.03	0.11	0.08	0.031	0.03	0.11	0.01	0.033
13	0.06	0.12	0.09	0.067	0.02	0.1	0.06	0.026	0.03	0.17	0.06	0.034
15	0.04	0.09	0.07	0.044	0.02	0.12	0.04	0.024	0.02	0.13	0.02	0.02
17	0.04	0.06	0.047	0.040	0.01	0.18	0.07	0.018	0.01	0.16	0.06	0.01
19	0.02	0.07	0.04	0.028	0.01	0.14	0.03	0.013	0.01	0.13	0.03	0.01

6.6.5. Experimental results

In order to validate the results obtained by simulation, a laboratory prototype has been built as shown in Fig. 6.28. The experimental setup parameters are: 1 kVA diode rectifier is taken as the non-linear load, the input supply voltage is 60 V, 50 Hz. The APF is made of 4 IGBT modules. The DC voltage is set at 150 V, filter inductor of 0.5 mH and DC bus capacitor of 1000μF. The switching frequency of the IGBT devices is 5 kHz. The source current waveform is stored in a Digital Storage Oscilloscope and then through Oscilloscope software, data is acquired to the personal computer. The used PC has a 1.46 GHz CPU and 1GB RAM. The sampling time in this case is fixed at 0.05ms.
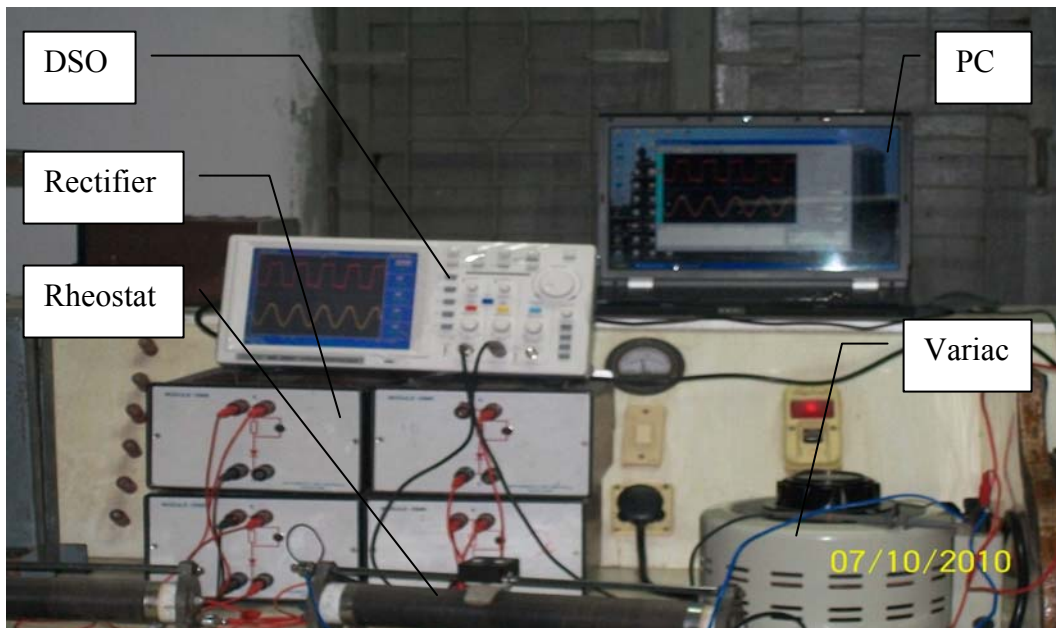
Fig. 6.28 Experimental setup for Harmonic elimination using HAPF
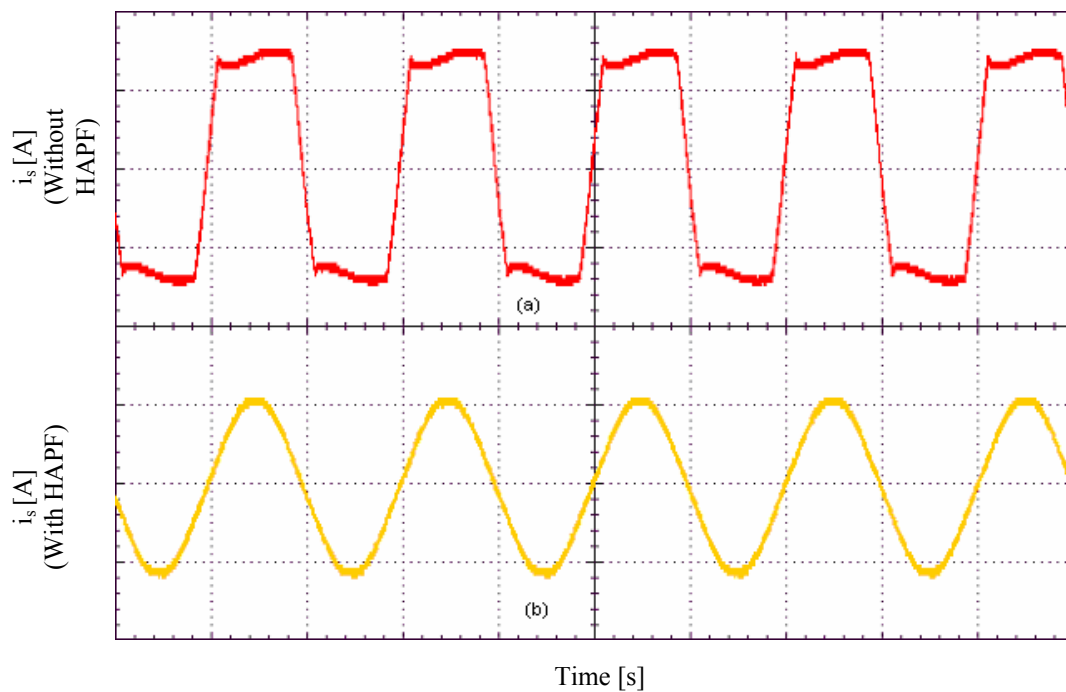
Fig.6.29 Experimental waveform of (a) source current without HAPF (b) source current with HAPF.
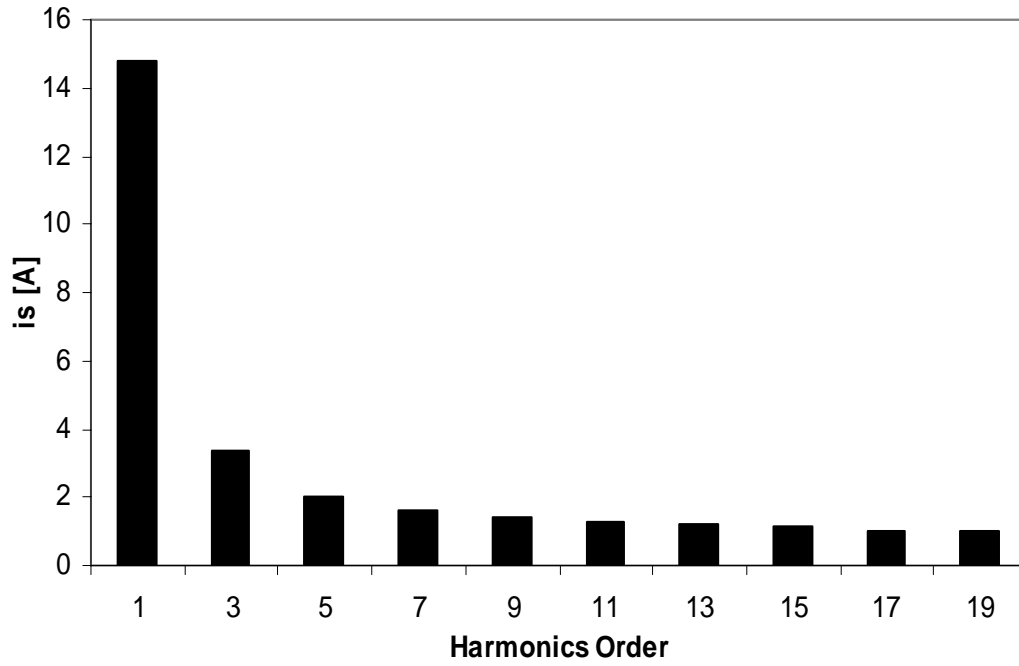
Fig.6.30 Source current spectrum without using filter
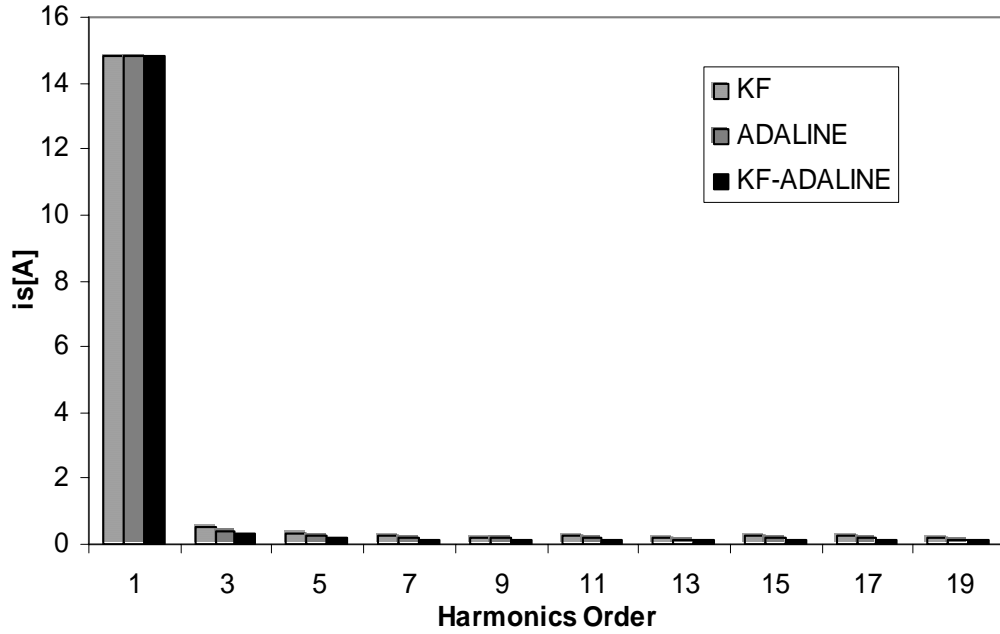
Fig.6.31 Comparison of Source current spectrum of HAPF using different methods

The steady state waveforms of the HAPF are shown in Fig. 6.29. Frequency spectra of source current before and after filtration using different methods are shown in figures 6.30 and 6.31 respectively. The THD of this current is reduced from 34.8 % to 3.4 %. From the results, it is clear that the HAPF using modified PWM technique has better ability to compensate the low frequency harmonics.

6.7. Chapter Summary

In this chapter, a comparative analysis of the performance of passive, active and hybrid power filters is presented. Simulation results show that the performance of shunt hybrid power filter is much better than other two. Harmonics components of signal in all the three cases are estimated by using KF-Adaline algorithm. The Total Harmonics Distortions (THD) of the shunt hybrid power filter using indirect current control algorithm is reduced to 1.82%, which is minimum among the three cases of filtering. This shunt hybrid power filter is effective and economic for solving harmonic problem in large capacity non-linear load. The real time simulation confirms the superiority of modified PWM control based HAPF.

Chapter-7

Summary and Conclusions

In this chapter, the conclusions of overall thesis are presented and some suggestions for future work are also proposed.

7.1 Summary of the Thesis Work

The thesis has mainly investigated on frequency and harmonics estimation of signal and development of HAPF with control technique for power conditioning. The novelty of the present work is the introduction of VLLMS to frequency estimation, EnKF to harmonics estimation and hybrid algorithms for both frequency and harmonics estimation. Finally the applications of hybrid algorithm to power system filter design for power conditioning.

- The problems and brief review of earlier techniques to power system frequency and harmonics estimation are discussed.

- Estimation of frequency of distorted signals, firstly using variants of recursive techniques such as RLS, ELS, Kalman Filter and LMS are presented. LMS outperforms over other three algorithms. For improvement in computational time and estimation error, secondly, a Variable Leaky Least Mean Square (VLLMS) algorithm based power system frequency estimation is proposed, a variable adaptation step size is introduced in estimation process. A quantized leak adjustment function is used for variation of leak. The performances of the new algorithm are studied at different situations of power system. The efficacies of the algorithm are verified on both simulation and experimental results.

- Four new hybrid algorithms (RLS-Adaline, KF-Adaline, RLS-BFO and Adaline-BFO) for power system frequency estimation are suggested. Initial choice of weight vector and Covariance matrix determines performance of RLS-Adaline and KF-Adaline algorithms. After the adaptation of the weight vector using RLS/KF algorithms, frequency of signal is estimated from updated weights. KF-Adaline performs better than RLS-Adaline at different level of noises and different signal changing conditions of power system. The performances of the next two proposed hybrid BFO algorithms i.e RLS-BFO and Adaline-BFO are dependent on the initial choice of maximum and minimum value of unknown parameters taken. If optimal choices of parameters are used, signal parameters can be converged faster. It is found that Adaline-BFO outperforms over BFO and RLS-BFO both in simulation and experimental results.

- A new algorithm called EnKF, for accurate estimation of amplitudes and phases of the harmonics contained in a voltage or current signal for power quality monitoring is suggested. Previously EnKF estimation has not been applied to power system area except some specialized applications such as weather forecasting, where initial states of model are highly uncertain and non-linear. Integer and non-integer multiple of harmonics, dc decaying offsets are successfully determined using EnKF by computer simulations. In case of fault condition, this algorithm is able to estimate the signal accurately. Results presented in this chapter indicate excellent accuracy (in terms of % age deviation in amplitude, deviation in phase angle and computational time) and convergence speed of the new algorithm in comparison to DFT, RLS, LMS, RLMS and KF algorithms. Laboratory test data is also used for validation of convergence property of the proposed EnKF algorithm.

- Harmonics estimation using combined signal processing and Neural Network technique (RLS-Adaline and KF-Adaline) is described. Subsequently, Evolutionary Computational technique such as Bacterial Foraging Optimization (BFO) is combined with signal processing or neural network technique for harmonics estimation. The way of implementation of the hybrid algorithms such as RLS-BFO and Adaline-BFO are the same as for frequency estimation but only there is change in number of unknown

parameters to be optimized. The performances of the proposed evolutionary computation hybrid approaches (RLS-BFO, Adaline-BFO) have been compared taking into account different power system changing conditions such as presence of inter and sub-harmonics in signal and also on data obtained from laboratory experiments.

- The application of hybrid algorithm (KF-Adaline) for designing a Hybrid Active Power Filter to mitigate the harmonic content of signal is presented. A comparative analysis of the performances of different estimation and elimination techniques are presented. Comparison shows that estimation using KF-Adaline is better than KF and Adaline algorithms. Similarly performance of harmonics mitigation using HAPF is better compared to passive and active filter. The Total Harmonics Distortions (THD) of HAPF using indirect current control algorithm is reduced to 1.82%, which is minimum among the three cases of filtering. Experimental results also confirm the superiority of modified PWM control based HAPF.

7.2 Thesis Contributions

The contributions of the Thesis are as follows.

- Critical assessment such as tracking time, computational time and estimation error of various estimation techniques applied to power system frequency and harmonics estimation.

- Development of improved LMS algorithm (VLLMS) for power system frequency estimation with introduction of a leakage factor and variable step size to avoid short comings such as poor convergence rate, more estimation error and more computational burden of the conventional LMS.

- The problems of KF applied to power system harmonics estimation such as maintenance of covariance matrix for higher order system and accurate tracking of harmonics in

system changing conditions have been resolved by applying EnKF under different real time power system situations.

- Developed two hybrid algorithms by hybridizing signal processing techniques such as RLS and KF with a neural network i.e RLS-Adaline and KF-Adaline for frequency and harmonics estimation. Frequency and Fundamental as well as harmonics components of amplitudes and phases are estimated for different cases of power system signal. These algorithms are also experimentally verified.

- Developed algorithms on hybridizing signal processing technique such as RLS and a neural network (Adaline) with Evolutionary computation Techniques such as RLS-BFO and Adaline-BFO for frequency and harmonics estimation with verification both through simulation taking different types of signals and experimentally by generating data in laboratory.

- Designed a HAPF for mitigation of harmonics occurring in a power system. Compared simulated results of HAPF with active and passive filter. Simulated results are also experimentally verified on laboratory prototype setup.

7.3 Conclusions

The research studies conducted resulted the following conclusions

- Four numbers of recursive algorithms such as RLS, ELS, KF and LMS have been applied to power system frequency estimation. Out of these algorithms LMS provides better estimation results compared to other three.
- For achieving more accuracy in estimation, step size of LMS is adapted and variation of leakage factor is introduced in the new proposed algorithm called VLLMS algorithm. It is found that estimation accuracy, tracking and computational time in case of VLLMS is better than LMS and VSSLMS algorithm.
- For harmonics estimation, a nonlinear state estimation approach called Ensemble Kalman Filter is developed. In case of EnKF, covariance matrix of Kalman Filter is replaced by

sample covariance and it is more feasible than covariance matrix. Estimation performance of EnKF is verified both by simulation and experimentation.

- Four hybrid algorithms such as RLS-Aadaline, KF-Adaline, RLS-BFO and Adaline-BFO are proposed. The efficacies of KF-Adaline and Adaline BFO are also verified using both simulation and experimental data.

- After estimation of harmonic content of distorted signal using different techniques, a Hybrid Active Power Filter with a modified PWM control technique is designed to eliminate the harmonic content present in source current signal.

7. 4 Future Scope of Work

- The proposed research work can be extended to design and develop a novel Hybrid Active Power Filter (HAPF) with a FPGA based digital controller for effective elimination of harmonics and reactive power compensation. With the advance of FPGA devices and integrated circuits (IC) technology, high efficient digital controller can be implemented in only one digital circuit. The control algorithms have been developed in VHSIC hardware description language (VHDL). This method is as flexible as any software solution, like developing the control algorithms in C-language for a DSP. Another important advantage of VHDL is that it is technology independent. The same algorithm can be synthesized into any FPGA and even has a possible direct path to a custom chip.

- This FPGA based controller can be applied to Aircraft electrical power system. It consists of mainly two or more engine driven generators to supply AC loads throughout the aircraft. Aircrafts need both AC and DC power. Transformer Rectifier Units (TRUs) convert AC power to DC power. These rectifier units are the main sources of harmonic generator in the aircraft Electric Power System. Increasing harmonics lead to malfunction of most sensitive equipments and circuits in the aircraft. Our future work in this area is to measure the harmonic content in the aircraft electric power system signal and then to design filter for effective mitigation of harmonic contents.

- Integrating Distributed Generation (DG) into electricity distribution network settles new needs for power quality monitoring because distributed generation units are usually connected to weak distribution network. DG units are likely to affect the system frequency. Since they are often not equipped with a load frequency control, so connecting a large no. of DG units to the grid should be carefully evaluated and planned. In future, this work can be extended by applying all the estimation techniques that are applied in the thesis, to power quality issues of distributed generation and simultaneously try to eliminate the harmonic content of the signal using suitable filtering techniques.

- Estimation of Frequency and Harmonics problems can also be extended in nonlinear frame work where techniques such as Nonlinear Least Square, H_∞ (Nonlinear setting) and EKF (Nonlinear setting) can be applied with further comparative assessment of the methods presented in the thesis.

References

[1] A. K. Pradhan, A. Routray and Abir Basak "Power System Frequency Estimation Using Least Mean Square Technique." *IEEE Trans. Power Del.*, vol. 20, no. 3, pp.1812-1816, 2005

[2] Bernard Widrow "Thinking about Thinking: The Discovery of the LMS Algorithm" *IEEE Signal Processing Magazine*, pp.100-103, 2005.

[3] Bernard Widrow, John McCool, and Michael Ball "The Complex LMS Algorithm" *Proceedings of the IEEE*, vol.63, no.4, pp.719-720, 1975.

[4] Raymond H. Kwong, Edward W. Johnston "A Variable Step Size LMS Algorithm" *IEEE Trans. on Signal Processing,* vol. 40, no.2, pp.1633-1642, 1992.

[5] Tyseer Aboulnasr and K. Mayyas "A Robust Variable Step-Size LMS-Type Algorithm: Analysis and Simulations" *IEEE Transactions on Signal Processing,* vol.43, no.3, pp.631-639, 1997.

[6] Wee-Peng Ang and B. Farhang-Boroujeny "A New Class of Gradient Adaptive Step-Size LMS Algorithms" *IEEE Transactions on Signal Processing*, vol.49, no.4, pp.805-810, 2001.

[7] Max Kemenetsky and Bernard Widrow "A Variable Leaky LMS Adaptive Algorithm"*38th IEEE Asilomar Conference on Signals, Systems & Computers*, vol.1, pp.125-128, 7-10 November,2004

[8] Vitor H. Nascimento and Ali H. Sayed "An Unbiased and Cost-Effective Leaky-LMS Filter"*30th IEEE Asilomar Conference on Signals, Systems & Computers*, vol.2, pp.1078-1082, 3-6 November,1996

[9] K. Mayyas and Tyseer Aboulnasr "Leaky LMS Algorithm: MSE Analysis for Gaussian Data" *IEEE Trans. on Signal Processing,* vol.45*,* no.4, 1997.

[10] Brian D. Rigling and Philip Schniter "Subspace Leaky LMS" *IEEE Signal Processing Letter*, vol.11, no.2, pp136-139, 2004.

[11] Orlando J. Tobias and Rui Seara "On the LMS Algorithm with Constant and Variable Leakage Factor in a Nonlinear Environment*" IEEE Trans. on Signal Processing,* vol. 54,no.9, pp.3448-3458, Sept.2006

[12] Scott C. Douglas "Performance Comparison of Two Implementations of the Leaky LMS Adaptive Filter" *IEEE Trans. on Signal Processing*, vol.45, no.8, 1997.

[13] P.K.Dash, A.K.Pradhan and G.Panda, "Frequency estimation of distorted power system signals using extended complex Kalman Filter." *IEEE Trans. on Power Del.*, vol. 14, no. 3, pp. 761-766, 1999.

[14] Chien-Hung Huang, Chien-Hsing Lee, Kuang-Jung Shih and Yaw-Juen Wang "Frequency Estimation of Distorted Power System Signals Using a Robust Algorithm" *IEEE Transactions on Power Delivery*, vol.23, no.1, pp.41-51, 2008.

[15] A. Routray, A. K. Pradhan and K. P. Rao "A Novel Kalman Filter for Frequency Estimation of Distorted Signals in Power Systems" *IEEE Transactions on Instrumentation and Measurement*, Vol.51, No.3, pp.469-479, 2002.

[16] P.K.Dash, R.K.Jena, G.Panda and A. Routray "An Extended Complex Kalman Filter for Frequency Measurement of Distorted Signals" *IEEE Transactions on Instrumentations and Measurement,* Vol.49, No.4, pp.746-753, 2000.

[17] A.K.Pradhan, A.Routray ,D.Sethi "Voltage Phasor Estimation Using Complex Linear Kalman Filter" *8th IEE International Conference on Developments in Power System Protection, IIT, Kharagpur*, vol.1, pp.24-27,5-8 April, 2004.

[18] M. J. Grimble "Adaptive Kalman Filter for Control of Systems with unknown disturbances" *IEE Proc.*, vol.128, no.6, pp.263-267, 1981.

[19] K. W. Chan and H. C. So "Accurate Frequency Estimation for Real Harmonic Sinusoids" *IEEE Signal Processing Letters*, vol.11, no.7, pp.609-612, 2004.

[20] Jin Jiang , Youmin Zhang "A revisit to block and recursive least squares for parameter estimation" *Computers and Electrical Engineering*, vol.30, pp.403-416, 2004

[21] Milenko B. Djuric, Zeljko R. Djurisic " Frequency measurement of distorted signals using Fourier and Zero crossing Techniques" *Electric Power System Research*, vol. 78, pp. 1407-1415, 2008

[22] Mohsen Mojiri, Masoud Karimi-Ghartemani and Alireza Bakhshai "Estimation of Power System Frequency Using an Adaptive Notch Filter" *IEEE Transactions on Instrumentation and Measurement*, vol.56, no.6, pp.2470-2477, 2007.

[23] T. S. Sidhu and M. S. Sachdev "An Iterative Technique for Fast and Accurate Measurement of Power System Frequency" *IEEE Transactions on Power Delivery*, vol.13, no.1, pp.109-115, 1998.

[24] M. Karimi-Ghartemani, M. R. Iravani "Wide-range, fast and robust estimation of power system frequency" *Electric Power System Research*, vol.65, pp.109-117, 2003.

[25] S.A. Soliman , R.A. Alammari , M.E. El-Hawary 'Frequency and harmonics evaluation in power network using fuzzy regression technique' *Electric Power System Research*, vol. 66, pp. 171-177., 2003

[26] P.K.Dash, D.P.Swain, A.Routray and A.C.Liew "An adaptive neural network for estimation of power system frequency" *Electric Power System Research*, vol.41, issue 3, pp. 203-210, 1997

[27] M.Gupta, S.Srivastava and J.R.P.Gupta "Power system frequency estimation using neural network and genetic algorithm" Proceedings of *Joint International Conference on Power System Technology and IEEE Power India Conference*, POWERCON 2008, pp. 1-5, 12-15 Oct. 2008

[28] M.Bertoluzzo, G.Buja, S.Castellan, P.Fiorentin " Real time estimation of power system frequency by neural network" Proceedings of *4th IEEE International Symposium on Diagnostics for Electric Machines, Power Electronics and Drives*, pp. 87-92, 24-26 Aug. 2003

[29] M.S. Sachdev, M.M. Giray "A Least Square technique for determining power system frequency" *IEEE Trans. Power Apparatus Syst.* Vol. 104, No.2, pp. 437-443, 1985

[30] V.V. Terzija, M.B.Djuric and B.D. Kovacevic, "Voltage Phasor and Local System Frequency Estimation Using Newton-Type Algorithms", *IEEE Trans. on Power Delivery,* Vol. 4, No. 3, pp. 1368-1374,1994

[31] R.Trapero,H.Sira-Ramirez and V.Feliu Batlle " On the algebraic identification of the frequencies, amplitudes and phases of two sinusoidal signals from their noisy sum" *International Journal of Control,*Vol.81,No.3,pp.507-518, 2008.

[32] Jin Jiang , Youmin Zhang, "A revisit to block and recursive least squares for parameter estimation" *Computers and Electrical Engineering,* Vol. 30, pp. 403-416, 2004.

[33] Tarlochan S.Sidhu, "Accurate Measurement of Power System Frequency Using a Digital Signal Processing Technique" *IEEE Transactions on Instrumentation and Measurement,* Vol.48*,* No.1, pp.75-81, 1999.

[34] D.C. Rife, R.R. Boorstyn, "Single tone parameter estimation from discrete time observations" *IEEE Trans. Infor. Theory*, Vol. 20, No. 5, pp. 591-598, 1974

[35] M.S. Sachdev, M.M. Giray, " Off-Nominal Frequency Measurements in Electric Power Systems" *IEEE Trans. on Power Delivery*, Vol.4, No.3, pp.1573-1578, 1989.

[36] Vladimir. V. Terzija "Improved Recursive Newton-Type Algorithm for Frequency and Spectra Estimation in Power Systems" *IEEE Trans. On Instrumentation and Measurement,* vol.52, No.5, pp. 1654-1659, October 2003.

[37] Karen Kennedy, Gordon Lightbody, Robert Yacamini, "Power System Harmonic Analysis Using the Kalman Filter" *IEEE Power Engineering Society General Meeting*, Vol.2, pp.752-757, 13-17th July 2003.

[38] Haili Ma, Adly A. Girgis "Identification and Tracking of Harmonic Sources in a Power System Using a Kalman Filter" *IEEE Transactions on Power Delivery*, Vol.11, No.3, pp.1659-1665, 1996.

[39] Ashwani Kumar, Biswarup Das, Jaydev Sharma "Robust dynamic state estimation of power system harmonics" *Electrical Power & Energy Systems*, vol.28, pp.65-74, 2006.

[40] Husam M.Beides, G. T .Heydt "Dynamic State Estimation of Power System Harmonics Using Kalman Filter Methodology" *IEEE Transactions on Power Delivery*, vol.6, no.4, pp.1663-1670, October 1991.

[41] P. K. Dash, A. K. Pradhan , G. Panda, R. K. Jena, S. K. Panda "On line tracking of time varying harmonics using an integrated complex Kalman Filter and Fourier Linear Combiner" *Proc. IEEE Conference on Power Engineering Society*, Singapore, vol.3, pp.1575-1580, 23-27 January, 2000

[42] Alberto Pigazo and Victor M.Moreno "$3\phi - 3\omega$ Signal Model for Power System Harmonics and Unbalance Identification Using Kalman Filtering" *IEEE Transactions on Power Delivery*, vol.23, no.2, pp.1260-1261, 2008.

[43] Maamar Bettayeb, Uvais Qidwai "Recursive estimation of power system harmonics" *Electric Power System Research*, vol.47, pp. 143-152, 1998

[44] E.A. Abu Al-Feilat, I. El-Amin, M. Bettayeb "Power System Harmonic Estimation a Comparative Study" *Electric Power System Research*, vol.29, issue 2, pp91-97, 1994.

[45] Tadeus Lobos, Andrzej Cichocki, Pawel Kostyla, Zbigniew Waclawek "Adaptive On-Line Learning Algorithm for Robust Estimation of Parameters of Noisy Sinusoidal Signals" *Artificial Neural Networks-ICANN, 97*, Springer Berlin/Heidelberg,vol.1327/1997, pp.1193-1198, April10, 2006

[46] Xiaohua Jiang, Ji King and Ali Emadi "A Power Harmonics Detection Approach Based on Least Squares Energy Minimization Principle" *The 30th Annual Conference of the IEEE Industrial Electronics Society, Busan, Korea*, pp.2934-2938, November 2-6,2004.

[47] T.Lobos, T.Kozina and H.J.Koglin "Power system harmonics estimation using linear least squares method and SVD" *IEE Proc. Generation, Transmission & Distributions*, vol.148, no.6, pp.567-572, 2001.

[48] Jorge Lazaro Dominguez, J. F. M. Arguelles, M. A. Z. Arrieta, B. L. Jaurieta, M. S. Benito and I. A. Zugazaga " New Quick convergence invariant digital filter for phasor estimation" *Electric Power System Research*, vol.79, issue.5, pp. 705-713, 2009

[49] Cai Tao, Duan Shanxu, Ren Ting and Liu Fangruli " A robust parametric method for power harmonics estimation based on M-estimators" *Measurement*, vol.43, issue.1, pp. 67-77, January 2010

[50] Ahmet S. Yilmatz, Ahmed Alkan, Musa H. Asyali "Application of parametric spectral estimation methods on detection of power system harmonics" *Electric Power System Research*, Vol-78, pp. 683-693, 2008.

[51] Y.Z. Liu, S. Chen "A Wavelet Based Model for On-line Tracking of Power System Harmonics using Kalman Filtering" in Proc. *IEEE Power Engineering Society Summer Meet.*, vol. 2, pp. 1237–1242, Jul. 2001

[52] Shyh-Jier Huang and Cheng-Tao Hsieh " Visualizing time-varying power system harmonics using a Morlet wavelet transform approach" *Electric Power Systems Research*, vol. 58, pp. 81-88, 2001

[53] Jan Mandel "A Brief Tutorial on the Ensemble Kalman Filter" *Center for Computational Mathematics report, University of Colorado at Denver and Health Sciences Center*, Denver, pp.1-5, 2007.

[54] Jan Mandel "Efficient Implementation of the Ensemble Kalman Filter" *Center for Computational Mathematics report, University of Colorado at Denver and Health Sciences Center*, Denver, pp.1-7, 2006.

[55] S. Gillijns, O. B. Mendoza, J. Chandrasekhar, B. L. R. De Moor, D.S. Bernstein and A. Ridley " What is the Ensemble Kalman Filter and How well does it Work" *Proceedings of the 2006 American Control Conference*, Minneapolis, Minnesota, USA, pp.4448-4453. June 14-16, 2008.

[56] P K Dash, A C Liew, D P Swain and B Mishra "Fast tracking of transient power system signals using fuzzy LMS algorithm" *Electrical Power & Energy Systems*, vol. 20, no. 8, pp. 555–561, 1998

[57] M. Joorabian, S.S. Mortazavi, A.A. Khayyami " Harmonics estimation in a power system using a novel-hybrid Least Square –Adaline algorithm" *Electric Power System Research*, vol.79, issue.1, pp. 107-116, 2009

[58] L. L. Lai, W. L. Chan, C. T. Tse, A. T. P. So "Real-Time Frequency and Harmonic Evaluation using Artificial Neural Networks" *IEEE Transactions on Power Delivery*, vol.14, no.1, pp.52-59, 1999.

[59] Josif J. Tomic, Miodrag D. Kusljevic and Vladimir V. Vujicic "A new Power System Digital Harmonic analyzer" *IEEE Transactions on Power Delivery*, vol.22, no.2, pp.772-780, 2007.

[60] P. K. Dash, D. P. Swain, A. Routray, A. C. Liew "Harmonic Estimation in a Power System using Adaptive Perceptrons" *IEE Proceedings of Generation, Transmissions & Distributions*, vol.143, no.6, pp.565-574, 1996.

[61] Hiroyuul Mori, Kenji Itou, Hiroshi Uematsu and Senji Tsuzuki " An artificial neural-net based method for predicting power system voltage Harmonics" *IEEE Trans. on Power Delivery*, vol.7, no.1,1992

[62] Hsiung cheng Lin "Intelligent neural network based fast power system Harmonics Estimation" *IEEE Trans. on Industrial Electronics*, vol. 54, no.1, 2007.

[63] V. Sureshkumar, P.S. Kannan, K. Kalaiselvi and D. Kavitha " Optimal Estimation of Harmonics in power system using Intelligent Computing Techniques" *Proceedings of International Joint conference on Neural Networks*, Orlando, Florida, USA, 12-17 August, 2007

[64] S. Ghodratollah Seifossadat, Morteza Razzaz, Mahmood Moghaddasian and Mehdi Monadi" Harmonics Estimation in Power System Using Adaptive Perceptrons based on a Genetic Algorithm" *WSEAS Trans. on Power Systems*, vol.2, issue 11, 2007

[65] Maamar Bettayeb and Uvais Qidwai "A Hybrid Least Squares-GA-Based Algorithm for Harmonic Estimation" *IEEE Transactions on Power Delivery*, vol.18, no.2, pp.377-382, 2003

[66] U. Qidwai, M. Bettayeb, "GA based nonlinear harmonic estimation" *IEEE Trans. Power Delivery,* December 1998.

[67] Kevin M.Passino "Biomimicry of Bacterial Foraging for Distributed Optimization and Control" *IEEE Control System Magazines*, pp.52-67, June 2002.

[68] Amitava Chatterjee and Fumitoshi Matsuno " Bacterial Foraging Techniques for solving EKF-based SLAM problems" *Proceedings of International Control Conferences (ICC2006), Glasgow, Scotland, United Kingdom*, 30th August-1st September, 2006

[69] S.Mishra "A Hybrid Least Square-Fuzzy Bacterial Foraging Strategy For Harmonic Estimation" *IEEE Transactions on Evolutionary Computation*, vol.9, no.1, pp.61-73, 2005.

[70] Dong Hwa Kim, Ajith Abraham, Jae Hoon Cho "A hybrid genetic algorithm and bacterial foraging approach for global optimization" *Information Sciences*, 177, pp.3918-3937, 2007

[71] M. Mojiri, M. K. Ghartemani and A. Bakhshai, " Processing of harmonics and interharmonics using an Adaptive Notch Filter" *IEEE Trans. on Power Delivery*, vol. 25, no. 2, pp. 534-542, 2010.

[72] V. J. Mathews and Z. Xie, "Stochastic gradient adaptive filters with gradient adaptive step size," *IEEE Trans. Signal Processing*, vol. 41, pp.2075–2087, 1993.

[73] A. Benveniste, M. Metivier, and P. Priouret, "*Adaptive Algorithms and Stochastic Approximation*". New York: Springer-Verlag, 1990.

[74] V. Panuska "A new form of the extended Kalman filter for parameter estimation in linear systems with correlated noise", *IEEE Trans on Automatic Control.,* vol. AC-25, pp. 229-235,1980.

[75] A. K. Deb, Jayadeva*, ,* M. Gopal, and Suresh Chandra, "SVM-Based Tree-Type Neural Networks as a Critic in Adaptive Critic Designs for Control" *IEEE Trans. On Neural network*, vol.18, no.4, pp.1016-1030, 2007.

[76] Z.G.Hou, L.Cheng and M. Tan, "Multicriteria optimization for Coordination of redundant robots using a dual neural network" *IEEE Trans. on SMC*" vol. 40, no.4, pp. 1075-1087, 2010.

[77] M.Z. Mohd Zain, M.O. Tokhi and Z. Mohamed, "Hybrid learning control schemes with input shaping of a flexible manipulator system," *Mechatronics*, vol. 16, pp. 209-219, 2006

[78] S. K. Aditya and D. Das "Design of load frequency controllers using genetic algorithm for two area interconnected hydro power system" *Intl. Journal of Electric Power Components and Systems*, vol.31, no. 1, pp. 81-84, 2003

[79] E. A. Merchan-Cruz and A. S. Morris "Fuzzy-GA-based Trajectory planner for robot manipulators sharing a common work place" *IEEE Trans. on Robotics*, vol. 22, no. 4, pp. 613-624, 2006

[80] B.K. Panigrahi , V. Ravikumar Pandi , R. Sharma , Swagatam Das , S.Das ,"Multiobjective bacteria foraging algorithm for electrical load dispatch problem" *Energy Conversion and Management*, 2010

[81] Y. R. Sood, N. P. Padhy and H. O. Gupta " Discussions of Optimal Power flow by Enhanced Genetic algorithm" *IEEE Trans. on Power System*, vol. 18, no. 3, pp. 1219-1219, 2003.

[82] Z.Ogonowski, Drying control system for spray booth with optimization of fuel consumption, *Applied Energy(Elsevier)*, 2010

[83] K.P.Basu, A. Asghar and S. Morris, "Elimination of inrush current in parallel transformers by sequential phase energization "*IEICE Electronic Express*, vol. 4, no. 5, pp. 147-152, 2007.

[84] A. De, D. Debnath and A. Chakraborty, "A Study on the Impact of Low-Amplitude Oscillatory Switching Transients on Grid Connected EHV Transformer Windings in a Longitudinal Power Supply System", *IEEE Tran. On Power Delivery*, vol.24, no. 2, pp. 679-686, 2009

[85] B. Singh, K. Al-Haddad, A. Chandra, "A Review of Active Power Filters for Power Quality Improvement," *IEEE Trans. on Industrial Electronics*, vol. 45, no.5, pp. 960-971, 1999.

[86] H. Akagi, "New trends in active filters for power conditioning*," IEEE Trans. Ind. Applicat.*, vol.32, no.6, pp. 1312-1322, 1996.

[87] H. Akagi, A. Nabae and S. Atoh "Control Strategy of Active Power Filters Using Multiple- Voltage Source PWM Converters", *IEEE Trans. on Indl. Applicat.*, Vol.IA-20, no.3, pp. 460-465, 1986.

[88] A. Chandra, B. Singh, B.N. Singh, K. Al-Haddad "An Improved Control Algorithm of Shunt Active Filter for Voltage Regulation, Harmonic Elimination, Power Factor Correction, and Balancing of Nonlinear Loads," *IEEE Trans. on Power Electronics*, vol. 15, no. 3, pp.495-507, 2000.

[89] S. Rahmani, K. Al-Haddad, H. Y. Kanaan and B. Singh, "Implementation and Simulation of Modified PWM with Two Current Control Techniques Applied To

Single-Phase Shunt Hybrid Power Filter," *IEE Proceedings -Electric Power Applications*, vol. 153, no. 03, pp. 317-326, 2006.

[90] S. Rahmani, K. Al-Haddad and H. Y. Kanaan, "A Comparative Study of Shunt Hybrid and Shunt Active Power Filters for Single-Phase Applications: Simulation and Experimental Validation" *Journal of Mathematics and Computers in Simulation, Transactions of IMACS*, *Elsevier*, vol.71, no.4-6, pp. 345-359, 2006.

[91] F. Z. Peng, M. Kohata, and H. Akagi, "Compensation characteristics of shunt active and series active filters" in Proc. *Chinese-Japanese Power Electron Conf.*, Beijing, Country, pp. 381-387, 1990.

[92] Rahmani, K. Al-Haddad and F. Fnaiech, "A Series Hybrid Power Filter To Compensate Harmonic Currents and Voltages", *IEEE Industrial Electronics Conference IECON 2002*, Seville, Spain Nov. 5 - 8, pp. 644- 649, 2002.

[93] S. Busao, L. Malesani and P. Mattavelli "Comparison of current control techniques for Active Applications", *IEEE Trans. Ind. Electronics*, vol. 45, pp. 722-729, 1998.

[94] F. Z. Peng, H. Akagi, and A. Nabae, "A new approach to harmonic compensation in power systems—A combined system of shunt passive and series active filters," *IEEE Trans. Ind. Appl.*, vol. 26, no. 6, pp. 983–990, 1990.

[95] F. Z. Peng, H. Akagi, and A. Nabae, "A new approach to harmonic compensation in power systems—A combined system of shunt passive and series active filters," in Conf. *Proc. IEEE-IAS Annu. Meeting*, pp. 874–880, 1988.

[96] H. Fujita and H. Akagi, "A practical approach to harmonic compensation in power systems: Series connection of passive and active filters," in Conf. *Proc. IEEE-IAS Annu. Meeting*, pp.1107–1112, 1990.

[97] H. Fujita and H. Akagi, "A practical approach to harmonic compensation in power systems: Series connection of passive and active filters," *IEEE Trans. Ind. Appl.,* vol. 27, no. 6, pp. 1020–1025, 1991.

[98] I. Takahashi and Y. Omura, "High power active filter using LC tuned filter," in Japanese *JIEE Trans. Ind. Appl.,* vol. 112-D, no. 9, pp. 823–828, 1992.

[99] N. Tokuda, Y. Ogihara, M. Oshima, and T. Miyata, "Active filter with series L-C circuit," in Conf. *Proc. IEEE-PES ICHPS,* pp. 242–249, 1994.

[100] M. Rastogi, N. Mohan, and A. A. Edris, "Filtering of harmonic currents and damping of resonances in power systems with a hybrid- active filter," in Conf. *Proc. IEEE-APEC,* Texas, USA, pp. 607–612, 1995.

[101] S. Bhattacharya, P. T. Cheng, and D. M. Divan, "Hybrid solutions for improving passive filter performance in high power applications," *IEEE Trans. Ind. Appl.,* vol. 33, no. 3, pp. 732–747, 1997.

[102] D. Basic, V. S. Ramsden, and P. K. Muttik, "Harmonic filtering of high-power 12-pulse rectifier loads with a selective hybrid filter system," *IEEE Trans. Ind. Electron.,* vol. 48, no. 6, pp. 1118–1127, 2001.

[103] D. Detjen, J. Jacobs, R. W. De Doncker, and H. G. Mall, "A new hybrid filter to dampen resonances and compensate harmonic currents in industrial power systems with power factor correction equipment," *IEEE Trans. Power Electron.*, vol. 16, no. 6, pp. 821–827, 2001.

[104] B. N. Singh, B. Singh, A. Chanda, and K. Al-Haddad, "Digital implementation of a new type of hybrid filter with simplified control strategy," in Conf. *Proc. IEEE-APEC*, Texas, USA, pp. 642–648, 1999.

[105] A. Chakraborty, S. Halder "Power System Analysis, Operation and Control" *PHI Publication*, Third Edition , New Delhi-2010

[106] Simon Haykin, Thomas Kailath, "*Adaptive Filter Theory*" 4th Edition, Pearson Education, 2007.

[107] J.M. Mendel, "*Lessons in Digital Estimation Theory*" Prentice-Hall, Englewood Cliffs, NJ, 1987.

[108] T. Soderstrom and P. Stocia "*System Identification*" Prentice-Hall, Englewood Cliffs,NJ,1989

[109] L. Ljung and T. Soderstrom "*Theory and Practice of Recursive Identification*" MIT Press, Cambridge, MA, 1983.

[110] L. Jung, "*System Identification-Theory for the User*", 2nd Edition, PTR Prentice Hall, Upper Saddle River, NJ, 1999.

Publications

In Journals

[1] B. Subudhi, P.K.Ray, A.M.Panda, and S.R.Mohanty, "A Comparative Study on different Power System Frequency Estimation Techniques" *Intl. Journal of Automation and Control*, vol.3, no. 2/3, pp. 202-215, 2009

[2] B. Subudhi, P.K.Ray and A.M.Panda, "Recursive Estimation of Power System Frequency by advanced signal processing techniques", *International Journal, AMSE, France*, vol.82, no. 1, pp. 16-26, 2009.

[3] B. Subudhi, P.K.Ray and A.M.Panda, "A Comparative study on Estimation Techniques with application to power signal frequency" *Archives of Control Sciences*, vol. 18, no.1, pp. 89-97, 2008.

[4] B.Subudhi and P.K.Ray, "Ensemble Kalman Filter based Power System Harmonics Estimation" *IET Generation, Transmission and Distribution* (Under Review)

[5] P.K.Ray and B. Subudhi, " BFO Optimized RLS algorithm for Power System Harmonics Estimation" *Applied Soft Computing, Elsevier* (Under Review)

In Conferences

[1] B. Subudhi and P.K.Ray, "A Hybrid Adaline Bacterial Foraging Approach for Power System Harmonics Estimation" IEEE Sponsored International Conference on Industrial Electronics, Control and Robotics, Rourkela, Dec. 28-30, 2010

[2] B. Subudhi, P.K.Ray, and A.M.Panda, " Estimation of Power System Harmonics using Hybrid RLS-Adaline and KF-Adaline Algorithms" *IEEE Conference, TENCON-09*, Singapore, Nov. 23-26, 2009.

[3] B.Subudhi and P.K.Ray, "A Comparative Study on Estimation of Power System Harmonics" *7th International R & D Conference*, Bhubaneswar, Feb. 4-6, 2009.

[4] B. Subudhi, P.K.Ray, S.R.Mohanty and A.M.Panda, "Parameter Estimation Techniques applied to Power Networks" *IEEE Conference, TENCON-08*, Hyderabad, Nov. 18-21, 2008.

[5] B. Subudhi, P.K.Ray and A.M.Panda, "Estimation of Power System Parameters Using Extended Least Square Techniques" *Proceeding of IEEE Sponsored Intl. Conference on Power System Analysis, Control and Optimization (PSACO)*, Visakhapatnam, pp.964-967, March 13-15, 2008.

[6] B. Subudhi, P.K.Ray and A.M.Panda, "Power System Control and Automation Using Different Parameter Estimation Techniques" *Proceeding of IEEE Sponsored Conference on Computational Inteligence, Control and Computer Vision in Robotics & Automation (CICCRA)*, Rourkela, pp.234-237, March 10-11, 2008.

Pravat Kumar Ray

Asst. Professor
Department of Electrical Engineering
Indira Gandhi Institute of Technology, Sarang
Orissa- 759146, India

Ph: +91-6760-240539

E-mail: pravat_ray@rediffmail.com

Qualification

- Ph. D. (Continuing)
  NIT Rourkela

- M.E (Power System Engineering)
  Bengal Engineering and Science University, Howrah [First Division]

- B.E (Electrical Engineering)
  Utkal University, Bhubaneswar, Orissa [First Division]

- +2 (Science)
  Council of Higher Secondary Education, Orissa [First Division]

- 10th
  Board of Secondary Education, Orissa [First Division]

Publications

- 03 Journal Papers

- 06 Conference Papers

Permanent Address

At/Po- Balabhadrapur, Via- Arnapal
Dist- Bhadrak, Orissa-756116, India

Date of Birth

04th November, 1975